DENITRIFICATION IN FUSARIUM: A CROSSROADS BETWEEN FUNGAL BIOLOGY AND EMISSION OF A MAJOR GREENHOUSE GAS

by

BLAKE A. OAKLEY

(Under the Direction of Anthony E. Glenn)

ABSTRACT

Denitrification is responsible for converting soluble nitrogen to gaseous forms as part of the nitrogen cycle. Denitrification has major implications for trends in intensive agriculture and global warming. Denitrification is primarily performed by specific types of microbes, including bacteria, archaea, and fungi. My research focused on fungal denitrification. I aimed to gain a holistic understanding of the denitrification pathway in the soil-borne maize pathogen *Fusarium verticillioides*. Prior to my involvement in the project, genes highly up-regulated (≥ 8-fold) in response to hypoxia and/or nitric oxide were found through transcriptome analysis of wild type *F. verticillioides*. This collection of genes was presumed to be directly or indirectly tied to fungal denitrification, nitrogen metabolism, and/or nitric oxide detoxification of reactive nitrogen oxides. My phylogenetic analyses revealed that fungal orthologs of dissimilatory nitrite reductase (DNI1) and nitric oxide reductase (NOR1) are nearly exclusive to the Ascomycota, and the ability to denitrify is limited to a select number of genera. Further, within the genus *Fusarium*, only select species complexes harbor denitrifiers. Prior to my arrival at UGA, some genes from the RNA-seq dataset hypothesized to be involved in denitrification were deleted using *Agrobacterium*-mediated fungal transformation. My research evaluated these deletion mutants

for their potential to grow under low-oxygen conditions, emit N_2O, produce fumonisins, and infect maize seedlings. Deletion of genes within the denitrification pathway had a marginal effect on fumonisin production and virulence. However, deletion of NOR1, a cytochrome P450 nitric oxide reductase, caused a significant decrease (99%) in N_2O production from *F. verticillioides*. Adding *FvNOR1* back into the deletion mutant background using protoplast complementation restored the wild type phenotype and conclusively demonstrated the genetic role of *NOR1* in N_2O production. Thus, NOR1 has been identified as a key target for mitigation of N_2O emissions from agricultural fields where *Fusarium* species are commonplace. My research increases understanding of the denitrification pathway in ascomycetes, assesses the phylogenetic limitedness of denitrification in fungi, and identifies a novel target for inhibition of fungal-derived agricultural N_2O emissions. My research results are anticipated to enable development of new solutions for mitigation of N loss and N_2O emissions.

INDEX WORKS: *Fusarium verticillioides*, denitrification, hypoxia, fungi, nitrous oxide emissions, nitrogen

DENITRIFICATION IN FUSARIUM: A CROSSROADS BETWEEN FUNGAL BIOLOGY AND EMISSION OF A MAJOR GREENHOUSE GAS

by

BLAKE A. OAKLEY

B.S., North Carolina State University, 2017

A Dissertation Submitted to the Graduate Faculty of The University of Georgia in Partial Fulfillment of the Requirements for the Degree

DOCTOR OF PHILOSOPHY

ATHENS, GEORGIA

2023

FUNGAL DENITRIFICATION IN FUSARIUM: A CROSSROADS BETWEEN FUNGAL BIOLOGY AND EMISSION OF A MAJOR GREENHOUSE GAS

by

BLAKE A. OAKLEY

Major Professor(s):	Anthony E. Glenn
Committee:	Scott E. Gold Marin T. Brewer Harald Scherm Shavannor M. Smith

Electronic Version Approved:

Ron Walcott
Dean of Graduate School
The University of Georgia
December 2023

DEDICATION

I dedicate this dissertation to a collective of people that are of great importance to me. First and foremost, I dedicate this dissertation to my late grandparents, Sandra Eleanor (1940-2022) and William Henry “Bill” (1938-2020) Oakley and John Knox Williams (1929-2022), who passed away during my Ph.D. Secondly, I dedicate this dissertation to my parents, Elizabeth Anne and Roger Dale Oakley, for their undying love for me and unwavering support of my academic career. Thirdly, I dedicate this dissertation to my best friends - Naish Lalloo, Robbie Mohney, Drew Hanford, Donald Gillis, and Kenton Hipsher - for being a much-needed distraction from work and always a source of encouragement. Fourth, I dedicate this dissertation to a special friend, Clara Grace Antoinette Coker, for her emotional support and guidance in all things from cooking to relationships. Lastly, I dedicate this dissertation to my professors, Drs. Scott E. Gold and Anthony E. Glenn, for being something more than academic advisors and extending support beyond research advice. Without these people, this dissertation would have never been written. For this reason, I can never give enough thanks to them for my intellectual, emotional, and spiritual growth over the past six years.

ACKNOWLEDGEMENTS

I acknowledge everyone that has assisted me in my personal and professional life from 2017-2023. I acknowledge my academic advisors and committee members including Dr. Anthony E. Glenn, Dr. Scott E. Gold, Dr. Marin T. Brewer, Dr. Shavannor M. Smith, and Dr. Harald Scherm. I acknowledge all past and present members of the Toxicology and Mycotoxin Research Unit (TMRU) at the USDA-ARS for their friendship and sound advice on experimental design, methods questions, data analysis and a lot more. Members include Nicole Crenshaw, Britton Glenn, Garrett Hibbs, Dr. Minglu "Hugo" Gao, Dr. Alex Blacutt, Dr. Shan Gao, Trevor Mitchell, Lily Lofton, Tam Stackhouse, Dr. Anthony Pokoo-Aikins, Dr. Thomas Baldwin, Larry Pierce, Callie McDonough, Dr. Revathi Shanmugasundaram, Shawn Cunningham, Kitisha Stimage, Britton Glenn, Drew Olson, Christine Miller, Jaci Hawkins, Dr. Kayla Pennerman, and Dr. Tim Satterlee, as well as many undergraduate researchers. I acknowledge all our collaborators who provided expertise, fungal and bacterial strains, plasmids, etc. including Dr. David Baltrus, Dr. Brian H. Kvitko, Dr. James Buck, Dr. Michelle Momany, Dr. Marin T. Brewer, Dr. Wei Shi, Dr. Paul Severns, Dr. Wayne A. Parrott, and Dr. Zachary Lewis. I acknowledge other graduate students and professors within the Plant Center, Department of Plant Pathology, Fungal Group, Mycology Graduate Student Organization, and Society of Aspiring Plant Pathologists (SAPPs) for their encouragement and feedback during my graduate career. I also acknowledge funding sources for research and travel including the University of Georgia Graduate School, SAPPs, Mycological Society of America (MSA), Genetics Society of America (GSA), and American Phytopathological Society (APS). If I have forgotten to acknowledge anyone who has helped me in my process, please recognize that your efforts were appreciated.

TABLE OF CONTENTS

Page

CHAPTER 1

INTRODUCTION AND LITERATURE REVIEW

Justification

Climate change results in droughts, tornadoes, ice melting, sea-level rise, saltwater intrusion, evaporation, shifts in flower/plant blooming times, and other planetary events, all of which are a consequence of the anthropogenic greenhouse effect and associated global warming. The National Aeronautics and Space Administration (NASA) and other scientific institutions have shown evidence that the global temperature has risen substantially since the early 20th century and has accelerated since the late 1970s.

Deforestation, land use, rice paddies, and livestock escalate the greenhouse effect partially through the release of greenhouse gases (GHGs), which are gas molecules that absorb thermal infrared radiation and prevent it from escaping into outer space. Examples include, water vapor, sulfur dioxide (SO_2), ozone (O_3), chlorofluorocarbons (CFCs), perfluorinated carbons (PFCs), halogenated fluorocarbons (HCFCs), hydrofluorocarbons (HFCs), methane (CH_4), carbon dioxide (CO_2), and nitrous oxide (N_2O). The latter, which is closely associated with agriculture, has a heat-trapping capacity 300-fold stronger than CO_2 (per molecule), and can destroy the stratospheric ozone layer (Gadani and Vyas, 2011; Snyder et al., 2009; Ravishankara et al., 2009; Pachauri et al., 2014; Sherman et al., 2012). The Intergovernmental Panel on Climate Change (IPCC) reports that approximately half of the cumulative GHG emissions between 1750 and 2011 have occurred in the last 40 years, and emissions have grown at a rate of 2.2% per year since 2000 (Edmonds et al., 2017). Scientists agree almost universally that as

global warming intensifies, climatic shifts and fluctuations will become more severe and they will affect the ability of agriculture to meet global food demands (Takle et al., 2013).

Plant protection plays a crucial role in being able to meet the global demand for food. Climatic variability has led to an increase in abiotic and biotic stressors that contribute to increases in plant disease due to changing environmental conditions that are conducive to plant pathogen development. These stressors exacerbate issues associated with plant health and food security (Juroszek and von Tiedemann, 2013). Direct yield losses due to plant pathogens, pests, and weeds account for a 20 to 40% loss in global agricultural productivity (Teng and Krupa, 1980; Teng, 1987; Oerke et al., 1994; Oerke, 2006; Oerke and Dehne, 1997; Oerke and Dehne, 2004). Additionally, plants infected by mycotoxigenic pathogens may harbor harmful secondary metabolites involved in various animal and human mycotoxicoses (Bennett and Klich, 2003).

As the world's population is expected to grow to almost 10 billion by 2050, agricultural demand will concurrently increase by approximately 50% (FAO, 2017). Unfortunately, greater agricultural inputs to achieve higher agricultural outputs (i.e., intensification) may contribute to increases in greenhouse gases, global warming, and climate change. The N cycle, specifically, has been profoundly disrupted by human activities. The Haber-Bosch process of industrial nitrogen fixation, the fixation of N_2 by cultivated legumes, and the burning of fossil fuels result in more fixed N per year than all natural processes combined (Fowler et al., 2013). Humankind has more than doubled the amount of inorganic and organic N applied to land areas since pre-industrial times to sustain food production in parallel with the growing population. High inputs of N in intensively managed agricultural systems may optimize plant yields, but can be costly and soluble N compounds can be lost to the environment. These N losses have resulted in

environmental problems such as eutrophication of fresh and marine waters and contamination of drinking water (Vitousek et al., 1997; Smith et al., 1999).

Denitrification plays direct and indirect roles in energy management, land usage management, plant disease management, food management, and climate change. Denitrification occurs in various ecosystems and is a complex, multi-factorial process involved in the global cycling of nitrogen, GHG emissions, fertilizer usage, soil dynamics, microbial diversity, and much more. Most importantly, denitrification affects agricultural ecosystems by reducing plant available nitrogen. I venture to study denitrification in fungi at a genomic scale to inform new strategies for inhibiting denitrification and the detrimental effects it has on crop production and on environmental and climate health.

Nitrogen cycle

The nitrogen cycle is the series of processes by which nitrogen and its compounds are converted in the environment and in living organisms. Biogeochemically, the nitrogen cycle is a network of reduction-oxidation (i.e., redox) reactions catalyzed by plants, fungi, bacteria, and archaea that cycle N through various ecosystems. Processes include nitrogen fixation, decomposition, ammonification, nitrification, denitrification, and assimilation. These processes modulate the oxidation state of N between fully reduced amines (e.g., ammonium) and fully oxidized nitrate (Coskun et al., 2017).

The largest pool of N in the biosphere is atmospheric di-nitrogen gas (N_2). Unfortunately, it is not directly available to most biological organisms. N enters the living world via biological or geochemical means (Coskun et al., 2017). N_2 is fixed by lightning or nitrogen-fixing bacteria and archaea (e.g., diazotrophic prokaryotes) that may be free-living or involved in symbiotic associations (Vitousek et al., 2013). N fixed by nitrogen-fixing bacteria/archaea in legume root

nodules is assimilated by the plant directly. Nitrogen-fixing microbes in the soil produce ammonium (NH_4^+) through ammonification. Ammonium is also produced by decomposition of biological organisms by aerobic and anaerobic microbes. At this stage, NH_4^+ may be absorbed through root uptake, participate in mineralization, or be immobilized and incorporated into amino acids and organic compounds (Hoffman et al., 2014; Krapp, 2015). NH_4^+ can also be oxidized by soil microbes to produce hydroxylamine (NH_2OH), nitrite (NO_2^-), and nitrate (NO_3^-) or transformed into hydrazine (N_2H_4) and N_2.

Nitrification is performed by a suite of microorganisms, including ammonia-oxidizing bacteria and archaea (AOB and AOA), nitrite-oxidizing bacteria (NOB), and comammox (complete ammonia oxidizers), which perform both oxidative steps in a single bacterium (Prosser and Nicol, 2012; Daims et al., 2015; van Kessel et al., 2015; Hayatsu et al., 2008). NO_3^- may be assimilated into plants or undergo denitrification by denitrifying microbes (e.g., bacteria, archaea, and fungi). Denitrification is the reverse reaction of nitrification. Denitrification reduces NO_3^- to NO_2^- to nitric oxide (NO) to N_2O and finally to N_2 to complete the biogeochemical cycle. Lesser known N cycle processes include dissimilatory nitrate reduction to ammonia (DNRA), anaerobic ammonium oxidation (anammox), and codenitrification. DNRA is the reduction of NO_3^- to NH_3 via NO_2^- by bacteria and fungi under anaerobic or low-oxygen conditions (Rutting et al., 2011). Anammox is the formation of N_2 from NO_2^- and NH_3 by bacteria via NO and hydrazine (N_2H_4) (Kartal et al., 2011; van Niftrik et al., 2012). Codenitrification is a hybrid reaction where one N atom originates from organic N and the other is from N_2O produced by denitrification (Muller et al., 2014). Denitrifying fungi, nitrifying archaea, anammox bacteria, aerobic denitrifying bacteria and heterotrophic nitrifying microorganisms are key players in the nitrogen cycle and N_2O production (Hayatsu et al., 2008). For instance, these different types of microbes play a major role

in three of the four main pathways for N_2O production in soil: 1) reduction of NO_2^- associated with nitrification, 2) reduction of NO_2^- associated with denitrification, 3) reduction of NO_2^- associated with organic N oxidation, and 4) codenitrification (Muller et al., 2014; Zhu et al., 2013).

At the molecular level, biological N-fixation occurs via a nitrogenase (NIF). Mineralization, immobilization, and root uptake of NH_3/NH_4^+ are moderated by non-denitrification-related enzymes (Coskun et al., 2017; Canfield et al., 2010). During anammox, NH_3/NH_4^+ is converted to N_2H_4 via hydrazine hydrolase (HH) and from N_2H_4 to N_2 via hydroxylamine oxidoreductase (HAO). During nitrification, conversion of NH_4^+ to NH_2OH occurs via an ammonium monooxygenase (AMO); NH_2OH to NO_2^- via a HAO; and NO_2^- to NO_3^- via a nitrite oxidoreductase (NXR). NO_3^- is reduced to NO_2^- by various nitrate reductases (NAS, NAR, NAP, EUK-NR). Denitrification/anammox and DNRA convert NO_2^- to either NO or NH_3 by dissimilatory nitrite reductase (NIR) or assimilatory nitrite reductase (NRF), respectively. In the denitrification pathway, NO is reduced to N_2O by a nitric oxide reductase (NOR) and N_2O is reduced to N_2 by a nitrous oxide reductase (NOS). In the anammox pathway, NO is shunted for formation of N_2H_4 by a HH (Coskun et al., 2017; Canfield et al., 2010).

This network of multi-functional enzymes and complex biological and geochemical processes is the driving force balancing immobile and mobile N in the environment. This natural equilibrium is maintained through biotic and abiotic processes that affect influx and efflux of N (Phillips et al., 2016). For example, denitrification and anammox may be a source of N_2O emissions when NO_3^- concentrations are elevated (non-limited), whereas, DNRA may remove N_2O (i.e., function as a N_2O sink) when NO_3^- levels are low (Zaman et al., 2008; Oertel et al., 2016; Hardison et al., 2015). Inorganic N entering soil via N-fixation, fertilization and deposition can have many fates, depending on the soil environment and the microbial community. This inter-

relationship between the global N cycle, the soil environment, and microbial diversity has been studied in many unique ecosystems, including temperate forest, tropical forest, arable, grassland, pasture, wetland, salt marsh, riparian, aquatic and agro-ecosystems (Regan et al., 2017; Pajares and Bohannan, 2016; Muller et al., 2014; Ettema et al., 1999; Salles et al., 2017; Schipper et al., 1993; Nguyen et al., 2017; Zaman et al., 2008; Maeda et al., 2015; Benckiser et al., 2015; Seitzinger et al., 2006).

Human disturbance of these ecosystems has caused detrimental impacts on community structure and characteristic diversity of microbes. Furthermore, more frequent extreme heat conditions, forecasted in the context of climate change, may significantly affect microbial communities that are important for N cycling and N_2O emissions. Data suggest that different microbial communities will respond differently to extreme heat conditions, and the type of N source applied will also have an interactive effect with temperature on microbial growth and N_2O emissions (Xu et al., 2016; Xu et al., 2017). Currently, nitrification and denitrification are the two most important microbial processes that contribute to GHGs and inefficient use of fertilizer N in agricultural environments. Although, research shows that effects of chronic N influx mostly negatively affect microbial biomass and activity, which could threaten the seemingly indefinite N-removal potential of denitrifiers in N-loaded systems (Ettema et al., 1999). Anthropogenic interference in the global N cycle has resulted in a severe imbalance of N that could have serious long-term consequences for our climate and Earth's biota.

Denitrification

Denitrification is a microbial-mediated process of stepwise reductions from NO_3^- to N_2, which includes four consecutive reductive reactions: NO_3^- -> NO_2^- -> NO -> N_2O -> N_2 (Knowles, 1982; Zumft, 1997). These sequential reductions are often coupled with energy-

capturing and energy-harvesting processes in heterotrophic microbes during anaerobic respiration, in which the nitrogen oxides are terminal electron acceptors. Shoun and Tanimoto (1991) showed dissimilatory reduction of NO_3^- to NO_2^- is an energetically favorable process (i.e., energy-capturing), whereas reduction of NO_2^- to N_2O might be energy-exhausting (i.e., energy-harvesting). Denitrification is phenotypically typified by N_2O production. However, reduction of nitrite to nitric oxide is widely considered to be the key step in the denitrification process because it maintains the balance between organic and inorganic nitrogen. Spatially distributed global models of denitrification suggest that continental shelf sediments account for the largest portion (44%) of total global denitrification, followed by terrestrial soils (22%) and oceanic oxygen minimum zones (14%). Freshwater systems (groundwater, lakes, rivers) account for about 20% and estuaries 1% of total global denitrification (Seitzinger et al., 2006). As agricultural production escalates, terrestrial soils may account for larger portions of the total global denitrification. Previous research shows that denitrification is the predominant source of soil-derived N_2O (Opdyke et al., 2009). Thus, N_2O emissions will increase concomitantly with agricultural outputs.

Early work in denitrification has focused mainly on eubacteria. Over 60 genera of bacteria from vastly different taxonomic and metabolic groups have been found to be capable of denitrification. Denitrification has also been shown in archaeal species (e.g., *Halobacterium denitrificans*) (Knowles, 1982; Zumft, 1997; Philippot et al., 2007). Bacterial denitrification was thought to work exclusively under anoxic conditions, but a wide variety of bacteria have been found to be able to carry out aerobic denitrification. Bacterial denitrifiers and fungal denitrifiers serve different roles in the denitrification process and these roles are defined by their molecular machinery. Most importantly, bacteria possess the gene encoding N_2O reductase (*nosZ*). The

fungal denitrification pathway is most often truncated meaning that fungi do not possess a homolog of *nosZ* and, thus, cannot generally reduce N_2O to N_2. This is concerning considering the only known biological sink for N_2O is its reduction to N_2 by microbes that possess the gene conferring this trait (Mothapo et al., 2015). Additionally, dissimilatory nitrate reductase (dNar) is common in bacteria and uncommon in fungi. There are only a few fungi that can reduce NO_3^- to NO_2^- via denitrification and examples include *Fusarium oxysporum* and *Fusarium fujikuroi* (Fuji and Takaya, 2008; Kobayashi et al., 1996). The majority of fungal denitrification begins with NO_2^- reduction versus bacterial denitrification that begins with NO_3^- reduction (Shoun and Tanimoto, 1991; Takaya, 2002; Zhou et al., 2010). Bacteria share a common ancestry with fungi for dissimilatory nitrite reductase (dNir) (Kim et al., 2009; Shoun et al., 2012). This may indicate that dNir and the ability to reduce NO_2^- to NO is conserved among prokaryotic and eukaryotic denitrifiers. However, bacteria and fungi are distinguished by the type of nitric oxide reductase (NOR) that they use to reduce NO. The involvement of cytochrome p450nor as a NOR is a unique feature of fungal denitrification, as opposed to cytochrome bc-type nitric oxide reductase, which is unique to bacterial denitrification (Takaya, 2009). Fungal NOR is a heme-cytochrome P450, which belongs to a family of structurally diverse and functionally versatile enzymes of the cytochrome P450 gene superfamily (Shoun and Tanimoto, 1991). These key differences between bacterial and fungal denitrification have been shown to help predict N_2O:N_2 ratios and downstream effects of denitrification based on surveys of microbial communities and ecosystem-specific abiotic factors. Fungi do not possess a homolog of the gene encoding NOS. For this reason, there has been growing interest in fungal denitrification because the end-product, N_2O, is a potent GHG and an ozone-depleting substance.

Fungi generally dominate microbial biomass in soils and play vital roles in ecosystem function, including nutrient cycling. Some fungi can grow under various O_2 conditions by using three types of energy-yielding metabolism, one of which is denitrification. The occurrence of denitrification was previously thought to be restricted to prokaryotes. Shoun and Tanimoto (1991) were the first to demonstrate that eukaryotes exhibit a marked denitrifying ability. Anaerobic evolution of N_2O from NO_3^- or NO_2^- was first shown in *F. oxysporum* (Shoun and Tanimoto, 1991), but dozens of studies have revealed a major contribution by fungi in the production of N_2O across a myriad of ecosystems. A foundational study by Maeda et al. (2015) tested 207 fungal isolates for their N_2O-producing ability. Seventy strains producing N_2O in pure culture were identified and were mostly species from the order *Hypocreales* – particularly *F. oxysporum* and *Trichoderma* spp. – and to a lesser extent species from the orders *Eurotiales*, *Sordariales,* and *Chaetosphaeriales* (Maeda et al., 2015). These results are consistent with parallel studies of N_2O-producing ability in fungal isolates from environmental and laboratory samples (Jirout et al., 2013; Wei et al., 2015; Mothapo et al., 2013). Further research showed a higher diversity of fungal denitrifiers in compost and agricultural soils (Novinscak et al., 2016) relative to other types of soils. Coincidentally, agricultural fields are one of the largest anthropogenic sources of atmospheric N_2O and fungi contribute substantially to these N_2O emissions in terrestrial environments (Wei et al., 2014).

Filamentous fungi usually inhabit normoxic environments by utilizing O_2 as a substrate for respiration and for the biosynthesis of some essential cellular components (e.g., sterols, fatty acids, heme). However, terrestrial soils are often prone to transient periods of hypoxia. The denitrification pathway can be used situationally by fungi as a metabolic and respiratory mechanism under hypoxic conditions. Zhou et al. (2001) determined that fungal denitrifying

activity requires a minimal amount of O_2 for induction, which is repressed by excess O_2. The optimal O_2 supply differs between denitrification substrates: 690 μmol O_2/h (g dry cell wt.)$^{-1}$ for NO_3^- and about 250 μmol O_2/h (g dry cell wt.)$^{-1}$ for NO_2^-. Takaya et al. (2003) validated the claim that induction of the mitochondrial NO_3^- respiration (denitrification) system in *F. oxysporum* requires the supply of low levels of O_2. They also found that O_2 and NO_3^- respiration function simultaneously in the mitochondria of fungal cells incubated under hypoxic, denitrifying conditions. Under these conditions, O_2 and NO_3^- both act as terminal electron acceptors and nitrate and nitrite reductases involved in fungal denitrification share the mitochondrial respiratory chain with cytochrome oxidase (Takaya et al., 2003). Hypoxia tolerance and hypoxia sensing allow fungi to rapidly adapt to O_2 stress in various macro- and microenvironments.

Environmental adaptability to hypoxia in fungi is driven by denitrification enzymes and influenced by O_2 levels. In aerobic environments, N_2O is produced at low levels. Although, N_2O production in fungi is highest when fungi are exposed to short anoxic spells or transient periods of hypoxia. Microbial environments, such as the soil and plant vasculature have the potential to become normoxic, anoxic, and hypoxic environments. For example, transient flooding during rainfall could lead to increases in N_2O release when water levels have dropped (Richardson et al., 2009). It has been experimentally shown, using a compact fluorescence ratiometric-based device, that the rhizosphere, developing seed, and plant vasculature experience spatial patterns of oxygen production and consumption (Tschiersch et al., 2012). Thus, both the soil and plant vasculature are major sinks for O_2 and can be hypoxic environments where fungal denitrification can occur.

Strategies for Mitigation and Inhibition of Denitrification

Denitrification is a necessary nutrient cycling process, but it is implicated in GHG emissions, ozone degradation, and N fertilizer losses. The ability to denitrify is phylogenetically diverse and, thus, it is unlikely that farming practices will ever be able to eliminate denitrifier-N_2O emissions from agriculture or prevent N loss. Even if complete prevention of N_2O emissions and N loss was a reality, it would not be desirable from a climate point of view (Benckiser et al., 2015). Thus, there is a concerted effort to inhibit microbial denitrifiers and mitigate the effects of denitrification through translational knowledge about modern agricultural practices, enzymology of denitrification, and abiotic effects on N_2O production.

Mitigation strategies may include agricultural practices, such as crop spacing, tillage, integrated inorganic fertilizer, residue and soil organic matter (SOM) management, or utilization of alternative N inputs associated with positive plant microbial interactions, such as N_2 fixing rhizobia or arbuscular endo-mycorrhizal fungi (Richardson et al., 2009; Andrews et al., 2011; Bender et al., 2014). Other potential strategies are: (1) to manipulate denitrification through inputs into the plant rhizosphere to change the composition of plant-derived carbon flow or nitrogen uptake demand, (2) to manipulate soil nitrogen concentrations and soil denitrification potential by breeding plant-release of biological nitrification and denitrification inhibitors, (3) to reduce application of high levels of NO_3^- fertilizer that stimulate rapid bacterial growth and lower copper availability, (4) to lime soils or add urine to increase activity of N_2O reductase, (5) to reduce sequestration and increase bioavailability of free copper ions in specific soil types, and (6) to optimize organic matter, pH, and/or N management practices for increase of N_2O reduction to N_2 in bacteria (Richardson et al., 2009; McMillan et al., 2016). It is important to remember that nitrification and denitrification end-products and by-products can be significantly modulated by

soil type, temperature, pH (McMillan et al., 2016), mineralogy, and organic carbon content (Singh et al., 2008).

Synthetic and non-synthetic chemicals are a popular and sometimes effective approach to inhibition of the denitrification pathway. Nitrification inhibitors include nitropyrin and dicyandiamide, synthetic compounds that affect the AMO enzymatic pathway in ammonia-oxidizing bacteria and reduce NO_3^- leaching and N_2O emissions (Singh et al., 2008; Andrews et al., 2011; Wu et al., 2017). Denitrification inhibitors include rotenone, antimycin A, and thenoyltrifluoroacetone, which affect nitrate and nitrite reductase activity (Kobayashi et al., 1996). Recently, pyrimidone- and triazinone-based compounds have been found to inhibit copper nitrite reductase (NirK) in *F. oxysporum* in the low micromolar range (Matsuoka et al., 2017). Hierarchical *in silico* screening approaches combined with pharmacophore modeling and molecular docking show promise for discovery of new bacterial and fungal nitrification and denitrification inhibitors (Matsuoka et al., 2017).

Direct and indirect inhibition of denitrification can also occur through biological denitrification inhibition (BDI) and biological nitrification inhibition (BNI), respectively. Exploitation of BNI and BDI may be a solution for development of low-nitrifying/denitrifying agronomic systems and improvement of plant N-nutrition. Sorgoleone and brachialactone are plant root exudates with BNI activity (Tesfamariam et al., 2014; Subbarao et al., 2009). Brachialactone appears to block both the AMO and hydroxylamine oxidoreductase enzymatic pathways in *Nitrosomonas* (Subbarao et al., 2009). Proanthocyanidins are secondary metabolites from *Fallopia* spp. that exhibit BDI activity (Bardon et al., 2014; Bardon et al., 2015). These proanthocyanidins can specifically inhibit membrane-bound NO_3-reductase by inducing enzymatic conformational changes through membrane disturbance (Bardon et al., 2016). This results in modification of root

N content and modification of root traits associated with nutrient acquisition capacity in *Fallopia* spp. (Bardon et al., 2017). However, fungal denitrifiers that lack a homolog of dNar (e.g., *Cylindrocarpon tonkinense*) may be unaffected by proanthocyanidins. A more advanced understanding of the processes associated with N_2O production and N metabolism offer management possibilities to lower net emissions.

Fusarium

Fusarium is a large genus of filamentous ascomycetous fungi within the Order Hypocreales and Family Nectriaceae (Nelson, 1992). Over 1,000 species have been identified as belonging to the genus *Fusarium.* Many *Fusarium* spp. are globally distributed in soil and are harmless saprophytes that constitute large portions of the soil microbial community. However, some species are facultative necrotrophic plant pathogens (Kistler, 1997; Roncero et al., 2003) and/or opportunistic animal and human pathogens (Boutati and Anaissie, 1997; Nucci and Anaissie, 2007). Molecular phylogenetic studies of the *Fusarium* genus indicate high molecular and functional diversity and interesting evolutionary relationships among genes and species (Watanbe et al., 2011; Summerell et al., 2010). Such diversity may be why *Fusarium* spp. are associated with hundreds of different plant hosts and are widely distributed in soil, water, aerial plant parts, plant residue, and other organic substrates (Nelson et al., 1994; Elvers et al., 1998).

Fusarium verticillioides (syn. *Fusarium moniliforme*, *Gibberella moniliformis*) is a soilborne mycotoxigenic fungus and a significant pathogen of maize that is of major global economic importance. Maize, or *Zea mays*, is a staple food crop globally and used in animal feed and industrial products. Rice, wheat, and maize provide at least 30% of the food calories to more than 4.5 billion people in 94 developing countries. In parts of Africa and Mesomaerica, maize alone contributes over 20% of food calories (Shiferaw et al., 2011). *Fusarium verticillioides* is a

perfect model system to study denitrification because it is a denitrifier that contains a single copy of each of the three denitrification genes (dNar, dNir, p450nor) required to reduce NO_3^- to N_2O. Additionally, it is ubiquitous in the soil of agricultural and terrestrial environments, it is a fungal endophyte, and a pathogenic agent of stalk rot and ear rot of maize. *F. verticillioides* occupies both soil and plant host environments, which are prone to temporary periods of hypoxia. It is likely that *F. verticillioides* induces genes thought to be involved in the denitrification pathway in other fungal systems to physiologically tolerate low-oxygen stress until oxygen levels return to normal (Takaya and Shoun, 2000; Zhou et al., 2001; Shoun et al., 2012; Fuji and Takaya, 2008; Kobayashi et al., 1996; Maeda et al., 2015). Many fungi within the order Hypocreales and within the genus *Fusarium* can reduce NO_3^- and NO_2^- anaerobically to form NO and N_2O (Mothapo et al., 2013; Jirout et al., 2013; Wei et al., 2015; Mothapo et al., 2015; Shoun et al., 1992). However, genes associated with the denitrification pathway have not been systematically and functionally characterized in any fungal species. Thus, eukaryotic denitrification is still not adequately understood.

Objectives

This research investigates the response of *F. verticillioides* to exposure of denitrification-inducing conditions and characterizes the biological effect of the loss of the genes involved in denitrification. To better grasp the breadth of denitrification in fungi and define the functional roles of fungal denitrification-associated genes, three objectives have been established:

1. Characterize the phylogenetic distribution of *F. verticillioides* denitrification-associated genes
2. Evaluate relationships between fungal denitrification, virulence *in planta,* and fumonisin production in *F. verticillioides*

3. Identify and characterize enzymes in fungal denitrifiers that can be targeted for reduction of N_2O emissions

Fungal denitrification is an understudied topic of research and the functionality of genes within this pathway and their effects on fungal biology are unclear. The purpose of my research is to thoroughly understand denitrification in fungi using phylogenetic, bioinformatic, and genomic approaches using *F. verticillioides* as a study system. In **Chapter 2**, *F. verticillioides* was exposed to diethylenetriamine (DETA) NONOate, a nitric oxide donor, or low levels of oxygen (i.e., hypoxia) and gene expression was characterized using RNA-seq. These two treatments were appropriate for inducing denitrification in *F. verticillioides* because fungal denitrification is repressed under normoxic conditions and fungal denitrifiers must have mechanisms to cope with endogenous NO produced via nitrate respiration as well as exogenous NO released by plants or competing microbes. Based on the data collected from the RNA-seq analysis, sixteen genes were identified that were up-regulated more than 8-fold in response to one or both treatments, three of which were the genes that encode the reductase enzymes that evolve NO_3^- to N_2O via denitrification. I explored my first objective by determining the evolutionary relationships and relative rarity of genes presumed to be associated with denitrification in fungi.

Some of the most notorious and economically important pathogens are fungi, but there is no literature about whether denitrification is tied to fungal pathogenicity. I hypothesize that the ability to denitrify in *F. verticillioides*, and other pathogenic fungal denitrifiers, may confer fitness advantages that enable them to infect their hosts successfully. To test this hypothesis, single-gene deletion mutants of key denitrification genes in *F. verticillioides* were created by Garrett Hibbs and RNA-seq data was mined to see if denitrification-associated genes are

differentially expressed *in planta* as we observed *in vitro*. In **Chapter 3**, mutants are used to examine the effects of gene deletion on fumonisin production and virulence to address the second objective.

Intensive application of N to agricultural systems results in notable N losses and increased emissions of N_2O due to denitrification, but there are no commercially available inhibitors to effectively reduce fungal N_2O production and/or loss of plant-available N. Identification and characterization of fungal enzymes that are essential to N_2O production will inform future development of compounds or technologies that inhibit fungal denitrification. To fulfill my third objective, a novel method to assess N_2O production using gas chromatography-electron capture detection was devised. Preliminary data suggested that deletion of *F. verticillioides* NOR1 had the greatest impact on N_2O emissions in culture media compared with NAR1 or DNI1. In **Chapter 4**, N_2O production in Δ*nor1* deletion mutants was investigated. Phylogenetics and motif analysis were also used to evaluate the sequence conservation of NOR1. From this data, the value of NOR1 as an enzymatic target for reduction of agricultural N_2O emissions was determined. As far as we know, this is the first study that functionally characterized genes directly, or indirectly, involved in fungal denitrification through systematic deletion and monitoring of phenotypic effects.

Literature Cited

Andrews, M., Edwards, G. R., Ridgway, H. J., Cameron, K. C., Di, H. J., & Raven, J. A. (2011). Positive plant microbial interactions in perennial ryegrass dairy pasture systems. Annals of Applied Biology, 159, 79-92.

Bardon, C., Piola, F., Bellvert, F., el Zahar Haichar, F., Comte, G., Meiffren, G., Pommier, T., Puijalon, S., Tsafack, N., & Poly, F. (2014). Evidence for biological denitrification inhibition (BDI) by plant secondary metabolites. New Phytologist, 204, 620-630.

Bardon, C., Piola, F., el Zahar Haichar, F., Meiffren, G., Comte, G., Missery, B., Balby, M., & Poly, F. (2015). Identification of B-type procyanidins in *Fallopia* spp. involved in biological denitrification inhibition. Environmental Microbiology, 18, 644-655.

Bardon, C., Poly, F., Piola, F., Pancton, M., Comte, G., Meiffren, G., & el Zahar Haichar, F. (2016). Mechanism of biological denitrification inhibition: procyanidins induce an allosteric transition of the membrane-bound nitrate reductase through membrane alteration. FEMS Microbiology Ecology, 92, 1-11.

Bardon, C., Poly, F., el Zahar Haichar, F., Le Roux, X., Simon, L., Meiffren, G., Comte, G., Rouifed, S., & Piola, F. (2017). Biological denitrification inhibition (BDI) with procyanidins induces modification of root traits, growth and N status in *Fallopia x bohemica*. Soil Biology & Biochemistry, 107, 41-49.

Benckiser, G., Schartel, T., & Weiske, A. (2015). Control of NO_3^- and N_2O emissions in agroecosystems: A review. Agronomy for Sustainable Development, 35, 1059-1074.

Bender, S. F., Plantenga, F., Neftel, A., Jocher, M., Oberholzer, H.-R., Kohl, L., Giles, M., Daniell, T. J., & van der Heijden, M. G. A. (2014). Symbiotic relationships between soil fungi and plants reduce N_2O emissions from soil. The ISME Journal, 8, 1336-1345.

Bennett, J. W. & Klich, M. (2003). Mycotoxins. Clinical Microbiology Reviews, 16, 497-516.

Blacutt, A. A., Gold, S. E., Voss, K. A., Gao, M., & Glenn, A. E. (2018). *Fusarium verticillioides*: Advancements in understanding the toxicity, virulence, and niche adaptations of a model mycotoxigenic pathogen of maize. Phytopathology, 108, 312-326.

Boutati, E. I. & Anaissie, E. J. (1997). *Fusarium*, a significant emerging pathogen in patients with hematologic malignancy: Ten years' experience at a cancer center and implications for management. Blood, 90, 999-1008.

Canfield, D. E., Glazer, A. N., & Falkowski, P. G. (2010). The evolution and future of Earth's nitrogen cycle. Science, 330, 192-196.

Coskun, D., Britto, D. T., Shi, W., & Kronzucker, H. J. (2017). How plant root exudates shape the nitrogen cycle. Trends in Plant Science, 22, 661-673.

Daims, H., Lebedeva, E. V., Pjevac, P., Han, P., Herbold, C., Albertsen, M., Jehmlich, N., Palatinszky, M., Vierheilig, J., Bulaev, A., Kirkegaard, R. H., von Bergen, M., Rattei, T., Bendinger, B., Nielsen, P. H., & Wagner, M. (2015). Complete nitrification by *Nitrospira* bacteria. Nature, 528, 504-509.

Edmonds, H. K., Lovell, J. E., & Knox Lovell, C. A. (2017). A new composite index for greenhouse gases: Climate science meets social science. Resources, 6, 1-16.

Elvers, K. T., Leeming, K., Moore, C. P., & Lappin-Scott, H. M. (1998). Bacterial-fungal biofilms in flowing water photo-processing tanks. Journal of Applied Microbiology, 84, 607-618.

Ettema, C. H., Lowrance, R., & Coleman, D. C. (1999). Riparian soil response to surface nitrogen input: temporal changes in denitrification, labile and microbial C and N pools, and bacterial and fungal respiration. Soil Biology & Biochemistry, 31, 1609-1624.

FAO. (2017). The future of food and agriculture – Trends and challenges. http://www.fao.org/3/a-i6583e.pdf. Accessed 22 November 2018.

Fowler, D., Coyle, M., Skiba, U., Sutton, M. A., Cape, J. N., Reis, S., Sheppard, L. J., Jenkins, A., Grizzetti, B., Galloway, J. N., Vitousek, P., Leach, A., Bouwman, A. F., Butterbach-Bahl, K., Dentener, F., Stevenson, D., Amann, M., & Voss, M. (2013). The global nitrogen cycle in the twenty-first century. Philosophical Transactions of The Royal Society B, 368, 1-13.

Fuji, T. & Takaya, N. (2008). Denitrification by the fungus *Fusarium oxysporum* involves NADH-nitrate reductase. Bioscience, Biotechnology, and Biochemistry, 72, 412-420.

Gadani, H. & Vyas, A. (2011). Anesthetic gases and global warming: Potentials, prevention and future of anesthesia. Anesthesia: Essays and Researches, 5, 5-10.

Hardison, A. K., Algar, C. K., Giblin, A. E., & Rich, J. J. (2015). Influence of organic carbon and nitrate loading on partitioning between dissimilatory nitrate reduction to ammonium (DNRA) and N_2 production. Geochimica et Cosmochimica Acta, 164, 146-160.

Hayatsu, M., Tago, K., & Saito, M. (2008). Various players in the nitrogen cycle: Diversity and functions of the microorganisms involved in nitrification and denitrification. Soil Science and Plant Nutrition, 54, 33-45.

Hoffman, B. M., Lukoyanov, D., Yang, Z-Y., Dean, D. R., & Seefeldt, L. C. (2014). Mechanism of nitrogen fixation by nitrogenase: The next stage. Chemical Reviews, 114, 4041-4062.

IPCC, 2014: Climate Change 2014: Synthesis Report. Contribution of Working Groups I, II and III to the Fifth Assessment Report of the Intergovernmental Panel on Climate Change [Core Writing Team, R.K. Pachauri and L.A. Meyer (eds.)]. IPCC, Geneva, Switzerland, 151 pp.

Jirout, J., Simek, M., & Elhottova, D. (2013). Fungal contribution to nitrous oxide emissions from cattle impacted soils. Chemosphere, 90, 565-572.

Juroszek, P. & von Tiedemann, A. (2013). Plant pathogens, insect pests and weeds in a changing global climate: a review of approaches, challenges, research gaps, key studies and concepts. Journal of Agricultural Science, 151, 163-188.

Kartal, B., Maalcke, W. J., de Almeida, N. M., Cirpus, I., Gloerich, J., Geerts, W., Op den Camp, H. J. M., Harhangi, H. R., Janssen-Megens, E. M., Francoijs, K-J., Stunnenberg, H. G., Keltjens, J. T., Jetten, M. S. M., & Strous, M. (2011). Molecular mechanisms of anaerobic ammonium oxidation. Nature, 479, 127-130.

Kim, S-W., Fushinobu, S., Zhou, S., Wakagi, T., & Shoun, H. (2009). Eukaryotic *nirK* genes encoding copper-containing nitrite reductase: Originating from the protomitochondrion? Applied and Environmental Microbiology, 75, 2652-2658.

Kistler, H. C. (1997). Genetic diversity in the plant-pathogenic fungus *Fusarium oxysporum*. Phytopathology, 87, 474-479.

Knowles, R. (1982). Denitrification. Microbiological Reviews, 46, 43-70.

Kobayashi, M., Matsuo, Y., Takimoto, A., Suzuki, S., Maruo, F., & Shoun, H. (1996). Denitrification, a novel type of respiratory metabolism in fungal mitochondrion. The Journal of Biological Chemistry, 271, 16263-16267.

Krapp, A. (2015). Plant nitrogen assimilation and its regulation: a complex puzzle with missing pieces. Current Opinion in Plant Biology, 25, 115-122.

Maeda, K., Spor, A., Edel-Hermann, V., Heraud, C., Breuil, M.-C., Bizouard, F., Toyoda, S., Yoshida, N., Steinberg, C., & Philippot, L. (2015). N_2O production, a widespread trait in fungi. Scientific Reports, 5, 1-7.

Matsuoka, M., Kumar, A., Muddassar, M., Matsuyama, A., Yoshida, M., & Zhang, K. Y. J. (2017). Discovery of fungal denitrification inhibitors by targeting copper nitrite reductase from *Fusarium oxysporum*. Journal of Chemical Information and Modeling, 57, 203-213.

McMillan, A. M. S., Pal, P., Phillips, R. L., Palmada, T., Berben, P. H., Jha, N., Saggar, S., & Luo, J. (2016). Can pH amendments in grazed pastures help reduce N_2O emissions from denitrification? – The effects of liming and urine addition on the completion of denitrification in fluvial and volcanic soils. Soil Biology & Biochemistry, 93, 90-104.

Mothapo, N. V., Chen, H., Cubeta, M. A., & Shi, Wei. (2013). Nitrous oxide producing activity of diverse fungi from distinct agroecosystems. Soil Biology & Biochemistry, 66, 94-101.

Mothapo, N., Chen, H., Cubeta, M. A., Grossman, J. M., Fuller, F., & Shi, W. (2015). Phylogenetic, taxonomic and functional diversity of fungal denitrifiers and associated N_2O production efficacy. Soil Biology & Biochemistry, 83, 160-175.

Muller, C., Laughlin, R. J., Spott, O., & Rutting, T. (2014). Quantification of N_2O emission pathways via a ^{15}N tracing model. Soil Biology & Biochemistry, 72, 44-54.

Nelson, P. E. (1992). Taxonomy and biology of *Fusarium moniliforme*. Mycopathologia, 117, 29-36.

Nelson, P. E., Dignani, M. C., & Anaissie, E. J. (1994). Taxonomy, biology, and clinical aspects of *Fusarium* species. Clinical Microbiology Reviews, 4, 479-504.

Nguyen, Q. V., Wu, D., Kong, X., Bol, R., Petersen, S. O., Jensen, L. S., Liu, S., Bruggemann, N., Glud, R. N., Larsen, M., & Bruun, S. (2017). Effects of cattle slurry and nitrification inhibitor application on spatial soil O_2 dynamics and N_2O production pathways. Soil Biology & Biochemistry, 114, 200-209.

Novinscak, A., Goyer, C., Zebarth, B. J., Burton, D. L., Chantigny, M. H., & Filion, M. (2016). Novel *P450nor* gene detection assay used to characterize the prevalence and diversity of soil fungal denitrifiers. Applied and Environmental Microbiology, 82, 4560-4569.

Nucci, M. & Anaissie, E. (2007). *Fusarium* infections in immunocompromised patients. Clinical Microbiology Reviews, 20, 695-704.

Oerke, E.-C. (2006). Crop losses to pests. Journal of Agricultural Science, 144, 31–43.

Oerke, E.-C., & Dehne, H.-W. (1997). Global crop production and the efficacy of crop protection – current situation and future trends. European Journal of Plant Pathology, 103, 203-215.

Oerke, E.-C., & Dehne, H.-W. (2004). Safeguarding production – losses in major crops and the role of crop protection. Crop Protection, 23, 275-285.

Oerke, E.-C., Dehne, H.-W., Schönbeck, F., & Weber, A. (1994). Crop production and crop protection. Estimated losses in major food and cash crops. Amsterdam: Elsevier.

Oertel, C., Matschullat, J., Zurba, K., Zimmerman, F., & Erasmi, S. (2016). Greenhouse gas emissions from soils – A review. Chemie der Erde, 76, 327-352.

Opdyke, M. R., Ostrom, N. E., & Ostrom, P. H. (2009). Evidence for the predominance of denitrification as a source of N_2O in temperate agricultural soils based on isotopologue measurements. Global Biogeochemical Cycles, 23, 1-10.

Pajares, S. & Bohannan, B. J. M. (2016). Ecology of nitrogen fixing, nitrifying, and denitrifying microorganisms in tropical forest soils. Frontiers in Microbiology, 7, 1-20.

Philippot, L. (2005). Denitrification in pathogenic bacteria: for better or worst? TRENDS in Microbiology, 13, 191-192.

Phillips, R. L., Song, B., McMillan, A. M. S., Grelet, G., Weir, B. S., Palmada, T., & Tobias, C. (2016). Chemical formation of hybrid di-nitrogen calls fungal codenitrification into question. Scientific Reports, 6, 1-8.

Prosser, J. I. & Nicol, G. W. (2012). Archaeal and bacterial ammonia-oxidizers in soil: the quest for niche specialization and differentiation. Trends in Microbiology, 20, 523-531.

Ravishankara, A. R., Daniel, J. S., & Portmann, R. W. (2009). The dominant ozone-depleting substance emitted in the 21st century. Science, 326, 123-125.

Regan, K., Stempfhuber, B., Schloter, M., Rasche, F., Prati, D., Philippot, L., Boeddinghaus, R. S., Kandeler, E., & Marhan, S. (2017). Spatial and temporal dynamics of nitrogen fixing, nitrifying and denitrifying microbes in an unfertilized grassland. Soil Biology & Biochemistry, 109, 214-226.

Richardson, D., Felgate, H., Watmough, N., Thomson, A., & Baggs, E. (2009). Mitigating release of the potent greenhouse gas N_2O from the nitrogen cycle – could enzymic regulation hold the key? Trends in Biotechnology, 27, 388-397.

Roncero, M. I. G., Hera, C., Ruiz-Rubio, M., Garcia Maceira, F. I., Madrid, M. P., Caracuel, Z., Calero, F., Delgado-Jarana, J., Roldan-Rodriguez, R., Martinez-Rocha, A. L., Velasco, C., Roa, J., Martin-Urdiroz, M., Cordoba, D., & Di Pietro, A. (2003). *Fusarium* as a model for studying virulence in soilborne plant pathogens. Physiological and Molecular Plant Pathology, 62, 87-98.

Rutting, T., Boeckx, P., Muller, C., & Klemedtsson, L. (2011). Assessment of the importance of dissimilatory nitrate reduction to ammonium for the terrestrial nitrogen cycle. Biogeosciences, 8, 1779-1791.

Salles, J. F., Pereira e Silva, M. C., Dini-Andreote, F., Dias, A. C. F., Guillaumaud, N., Poly, F., & van Elsas, J. D. (2017). Successional patterns of key genes and processes involved in the microbial nitrogen cycle in a salt marsh chronosequence. Biogeochemistry, 132, 185-201.

Schipper, L. A., Cooper, A. B., Harfoot, C. G., & Dyck, W. J. (1993). Regulators of denitrification in an organic riparian soil. Soil Biology & Biochemistry, 25, 925-933.

Seitzinger, S., Harrison, J. A., Bohlke, J. K., Bouwman, A. F., Lowrance, R., Peterson, B., Tobias, C., & Van Drecht, G. (2006). Denitrification across landscapes and waterscapes: A synthesis. Ecological Applications, 16, 2064-2090.

Sherman, J., Le, C., Lamers, V., & Eckelman, M. (2012). Life cycle greenhouse gas emissions of anesthetic drugs. Anesthesia & Analgesia, 114, 1086-1090.

Shiferaw, B., Prasanna, B. M., Hellin, J., & Banziger, M. (2011). Crops that feed the world 6. Past successes and future challenges to the role played by maize in global food security. Food Security, 3, 307-327.

Shoun, H. & Tanimoto, T. (1991). Denitrification by the fungus *Fusarium oxysporum* and involvement of cytochrome P-450 in the respiratory nitrite reduction. The Journal of Biological Chemistry, 266, 11078-11082.

Shoun, H., Kim, D.-H., Uchiyama, H., & Sugiyama, J. (1992). Denitrification by fungi. FEMS Microbiology Letters, 94, 277-282.

Shoun, H., Fushinobu, S., Jiang, L., Kim, S.-W., & Wakagi, T. (2012). Fungal denitrification and nitric oxide reductase cytochrome P450nor. Philosophical Transactions: Biological Sciences, 367, 1186-1194.

Singh, J., Saggar, S., Giltrap, D. L., & Bolan, N. S. (2008). Decomposition of dicyandiamide (DCD) in three contrasting soils and its effect on nitrous oxide emission, soil respiratory activity, and microbial biomass – an incubation study. Australian Journal of Soil Research, 46, 517-525.

Smith, V. H., Tilman, G. D., & Nekola, J. C. (1999). Eutrophication: impacts of excess nutrient inputs on freshwater, marine, and terrestrial ecosystems. Environmental Pollution, 100, 179-196.

Slot, J. C. & Hibbett, D. S. (2007). Horizontal transfer of a nitrate assimilation gene cluster and ecological transitions in fungi: A phylogenetic study. PLoS One, 1-8.

Snyder, C.S., Bruulsema, T. W., Jensen, T. L., & Fixen, P. E. (2009). Review of greenhouse gas emissions from crop production systems and fertilizer management effects. Agriculture, Ecosystems and Environment, 133, 247-266.

Subbarao, G. V., Nakahara, K., Hurtado, M. P., Ono, H., Moreta, D. E., Salcedo, A. F., Yoshihashi, A. T., Ishikawa, T., Ishitani, M., Ohnishi-Kameyama, M., Yoshida, M., Rondon, M., Rao, I. M., Lascano, C. E., Berry, W. L., Ito, O., & Schlesinger, W. H. (2009). Evidence for biological nitrification inhibition in *Brachiaria* pastures. Proceedings of the National Academy of Sciences of the United States of America, 106, 17302-17307.

Summerell, B. A. Laurence, M. H. Liew, E. C. Y., & Leslie, J. F. (2010). Biogeography and phylogeography of *Fusarium*: a review. Fungal Diversity, 44, 3-13.

Takaya, N. & Shoun, H. (2000). Nitric oxide reduction, the last step in denitrification by *Fusarium oxysporum*, is obligatorily mediated by cytochrome P450nor. Molecular and General Genetics, 263, 342-348.

Takaya, N. (2002). Dissimilatory nitrate reduction metabolisms and their control in fungi. Journal of Bioscience and Bioengineering, 94, 506-510.

Takaya, N., Kuwazaki, S., Adachi, Y., Suzuki, S., Kikuchi, T., Nakamura, H., Shiro, Y., & Shoun, H. (2003). Hybrid respiration in the denitrifying mitochondria of *Fusarium oxysporum*. Journal of Biochemistry, 133, 461-465.

Takaya, N. (2009). Response to hypoxia, reduction of electron acceptors, and subsequent survival by filamentous fungi. Bioscience, Biotechnology, and Biochemistry, 73, 1-8.

Takle, E. G., Gustafson, D., Beachy, R., Nelson, G. C., Mason-D 'Croz, D., & Palazzo, A. (2013). US Food Security and Climate Change: Agricultural Futures. Economics, 7, 2013-2034.

Teng, P. S. (Ed.). (1987). Crop loss assessment and pest management. St Paul: APS Press.

Teng, P. S., & Krupa, S. V. (Eds). (1980). Assessment of losses which constrain production and crop improvement in agriculture and forestry. Proceedings of the E. C. Stackman Commemorative Symposium. St. Paul: University of Minnesota.

Tesfamariam, T., Yoshinaga, H., Deshpande, S. P., Srinivasa Rao, P., Sahrawat, K. L., Ando, Y., Nakahara, K., Hash, C. T., & Subbarao, G. V. (2014). Biological nitrification inhibition in sorghum: the role of sorgoleone production. Plant and Soil, 379, 325-335.

Tschiersch, H., Liebsch, G., Borisjuk, L., Stangelmayer, A., & Rolletschek, H. (2012). An imaging method for oxygen distribution, respiration and photosynthesis at a microscopic level of resolution. New Phytologist, 196, 926-936.

van Kessel, M. A. H. J., Speth, D. R., Albertsen, M., Nielsen, P. H., Op den Camp, H. J. M., Kartal, B., Jetten, M. S. M., & Lucker, S. (2015). Complete denitrification by a single microorganism. Nature, 528, 555-559.

van Niftrik, L. & Jetten, M. S. M. (2012). Anaerobic ammonium-oxidizing bacteria: Unique microorganisms with exceptional properties. Microbiology and Molecular Biology Reviews, 76, 585-596.

Vitousek, P .M., Aber, J. D., Howarth, R. W., Likens, G. E., Matson, P. A., Schindler, D. W., Schlesinger, W. H., & Tilman, D. G. (1997). Human alteration of the global nitrogen cycle: Sources and consequences. Ecological Applications, 7, 737-750.

Vitousek, P. M., Menge, D. N. L., Reed, S. C., & Cleveland, C. C. (2013). Biological nitrogen fixation: rates, patterns and ecological controls in terrestrial ecosystems. Philosophical Transactions of The Royal Society B, 368, 1-9.

Watanbe, M., Yonezawa, T., Lee, K.-i., Kumagai, S., Sugita-Konishi, Y., Goto, K., & Hara-Kudo, Y. (2011). Molecular phylogeny of the higher and lower taxonomy of the *Fusarium* genus and differences in the evolutionary histories of multiple genes. BMC Evolutionary Biology, 11, 1-16.

Wei, W., Isobe, K., Shiratori, Y., Nishizawa, T., Ohte, N., Otsuka, S., & Senoo, K. (2014). N_2O emission from cropland field soil through fungal denitrification after surface applications of organic fertilizer. Soil Biology & Biochemistry, 69, 157-167.

Wei, W., Isobe, K., Shiratori, Y., Nishizawa, T., Ohte, N., Ise, Y., Otsuka, S., & Senoo, K. (2015). Development of PCR primers targeting fungal *nirK* to study fungal denitrification in the environment. Soil Biology & Biochemistry, 81, 282-286.

Wu, D., Senbayram, M., Well, R., Bruggemann, N., Pfeiffer, B., Loick, N., Stempfhuber, B., Dittert, K., & Bol, R. (2017). Nitrification inhibitors mitigate N_2O emissions more effectively under straw-induced conditions favoring denitrification. Soil Biology & Biochemistry, 104, 197-207.

Xu, X., Ran, Y., Li, Y., Zhang, Q., Liu, Y., Pan, H., Guan, X., Li, J., Shi, J., Dong, L., Li, Z., Di, H., & Xu, J. (2016). Warmer and drier conditions alter the nitrifier and denitrifier communities and reduce N_2O emissions in fertilized vegetable soils. Agriculture, Ecosystems and Environment, 231, 133-142.

Xu, X., Liu, X., Li, Y., Ran, Y., Liu, Y., Zhang, Q., Li, Z., He, Y., Xu, J., & Di H. (2017). High temperatures inhibited the growth of soil bacteria and archaea but not that of fungi and altered nitrous oxide production mechanisms from different nitrogen sources in an acidic soil. Soil Biology & Biochemistry, 107, 168-179.

Zaman, M., Nguyen, M. L., Gold, A. J., Groffman, P. M., Kellogg, D. Q., & Wilcock, R. J. (2008). Nitrous oxide generation, denitrification, and nitrate removal in a seepage wetland intercepting surface and subsurface flows from a grazed dairy catchment. Australian Journal of Soil Research, 46, 565-577.

Zhou, Z., Takaya, N., Antonina, M., Sakairi, C., & Shoun, H. (2001). Oxygen requirement for denitrification by the fungus *Fusarium oxysporum*. Archives of Microbiology, 175, 19-25.

Zhou, Z., Takaya, N., & Shoun, H. (2010). Multi-energy metabolic mechanisms of the fungus *Fusarium oxysporum* in low oxygen environments. Bioscience, Biotechnology and Biochemistry, 74, 2431-2437.

Zhu, X., Burger, M., Doane, T. A., & Horwath, W. R. (2013). Ammonia oxidation pathways and nitrifier denitrification are significant sources of N_2O and NO under low oxygen availability. Proceedings of the National Academy of Sciences of the United States of America, 110, 6328-6333.

Zumft, W. G. (1997). Cell biology and molecular basis of denitrification. Microbiology and Molecular Biology Reviews, 61, 533-616.

CHAPTER 2

PHYLOGENETIC AND PHYLOGENOMIC CHARACTERIZATION OF DENITRIFICATION-ASSOCIATED PROTEINS IN FUNGI[1]

[1] Oakley BA, Gao M, Gu X, Gold SE, and Glenn AE. To be submitted to *Frontiers in Microbiology*.

Abstract

Denitrification is activated under hypoxic or anoxic conditions and converts soluble nitrogen (N) oxides such as nitrate and nitrite to gaseous N oxides including nitric oxide (NO), nitrous oxide (N_2O), and di-nitrogen (N_2). Denitrification has become a major source of N loss and N_2O emissions in agriculture due to increasing anthropogenic reliance on synthetic nitrogen fertilizers. Denitrifying fungi are probably the main culprits responsible for rising N_2O emissions from agricultural sources since they lack the nitrous oxide reductase that bacteria use to reduce N_2O to the benign N_2. To reduce greenhouse gas emissions and slow the acceleration of climate change, we must develop solutions to inhibit fungal denitrification and its concomitant N_2O production. However, the ability to denitrify is an uncommon, largely uncharacterized trait in the fungal kingdom. Here, we use RNA-seq to identify genes in the soil-borne mycotoxigenic fungus, *Fusarium verticillioides*, associated with hypoxic respiration and nitric oxide detoxification. Genes up-regulated more than eight-fold in response to one or both treatments were further investigated to gauge their importance in fungal denitrification. Publicly-available RNA-seq data from FungiDB confirmed that genes highly up-regulated *in vitro* are also upregulated *in planta* when *F. verticillioides* infects maize roots. Using the *F. verticillioides* RNA-seq data and widely catalogued protein sequence data, we evaluated the phylogenetic limitedness of denitrification across fungi and found that dissimilatory nitrate and nitrite reductase and nitric oxide reductase are narrowly distributed, whereas assimilatory nitrate and nitrite reductase are more broadly distributed. We also used phylogenomics to explore the diversity of denitrification capable *Fusarium* species. Based on our analysis, denitrifying *Fusarium* species are confined to a few species complexes and sections, suggesting that the ability to denitrify is a trait that was gained or lost from the most recent common ancestor of the

genus *Fusarium*. Collectively, we determined that denitrification in fungi is exclusive to the phylum Ascomycota because there are no fungi with orthologs of both dissimilatory nitrite reductase and nitric oxide reductase outside of the Ascomycota. Additionally, the ability to denitrify may influence the pathogenicity and lifestyle of some *Fusarium* species by conferring a fitness advantage under adverse conditions.

Introduction

The global nitrogen (N) cycle is central to Earth's biogeochemistry and maintains Earth's N balance. However, since the dawn of the Green Revolution, humans have become increasingly reliant on fixed N to achieve maximal agricultural productivity. This increased reliance on synthetic N fertilizers has accelerated the N cycle (Galloway et al., 2004). Unfortunately, anthropogenic alteration of the natural flow of N has caused a massive imbalance in the N cycle, which has severe implications for environmental and human health and agricultural productivity. One of the effects of this perturbation of the N cycle has been a 20% increase over the past 100 years in atmospheric nitrous oxide (N_2O), a long-lived potent greenhouse gas that also damages the stratospheric ozone layer (Galloway et al., 2008; Canfield et al., 2010). This massive increase in N_2O emissions is largely due to denitrification, which is one of the key processes of the N cycle, alongside biological N fixation and nitrification (Li et al., 2023).

Denitrification reduces the N overload of aquatic ecosystems by converting soluble N oxides (e.g., NO_3^-, NO_2^-) to gaseous N oxides (e.g., NO, N_2O, N_2), thereby limiting human pollution of water sources (Bouwman et al., 2013). In contrast, denitrification is problematic in agriculture because it results in N loss by removing plant-available N from the soil (Fang et al., 2015). This is compounded by the fact that synthetic fertilizers increase denitrifier abundance; thus, increasing soil N_2O emissions (Bouwman et al., 2002; Millar et al., 2010; Shcherbak et al., 2014; Wang et al., 2020). Of the total amount of fertilizer N applied to crop systems globally (~115 Tg N $year^{-1}$; FAO, 2016), 50-70% is lost to the surrounding environment due to leaching and denitrification (Cassman et al., 2002; Ladha et al., 2016; Schlesinger, 2009; Coskun et al., 2017). Global estimates of terrestrial denitrification range from 100 to 250 Tg-N $year^{-1}$, which is equivalent to about 50% of newly fixed terrestrial N (Fowler et al., 2013; Scheer et al., 2020). In

a study of N losses from a heavy clay soil under grass, denitrification was responsible for 90% of the loss of N applied to the field as fertilizer and manure (van der Salm et al., 2007). Denitrification is also concerning for Earth's climate since the global warming potential of N_2O is 300-times higher than CO_2 and the compound has a long atmospheric lifetime (110 ± 6 years) (Ravishankara et al., 2009, Pachauri et al., 2014). This problem is further exacerbated considering global warming can boost denitrification rates in a positive feedback loop (Veraart et al., 2011).

Denitrification is the oxygen-regulated, microbe-mediated chemical reduction of nitrate (NO_3^-) to nitrite (NO_2^-), nitric oxide (NO), the greenhouse gas nitrous oxide (N_2O), and dinitrogen (N_2) (Zumft, 1997). The ability to denitrify was originally thought to be exclusive to the prokaryotes, bacteria and archaea. There is also conclusive evidence that benthic foraminifera can denitrify (Risgaard-Petersen et al., 2006; Woehle et al., 2018; Choquel et al., 2021; Woehle et al., 2022), but they do not contribute significantly to N_2O emissions from terrestrial or agricultural environments. Most eukaryotic organisms cannot denitrify due to lack of genetic potential. Over the past 30 years it has become apparent that the most common and important eukaryotic denitrifiers in agriculture are fungi, and they will be the focus of this paper.

There are genetic and biochemical differences between prokaryotic and fungal denitrification. The canonical denitrification pathway in bacteria encompasses four enzymes encoded by gene clusters – (1) napEDABC, a dissimilatory nitrate reductase that reduces NO_3^- to NO_2^-, (2) nirK, a dissimilatory nitrite reductase that reduces NO_2^- to NO, (3) norCBQD, a nitric oxide reductase that reduces NO to N_2O, and (4) nosRZDFYLX, a nitrous oxide reductase that reduces N_2O to N_2 (Bedmar et al., 2005). Fungi have single gene functional homologs, most frequently unlinked, of the prokaryote encoded enzymes, dNAR, dNIR, and p450nor (Zumft et

al., 1994; Ye et al., 1994). But fungi differ from bacteria in that they do not possess a gene that encodes nitrous oxide reductase (nosZ) (Morozkina and Kurakov, 2007). This means that fungi cannot convert the greenhouse gas N_2O into benign atmospheric N_2. This results in fungi being the major contributors to N_2O emissions across a variety of aquatic, terrestrial, and agricultural ecosystems (Wankel et al., 2017; Crenshaw et al., 2008; Yanai et al., 2007; Laughlin and Stevens, 2002; Laughlin et al., 2009; Castellano-Hinjosa et al., 2021; Ma et al., 2017; Castaldi and Smith, 1998). However, there are significant gaps in our understanding of which fungal taxa are able to denitrify and their associated denitrification capabilities.

To be a fungal denitrifier, the minimum requirement is the genomic presence and function of dNIR and p450nor to convert NO_2^-, a soluble nitrogen oxide, to N_2O, a gaseous nitrogen oxide (Shoun et al., 2012). These are the minimum requirements because fungi do not need dNAR to utilize nitrate for denitrification. For example, *Cylindrocarpon tonkinense* (syn. *Fusarium tonkinense*) is a denitrifying fungus that lacks an ortholog of dNAR and uses aNAR to reduce nitrate to nitrite (Watsuji et al., 2003). Using these criteria, fungi that have p450nor but lack dNIR are N_2O producers, but they are not denitrifiers. There are numerous reports of fungi and their ability to produce N_2O (Tsuruta et al., 1998; Mothapo et al., 2013; Mothapo et al., 2015; Maeda et al., 2015), but these studies sometimes inappropriately link N_2O production to denitrification without supporting genomic data. For example, Tsuruta et al. (1998) state that *Cutaneotrichosporon cutaneum* (*Cc*), a basidiomycetous yeast, can convert NO_2^- to N_2O, but they could not detect activity of dNIR in their cell-free extracts. Currently available genomic data indicates that *C. cutaneum* does not possess a dNIR ortholog; thus, this yeast is disqualified as a denitrifier. To reduce N loss and N_2O emissions that are an unintended product of fertilizer

application, the disconnect between denitrification potential and N_2O production must be clarified.

Fungal denitrification involves a series of steps that likely requires a wide array of functionally distinct proteins to efficiently convert inorganic nitrogen into energy, but some of the encoding genes are unknown and their roles have not been elucidated. In this report, RNA-seq was used to identify genes presumed to be required for, or associated with, the fungal denitrification pathway by exposing *Fusarium verticillioides* to either low-oxygen concentrations or a NO donor, both of which are conditions that the fungus would encounter while undergoing denitrification. Then, phylogenetic and phylogenomic approaches were used to assess these genes to determine which fungi are genetically capable of denitrifying and how common these *F. verticillioides* homologs are in the Kingdom Fungi. The findings reported here provide a better understanding of fungal denitrification and may help develop targeted solutions to reduce N loss and ever-increasing N_2O emissions.

Materials & Methods

Fungal and bacterial strains, culture media, and growth conditions

The wild-type strain *Fusarium verticillioides* M-3125 from the Fusarium Research Center (FRC) was used throughout this study and was routinely grown at 27° C in the dark for 3 days on a shaker incubator at 250 rpm in either (i) potato dextrose broth (PDB; Neogen Food Safety) buffered with 0.1 M sodium phosphate (Na_3PO_4) (pH = 7.0-7.4) or (ii) glycerol peptone (GP) medium. This GP medium contains 1% glycerol, 0.2% peptone, and trace elements. Trace elements (per 100 mL) include 5.0 g citric acid, 5.0 g $ZnSO_4 \bullet 6H_2O$, 1.0 g $Fe(NH_4)_2(SO_4)_2 \bullet 6H_2O$, 0.25 g $CuSO_4 \bullet 5H_2O$, 0.05 g $MnSO_4$, 0.05 g H_3BO_3, and 0.05 g $Na_2MoO_4 \bullet 2H_2O$. For the RNA-seq study, wild type *F. verticillioides* was grown in the two

media and exposed to normal and NO or hypoxia treatment conditions depending on the nature of the experiment as described below.

RNA-seq: Nitric Oxide Exposure vs. Control

Transcriptional analysis was used to test the response of *F. verticillioides* M-3125 to nitric oxide (NO). The fungus was inoculated into PDB buffered with 0.1 M sodium phosphate and cultured for 3 days at 27ºC at 250 rpm. As the untreated control, 1 mL of culture was transferred to lysing matrix S tubes (MP Biomedicals, LLC, Santa Ana, CA, USA), centrifuged at 10,000 x g for 5 min at 4ºC, and the supernatant discarded. Lysis buffer (PureLink® RNA Mini Kit, Thermo Fisher Scientific) was immediately added to the fungal cell pellet, and the samples homogenized at a speed of 6 m/sec with two segments of 30 s with a 1 min rest on ice between segments using the FastPrep-24™ 5G Instrument (MP Biomedicals). Total RNA was extracted following the manufacturer's instructions (PureLink® RNA Mini Kit, Thermo Fisher Scientific). The NO treated samples were also cultured in buffered PDB for 3 days followed by 30 min exposure to 1.5 mM diethylenetriamine (DETA) NONOate (Cayman Chemical, Ann Arbor, MI, USA) dissolved in 0.01 M NaOH, and the samples were then harvested for RNA extraction as stated above. Six libraries (wild type *F. verticillioides* treated with and without 1.5 mM DETA NONOate for 30 min, with three biological replicates each) were prepared and sequenced on an Illumina NextSeq (75 Cycles) High Output Flow Cell (paired end, 75 bp read length) by the Georgia Genomics Facility at the University of Georgia.

RNA-seq: Hypoxia vs. Normoxia

Transcriptional response to hypoxia was conducted by initially growing M-3125 in 50 mL GP medium for 3 days as above. The fungus (0.1 mL) was then inoculated into six replicate tubes containing 3 mL of GP medium and grown for 3 days. The tubes were centrifuged to pellet

the fungus, and the supernatant was decanted. Then, 3 mL of GP medium amended with 10 mM $NaNO_3$ was added to each tube and the pellets were resuspended. Three of the tubes had their caps snapped close to induce hypoxia, while the caps of the other three tubes were kept loose to allow for air exchange. The cultures were incubated as before for 24 h, centrifuged again to pellet the fungus, and the supernatant was removed. To extract and sequence the RNA, 1 mL of lysis buffer was added and the fungal samples transferred to matrix S tubes for homogenization and processing as noted above.

RNA-seq data analysis

Raw RNAseq reads were subject to quality control by fastqc (Andrews, 2010; http://www.bioinformatics.babraham.ac.uk/projects/fastqc/), followed by removal of low-quality reads (Phred score <20) and Illumina sequencing adapters using Trimmomatic 0.25 (Bolger et al., 2014). The genome for *F. verticillioides* (Ma et al., 2010) was downloaded from FungiDB (Amos et al., 2022; Basenko et al., 2018; www.fungidb.org). Mapping of the filtered paired-end reads against the *F. verticillioides* genome was performed using the align function in the Rsubread package (Liao et al., 2013) in Bioconductor (www.bioconductor.org). Read counting, normalization, and expression level (FPKM) calculations were executed using the featurecount function in Rsubread using the default settings. Differential gene expression analysis was then performed using edgeR (Robinson et al., 2010) and DESeq (Anders and Huber, 2010) packages by applying a false discovery rate threshold of < 0.05 for the adjusted *p*-value. The NO exposure RNA-seq dataset discussed in this publication has been deposited in NCBI's Gene Expression Omnibus (Edgar et al., 2002; Barrett et al., 2013) and is accessible through GEO Series accession number GSE118800

(https://www.ncbi.nlm.nih.gov/geo/query/acc.cgi?acc=GSE118800). The hypoxia RNA-seq dataset is being submitted now but does not yet have an accession number.

Genome database search and sequence retrieval

The protein sequences of genes in Table 2.1 were downloaded from FungiDB (Release 57; April 21, 2022) in FASTA format. NCBI's Protein Basic Local Alignment Search Tool (protein-protein BLAST) algorithm (BLAST+ v2.13.0; https://blast.ncbi.nlm.nih.gov/Blast.cgi) was used to identify fungal and oomycete protein sequences that are similar to the aforementioned genes from the RNA-seq experiment (Altschul et al., 1990; Johnson et al., 2008; Boratyn et al., 2013). Searches were confined to the reference proteins (refseq_protein) database with "Uncultured/environmental sample sequences" excluded. Searches were filtered to only include Fungi (taxid:4751) and Oomycota (taxid:4762) and further filtered to only retain sequences with an e-value of 9E-40 or lower. Algorithm parameters, including general and scoring parameters as well as filters and masking, were all set to default except for the max target sequences (5,000, not 100). Oomycetes were included despite not being "true" fungi to confirm their inability to denitrify.

Additional sequence data was added to the dataset of each protein in the form of the protein's respective orthogroup (OG) from OrthoMCL DB (Release 6.11; June 23, 2022; https://orthomcl.org/orthomcl/app/static-content/OrthoMCL/about.html) (Li et al., 2003; Chen et al., 2006; Chen et al., 2007; Fischer et al., 2011). To form these OGs, the OrthoMCL algorithm was employed on proteins from a set of 150 core species. These 150 species were chosen based on proteome quality and widespread placement across the tree of life. Each core protein was placed into a core ortholog group consisting of one or more proteins. The proteins from hundreds of additional organisms, termed peripheral organisms, are mapped into the core groups. To do

this, NCBI BLASTP was used to compare each peripheral protein to each core protein in the core groups. Each peripheral protein was assigned to the core group containing the core protein with the best BLAST score, but only if the e-value was <1E-5 and the percent match length was ≥50%. OrthoMCL DB data for each protein was manually filtered to exclude Bacteria, Archaea, and any non-fungal or non-oomycete eukaryotes. Duplicate sequences of the same species-strain combination, redundant sequences from different strains of the same species, and any sequences that were abnormally short or long, causing short (Dick et al., 2017) or long branch attraction (Bergsten, 2005), were also removed from each dataset.

Construction of phylogenies for genes identified by RNA-seq

The final datasets for NAR1 (FVEG_01721)/NIA1 (FVEG_07298), DNI1 (FVEG_08676), NOR1 (FVEG_10773), FHB1/FHB2 (FVEG_11186/FVEG_13827), and FNT1/FNT2 (FVEG_03704/FVEG_08384) consisted of 1,045, 76, 110, 570, and 310 sequences, respectively. These sequences were subjected to multiple sequence alignment (MSA) using MAFFT (v7.490; Katoh et al., 2002; Katoh and Standley, 2013) in Geneious Prime® 2022.2.1 (Build 2022-07-07 13:25). FastTree (v2.1.11; Price et al., 2009; Price et al., 2010) was used to evaluate the preliminary phylogenies. The outgroup or the most basal clade was identified via the FastTree maximum-likelihood (ML) tree. The protein alignments were re-used to build maximum likelihood trees using IQ-TREE (v1.6.12; Nguyen et al., 2015; Minh et al., 2020). ModelFinder (Kalyaanamoorthy et al., 2017) was used to identify the best substitution model for each dataset. “LG+R10” (NAR1/NIA1), “JTT+I+G4” (DNI1), “LG+G4” (NOR1), “LG+F+R10” (FHB1/FHB2), and “LG+R8” (FNT1/FNT2) were determined to be the best amino-acid exchange rate matrices for each dataset according to the Bayesian Information Criterion. A description of each of the datasets’ optimal substitution model is included in Supplementary

Table S2.1. For more information regarding IQ-TREE sequence alignment, substitution model, tree statistics and BIC values, see Supplementary Tables S2.2-2.6.

All phylogenies were re-run with the respective substitution model specified above using the Ultrafast Bootstrap (UFBoot; Hoang et al., 2018) analysis in combination with the SH-like approximate likelihood ratio test (SH-aLRT branch test; Guindon et al., 2010) with 1000 replicates. UFBoot was used to overcome the computational costs required by nonparametric bootstrap estimation (Felsenstein, 1985). The resulting phylogenies were visualized and edited in FigTree (v1.4.4).

Phylogenomics and ortholog analysis in *Fusarium*

Phylogenomics was used to identify orthologs of proteins of interest, as identified by RNA-seq, in the fungal genus *Fusarium.* We used a representative sample of the known diversity of *Fusarium* fungi because many of the known species do not have a publicly available genome. NCBI's "Genome" page (https://www.ncbi.nlm.nih.gov/datasets/genome/) was used to download reference genomes for *Fusarium.* Genomes that were not annotated or did not have a corresponding proteome were excluded. In total, 75 *Fusarium* proteomes were used. This dataset consisted of 54 unique species of *Fusarium,* nine undescribed *Fusarium* sp., eight strains and formae speciales of *F. oxysporum,* two strains of *F. poae,* two strains of *F. fujikuroi,* and two strains of *F. odoratissimum.* Multiple strains or races of the same species were included to detect any strain-level differences in fungal denitrification capabilities (e.g., *F. poae* 2516 and *F. poae* DAOMC 252244). Two different assemblies of *Fusarium graminearum* (*Fg*) strain PH-1 were also included as an internal control (*F. graminearum*: GCA_000240135.3, GCA_900044135.1).

OrthoFinder (Emms and Kelly, 2015; Emms and Kelly, 2019) was used for phylogenetic orthology inference and comparative genomics. The 75 *Fusarium* proteomes assessed were

collated as a single dataset and used as the input. From this input, OrthoFinder analyzed the proteomes, found orthogroups and orthologs, and automatically inferred orthogroups for all species and generated a complete set of rooted gene trees. It also identified all gene duplication events in those gene trees. Resolved gene trees were interpreted based on the inference of orthologs and gene duplication events. OrthoFinder carried out a duplication-loss-coalescence analysis to identify the most parsimonious interpretation of the gene trees.

To infer the best species tree, OrthoFinder uses multiple algorithms, including STAG (Species Tree Inference from All Genes; Emms and Kelly, preprint) and STRIDE (Species Tree Root Inference from Gene Duplication Events; Emms and Kelly, 2017) to identify a set of all orthogroups with all species present, regardless of gene copy number, and calculates a matrix of pairwise species distances for each orthogroup. The distance between each species pair is the tree distance for the closest pair of genes from that species pair in the gene tree. A consensus tree of all these individual species trees was calculated as the final species tree. The support value for each bipartition is the number of individual species trees that contained that bipartition. This data was used to draw conclusions about differences in fungal denitrification potential among *Fusarium* spp. and determine if those differences may affect lifestyle preferences among members of the genus *Fusarium*.

Results & Discussion

RNA-seq analysis identified 16 genes in *F. verticillioides* presumed to be involved in nitrogen metabolism and fungal denitrification

As a basis for this study, we hypothesized that genes associated with the denitrification pathway may be linked to NO detoxification as well as alternative respiration. To test this, two different RNA-seq experiments were conducted in the hopes of seeing an overlap in highly

induced genes across both datasets. One experiment compared gene expression levels in wild type *F. verticillioides* when grown in a normoxic versus hypoxic environment, and the second experiment evaluated expression levels when *F. verticillioides* was either exposed to exogenous NO or not. The rationale for using the experimental treatments described above is that the denitrification pathway in fungi is induced under low-oxygen conditions (Zhou et al., 2001) and as a plant pathogen, *F. verticillioides* likely frequently encounters hypoxic environments and the nitrosative stressor NO in the soil and during infection of maize. Specifically, Tschiersch et al. (2012) confirmed the vascular tissues of monocots and dicots as the major stem sink for oxygen, meaning the plant vasculature can become a temporary hypoxic environment. Additionally, many research groups have demonstrated that NO is an important signaling molecule and plays a major role in mediating the defense response in plants (Zhang et al., 2007; Sang et al., 2008; Bellin et al., 2013). The aforementioned findings are reasons we speculated that *F. verticillioides* may utilize its ability to denitrify to successfully infect maize while overcoming abiotic and biotic challenges such as reduced oxygen availability and fungal- (endogenous) and plant-induced (exogenous) NO release.

RNA-seq analysis revealed that a combination of 1,503 genes were induced in wild type *F. verticillioides* when the fungus was either exposed to NO or grown under hypoxic conditions. Hypoxia-treated samples had 1,454 induced genes, whereas NO-treated samples had 59 induced genes (Figure 2.1). Sixteen genes were induced eight-fold or more in a single treatment and ten genes were induced eight-fold or more in both treatments (Table 2.1). The putative functions of genes in Table 2.1 include nitrate, nitrite, and nitric oxide reductases, a transcriptional regulator, a nitrate-specific regulator, flavohemoglobins, an oxalate decarboxylase, a formate dehydrogenase, a protein of unknown function, and various types of transporters, including

formate/nitrite transporters, a nitrate/nitrite transporter, and an ABC transporter. Of the 16 genes in Table 2.1, all three of the key denitrification genes (FVEG_01721, NAR1; FVEG_08676, DNI1; FVEG_10773, NOR1) were present. NAR1, DNI1, and NOR1 had a $\log_2$ fold-change of 1.7, 7.6, and 5.0, respectively, when exposed to 1.5 mM DETA-NONOate compared with no exposure (Supplementary Table S2.7). NAR1, DNI1, and NOR1 had a $\log_2$ fold-change of 3.3 ($base_2$ = 9.9), 9.7 ($base_2$ = 831.8), and 14.1 ($base_2$ = 17,559.9), respectively, when grown in a hypoxic environment compared with a normoxic environment (Supplementary Table S2.8). These findings supported our hypothesis that the ability of fungi to use N oxides as terminal electron acceptors may serve a dual purpose in coping with nitrosative stressors such as NO and survival under hypoxic conditions, leading to increased denitrification in hypoxic environments such as saturated soils.

Enriched metabolic pathways of NAR1 and DNI1, as determined by KEGG (Kyoto Encyclopedia of Genes and Genomes), are limited to amino sugar and nucleotide sugar metabolism (1.6.2.2) and nitrogen metabolism (1.7.1.1; 1.7.1.3; 1.7.2.1). NOR1, however, is predicted to be involved in many diverse types of metabolism ranging from aminobenzoate degradation (1.14.14.-, 1.14.14.1), arachidonic acid metabolism (1.14.14.1), biosynthesis of type II polyketide products (1.14.14.-), biosynthesis of various alkaloids (1.14.14.-), biosynthesis of various plant and other secondary metabolites (1.14.14.-), biotin metabolism (1.14.14.46), caffeine metabolism (1.14.14.1), chlorocyclohexane and chlorobenzene degradation (1.14.14.-), drug metabolism by cytochrome P450 and other enzymes (1.14.14.-, 1.14.14.1), fatty acid degradation (1.14.14.1), indole alkaloid biosynthesis (1.14.14.-), linoleic acid metabolism (1.14.14.1), metabolism of xenobiotics by cytochrome P450 (1.14.14.-), nitrogen metabolism (1.7.1.14), phenylpropanoid biosynthesis (1.11.1.7), retinol metabolism (1.14.14.1),

staurosporine biosynthesis (1.14.14.-), steroid degradation (1.14.15.29), steroid hormone biosynthesis (1.14.14.1), and tryptophan metabolism (1.14.14.1). This diversity of metabolic reactions mediated by p450nor may imply an unelucidated role in secondary metabolism (SM).

In planta gene expression of _F. verticillioides_ in an independent RNA-seq study from the literature

We did not conduct *in planta* expression studies with *F. verticillioides* to validate the RNA-seq results. Instead, using FungiDB, we mined publicly-available expression data from an independent RNA-seq study by Niehaus et al. (2016) that examined transcriptional changes in *F. verticillioides* during maize root infection. This was done to see if the genes identified through the *in vitro* assay were differentially regulated *in planta.* RNA-seq data mined from Niehaus et al. (2016) revealed that dNAR, dNIR, and NOR1 were all up-regulated significantly compared with control conditions suggesting that the denitrification pathway is active in *F. verticillioides* during plant infection (Figure 2.2).

There is substantial evidence in the literature that inorganic nitrogen metabolism (i.e., denitrification) is a virulence factor in some plant and human pathogenic bacterial denitrifiers such as *Ralstonia solanacearum* (Dalsing et al., 2015), *Pseudomonas aeruginosa* (Lichtenberg et al., 2021), *Brucella melitensis, Neisseria gonorrhoeae,* and *Mycobacterium bovis* (Philippot, 2005). This gives further credence to the hypothesis that the ability to evolve nitrate or nitrite to nitrous oxide may play a role in virulence. Thus, it is likely that *F. verticillioides* utilizes the denitrification pathway during infection of maize to respire, produce energy, and detoxify fungal- and plant-derived NO.

Ortholog analysis of dNAR, dNIR, and p450nor in *Fusarium verticillioides*

Using OrthoMCL, orthologs of NAR1, DNI1, and NOR1 in *F. verticillioides* were sought after to assess if these genes were unique. OG6_100179 contains NAR1, the dissimilatory nitrate reductase, NIA1, the assimilatory nitrite reductase, and ten other *F. verticillioides* orthologs. Besides NAR1 and NIA1, the most up-regulated *F. verticillioides* gene among OG6_100179 was FVEG_12090. FVEG_12090 encodes a protein with domain architecture similar to NIA1 (data not shown) meaning it probably functions as an assimilatory nitrate reductase. There is functional redundancy between NAR1, NIA1, and likely FVEG_12090 to reduce NO_3^- to NO_2^-, but NIA1 and FVEG_12090 reduce NO_3^- for N assimilation whereas NAR1 reduces NO_3^- for N dissimilation. There are two presumed *F. verticillioides* NAR1-like proteins in this OG that share domain architecture with NAR1, FVEG_07620 and FVEG_13790, but their expression was not significantly differentially regulated in the RNA-seq dataset (Figure 2.3). The other seven orthologs have 'mix-and-match' domain architecture and were lowly expressed relative to NAR1 and NIA1; thus, these genes do not appear to function as dissimilatory or assimilatory nitrate reductases.

DNI1 (FVEG_08676), which is in orthogroup (OG) OG6_124759, does not have any additional orthology in *F. verticillioides* (Figure 2.4), so it is presumed to be the only dissimilatory nitrite reductase in the genome of *F. verticillioides.* This makes DNI1 functionally special because it is the only nitrite-reducing enzyme in the dissimilatory system. NOR1 is in OG OG6_110453, which includes one other *F. verticillioides* gene, FVEG_05499. FVEG_05499 does not have P450 domains nor does it have the cytochrome P450 motif that is characteristic of a majority of cytochrome P450 nitric oxide reductases (data not shown). FVEG_05499 was also not significantly expressed in our RNA-seq dataset (Figure 2.5). Based on expression data and

ortholog analysis of OGs containing NAR1, DNI1, and NOR1, these three are the only genes that appear to be directly involved in denitrification in *F. verticillioides.*

Phylogenetic analyses suggest that fungal denitrification is likely restricted to the phylum Ascomycota

Our collective analysis of dNAR, dNIR, and p450nor, the three key denitrification genes, suggests that fungal denitrifiers are phylogenetically limited to the fungal phylum Ascomycota. In the dNAR/aNAR phylogeny (Figure 2.6), dNAR's distribution is highly limited whereas aNAR's distribution is very broad. Most fungi, except for some yeasts, can assimilate nitrate (Siverio, 2002; Song et al., 2007; Gorfer et al., 2011; Schinko et al., 2013), so it is not surprising that aNAR's phylogenetic distribution, relative to dNAR, is much broader. dNAR and aNAR are found in the same phylogeny due to the overlap in domain architecture between the two types of nitrate reductases (data not shown). This phylogeny includes oomycetes and fungi from Basidiomycota, Ascomycota, and other fungal phyla like the Mucoromycota. Notably, fungi from economically important genera including *Fusarium*, *Aspergillus*, *Colletotrichum*, *Trichoderma*, *Alternaria*, and *Penicillium* are heavily featured.

The p450nor phylogeny (Figure 2.7) focuses attention on a variety of animal and plant pathogens within the Ascomycota. As with the dNAR/aNAR phylogeny, *Fusarium* spp. and *Aspergillus* spp. are the genera that appear most frequently, but both *Colletotrichum* and *Trichoderma* also have numerous p450nor entries. Across the three phylogenies, p450nor is more abundant than dNAR or dNIR. This is consistent with a study by Higgins et al. (2018) where p450nor was twice as abundant compared with napA (dNAR) and nirK (dNIR). This discrepancy in gene abundance between the three denitrification genes indicates a disconnect between p450nor presence and denitrification potential. It is possible that p450nor functions

differently in non-denitrifying fungi versus denitrifying fungi, but it is unclear what the role of p450nor is, besides NO detoxification, in fungi that cannot denitrify. In a separate analysis of p450nor distribution across agriculturally and economically important fungi, p450nor distribution was found to be almost exclusively limited to the phylum Ascomycota with the exception of a few basidiomycetous yeasts (Oakley et al., submitted). Using a different NCBI database (refseq_protein vs. non-redundant protein), a different dataset (110 vs. 198 sequences), and a different substitution model (LG+G4 vs. JTTDCMut+R5), similar results were found; p450nor distribution is confined to the phylum Ascomycota.

The dNIR phylogeny (Figure 2.8) is indicative of the rarity of dNIR in fungi. This phylogeny has the least number of sequences out of the phylogenies for dNAR, dNIR, and p450nor. This is likely because the dNIR phylogeny does not include the assimilatory nitrite reductase (aNIR) that is functionally distinct from dNIR. In contrast to dNAR and aNAR, dNIR and aNIR do not share any protein domains (data not shown). The taxa in this phylogeny are exclusively within the Ascomycota. The most prevalent genera in the dNIR phylogeny are, again, *Fusarium* and *Aspergillus*. The only species of *Trichoderma* and *Penicillium* present are *T. asperellum* CBS 433.97 (XP_024766708.1) and *P. solitum* IBT 29525 (XP_040815834.1). We are aware that the databases used to acquire the sequence data may bias the results, but to ensure that data sampling did not influence conclusions about the breadth of dNIR, *F. verticillioides* dNIR (FVEG_08676) was used as the query protein in a protein BLAST search of the Basidiomycota (taxid:5204) using the refseq_protein database. We chose not to query against other fungal phyla beyond Basidiomycota because no fungus outside of the Dikarya has ever been shown to denitrify. Only three sequences were returned, and they were *Acaromyces ingoldii* (XP_025374844.1), *Trichosporon asahii* var. *asahii* CBS 2479 (XP_014177996.1), and

Rhizoctonia solani (XP_043180825.1). The e-value of these three sequences was 0.002 or higher and query coverage (< 46%) and sequence identity (< 30.39%) was very low, suggesting that there are no orthologs of dNIR in the Basidiomycota when searching the refseq_protein database. This increased confidence in the original interpretation of the dNIR phylogeny that dNIR is exclusive to the Ascomycota.

The dNIR phylogeny reveals that dNIR is even more limited than p450nor in its distribution, and it too is exclusive to the Ascomycota. The lack of, or scarcity of, dNIR and p450nor orthologs in other fungal phyla beyond the Ascomycota suggests that the ability to denitrify among the fungi is mostly restricted to that phylum. This is a novel discovery because the phylogenetic limitedness of fungal denitrification has not been evaluated until now. Higgins et al. (2018) studied the independent distribution of dNAR, dNIR, and p450nor in over 700 fungal genomes, but we are unaware of any studies using phylogenetics of dNAR, dNIR, and p450nor as a proxy for pinpointing which fungal phyla can denitrify.

Inferred species tree of 73 unique *Fusarium* proteomes shows discordance between the evolution of the genus *Fusarium* and denitrification-associated proteins

OrthoFinder analysis of *Fusarium* showed discordance between the evolution of denitrification-associated genes and evolution of the genus *Fusarium*, as informed by the inferred species tree (Figure 2.9) and the individual resolved gene trees for dNAR (Figure 2.10), dNIR (Figure 2.11), and p450nor (Figure 2.12). The OrthoFinder analysis outputs statistics summarizing the phylogenomic analysis and this data is displayed in Table 2.2. Of the 75 proteomes, there were 1,133,937 genes, and the number of genes assigned to orthogroups was 1,118,700, or 98.7%. There were only 15,237 unassigned genes (1.3%). The number of orthogroups totaled 27,687, and 557 (2.0%) of those were species-specific orthogroups. The

number of genes within those species-specific orthogroups was 1,613 (0.1%). The number of orthogroups with all species present was 3,042, and the number of single copy orthologs was 628. OrthoFinder species-specific summary statistics of the primary fungus of interest, *F. verticillioides*, is shown in Table 2.3. The *F. verticillioides* 7600 proteome (GCA_000149555.1) has 20,553 proteins and the number of these encoding genes in orthogroups was 20,044 (97.5%); thus, there were only 509 (2.5%) unassigned genes. The number of orthogroups containing *F. verticillioides* was 13,280 (48.0%), meaning that 52.0% of orthogroups in this analysis do not include proteins from *F. verticillioides.* The number of species-specific orthogroups across all *Fusarium* spp. was 88, and the number of genes within those species-specific orthogroups was 331 (1.6%).

There are no putative xenologs (i.e., homologs resulting from horizontal gene transfer (HGT) between two organisms) of the *F. verticillioides* genes in Table 2.1 in any of the other 72 unique *Fusarium* species-strain combinations (data not shown). This means OrthoFinder did not detect any homologous genes from Table 2.1 derived from horizontal transfer or lineage fusion for the rest of the *Fusarium* dataset. This implies that the denitrification-associated genes in *Fusarium* were vertically inherited and present before speciation from the most recent common ancestor. This result is backed by a broad analysis of p450nor in fungi along with denitrification enzyme genes napA (dNAR) and nirK (dNIR). In this analysis, Higgins et al. (2018) found a likely actinobacterial origin of p450nor enzymes while the other enzymes were thought to be of proteobacterial origin. This is supported by several other studies that say that nirK genes have the same ancestor as their bacterial counterpart (Shoun et al., 2012). In contrast, the close homology of the prokaryotic and eukaryotic cytochrome p450s suggests horizontal transfer of a cytochrome p450 gene from bacteria and subsequent modulation of its function to become p450nor (Kizawa

et al., 1991; Shoun et al., 1992). We, and others, speculate that a prototype p450 gene would have encoded a usual monooxygenase, whereas fungi would have modified the gene to possess nitric oxide reductase activity. Fungal p450nor is not found among bacteria, and it has not been shown to be involved in bacterial denitrification systems (Usuda et al., 1995).

The inferred species tree (Figure 2.9) has a dissimilar number of clades, and groupings of species within those clades, when compared with the resolved gene trees of dNAR (Figure 2.10), dNIR (Figure 2.11), and p450nor (Figure 2.12). Neither dNAR, dNIR, nor p450nor were found in every *Fusarium* species evaluated. The distribution of these genes also varied. Of the three key denitrification genes, p450nor had the broadest distribution, and dNAR had the narrowest distribution. This is confounding because, in theory, dNAR, dNIR, and p450nor should be present in all *Fusarium* species if the genes were horizontally transferred from bacteria to an early-diverging lineage of fungi. To evaluate this hypothesis, the OrthoFinder dataset was searched through to identify which of the 73 unique *Fusarium* species-strain combinations had various combinations of the three enzymes important in fungal denitrification (i.e., dNAR, dNIR, p450nor). Data from this search was compiled to know which of the *Fusarium* spp. in our dataset were denitrifiers or non-denitrifiers and to discover if there is a relationship between the ability to denitrify and lifestyle preferences (e.g., foliar vs. vascular, soil-borne vs. air-borne).

The fungal genus *Fusarium* has more than 50 denitrification capable species

Based on the ortholog analysis of the proteomes of 73 unique *Fusarium* species-strain combinations, 31.51% (23) have a dNAR ortholog; 71.24% (52) have a dNIR ortholog; and 84.94% (62) have a NOR1 ortholog (Table 2.4). 15.07% (11) do not have an ortholog of any of the three genes encoding reductases important to fungal denitrification including *F. zealandicum* NRRL 22465, *F. coffeatum* FIESC_28, *F. irregulare* CF00143, *F. sp.* FIESC RH6, *F.*

langsethiae FI201059, *F. sporotrichioides* NRRL 3299, *F. poae* 2516, *F. poae* DAOMC 252244, *F. venenatum* A3/5, *F. pseudograminearum* CS3096, and *F. culmorum* Class2-1B. Out of 73 *Fusarium* species and strains, 52 (71.2%) are predicted to denitrify based on the presence of genes with orthology to dNIR and p450nor in their genome. Only two (2.74%) species, *F. gaditjirri* and *F. mundagurra*, have an ortholog of dNAR and p450nor, but lack a dNIR ortholog. No *Fusarium* species examined had a combination of dNAR and dNIR but lacked p450nor; similarly, there were none that only had dNAR or dNIR.

The number of *Fusarium* species and strains that have at least one ortholog of dNAR, dNIR, and p450nor was 21 (28.77%). These species are "complete" denitrifiers, which means that they have the complete fungal denitrification pathway and may convert NO_3^- to N_2O without assistance from other microbes or assimilatory nitrate reductases. Complete denitrifiers include *F. verticillioides* 7600, *F. oxysporum* f. sp. *cubense* 160527, *F. oxysporum* Fo47, *F. oxysporum* f. sp. *conglutinans* Fo5176, *F. musae* F31, *F. duplospermum* NRRL 62584, *F. kuroshium* UCR3666, *F. oligoseptatum* NRRL 62579, *F. floridanum* NRRL 62606, *F. ambrosium* NRRL 20438, *F.* sp. Ph1, *F. keratoplasticum* Fu6.1, *F. oxysporum* f. sp. *cubense* Race 1, *F. oxysporum* NRRL 39464, *F. oxysporum* f. sp. *conglutinans* Race 2 54008, *F. acutatum* NRRL 13308, *F. anthophilum* NRRL 25214, *F. tjaetaba* NRRL 66243, *F. napiforme* NRRL 25196, *F. pseudoanthophilum* NRRL 25211, and *F. coicis* NRRL 66233.

The combination of dNIR and p450nor was found in 31 (42.47%) of the 73 proteomes. These fungi are not "complete" denitrifiers, but they do have a partial pathway that includes at least one ortholog of dNIR and p450nor. The genomic presence of both dNIR and p450nor satisfies the minimum requirements for fungal denitrification; the fungus can convert NO_2^- to N_2O. These fungi include *F. falciforme* Fu3.1, *F.* sp. LHS14.1, *F. vanettenii* 77-13-4, *F. solani-*

melongenae CRI 24-3, *F. solani* FSSC 5 MPI-SDFR-AT-0091, *F.* sp. FIESC 12 MPI-CAGE-AA-0113, *F. oxysporum* f. sp. *cepae* FoC_Fus2, *F. oxysporum* NRRL 32931, *F. odoratissimum* Race 4, *F. odoratissimum* NRRL 54006, *F. bulbicola* NRRL 25176, *F. mexicanum* NRRL 53147, *F.* sp. NRRL 52700, *F. phyllophilum* NRRL 13617, *F. subglutinans* NRRL 66333, *F. redolens* MPI-CAGE-AT-0023, *F. chuoi* FFSC RH1, *F. mangiferae* MRC7560, *F.* sp. NRRL 25303, *F. proliferatum* ET1, *F. fujikuroi* I1.3, *F. fujikuroi* IMI 58289, *F. globosum* NRRL 26131, *F. denticulatum* NRRL 25311, *F. pseudocircinatum* NRRL 36939, *F. austroafricanum* NRRL 25196, *F.* sp. MPI-SDFR-AT-0072, *F.* sp. DS 682, *F. decemcellulare* NRRL 13412, and *F. albosuccineum* NRRL 20459. Fungi that lack dNAR but possess at least one ortholog of dNIR and p450nor may still be able to reduce NO_3^- to NO_2^- using assimilatory nitrate reductase (aNAR). The assimilatory nitrate-reducing system is ubiquitously distributed among plants and microorganisms and long thought to function independently of the dissimilatory nitrate-reducing system. Preliminary studies show that deletion of dNAR (*F. verticillioides* NAR1) does not greatly impact N_2O production or fungal growth even when the fungus is grown in a medium amended with NO_3^- (data not shown). This suggests that there is crosstalk between the assimilatory and dissimilatory nitrogen metabolism pathways in *F. verticillioides*. This finding is bolstered by a study where *Cylindrocarpon tonkinense* (syn. *Fusarium tonkinense*) was shown to use the assimilatory system for dissimilatory purposes (i.e., producing ATP via denitrification) (Watsuji et al., 2003).

Only 10.96% (8/73) of *Fusarium* species and strains examined have a p450nor ortholog but lack dNAR and dNIR; these fungi are as follows: *F. graminearum* PH-1, *F. heterosporum* NRRL 20693, *F. tricinctum* MPI-SDFR-AT-0068, *F. sp.* NRRL 66182, *F. beomiforme* NRRL 25174, *F. torreyae* CF00136, *F. sarcochroum* NRRL 20472, and *F. graminum* FIESC 12 MPI-

CAGE-AA-0113. Non-denitrifying fungi that possess p450nor can produce N_2O, albeit in significantly lower amounts than complete or incomplete denitrifiers. It was previously reported that *F. graminearum*, the causal agent of Fusarium head blight of wheat (*Triticum aestivum*), produced a small amount of N_2O (0.08 ppm N_2O/mg) in an *in vitro* assay despite genomic data showing that it had no dNIR enzyme (Oakley et al., submitted). These results dispelled the notion that all N_2O-producing fungi are denitrifiers. At minimum, a denitrifying fungus must have a functional dNIR and p450nor enzyme to carry out the reduction of NO_2^- to N_2O.

As confirmation of the relative rarity of denitrification genes in the genus *Fusarium,* especially dNAR and dNIR, the frequency of occurrence of the other genes in Table 2.1 in the proteomes analyzed by OrthoFinder was examined. The flavohemoglobins (flavoHBs), or nitric oxide dioxygenases, are prime examples of single-protein metabolic modules, detoxifying NO to NO_3^-. These standalone metabolic units may be prone to gene duplication (GD) and HGT. Of the proteomes analyzed, 99% (72/73) had an ortholog of FHB1 (FVEG_11186); the only species lacking a FHB1 ortholog was *F. culmorum* Class2-1B (Supplementary Figure S2.1). Comparatively, 34 (47%) of the proteomes did not have an ortholog of FHB2 (FVEG_13827; Supplementary Figure S2.2). The phylogenetic analyses of the flavoHBs (Supplementary Figure S2.3) identified a third flavoHB (FVEG_14660), but it is not in the same OG (OG0003335) as FHB1 (FVEG_11186) or FHB2 (FVEG_13827), which are found in OGs OG0007166 and OG0012021, respectively. One-hundred percent (73/73) of the proteomes had this FHB3 ortholog (Supplementary Figure S2.4), but FHB3 was lowly expressed relative to FHB1 and FHB2 in *F. verticillioides* in both RNA-seq experiments (Supplementary Figure S2.5).

The fact that none of the flavoHBs are in the same orthogroup implies that each flavoHB in *F. verticillioides* has a unique evolutionary history. FlavoHBs function independently, so it is

thought they represent “plug-and-play” proteins for ecological arms races. Wisecaver et al., (2016) did a reconstruction of the evolutionary history of 3,318 flavoHB protein sequences that showed evidence of recurrent HGT at multiple evolutionary scales including intrabacterial HGT and HGT from bacteria to eukaryotes. Other flavoHBs arose via GD, which is why many filamentous fungi possess two flavoHBs that are differentially targeted to the cytosol and mitochondria to confer protection against external and internal sources of NO, respectively (Wisecaver et al., 2016). If a p450nor enzyme’s only function is to detoxify NO by reducing it to N_2O, it is puzzling why so many *Fusarium* spp. have integrated multiple flavoHBs into their genome that also function to detoxify NO. In fact, Higgins et al. (2018) found that there is a high correlation between p450nor and co-occurrence with genes encoding NO-detoxifying flavoHBs. This co-occurrence of p450nor with flavoHBs spurs questions about p450nor’s role outside of NO detoxification.

Analogous to our phylogenetic assessment of the flavoHBs, we identified a third formate/nitrite transporter (FNT3; FVEG_14575) (Supplementary Figure S2.6) that is not in the same OG (OG0013118; Supplementary Figure S2.7) as FNT1 and FNT2, which are in OG0000462 (Supplementary Figure S2.8). Of the 73 *Fusarium* species and strains included in the phylogenomic analysis, 31.5% (23/73) have three formate/nitrite transporter (FNT) homologs (e.g., FVEG_03704 + FVEG_08384 + FVEG_14575) and 54.8% (40/73) have two homologs. Some *Fusarium* species (4.1%; 3/73) have more than three FNT homologs and 9.6% (7/73) of tested species and strains have a single FNT. These include *F.* sp. MPI-SDFR-AT-0072 (5), *F. falciforme* Fu3.1 (4), *F. odoratissimum* NRRL 54006 (4), *F.* sp. LHS14.1 (1), *F. pseudograminearum* CS3096 (1), *F. odoratissimum* race 4 (1), *F langsethiae* Fl201059 (1), *F. sporotrichioides* NRRL 3299 (1), *F. floridanum* NRRL 62606 (1), and *F. zealandicum* NRRL

22465 (1). These results imply that FNT3 may have a different ancestry than FNT1 and FNT2. All three FNTs were significantly up-regulated when treated with 1.5 mM DETA-NONOate, FNT3 having the lowest expression. FNT1 (FVEG_03704) was significantly down-regulated when *F. verticillioides* was grown under low-oxygen conditions while FNT2 and FNT3 were significantly up-regulated, with FNT3 having the highest relative gene expression (Supplementary Figure S2.9).

NRT1 (FVEG_00877), FDH1 (FVEG_04761), NIA1 (FVEG_07298), NII1 (FVEG_02069), FNT1/FNT2 (FVEG_03704/FVEG_08384), FHB1 (FVEG_11186), FVEG_03775, and FVEG_10401 were found in 99-100% of the 73 unique species-strain combinations. These findings suggest that the genes that are not directly involved in denitrification commonly occur in genomes of fungi regardless of denitrification potential. The role, if any, of these proteins in the *F. verticillioides* denitrification pathway are largely uncharacterized. However, formate has been shown to be essential in regulating the denitrification pathway (Ma et al., 2008) and a gene with orthology to FDH1 (FVEG_04761), a formate dehydrogenase, in *F. oxysporum* was proven be coupled to dNAR and a ubiquinone/ubiquinol pool to facilitate dissimilation of NO_3^- (Uchimura et al., 2002). Additionally, Kuwazaki et al. (2003) showed that pyruvate is catabolized anaerobically by *F. oxysporum* to form formate and acetate and addition of nitrate decreased the accumulation of formate in the medium with concomitant formation of NO_2^- and N_2O. Together these results suggest that fungi use a unique metabolic pathway mediated by pyruvate-formate lyase to supply electrons via formate to fungal denitrification.

F. gaditjirri NRRL 45417, *F. musae* F31, and *F. odoratissimum* Race 4 are the only species-strains without a FVEG_10772 ortholog. FVEG_10772 is a hypothetical protein (172 aa)

with no predicted function, but it has a sulfite reductase domain (data not shown). It is of particular interest because in most cases where a *Fusarium* species has an ortholog of p450nor, an ortholog of FVEG_10772 is positioned upstream of it on the chromosome. The positionality of orthologs of FVEG_10772 and p450nor in *Fusarium* further raises questions about a potential role of p450nor in secondary metabolism. *F. floridanum* NRRL 62606 and both strains of *F. fujikuroi* (I1.3 and IMI 58289) lack an ortholog of FVEG_12326, an oxalate decarboxylase that catalyzes the conversion of oxalate to formate and CO_2. FVEG_12326 may function to supply extra formate to the coupling of dNAR and formate dehydrogenase for the reduction of NO_3^- to NO_2^-. Future investigation will be required to discover what the function of these proteins are in non-denitrifying and denitrifying fungi of the *Fusarium* genus.

Genomic potential to denitrify is found in a select number of *Fusarium* species complexes

Through this analysis of a diversity of *Fusarium* proteomes, it was found that complete and incomplete denitrifiers are found primarily in the Fujikuroi, Oxysporum, Solani, and Decemcellulare species complexes (O'Donnell et al., 2013). In parallel, non-denitrifying *Fusarium* species were found to be limited to a few sections and species complexes, taxonomic ranks below the genus level, including *F. culmorum, F. pseudograminearum, F. venenatum, F. graminearum,* and *F. heterosporum* (Discolor section), and *F. sporotrichioides, F. langsethiae, F. poae,* and *F. tricinctum* (Martiella section) (O'Donnell et al., 2013). Additionally, many species in the Sambucinum and Heterosporum species complexes do not have the ability to denitrify due to the lack of a dNIR ortholog. When examining the lifestyles of these fungi, it is apparent that the presence of a complete, or incomplete, denitrification pathway may influence fungal lifestyle preferences and survival in various macro- and micro-ecosystems. One example is that *F. oxysporum,* a denitrifier with multiple orthologs of p450nor, and *F. graminearum,* a

p450nor-containing non-denitrifier, have distinct lifestyles. *F. oxysporum* is a wilt-causing pathogen that infects through the roots and the plant vasculature, whereas *F. graminearum* is a foliar pathogen that most commonly infects through airborne spores landing on the heads of susceptible cereals. This difference in infection strategy may be partially due to their ability to denitrify or not. Differences in the ability to denitrify were also observed at a sub-species level for *Fusarium oxysporum* fungi. Out of the eight different strains, races, and formae speciales of *F. oxysporum*, six have the potential to reduce NO_3^- to N_2O including *F. oxysporum* Fo47, *F. oxysporum* f. sp. *conglutinans*, *F. oxysporum* f. sp. *cubense* race 1, *F. oxysporum* f. sp. *cubense* 160527, *F. oxysporum* NRRL 39464, and *F. oxysporum* f. sp. *conglutinans* race 2 54008; while two others, *F. oxysporum* f. sp. *cepae* FoC_Fus2 and *F. oxysporum* NRRL 32931, only have the potential to reduce NO_2^- to N_2O (i.e., incomplete denitrifiers).

Out of the sample population tested, only select *Fusarium* species and formae speciales fit the criteria of a denitrifier; thus, it is likely that some *Fusarium* species underwent gene loss during speciation. In an inter-genome analysis of gene family changes across fungal evolution inferred from 123 fungi and relatives, Merényi et al. (2023) described that the genomes of pre-fungal ancestors, such as protists, evolved into the typical filamentous fungal genome through gradual gene loss, turnover, and several large duplication events. Protists are thought to have arisen from bacteria. Because protists are suspected to have played a major role in eukaryotic evolution and are hypothesized to be the origin of eukaryotic cells from prokaryotic ancestries (eukaryogenesis) via endosymbiosis, it is probable that the denitrification pathway was vertically transferred from bacteria to early eukaryotes to fungi. Once in fungi, the denitrification genes may have been lost if they did not confer an evolutionary advantage to a specific fungus.

Skamnioti et al. (2008) investigated the contribution of gene families to the evolutionary forces shaping the diversity of lifestyles among five Ascomycota fungi. They found that the inventory of cutinase genes for each fungal species depends on the requirements of that fungus to successfully complete its life cycle. Therefore, fungi such as *Magnaporthe oryzae* and *F. graminearum* have an arsenal of cutinase genes due to their plant pathogenic lifestyle. This same logic may apply to *Fusarium* denitrifiers. Non-denitrifying *Fusarium* species that lack the genomic potential to denitrify may have experienced gene loss over time due to species-specific adaptations or changes in their ecological niches.

This report is the first study, to our knowledge, that assessed denitrification in the genus *Fusarium* using RNA sequencing, phylogenetics, and phylogenomics. More than ten genes were identified that are hypothesized to be important to fungal denitrification and orthologs of those genes in *F. verticillioides* were analyzed. Evidence for the incongruence of evolutionary histories between dNAR, dNIR, p450nor, and *Fusarium* species was also provided. Additionally, sub-groups of *Fusarium* fungi that have the highest frequency of denitrifiers and non-denitrifiers were pinpointed. This report is intended to inform future studies of denitrification in fungi and aid in community understanding of what a fungal denitrifier is and its genomic characteristics.

Literature Cited

Altschul, S. F., Gish, W., Miller, W., Myers, E. W., and Lipman, D. J. (1990). Basic local alignment search tool. J. Mol. Biol. 215, 403-410. doi: 10.1016/S0022-2836(05)80360-2

Amos, B. et al. (2022). VEuPathDB: the eukaryotic pathogen, vector and host bioinformatics resource center. Nucleic Acids Res. 50, D898-D911. doi: 10.1093/nar/gkab929

Anders, S. and Huber, W. (2010). Differential expression analysis for sequence count data. Genome Biol. 11, R106. doi: 10.1186/gb-2010-11-10-r106

Andrews, S. (2010). FastQC: a quality control tool for high throughput sequence data. Available online at: http://www.bioinformatics.babraham.ac.uk/projects/fastqc

Barrett, T., Wilhite, S. E., Ledoux, P., Evangelista, C., Kim, I. F., Tomashevsky, M., Marshall, K. A., Phillippy, K. H., Sherman, P. M., Holko, M., Yefanov, A., Lee, H., Zhang, N., Robertson, C. L., Serova, N., Davis, S., and Soboleva, A. (2013). NCBI GEO: archive for functional genomics data sets – update. Nucleic Acids Res. 41, D991-D995. doi: 10.1093/nar/gks1193

Basenko, E. Y. et al. (2018). FungiDB: An integrated bioinformatic resource for fungi and oomycetes. J. Fungi. 4, 39. doi: 10.3390/jof4010039

Bedmar, E. J., Robles, E. F., and Delgado, M. J. (2005). The complete denitrification pathway of the symbiotic, nitrogen-fixing bacterium *Bradyrhizobium japonicum.* Biochem. Soc. Trans. 33, 141-144. doi: 10.1042/BST0330141

Bellin, D., Asai, S., Delledonne, M., and Yoshioka, H. (2013). Nitric oxide as a mediator for defense responses. Mol. Plant Microbe Interact. 26, 271-277. doi: 10.1094/MPMI-09-12-0214-CR

Bergsten, J. (2005). A review of long-branch attraction. Cladistics. 21, 163-193.

Bolger, A. M., Lohse, M., and Usadel, B. (2014). Trimmomatic: a flexible trimmer for Illumina sequence data. Bioinformatics. 30, 2114-2120. doi: 10.1093/bioinformatics/btu170

Boratyn, G. M. et al. (2013). BLAST: a more efficient report with usability improvements. Nucleic Acids Res. 41, W29-W33. doi: 10.1093/nar/gkt282

Bouwman, A. F., Beusen, A. H. W., Griffioen, J., Van Groenigen, J. W., Hefting, M. M., Oenema, O., Van Puijenbroek, P. J. T. M., Seitzinger, S., Slomp, C. P., and Stehfest, E. (2013). Global trends and uncertainties in terrestrial denitrification and N_2O emissions. Phil. Trans. R. Soc. B. 368, 20130112. doi: 10.1098/rstb.2013.0112

Bouwman, A. F., Boumans, L. J. M., and Batjes, N. H. (2002). Emissions of N_2O and NO from fertilized fields: Summary of available measurement data. Glob. Biogeochem. Cycles. 16, 1058. doi: 10.1029/2001GB001811

Canfield, D. E., Glazer, A. N., and Falkowski, P. G. (2010). The evolution and future of Earth's nitrogen cycle. Science. 330, 192-196. doi: 10.1126/science.1186120

Cassman, K.G. et al. (2002) Agroecosystems, nitrogen-use efficiency, and nitrogen management. AMBIO 31, 132–140.

Castaldi, S. and Smith, K. A. (1998). Effect of cycloheximide on N_2O and NO_3^- production in a forest and an agricultural soil. Biol. Fertil. Soils. 27, 27-34.

Castellano-Hinojosa, A., Le Cocq, K., Charteris, A. F., Abadie, M., Chadwick, D. R., Clark, I. M., González-López, J., Bedmar, E. J., and Cardenas, L. M. (2021). Relative contributions of bacteria and fungi to nitrous oxide emissions following nitrate application in soils representing different land uses. Int. Biodeterior. Biodegrad. 159, 105199. doi: 10.1016/j.ibiod.2021.105199

Chen, F., Mackey, A. J., Stoeckert, Jr., C. J., and Roos, D. S. (2006). OrthoMCL-DB: querying a comprehensive multi-species collection of ortholog groups. Nucleic Acids Res. 34, D363-D368. doi: 10.1093/nar/gkj123

Chen, F., Mackey, A. J., Vermunt, J. K., and Roos, D. S. (2007). Assessing performance of orthology detection strategies applied to eukaryotic genomes. PLoS ONE. 2, e383. doi: 10.1371/journal.pone.0000383

Choquel, C., Geslin, E., Metzger, E., Filipsson, H. L., Risgaard-Petersen, N., Launeau, P., Giraud, M., Jauffrais, T., Jesus, B., and Mouret, A. (2021). Denitrification by benthic foraminifera and their contribution to N-loss from a fjord environment. Biogeosciences. 18, 327-341. doi: 10.5194/bg-18-327-2021

Coskun, D., Britto, D. T., Shi, W., and Kronzucker, H. J. (2017). How plant root exudates shape the nitrogen cycle. Trends Plant Sci. 22, 661-673. doi: 10.1016/j.tplants.2017.05.004

Dalsing, B. L., Truchon, A. N., Gonzalez-Orta, E. T., Milling, A. S., and Allen, C. (2015). *Ralstonia solanacearum* uses inorganic nitrogen metabolism for virulence, ATP production, and detoxification in the oxygen-limited host xylem environment. mBio. 6, e02471-14. doi: 10.1128/mBio.02471-14

Dick, A. A., Harlow, T. J., and Gogarten, J. P. (2017). Short branches lead to systematic artifacts when BLAST searches are used as surrogate for phylogenetic reconstruction. Mol. Phylogenet. Evol. 107, 338-344. doi: 10.1016/j.ympev.2016.11.016

Edgar, R., Domrachev, M., and Lash, A. E. (2002). Gene Expression Omnibus: NCBI gene expression and hybridization array data repository. Nucleic Acids Res. 30, 207-210. doi: 10.1093/nar/30.1.207

Emms, D. M. and Kelly, S. (2015). OrthoFinder: solving fundamental biases in whole genome comparisons dramatically improves orthogroup inference accuracy. Genome Biol. 16, 157. doi: 10.1186/s13059-015-0721-2

Emms, D. M. and Kelly, S. (2017). STRIDE: Species Tree Root Inference from Gene Duplication Events. Mol. Biol. Evol. 34, 3267-3278. doi: 10.1093/molbev/msx259

Emms, D. M. and Kelly, S. (2019). OrthoFinder: phylogenetic orthology inference for comparative genomics. Genome Biol. 20, 238. doi: 10.1186/s13059-019-1832-y

Emms, D. M. and Kelly, S. (preprint). STAG: Species Tree Inference from All Genes. bioRxiv. doi: 10.1101/267914

Fang, Y. et al. (2015). Microbial denitrification dominates nitrate losses from forest ecosystems. Proc. Natl. Acad. Sci. U.S.A. 112, 1470-1474. doi: 10.1073/pnas.1416776112

Felsenstein, J. (1985). Confidence limits on phylogenies: An approach using the bootstrap. Evolution. 39, 783-791.

Fischer, S., Brunk, B. P., Chen, F., Gao, X., Harb, O. S., Iodice, J. B., Shanmugam, D., Roos, D. S., and Stoeckert, Jr., C. J. (2011). Using OrthoMCL to assign proteins to OrthoMCL-DB groups or to cluster proteomes into new ortholog groups. Curr. Protoc. Bioinformatics. Chapter 6:6.12.1-6.12.19. doi: 10.1002/0471250953.bi0612s35

Food and Agriculture Organization of the United Nations (2016) World Fertilizer Trends and Outlook to 2019: Summary Report, FAO.

Fowler, D. et al. (2013). The global nitrogen cycle in the twenty-first century. Phil. Trans. R. Soc. B. 368, 20130164. doi: 10.1098/rstb.2013.0164

Galloway, J. N., Dentener, F. J., Capone, D. G., Boyer, E. W., Howarth, R. W., Seitzinger, S. P., Asner, G. P., Cleveland, C. C., Green, P. A., Holland, E. A., Karl, D. M. Michaels, A. F.,

Porter, J. H., Townsend, A. R., and Vörösmarty, C. J. (2004). Nitrogen cycles: past, present, and future. Biogeochemistry. 70, 153-226. doi: 10.1007/s10533-004-0370-0

Galloway, J. N., Townsend, A. R., Erisman, J. W., Bekunda, M., Cai, Z., Freney, J. R., Martinelli, L. A., Seitzinger, S. P., and Sutton, M. A. (2008). Transformation of the nitrogen cycle: Recent trends, questions, and potential solutions. Science. 320, 889-892. doi: 10.1126/science.1136674

Gorfer, M., Blumhoff, M., Klaubauf, S., Urban, A., Inselsbacher, E., Bandian, D., Mitter, B., Sessitsch, A., Wanek, W., and Strauss, J. (2011). Community profiling and gene expression of fungal assimilatory nitrate reductases in agricultural soil. ISME J. 5, 1771-1783.

Gu, X., Fu, Y-X., and Li, W-H. (1995). Maximum likelihood estimation of the heterogeneity of substitution rate among nucleotide sites. Mol. Biol. Evol. 12, 546-557.

Guindon, S., Dufayard, J-F., Lefort, V., Anisimova, M., Hordijk, W., and Gascuel, O. (2010). New algorithms and methods to estimate maximum-likelihood phylogenies: Assessing the performance of PhyML 3.0. Syst. Biol. 59, 307-321. doi: 10.1093/sysbio/syq010

Higgins, S. A., Schadt, C. W., Matheny, P. B., Löffler, F. E. (2018). Phylogenomics reveal the dynamic evolution of fungal nitric oxide reductases and their relationship to secondary metabolism. Genome Biol. Evol. 10, 2474-2489. doi: 10.1093/gbe/evy187

Hoang, D. T., Chernomor, O., von Haeseler, A., Minh, B. Q., and Vinh, L. S. (2018). UFBoot2: Improving the ultrafast bootstrap approximation. Mol. Biol. Evol. 35, 518-522. doi: 10.1093/molbev/msx281

Johnson, M., Zaretskaya, I., Raytselis, Y., Merezhuk, Y., McGinnis, S., and Madden, T. L. (2008). NCBI BLAST: a better web interface. Nucleic Acids Res. 36, W5-W9. doi: 10.1093/nar/gkn201

Jones, D. T., Taylor, W. R., and Thornton, J. M. (1992). The rapid generation of mutation data matrices from protein sequences. CABIOS. 8, 275-282.

Kalyaanamoorthy, S., Minh, B. Q., Wong, T. K. F., von Haeseler, A., and Jermiin, L. S. (2017). ModelFinder: fast model selection for accurate phylogenetic estimates. Nat. Methods. 14, 587-589. doi: 10.1038/nmeth.4285

Katoh, K., Misawa, K., Kuma, K-i., and Miyata, T. (2002). MAFFT: a novel method for rapid multiple sequence alignment based on fast Fourier transform. Nucleic Acids Res. 30, 3059-3066.

Katoh, K. and Standley, D. M. (2013). MAFFT multiple sequence alignment software version 7: Improvements in performance and usability. Mol. Biol. Evol. 30, 772-780. doi: 10.1093/molbev/mst010

Kizawa, H., Tomura, D., Oda, M., Fukamizu, A., Hoshino, T., Gotoh, O., Yasui, T., and Shoun, H. (1991). Nucleotide sequence of the unique nitrate/nitrite-inducible cytochrome P-450 cDNA from *Fusarium oxysporum.* J. Biol. Chem. 266, 10632-10637.

Kuwazaki, S., Takaya, N., Nakamura, A., and Shoun, H. (2003). Formate-forming fungal catabolic pathway to supply electrons to nitrate respiration. Biosci. Biotechnol. Biochem. 67, 937-939. doi: 10.1271/bbb.67.937

Ladha, J.K. et al. (2016) Global nitrogen budgets in cereals: a 50-year assessment for maize, rice, and wheat production systems. Sci. Rep. 6, 19355.

Laughlin, R. J., Rütting, T., Müller, C., Watson, C. J., and Stevens, R. J. (2009). Effect of acetate on soil respiration, N_2O emissions and gross N transformations related to fungi and bacteria in a grassland soil. Appl. Soil Ecol. 42, 25-30. doi: 10.1016/j.apsoil.2009.01.004

Laughlin, R. J. and Stevens, R. J. (2002). Evidence for fungal dominance of denitrification and codenitrification in a grassland soil. Soil Sci. Soc. Am. J. 66, 1540-1548.

Le, S. Q. and Gascuel, O. (2008). An improved general amino acid replacement matrix. Mol. Biol. Evol. 25, 1307-1320. doi: 10.1093/molbev/msn067

Li, L., Stoeckert, Jr., C. J., and Roos, D. S. (2003). OrthoMCL: Identification of ortholog groups for eukaryotic genomes. Genome Res. 13, 2178-2189. doi: 10.1101/gr.1224503

Li, X., Gao, D., Li, Y., Zheng, Y., Dong, H., Liang, X., Liu, M., and Hou, L. (2023). Increased nitrogen loading facilitates nitrous oxide production through fungal and chemodenitrification in estuarine and coastal sediments. Environ. Sci. Technol. 57, 2660-2671. doi: 10.1021/acs.est.2c06602

Liao, Y., Smyth, G. K., and Shi, W. (2013). The Subread aligner: fast, accurate and scalable read mapping by seed-and-vote. Nucleic Acids Res. 41, e108. doi: 10.1093/nar/gkt214

Lichtenberg, M., Line, L., Schrameyer, V., Jakobsen, T. H., Rybtke, M. L., Toyofuku, M., Nomura, N., Kolpen, M., Tolker-Nielsen, T., Kühl, M., Bjarnsholt, T., and Jensen, P. O. (2021). Nitric-oxide-driven oxygen release in anoxic *Pseudomonas aeruginosa.* iScience. 24, 103404. doi: 10.1016/j.isci.2021.103404

Ma, L-J. et al. (2010). Comparative genomics reveals mobile pathogenicity chromosomes in *Fusarium.* Nature. 464, 367-373. doi: 10.1038/nature08850

Ma, S., Shan, J., and Yan, X. (2017). N_2O emissions dominated by fungi in an intensively managed vegetable field converted from wheat-rice rotation. Appl. Soil Ecol. 116, 23-29. doi: 10.1016/j.apsoil.2017.03.021

Ma, W. K., Farrell, R. E., and Siciliano, S. D. (2008). Soil formate regulates the fungal nitrous oxide emission pathway. Appl. Environ. Microbiol. 74, 6690-6696. doi: 10.1128/AEM.00797-08

Maeda, K., Spor, A., Edel-Hermann, V., Heraud, C., Breuil, M-C., Bizouard, F., Toyoda, S., Yoshia, N., Steinberg, C., and Philippot, L. (2015). N_2O production, a widespread trait in fungi. Sci. Rep. 5, 9697. doi: 10.1038/srep09697

Merényi, Z., Krizsán, K., Sahu, N., Liu, X-B., Bálint, B., Stajich, J. E., Spatafora, J. W., and Nagy, L. G. (2023). Genomes of fungi and relatives reveal delayed loss of ancestral gene families and evolution of key fungal traits. Nat. Ecol. Evol. 7, 1221-1231. doi: 10.1038/s41559-023-02095-9

Millar, N., Robertson, G. P., Grace, P. R., Gehl, R. J., and Hoben, J. P. (2010). Nitrogen fertilizer management for nitrous oxide (N_2O) mitigation in intensive corn (Maize) production: an emissions reduction protocol for U.S. Midwest agriculture. Mitig. Adapt Strateg. Glob. Change. 15, 185-204. doi: 10.1007/s11027-010-9212-7

Minh, B. Q., Nguyen, M. A. T., and von Haeseler, A. (2013). Ultrafast approximation for phylogenetic bootstrap. Mol. Biol. Evol. 30, 1188-1195. doi: 10.1093/molbev/mst024

Minh, B. Q., Schmidt, H. A., Chernomor, O., Schrempf, D., Woodhams, M. D., von Haeseler, A., and Lanfear, R. (2020). IQ-TREE 2: New models and efficient methods for phylogenetic inference in the genomic era. Mol. Biol. Evol. 37, 1530-1534. doi: 10.1093/molbev/msaa015

Morozkina, E. V. and Kurakov, A. V. (2007). Dissimilatory nitrate reduction in fungi under conditions of hypoxia and anoxia: A review. Appl. Biochem. Microbiol. 43, 544-549. doi: 10.1134/S0003683807050079

Mothapo, N., Chen, H., Cubeta, M. A., Grossman, J. M., Fuller, F., and Shi, W. (2015). Phylogenetic, taxonomic and functional diversity of fungal denitrifiers and associated N_2O production efficacy. Soil Biol. Biochem. 83, 160-175. doi: 10.1016/j.soilbio.2015.02.001

Mothapo, N. V., Chen, H., Cubeta, M. A., and Shi, W. (2013). Nitrous oxide producing activity of diverse fungi from distinct agroecosystems. Soil Biol. Biochem. 66, 94-101. doi: 10.1016/j.soilbio.2013.07.004

Nguyen, L-T., Schmidt, H. A., von Haeseler, A., and Minh, B. Q. (2015). IQ-TREE: A fast and effective stochastic algorithm for estimating maximum-likelihood phylogenies. Mol. Biol. Evol. 32, 268-274. doi: 10.1093/molbev/msu300

Niehaus, E-M. et al. (2016). Comparative "omics" of the *Fusarium fujikuroi* species complex highlights differences in genetic potential and metabolite synthesis. Genome Biol. Evol. 8, 3574-3599. doi: 10.1093/gbe/evw259

O'Donnell, K., Rooney, A. P., Proctor, R. H., Brown, D. W., McCormick, S. P., Ward, T. J., Frandsen, R. J. N., Lysøe, E., Rehner, S. A., Aoki, T., Robert, V. A. R. G., Crous, P. W., Groenewald, J. Z., Kang, S., and Geiser, D. M. (2013). Phylogenetic analyses of *RPB1* and *RPB2* support a middle Cretaceous origin for a clade comprising all agriculturally and medically important fusaria. Fungal Genet. Biol. 52, 20-31. doi: 10.1016/j.fgb.2012.12.004

Oakley, B. A., Mitchell, T. R., Read, Q. D., Hibbs, G. T., Baldwin, T. T., Gold, S. E., and Glenn, A. E. (submitted). Identification of a key enzyme target for reducing agricultural emissions of nitrous oxide. Science Advances.

Pachauri, R.K. et al. (2014). Climate change 2014: synthesis report – contribution of working groups I, II and III to the fifth assessment report of the intergovernmental panel on climate change, IPCC.

Philippot, L. (2005). Denitrification in pathogenic bacteria: for better or worst? Trends Microbiol. 13, 191-192. doi: 10.1016/j.tim.2005.03.001

Price, M. N., Dehal, P. S., and Arkin, A. P. (2009). FastTree: Computing large minimum evolution trees with profiles instead of a distance matrix. Mol. Biol. Evol. 26, 1641-1650. doi: 10.1093/molbev/msp077

Price, M. N., Dehal, P. S., and Arkin, A. P. (2010). FastTree 2 – Approximately maximum-likelihood trees for large alignments. PLoS ONE. 5, e9490. doi: 10.1371/journal.pone.0009490

Ravishankara, A. R., Daniel, J. S., and Portmann, R. W. (2009). Nitrous oxide (N_2O): The dominant ozone-depleting substance emitted in the 21st century. Science. 326, 123-125. doi: 10.1126/science.1176985

Revsbech, N. P., Cedhagen, T., and van der Zwaan, G. J. (2006). Evidence for complete denitrification in a benthic foraminifer. Nature. 443, 93-96. doi: 10.1038/nature05070

Risgaard-Petersen, N., Langezaal, A. M., Ingvardsen, S., Schmid, M. C., Jetten, M. S. M., Op den Camp, H. J. M., Derksen, J. W. M., Piña-Ochoa, E., Eriksson, S. P., Nielsen, L. P.,

Woehle, C., Roy, A-S. Glock, N., Wein, T., Weissenbach, J., Rosenstiel, P., Hiebenthal, C., Michels, J., Schönfeld, J., and Dagan, T. (2018). A novel eukaryotic denitrification pathway in foraminifera. Curr. Biol. 28, 2536-2543. doi: 10.1016/j.cub.2018.06.027

Robinson, M. D., McCarthy, D. J., and Smyth, G. K. (2010). edgeR: a Bioconductor package for differential expression analysis of digital gene expression data. Bioinformatics. 26, 139-140. doi: 10.1093/bioinformatics/btp616

Sang, J., Zhang, A., Lin, F., Tan, M., and Jiang, M. (2008). Cross-talk between calcium-calmodulin and nitric oxide in abscisic acid signaling in leaves of maize plants. Cell Res. 18, 577-588. doi: 10.1038/cr.2008.39

Scheer, C., Fuchs, K., Pelster, D. E., and Butterbach-Bahl, K. (2020). Estimating global terrestrial denitrification from measured N_2O: (N_2O + N_2) product ratios. Curr. Opin. Environ. Sustain. 47, 72-80. doi: 10.1016/j.cosust.2020.07.005

Schinko, T., Gallmetzer, A., Amillis, S., and Strauss, J. (2013). Pseudo-constitutivity of nitrate-responsive genes in nitrate reductase mutants. Fungal Genet. Biol. 54, 34-41. doi: 10.1016/j.fgb.2013.02.003

Schlesinger, W.H. (2009). On the fate of anthropogenic nitrogen. Proc. Natl. Acad. Sci. U. S. A. 106, 203–208.

Shcherbak, I., Millar, N., and Robertson, G. P. (2014). Global metaanalysis of the nonlinear response of soil nitrous oxide (N_2O) emissions to fertilizer nitrogen. Proc. Natl. Acad. Sci. U.S.A. 111, 9199-9204. doi: 10.1073/pnas.1322434111

Shoun, H., Fushinobu, S., Jiang, L., Kim, S-W., and Wakagi, T. (2012). Fungal denitrification and nitric oxide reductase cytochrome P450nor. Phil. Trans. R. Soc. B. 367, 1186-1194. doi: 10.1098/rstb.2011.0335

Shoun, H., Kim, D-H., Uchiyama, H., and Sugiyama, J. (1992). Denitrification by fungi. FEMS Microbiol. Lett. 94, 277-282.

Siverio, J. M. (2002). Assimilation of nitrate by yeasts. FEMS Microbiol. Rev. 26, 277-284.

Skamnioti, P., Furlong, R. F., and Gurr, S. J. (2008). The fate of gene duplicates in the genomes of fungal pathogens. Commun. Integr. Biol. 1, 196-198.

Song, M., Xu, X., Hu, Q., Tian, Y., Ouyang, H., and Zhou, C. (2007). Interactions of plant species mediated plant competition for inorganic nitrogen with soil microorganisms in an alpine meadow. Plant Soil. 297, 127-137. doi: 10.1007/s11104-007-9326-1

Soubrier, J., Steel, M., Lee, M. S. Y., Der Sarkissian, C., Guindon, S., Ho, S. Y. W., and Cooper, A. (2012). The influence of rate heterogeneity among sites on the time dependence of molecular rates. Mol. Biol. Evol. 29, 3345-3358. doi: 10.1093/molbev/mss140

Trivedi, R. and Nagarajaram, H. A. (2020). Substitution scoring matrices for proteins – An overview. Protein Sci. 29, 2150-2163. doi: 10.1002/pro.3954

Tschiersch, H., Liebsch, G., Borisjuk, L., Stangelmayer, A., and Rolletschek, H. (2012). An imaging method for oxygen distribution, respiration and photosynthesis at a microscopic level of resolution. New Phytol. 196, 926-936. doi: 10.1111/j.1469-8137.2012.04295.x

Tsuruta, S., Takaya, N., Zhang, L., Shoun, H., Kimura, K., Hamamoto, M., and Nakase, T. (1998). Denitrification by yeasts and occurrence of cytochrome P450nor in *Trichosporon cutaneum*. FEMS Microbiol. Lett. 168, 105-110.

Uchimura, H., Enjoji, H., Seki, T., Taguchi, A., Takaya, N., and Shoun, H. (2002). Nitrate reductase-formate dehydrogenase couple involved in the fungal denitrification by *Fusarium oxysporum*. J. Biochem. 131, 579-586.

Usuda, K., Toritsuka, N., Matsuo, Y., Kim, D-H., and Shoun, H. (1995). Denitrification by the fungus *Cylindrocarpon tonkinense*: anaerobic cell growth and two isozyme forms of cytochrome P-450nor. Appl. Environ. Microbiol. 61, 883-889.

van der Salm, C., Dolfing, J., Heinen, M., and Velthof, G. L. (2007). Estimation of nitrogen losses via denitrification from a heavy clay soil under grass. Agric. Ecosyst. Environ. 119, 311-319. doi: 10.1016/j.agee.2006.07.018

Veraart, A. J., de Klein, J. J. M., and Scheffer, M. (2011). Warming can boost denitrification disproportionately due to altered oxygen dynamics. PLoS One. 6, e18508. doi: 10.1371/journal.pone.0018508

Wang, Y., Ji, H., Wang, R., Hu, Y., and Guo, S. (2020). Synthetic fertilizer increases denitrifier abundance and depletes subsoil total N in a long-term fertilization experiment. Front. Microbiol. 11, 2026. doi: 10.3389/fmicb.2020.02026

Wankel, S. D., Ziebis, W., Buchwald, C., Charoenpong, C., de Beer, D., Dentinger, J., Xu, Z., and Zengler, K. (2017). Evidence for fungal and chemodenitrification based N_2O flux from nitrogen impacted coastal sediments. Nat. Commun. 8, 15595. doi: 10.1038/ncomms15595

Crenshaw, C. L., Lauber, C., Sinsabaugh, R. L., and Stavely, L. K. (2008). Fungal control of nitrous oxide production in semiarid grassland. Biogeochemistry. 87, 17-27. doi: 10.1007/s10533-007-9165-4

Watsuji, T. O., Takaya, N., Nakamura, A., and Shoun, H. (2003). Denitrification of nitrate by the fungus *Cylindrocarpon tonkinense.* Biosci. Biotechnol. Biochem. 67, 1115-1120. doi: 10.1271/bbb.67.1115

Wisecaver, J. H., Alexander, W. G., King, S. B., Hittinger, C. T., and Rokas, A. (2016). Dynamic evolution of nitric oxide detoxifying flavohemoglobins, a family of single-protein metabolic modules in bacteria and eukaryotes. Mol. Biol. Evol. 33, 1979-1987. doi: 10.1093/molbev/msw073

Woehle, C., Roy, A-S., Glock, N., Michels, J., Wein, T., Weissenbach, J., Romero, D., Hiebenthal, C., Gorb, S. N., Schönfeld, J., and Dagan, T. (2022). Denitrification in foraminifera has an ancient origin and is complemented by associated bacteria. Proc. Natl. Acad. Sci. U.S.A. 119, e2200198119. doi: 10.1073/pnas.2200198119

Yanai, Y., Toyota, K., Morishita, T., Takakai, F., Hatano, R., Limin, S. H., Darung, U., and Dohong, S. (2007). Fungal N_2O production in an arable peat soil in Central Kalimantan, Indonesia. Soil Sci. Plant Nutr. 53, 806-811. doi: 10.1111/j.1747-0765.2007.00201.x

Yang, Z. (1994). Maximum likelihood phylogenetic estimation from DNA sequences with variable rates over sites: Approximate methods. J. Mol. Evol. 39, 306-314.

Yang, Z. (1995). A space-time process model for the evolution of DNA sequences. Genetics. 139, 993-1005.

Ye, R. W., Averill, B. A., and Tiedje, J. M. (1994). Denitrification: Production and consumption of nitric oxide. Appl. Environ. Microbiol. 60, 1053-1058.

Zhang, A., Jiang, M., Zhang, J., Ding, H., Xu, S., Hu, X., and Tan, M. (2007). Nitric oxide induced by hydrogen peroxide mediates abscisic acid-induced activation of the mitogen-activated protein kinase cascade involved in antioxidant defense in maize leaves. New Phytol. 175, 36-50. doi: 10.1111/j.1469-8137.2007.02071.x

Zhou, Z., Takaya, N., Sakairi, M. A. C., and Shoun, H. (2001). Oxygen requirement for denitrification by the fungus *Fusarium oxysporum.* Arch. Microbiol. 175, 19-25. doi: 10.1007/s002030000231

Zumft, W. G. (1997). Cell biology and molecular basis of denitrification. Microbiol. Mol. Biol. Rev. 61, 533-616

Zumft, W. G., Braun, C., and Cuypers, H. (1994). Nitric oxide reductase from *Pseudomonas stutzeri* - Primary structure and gene organization of a novel bacterial cytochrome *bc* complex. Eur. J. Biochem. 219, 481-490.

Tables

Table 2.1. log2 fold change of denitrification-associated *Fusarium verticillioides* genes in response to nitric oxide or hypoxia.

Locus	Gene	Putative Function	log2 NO[b]	log2 Hypoxia[c]
FVEG_07298[a]	*NIA1*	Assimilatory nitrate reductase	4.5	5.3
FVEG_02069	*NII1*	Assimilatory nitrite reductase	6.3	2.3
FVEG_01721	*NAR1*	Dissimilatory nitrate reductase	1.7	3.3
FVEG_08676[a]	*DNI1*	Dissimilatory nitrite reductase	7.6	9.7
FVEG_10773[a]	*NOR1*	P450 Nitric oxide reductase	5.0	14.1
FVEG_11186[a]	*FHB1*	Flavohemoglobin	3.0	4.8
FVEG_13827	*FHB2*	Flavohemoglobin	2.3	4.9
FVEG_08384[a]	*FNT1*	Formate/nitrite transporter	3.6	3.6
FVEG_03704	*FNT2*	Formate/nitrite transporter	2.1	-4.3
FVEG_04761[a]	*FDH1*	Formate dehydrogenase	3.7	3.4
FVEG_00877	*NRT1*	Nitrate transporter	3.5	-4.9
FVEG_04246	*NIR1*	Nitrate specific regulator	-0.1	-0.7
FVEG_12326[a]	FVEG_12326	Oxalate decarboxylase	3.2	3.1
FVEG_10772[a]	FVEG_10772	Unknown	4.0	5.8
FVEG_10401[a]	FVEG_10401	Transcriptional regulator	5.4	3.0
FVEG_03775[a]	FVEG_03775	ABC transporter	3.5	4.0

A table of 16 genes that were significantly differentially regulated in response to NO, hypoxia or both using RNA-seq. The locus tag (FVEG_XXXXX) is the identifier systematically applied to genes in the genome. Locus tags are used as a surrogate gene name when a gene name has not been determined. The gene name is the designation commonly used by the biological

community. The putative function is a prediction of the protein a gene is believed to encode based on sequence similarities to already characterized/named genes.

[a]Ten genes were induced ≥8-fold in response to both nitric oxide (NO) and hypoxia. Six other genes of interest involving metabolism of nitrogen oxides were induced ≥8-fold in response to only one of the two treatments.
[b] Change in gene expression (presented as log2 values) due to exposure to nitric oxide (NO).
[c] Change in gene expression (presented as log2 values) due to hypoxic growth conditions.

Table 2.2. Summary statistics of OrthoFinder2 analysis of 75 *Fusarium* proteomes

Number of species	75
Number of genes	1133937
Number of genes in orthogroups	1118700
Number of unassigned genes	15237
Percentage of genes in orthogroups	98.7
Percentage of unassigned genes	1.3
Number of orthogroups	27687
Number of species-specific orthogroups	557
Number of genes in species-specific orthogroups	1613
Percentage of genes in species-specific orthogroups	0.1
Mean orthogroup size	40.4
Median orthogroup size	20.0
G50 (assigned genes)	76
G50 (all genes)	76
O50 (assigned genes)	5537
O50 (all genes)	5637
Number of orthogroups with all species present	3042
Number of single-copy orthologs	628

Average number of genes per-species in orthogroup	Number of orthogroups	Percentage of orthogroups	Number of genes	Percentage of genes
<1	20367	73.6	425034	38.0
1	6822	24.6	588138	52.6
2	364	1.3	64489	5.8
3	87	0.3	22040	2.0
4	27	0.1	8818	0.8
5	10	0.0	4128	0.4
6	3	0.0	1489	0.1
7	4	0.0	2248	0.2
8	1	0.0	607	0.1
9	0	0.0	0	0.0
10	1	0.0	824	0.1
11-15	1	0.0	885	0.1
16-20	0	0.0	0	0.0
21-50	0	0.0	0	0.0
51-100	0	0.0	0	0.0
101-150	0	0.0	0	0.0
151-200	0	0.0	0	0.0
201-500	0	0.0	0	0.0
501-1000	0	0.0	0	0.0

Table 2.3. Species-specific summary statistics from OrthoFinder 2 analysis of *Fusarium verticillioides* 7600 proteome (GCA_000149555.1)

	GCA_000149555.1_protein
Number of genes	20553
Number of genes in orthogroups	20044
Number of unassigned genes	509
Percentage of genes in orthogroups	97.5
Percentage of unassigned genes	2.5
Number of orthogroups containing species	13280
Percentage of orthogroups containing species	48.0
Number of species-specific orthogroups	88
Number of genes in species-specific orthogroups	331
Percentage of genes in species-specific orthogroups	1.6

Table 2.4. Pairwise combinations of fungal denitrification reductase enzymes and their frequency of occurrence in genomes of 73 different species-strains of *Fusarium* fungi.

Fungal denitrification reductase enzymes	% of *Fusarium* species-strain combinations
dNAR + dNIR + NOR[a]	28.77 (= 21/73)
dNAR + dNIR[c]	0.00 (= 0/73)
dNIR + NOR[b]	42.47 (=31/73)
dNAR + NOR[c]	2.74 (= 2/73)
dNAR[c]	0.00 (= 0/73)
dNIR[c]	0.00 (=0/73)
NOR[c]	10.96 (= 8/73)
None[c]	15.07 (= 11/73)
Total	100.00 (= 73/73)

[a] dNAR + dNIR + NOR are the three enzymes a fungus needs to convert NO_3^- to N_2O and be a "complete" fungal denitrifier; [b] dNIR + NOR are the essential enzymes needed to convert NO_2^- to N_2O and be an "incomplete" fungal denitrifier; [c] Any fungus that is not predicted to have at least dNIR + NOR is not a denitrifier

Figures

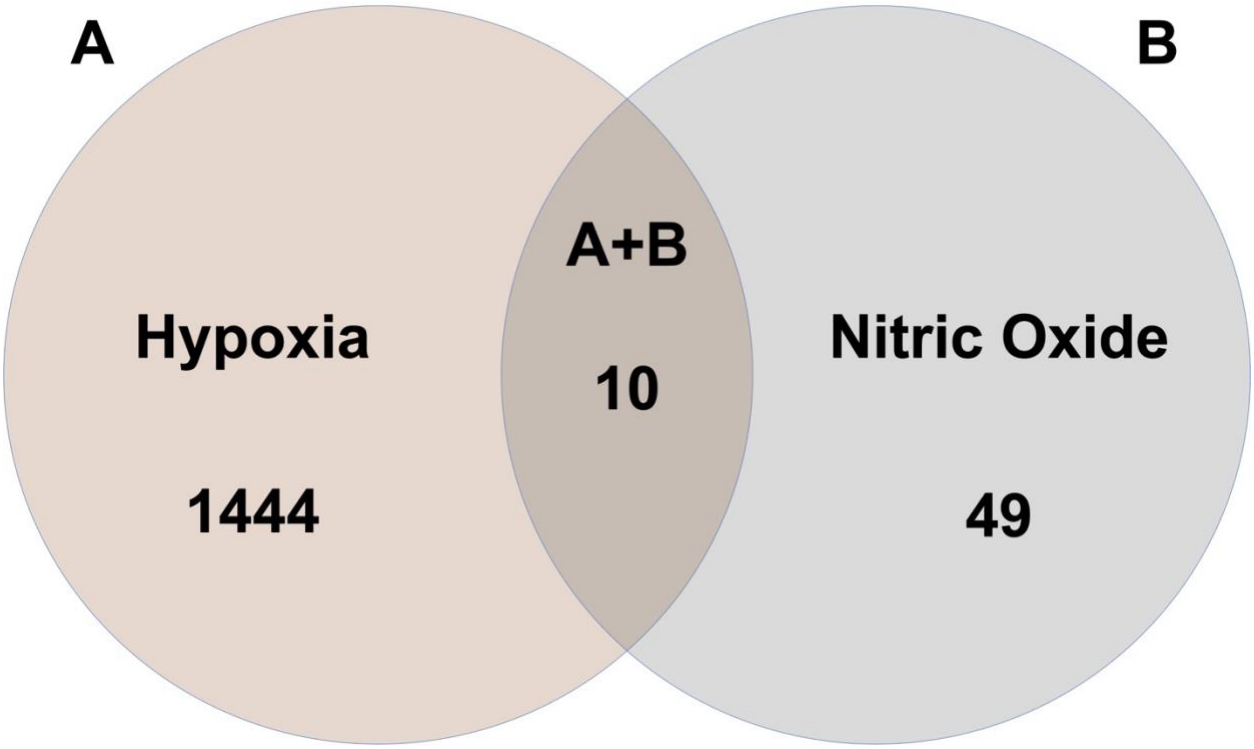

Figure 2.1. **Venn diagram of the number of differentially expressed genes in wild-type *Fusarium verticillioides* when (A) grown under hypoxia or (B) treated with DETA-NONOate, a NO donor.** The genes represented in the A or B circles of the Venn diagram are those that were up- or down-regulated more than 2-fold in a single treatment. The genes represented in the intersecting A+B portion were up- or down-regulated more than eight-fold across both treatments.

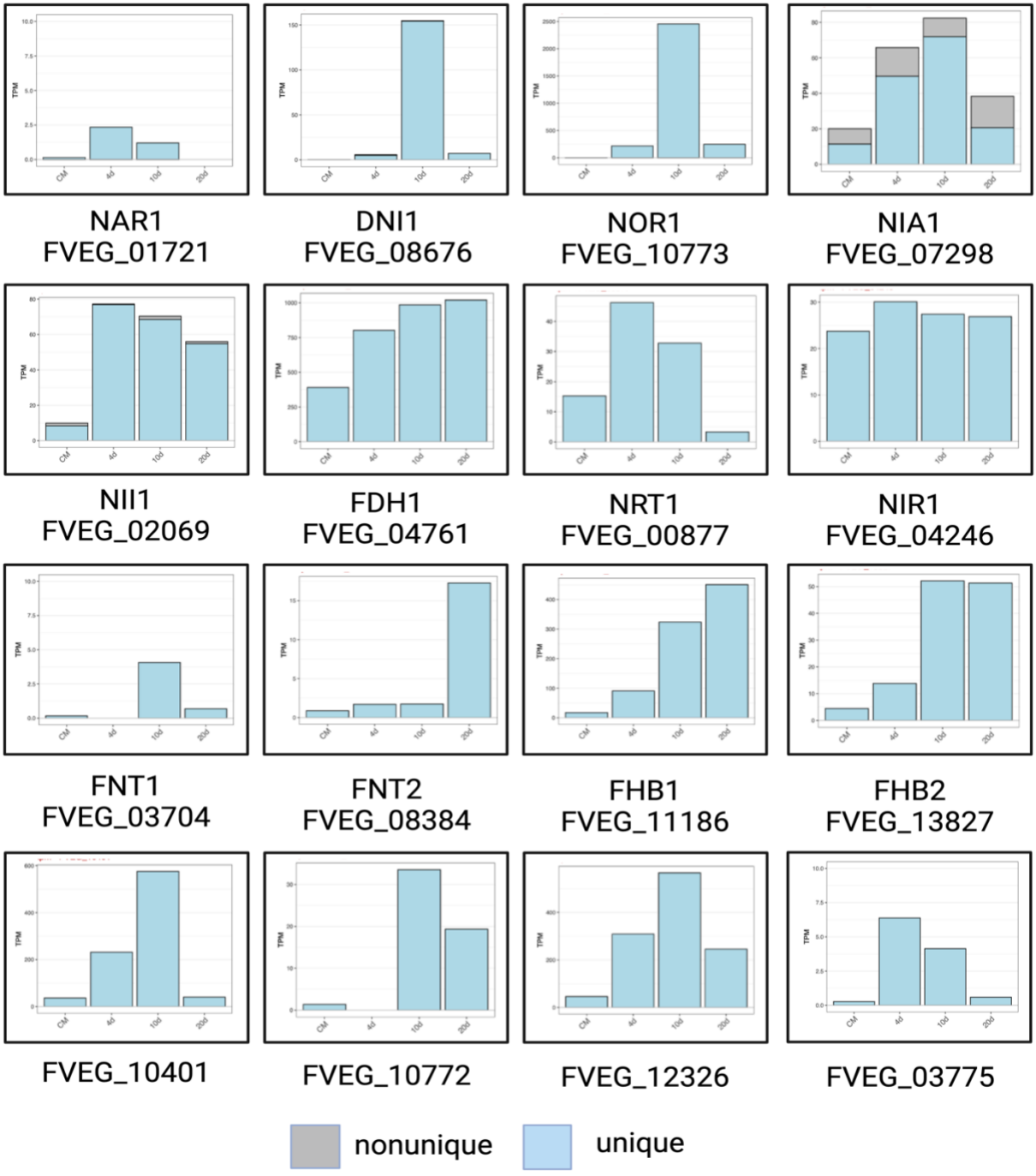

Figure 2.2. Transcriptional analysis of *Fusarium verticillioides* during infection of maize seedlings or when grown *in vitro* on CM agar. Transcript abundance is measured in transcripts per million (TPM). CM = culture medium; 4d, 10d, and 20d are timepoints for RNA-sampling from maize roots. Gray bars represent nonunique reads and blue bars represent unique reads. This RNA-seq data was mined from Niehaus et al. (2016) and FungiDB. Created with BioRender.com

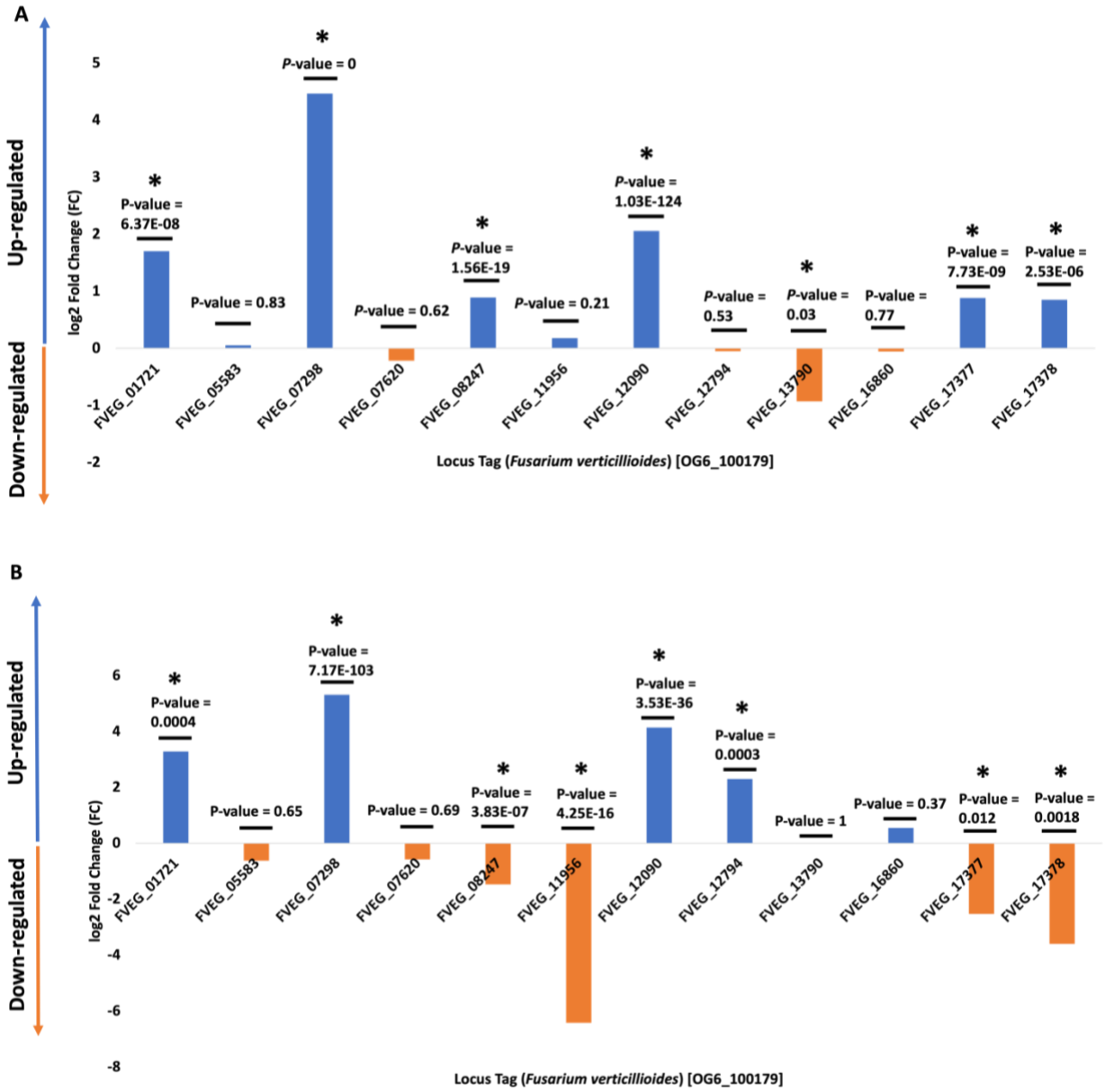

Figure 2.3. Expression levels of all genes within the OrthoMCL orthogroup OG6_100179 across both RNA-seq experiments. Expression levels have been transformed to log2 fold-change. Significantly up-regulated (blue) or down-regulated (orange) genes, as determined by p-value statistic, are indicated by an asterisk. (A) 0 vs. 1.5 mM DETA-NONOate; (B) Normoxia vs. Hypoxia

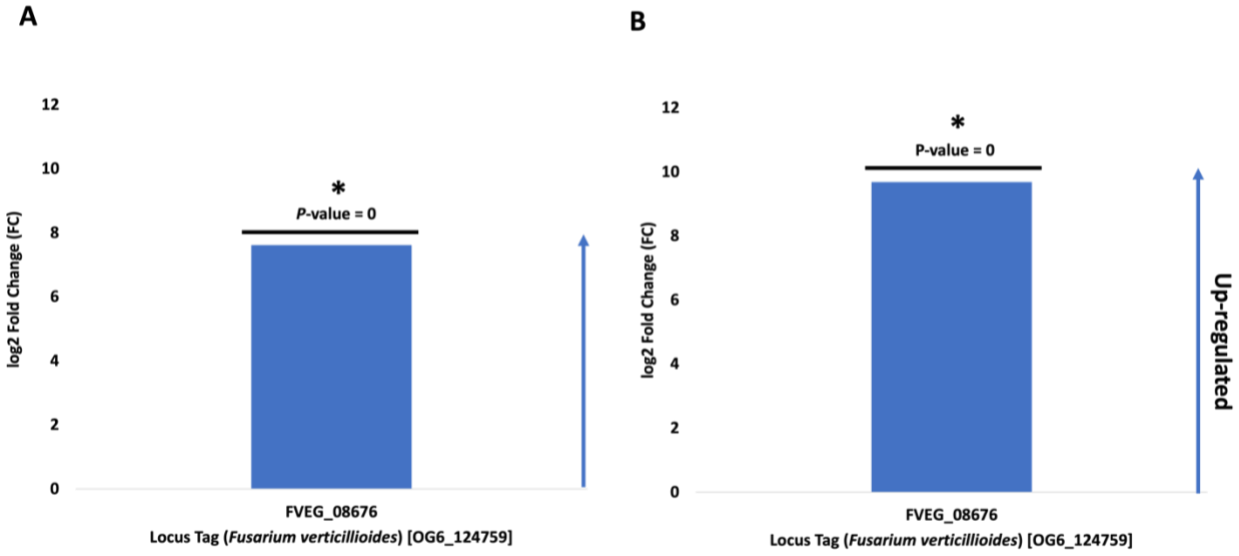

Figure 2.4. Expression levels of the single wild type *Fusarium verticillioides* gene (FVEG_08676) within the OrthoMCL orthogroup OG6_124759 across both RNA-seq experiments. Expression levels have been transformed to log2 fold-change. Significantly up-regulated (blue) genes, as determined by *p*-value statistic, are indicated by an asterisk. (A) 0 vs. 1.5 mM DETA-NONOate; (B) Normoxia vs. Hypoxia

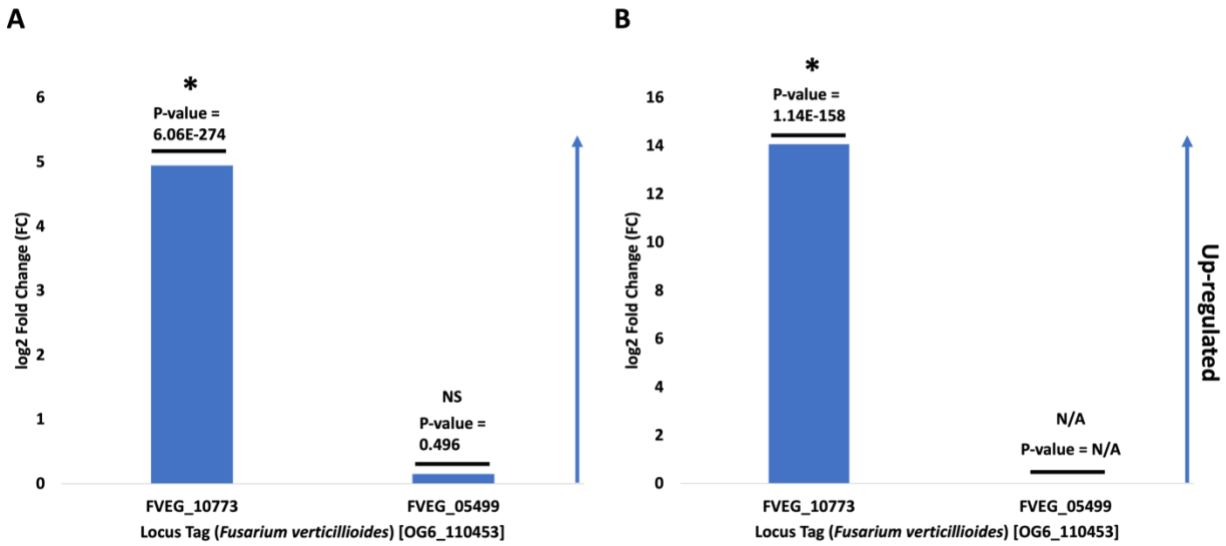

Figure 2.5. Expression levels of FVEG_10773 and FVEG_05499 genes of *Fusarium verticillioides* within the OrthoMCL orthogroup OG6_110453 across both RNA-seq experiments. Expression levels have been transformed to log2 fold-change. FVEG_10773 but not FVEG_05499 was up-regulated as determined by the *p*-value statistic, which is indicated by an asterisk. (A) 0 vs. 1.5 mM DETA-NONOate; (B) Normoxia vs. Hypoxia

Figure 2.6. Protein tree of assimilatory (NIA1) and dissimilatory nitrate reductase (NAR1) from fungi and Oomycota. A dataset of 1,040 sequences was aligned using MAFFT. A clade containing *Pseudomonas aeruginosa* Q9HTF3 and Q9HUT1 was used as the outgroup. The phylogeny is rooted to the sole bacterial species in the phylogeny. Maximum-likelihood trees were built using IQ-TREE (v1.6.12). ModelFinder identified the best substitution model as LG+R10 according to Bayesian Information Criterion (BIC). The phylogeny was re-run using the LG+R10 model with 1,000 SH-aLRT and UFBoot replicates to assess phylogenetic relationships. The branch labels are colored according to split support values represented as SH-aLRT support (%) / ultrafast bootstrap support (%). Clades are not collapsed and support values for relationships between samples at sub-genus level clades and at individual branches are shown in this representation. Scale bar (0.9) is at the bottom of the phylogeny. Important fungal genera are colored as follows: *Fusarium* (red), *Trichoderma* (green), *Alternaria* (blue), *Colletotrichum* (purple), *Penicillium* (orange), and *Aspergillus* (pink); other fungal genera are colored black. Tree visualization was done using FigTree (v1.4.4).

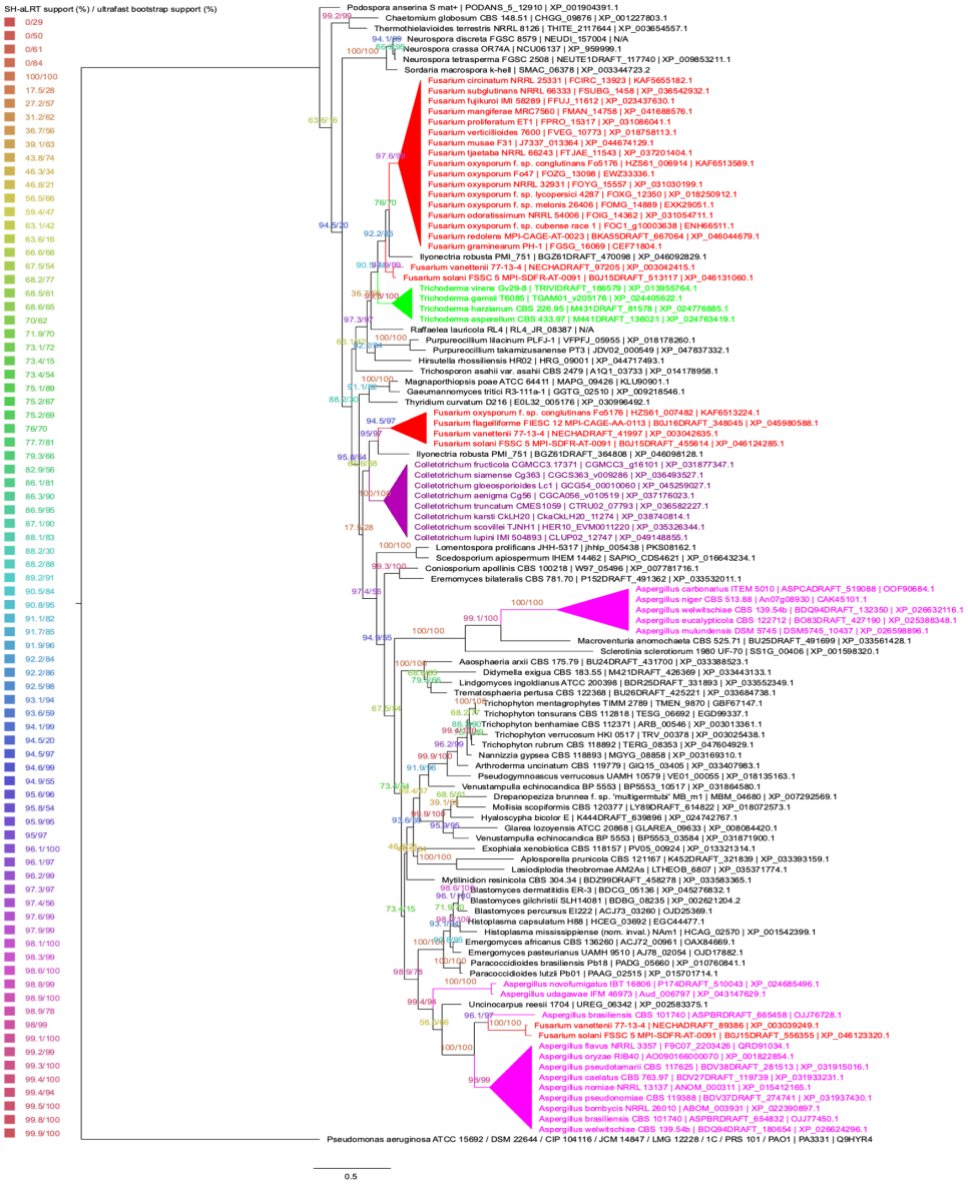

Figure 2.7. Protein tree of cytochrome P450 nitric oxide reductase (NOR1) from fungi A dataset of 110 sequences was aligned using MAFFT. *Pseudomonas aeruginosa* Q9HYR4 was used as the outgroup and the phylogeny is rooted to this sole bacterium included. Maximum-likelihood trees were built using IQ-TREE (v1.6.12). ModelFinder identified the best substitution model as LG+G4 according to Bayesian Information Criterion (BIC). The phylogeny was run using the LG+G4 model with 1,000 SH-aLRT and UFBoot replicates to assess phylogenetic relationships. The branch labels are colored according to split support values represented as SH-aLRT support (%) / ultrafast bootstrap support (%). Clades are not collapsed and support values for relationships between samples at sub-genus level clades and at individual branches are shown in this representation. Scale bar (0.5) is at the bottom of the phylogeny. Important fungal genera are colored as follows: *Fusarium* (red), *Trichoderma* (green), *Colletotrichum* (purple), *Penicillium* (orange), and *Aspergillus* (pink); other fungal genera are colored black. Tree visualization was done using FigTree (v1.4.4).

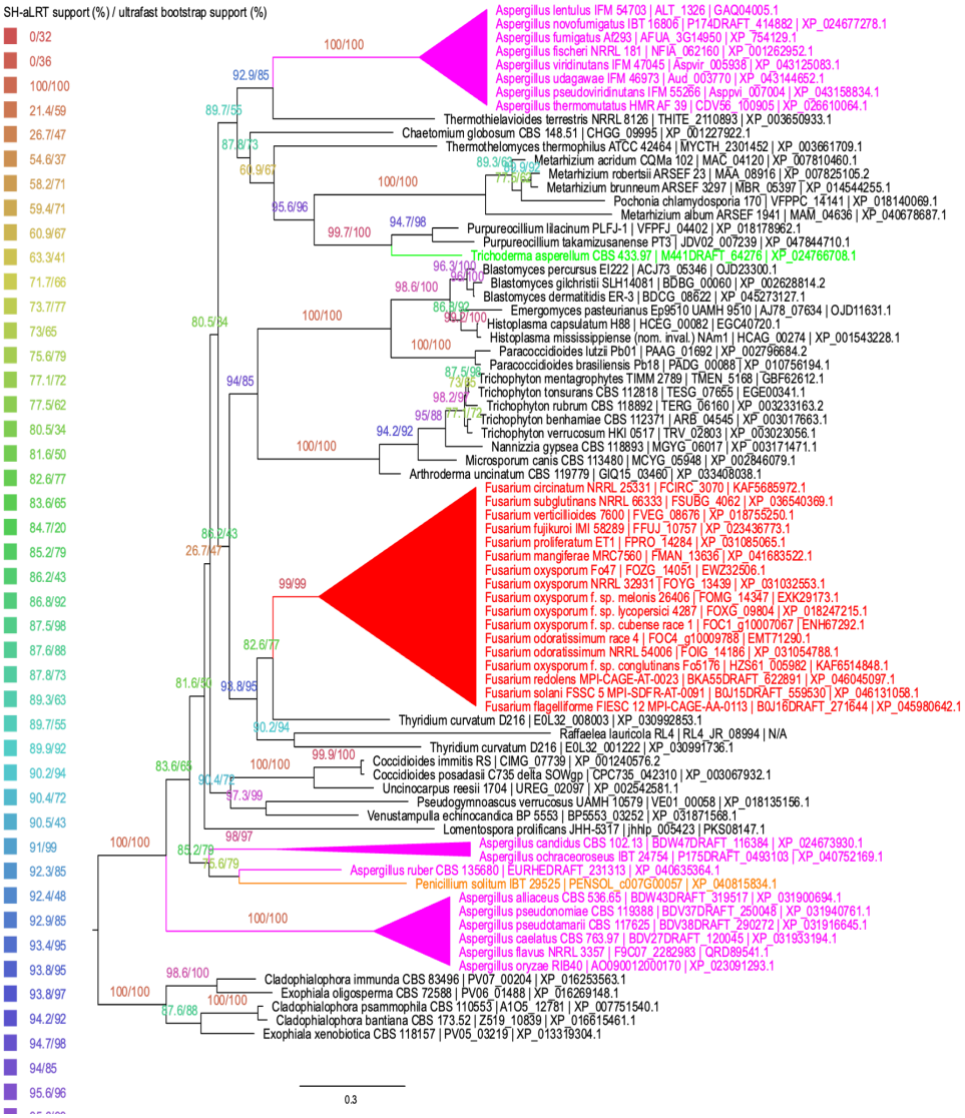

Figure 2.8. Protein tree of dissimilatory nitrite reductase (DNI1) from fungi. A dataset of 76 sequences was aligned using MAFFT. A clade containing *Cladophialophora immunda* CBS 83496 PV07_00204, *Exophiala oligosperma* CBS 72588 PV06_01488, *Cladophialophora psammophila* CBS 110553 A1O5_12781, *Cladophialophora bantiana* CBS 173.52 Z519_10839, and *Exophiala xenobiotica* CBS 118157 PV05_03219 was used as the outgroup. Maximum-likelihood trees were built using IQ-TREE (v1.6.12). ModelFinder identified the best substitution model as JTT+I+G4 according to Bayesian Information Criterion (BIC). The phylogeny was re-run using the JTT+I+G4 model with 1,000 SH-aLRT and UFBoot replicates to assess phylogenetic relationships. The branch labels are colored according to split support values represented as SH-aLRT support (%) / ultrafast bootstrap support (%). Clades are not collapsed and support values for relationships between samples at sub-genus level clades and at individual branches are visible in this representation. Scale bar (0.3) is at the bottom of the phylogeny. Important fungal genera are colored as follows: *Fusarium* (red), *Trichoderma* (green), *Colletotrichum* (purple), *Penicillium* (orange), and *Aspergillus* (pink); other fungal genera are colored black. Tree visualization was done using FigTree (v1.4.4).

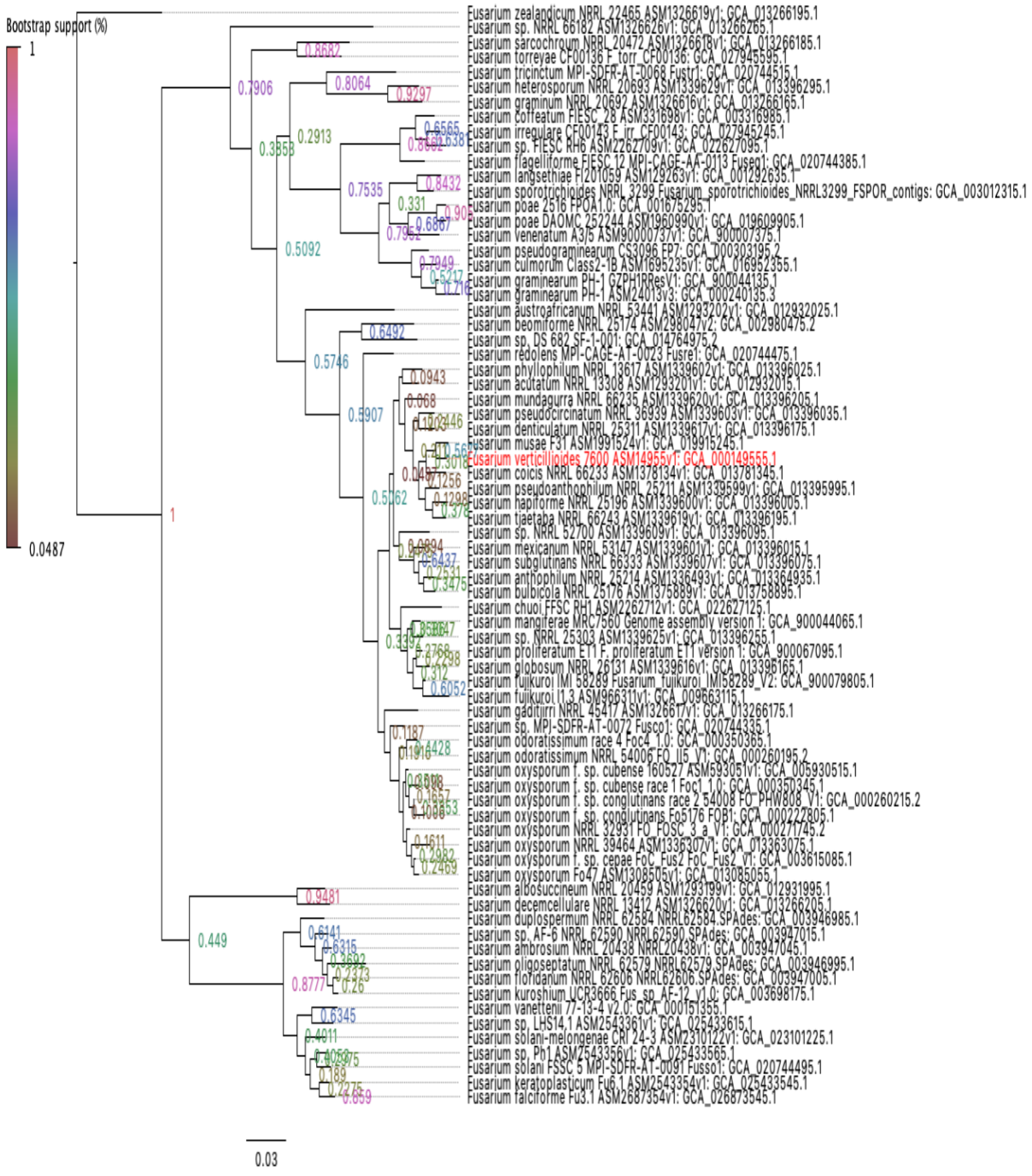

Figure 2.9. Inferred species tree based on OrthoFinder analysis of proteomes from 73 *Fusarium* species-strain combinations. This tree has been inferred using the STAG algorithm and rooted using the STRIDE algorithm. This tree is rooted to *Fusarium zealandicum* NRRL 22465. *Fusarium verticillioides* 7600, the primary fungus of interest in this paper, has been highlighted in red. Scale bar is 0.03. Support values are represented as bootstrap support (%). Node labels are colored according to bootstrap support (0.0487-1). Tree visualization was done using FigTree (v1.4.4).

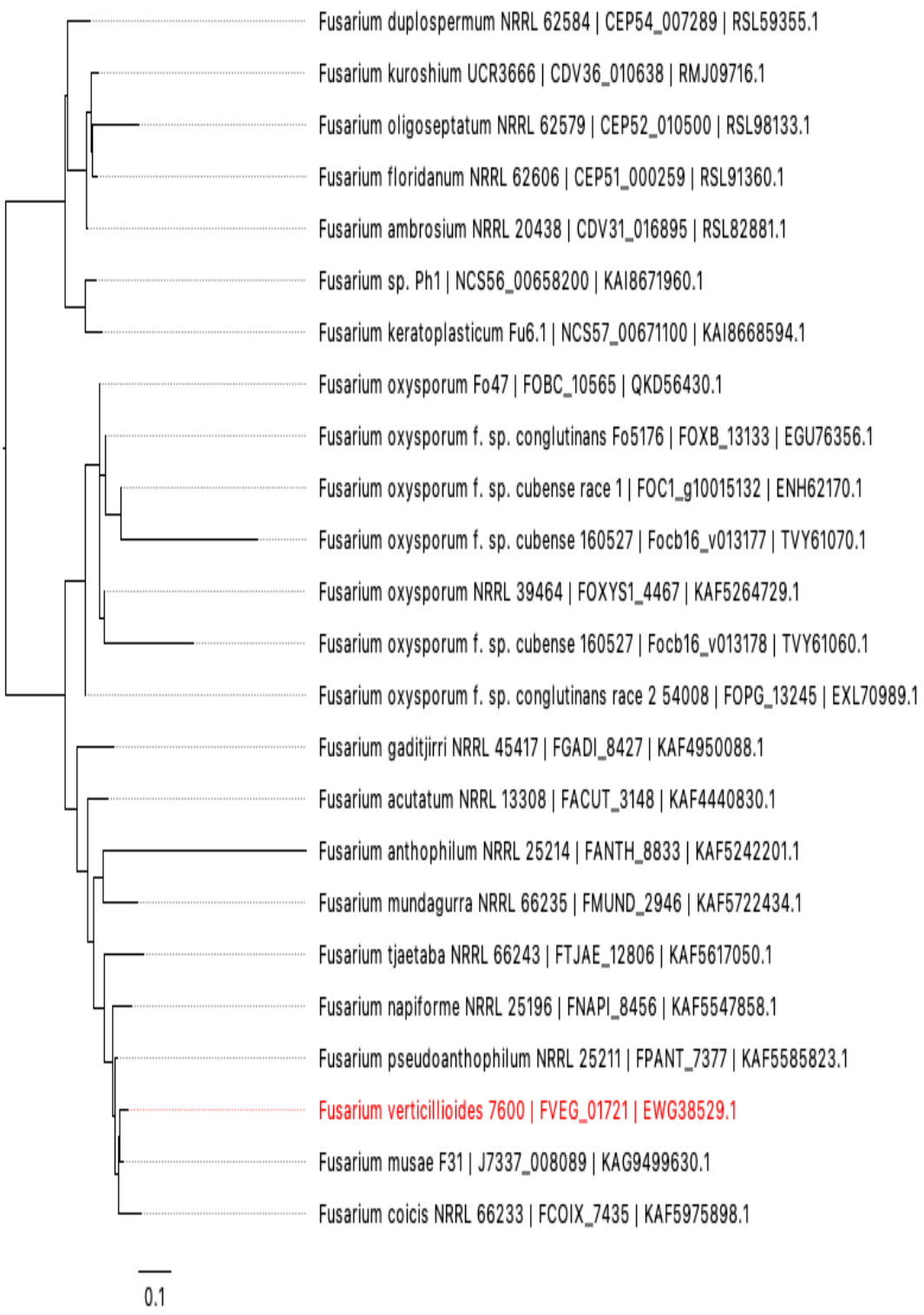

Figure 2.10. OrthoFinder-based resolved gene tree of orthogroup (OG) OG0013215. NAR1 from *Fusarium verticillioides* (dNAR; FVEG_01721; EWG38529.1) is highlighted in red. Scale bar is 0.1. No support values were calculated. The tree is rooted to the most basal sister clade containing seven different species. Tree visualization was done using FigTree (v1.4.4).

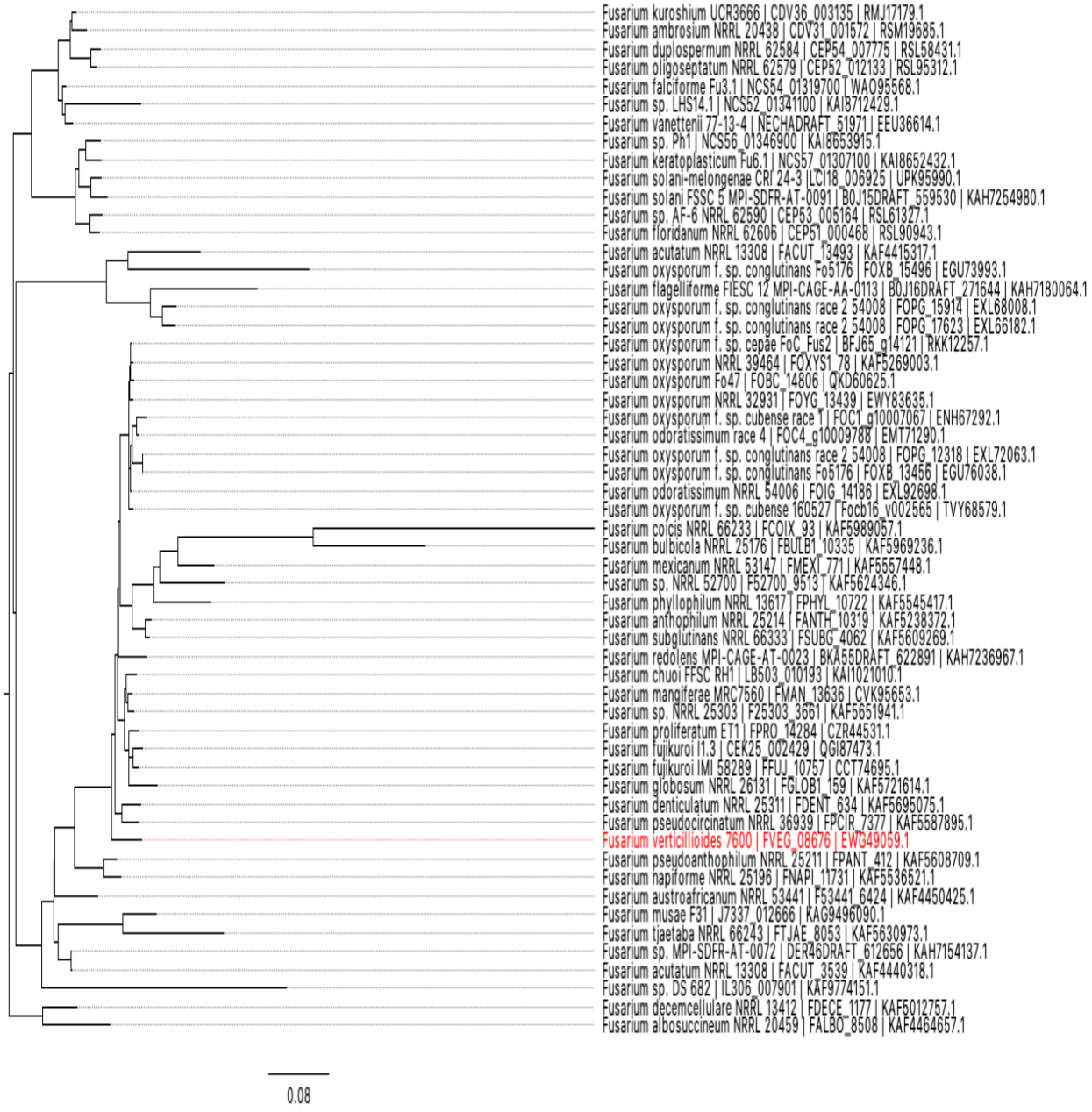

Figure 2.11. OrthoFinder-based resolved gene tree of orthogroup (OG) OG0010514. *Fusarium verticillioides* DNI1 (dNIR; FVEG_08676; EWG49059.1) is highlighted in red. Scale bar is 0.08. No support values were calculated. The tree is rooted to the most basal sister clade, which contains *Fusarium decemcellulare* NRRL 13412 FDECE_1177 (KAF5012757.1) and *Fusarium albosuccineum* NRRL 20459 FALBO_8508 (KAF4464657.1). Tree visualization was done using FigTree (v1.4.4).

Figure 2.12. OrthoFinder-based resolved gene tree of orthogroup (OG) OG0001521. *Fusarium verticillioides* NOR1 (p450nor; FVEG_10773; EWG51922.1) is highlighted in red. Scale bar is 0.3. No support values were calculated. The tree is rooted to the most basal sister clade. Tree visualization was done using FigTree (v1.4.4).

Supplemental Tables

Supplementary Table S2.1. All substitution models used for protein tree construction.

Dataset	Substitution model	Amino-acid exchange rate matrix[a]	Amino-acid frequencies	Rate heterogeneity across sites	Reference(s)
NAR1/NIA1	LG+R10	LG	N/A	+R10	Le and Gascuel, 2008; Yang, 1995; Soubrier et al., 2012
DNI1	JTT+I+G4	JTT	N/A	+I+G4	Jones et al., 1992; Gu et al., 1995
NOR1	LG+G4	LG	N/A	+G4	Le and Gascuel, 2008; Yang, 1994
FHB1/FHB2	LG+F+R10	LG	+F	+R10	Le and Gascuel, 2008; Yang, 1995; Soubrier et al., 2012
FNT1/FNT2	LG+R8	LG	N/A	+R8	Le and Gascuel, 2008; Yang, 1995; Soubrier et al., 2012

Amino-acid exchange rate matrix, amino-acid frequencies, and rate heterogeneity across sites are specified for each substitution model, if applicable. For more information about the substitution models used in this study, examine the references above and/or go to this website: http://www.iqtree.org/doc/Substitution-Models

[a] An amino-acid exchange rate matrix is a 20 × 20 matrix that describes the frequency at which a character in a protein sequence changes to other character states over evolutionary time. This information is often in the form of log odds of finding two specific character states aligned and depends on the assumed number of evolutionary changes or sequence dissimilarity between compared sequences (Trivedi and Nagarajaram, 2020).

Supplementary Table S2.2. IQ-TREE sequence alignment, substitution model, and tree statistics for ModelFinder analysis of assimilatory (aNAR) and dissimilatory (dNAR) nitrate reductase dataset

Sequence Alignment			
Input Data	# of Invariant Sites	# of Parsimony Informative Sites	# of Distinct Site Patterns
1045 sequences with 4073 amino acid sites	1510 (= 37.07% of all sites)	1852	3201

Substitution Process		
Model of Substitution	Model of Rate Heterogeneity	Relative Rates (and Proportion)
LG+R10	FreeRate with 10 categories	1) 0.0336 (0.0348) 2) 0.1103 (0.0528) 3) 0.2230 (0.0765) 4) 0.3290 (0.0974) 5) 0.4942 (0.1139) 6) 0.6841 (0.0757) 7) 0.9038 (0.1157) 8) 1.1428 (0.1137) 9) 1.5454 (0.1257) 10) 2.0989 (0.1940)

Maximum Likelihood Tree							
Log-Likelihood of the Tree	Unconstrained Log-Likelihood (without tree)	# of Free Parameters[a]	AIC[b]	AICc[c]	BIC[d]	Total Tree Length (Sum of Branch Lengths)	Sum of Internal Branch Lengths
-470394.67	-31668.04	2101	9449 91.34	9494 72.62	9582 53.13	390.39	161.63 (41.40% of tree length)

[a] Number of branches + number of model parameters
[b] Akaike Information Criterion score
[c] Corrected Akaike Information Criterion score
[d] Bayesian Information Criterion score

Supplementary Table S2.3. IQ-TREE sequence alignment, substitution model, and tree statistics for ModelFinder analysis of dissimilatory nitrite reductase (dNIR) dataset

Sequence Alignment			
Input Data	# of Invariant Sites	# of Parsimony Informative Sites	# of Distinct Site Patterns
76 sequences with 750 amino acid sites	288 (= 38.40% of all sites)	385	563

Substitution Process		
Model of Substitution	Model of Rate Heterogeneity	Relative Rates (and Proportion)
JTT+I+G4	Invar+Gamma with 4 categories	0) 0 (0.1267) 1) 0.1182 (0.2183) 2) 0.4823 (0.2183) 3) 1.1067 (0.2183) 4) 2.8733 (0.2183)

Maximum Likelihood Tree							
Log-Likelihood of the Tree	Unconstrained Log-Likelihood (without tree)	# of Free Parameters[a]	AIC[b]	AICc[c]	BIC[d]	Total Tree Length (Sum of Branch Lengths)	Sum of Internal Branch Lengths
-22523.43	-4553.79	151	45348.87	45425.63	46046.50	16.75	7.02 (41.93% of tree length)

[a] Number of branches + number of model parameters
[b] Akaike Information Criterion score
[c] Corrected Akaike Information Criterion score
[d] Bayesian Information Criterion score

Supplementary Table S2.4. IQ-TREE sequence alignment, substitution model, and tree statistics for ModelFinder analysis of nitric oxide reductase (p450nor) dataset

Sequence Alignment			
Input Data	# of Invariant Sites	# of Parsimony Informative Sites	# of Distinct Site Patterns
110 sequences with 698 amino acid sites	181 (= 25.93% of all sites)	390	637

Substitution Process		
Model of Substitution	Model of Rate Heterogeneity	Relative Rates (and Proportion)
LG+G4	Gamma with 4 categories	1) 0.1306 (0.2500) 2) 0.4670 (0.2500) 3) 0.9945 (0.2500) 4) 2.4079 (0.2500)

Maximum Likelihood Tree							
Log-Likelihood of the Tree	Unconstrained Log-Likelihood (without tree)	# of Free Parameters[a]	AIC[b]	AICc[c]	BIC[d]	Total Tree Length (Sum of Branch Lengths)	Sum of Internal Branch Lengths
-28935.12	-4468.33	218	58306.23	58505.57	59297.74	21.66	8.30 (38.32% of tree length)

[a] Number of branches + number of model parameters
[b] Akaike Information Criterion score
[c] Corrected Akaike Information Criterion score
[d] Bayesian Information Criterion score

Supplementary Table S2.5. IQ-TREE sequence alignment, substitution model, and tree statistics for ModelFinder analysis of flavohemoglobin (flavoHB) dataset

Sequence Alignment			
Input Data	# of Invariant Sites	# of Parsimony Informative Sites	# of Distinct Site Patterns
570 sequences with 1783 amino acid sites	618 (= 34.66% of all sites)	742	1478

Substitution Process		
Model of Substitution	Model of Rate Heterogeneity	Relative Rates (and Proportion)
LG+F+R10	FreeRate with 10 categories	1) 0.0292 (0.0369) 2) 0.0916 (0.0611) 3) 0.1993 (0.0582) 4) 0.3435 (0.1082) 5) 0.5551 (0.0852) 6) 0.7471 (0.1169) 7) 0.9822 (0.1283) 8) 1.3126 (0.1453) 9) 1.6599 (0.1740) 10) 2.3802 (0.0859)

Maximum Likelihood Tree							
Log-Likelihood of the Tree	Unconstrained Log-Likelihood (without tree)	# of Free Parameters[a]	AIC[b]	AICc[c]	BIC[d]	Total Tree Length (Sum of Branch Lengths)	Sum of Internal Branch Lengths
-171018.69	-12763.59	1164	344365.39	348753.93	350751.15	189.53	82.86 (43.72% of tree length)

[a] Number of branches + number of model parameters
[b] Akaike Information Criterion score
[c] Corrected Akaike Information Criterion score
[d] Bayesian Information Criterion score

Supplementary Table S2.6. IQ-TREE sequence alignment, substitution model, and tree statistics for ModelFinder analysis of formate/nitrite transporter (FNT) dataset

Sequence Alignment			
Input Data	# of Invariant Sites	# of Parsimony Informative Sites	# of Distinct Site Patterns
310 sequences with 2023 amino acid sites	971 (= 47.99% of all sites)	740	1352

Substitution Process		
Model of Substitution	Model of Rate Heterogeneity	Relative Rates (and Proportion)
LG+R8	FreeRate with 8 categories	1) 0.0500 (0.0348) 2) 0.1586 (0.0793) 3) 0.2824 (0.1253) 4) 0.4367 (0.1278) 5) 0.6775 (0.1310) 6) 1.1557 (0.0600) 7)1.1923 (0.1660) 8) 1.9518 (0.2759)

Maximum Likelihood Tree							
Log-Likelihood of the Tree	Unconstrained Log-Likelihood (without tree)	# of Free Parameters[a]	AIC[b]	AICc[c]	BIC[d]	Total Tree Length (Sum of Branch Lengths)	Sum of Internal Branch Lengths
-89329.47	-13247.98	625	179908.94	180469.07	183416.65	149.09	61.93 (41.54% of tree length)

[a] Number of branches + number of model parameters
[b] Akaike Information Criterion score
[c] Corrected Akaike Information Criterion score
[d] Bayesian Information Criterion score

Supplementary Table S2.7. Induction of denitrification-associated genes in wild-type *Fusarium verticillioides* when exposed to nitric oxide.

Locus Tag[a]	baseMean[b]	log2 Fold Change[c]	lfcSE[d]	stat[e]	p-value[f]	padj[g]
FVEG_03775	45.18	3.5	0.3333	10.5191	7.05E-26	2.10E-24
FVEG_04761	167285.88	3.7	0.1192	30.7638	7.99E-208	5.86E-205
FVEG_07298	19359.80	4.5	0.1133	39.3762	0	0
FVEG_08384	519.79	3.6	0.1666	21.5426	6.21E-103	1.57E-100
FVEG_08676	3104.51	7.6	0.18357	41.5023	0	0
FVEG_10401	3478.35	5.4	0.1238	43.6034	0	0
FVEG_10772	201.66	4.0	0.2053	19.2641	1.07E-82	1.97E-80
FVEG_10773	2992.06	5.0	0.1399	35.3642	6.06E-274	7.04E-271
FVEG_11186	10089.05	3.0	0.1741	16.9436	2.15E-64	2.93E-62
FVEG_12326	11053.84	3.2	0.0968	32.9967	9.03E-239	7.86E-236
FVEG_01721	30.19	1.7	0.3148	5.4080	6.37E-08	4.67E-07
FVEG_02069	28701.88	6.3	0.0984	64.3899	0	0
FVEG_13827	244.91	2.3	0.1500	14.9941	8.02E-51	7.35E-49
FVEG_00877	7400.41	3.5	0.1233	27.9719	3.56E-172	2.07E-169
FVEG_03704	10.50	2.1	0.4309	4.7713	1.83E-06	1.09E-05
FVEG_04246	3186.41	-0.1	0.1086	-1.2692	0.204334	0.327195

This table includes putative denitrification-associated genes differentially expressed in *F. verticillioides* M-3125 when the fungus is exposed to exogenous nitric oxide.

[a] Locus tag is the gene identifier
[b] baseMean is the average of the normalized count values, dividing by size factors, taken over all samples
[c] log2 fold change is the effect size estimate after logarithmic transformation; this value indicates the difference in expression of the query group (e.g., FVEG_10773) compared with the reference group (e.g., beta-tubulin; FVEG_04081)
[d] lfcSE is the standard error of the logarithmized fold change
[e] stat is the test statistic
[f] *p*-value is the statistical measurement used to validate the query gene's expression compared to a control gene
[g] padj is the adjusted *p*-value.

Supplementary Table S2.8. Induction of denitrification-associated genes in wild-type *Fusarium verticillioides* when grown under low-oxygen conditions.

Locus Tag[a]	baseMean[b]	log2 Fold Change[c]	lfcSE[d]	stat[e]	*p*-value[f]	padj[g]
FVEG_03775	12.72	4.0	0.6630	5.9776	2.26E-09	7.67E-09
FVEG_04761	7978.51	3.4	0.6138	5.5625	2.66E-08	8.19E-08
FVEG_07298	16924.32	5.3	0.2463	21.5360	7.17E-103	4.97E-101
FVEG_08384	3162.73	3.6	0.6262	5.6682	1.44E-08	4.55E-08
FVEG_08676	6234.06	9.7	1.2362	7.8373	NA	NA
FVEG_10401	332.42	3.0	0.2145	13.9859	1.90E-44	3.41E-43
FVEG_10772	90.63	5.8	0.4090	14.0917	4.27E-45	7.83E-44
FVEG_10773	25486.64	14.1	0.5242	26.8389	1.14E-158	2.36E-156
FVEG_11186	15969.82	4.8	0.5369	8.8994	5.62E-19	3.75E-18
FVEG_12326	31.91	3.1	1.0415	3.0140	0.002578647	0.004476687
FVEG_01721	14.65	3.3	0.9241	3.5460	0.000391074	0.000757809
FVEG_02069	26638.01	2.3	0.3087	7.5062	6.09E-14	2.99E-13
FVEG_13827	1766.23	4.9	0.3225	15.1639	6.13E-52	1.34E-50
FVEG_00877	12562.90	-4.9	0.3518	-13.7970	2.66E-43	4.62E-42
FVEG_03704	14.21	-4.3	1.2035	-3.5920	0.000328206	0.000642431
FVEG_04246	919.46	-0.7	0.0835	-8.8731	7.12E-19	4.71E-18

This table includes putative denitrification-associated genes differentially expressed in *F. verticillioides* M-3125 when the fungus is exposed to low-oxygen conditions.

[a] Locus tag is the gene identifier
[b] baseMean is the average of the normalized count values, dividing by size factors, taken over all samples
[c] log2 fold change is the effect size estimate after logarithmic transformation; this value indicates the difference in expression of the query group (e.g., FVEG_10773) compared with the reference group (e.g., beta-tubulin; FVEG_04081)
[d] lfcSE is the standard error of the logarithmized fold change
[e] stat is the test statistic
[f] *p*-value is the statistical measurement used to validate the query gene's expression compared to a control gene
[g] padj is the adjusted *p*-value.

Supplemental Figures

Supplementary Figure S2.1. OrthoFinder-based resolved gene tree of orthogroup (OG) OG0007166. *Fusarium verticillioides* FHB1 (FVEG_11186; EWG52435.1) is highlighted in red. Scale bar is 0.07. No support values were calculated. The tree is rooted to *Fusarium zealandicum* NRRL 22465 FZEAL_6067 (KAF4977403.1). Tree visualization was done using FigTree (v1.4.4).

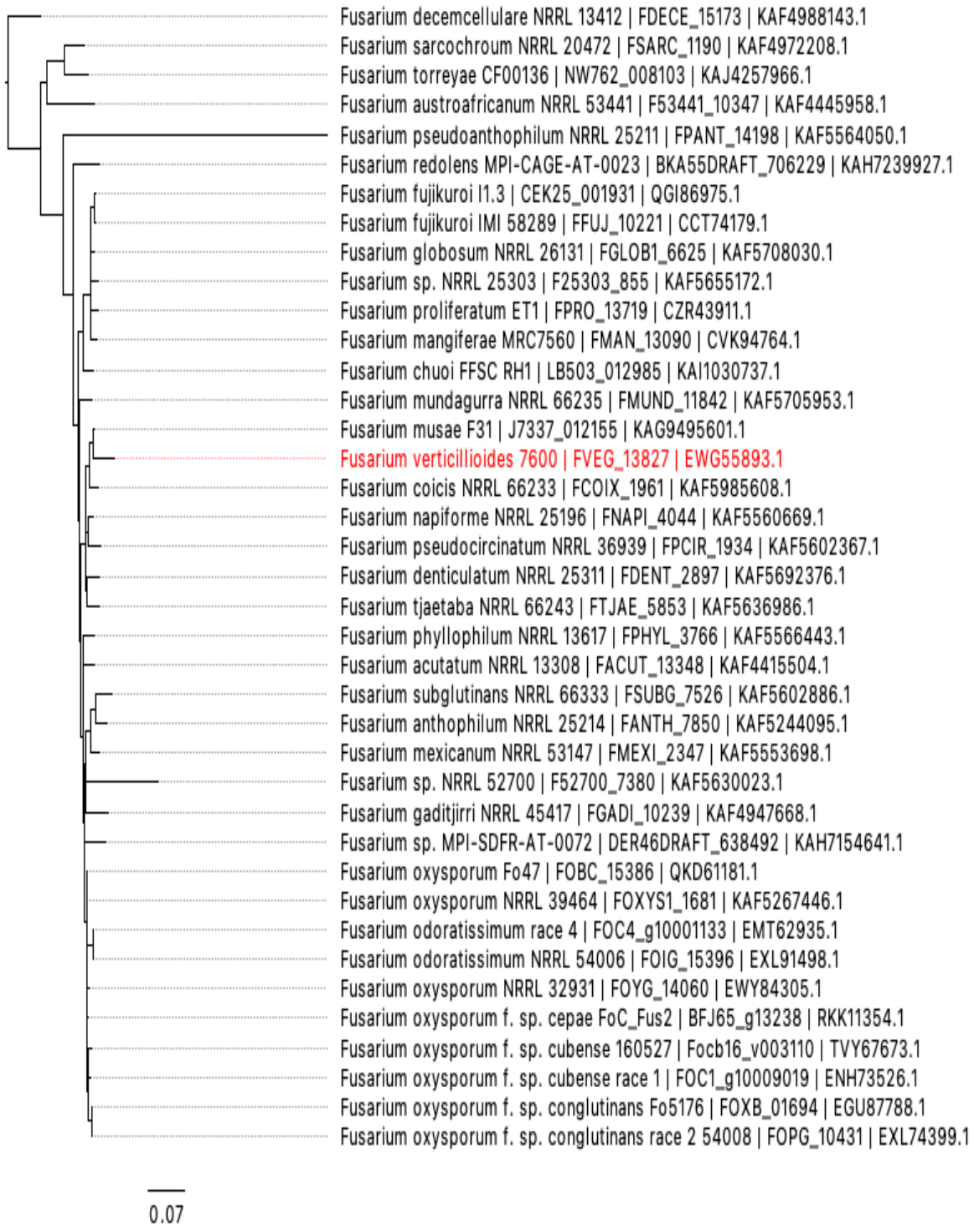

Supplementary Figure S2.2. OrthoFinder-based resolved gene tree of orthogroup (OG) OG0012021. *Fusarium verticillioides* FHB2 (FVEG_13827; EWG55893.1) is highlighted in red. Scale bar is 0.07. No support values were calculated. The tree is rooted to *Fusarium decemcellulare* NRRL 13412 FDECE_15173. Tree visualization was done using FigTree (v1.4.4).

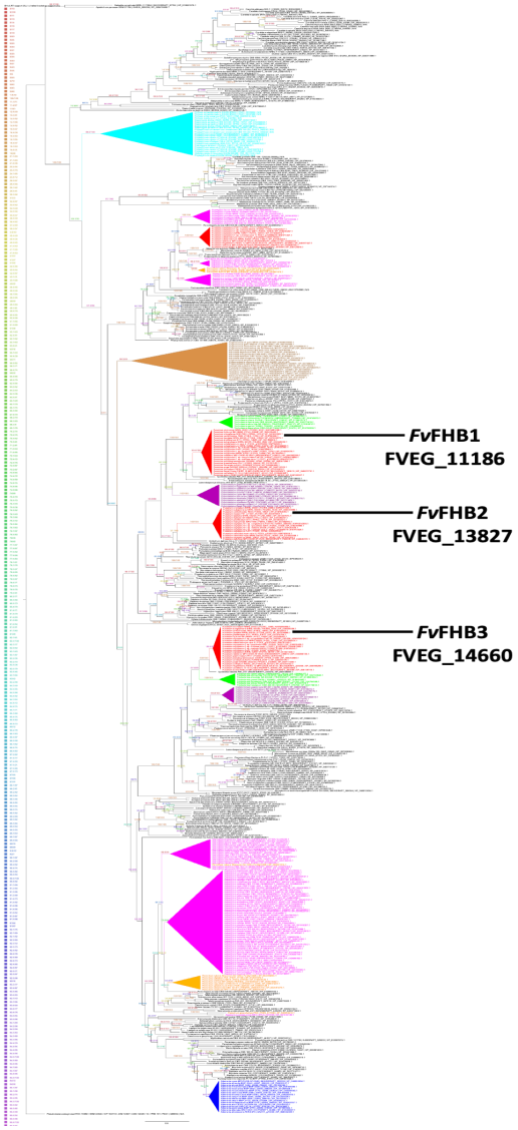

Supplementary Figure S2.3. Protein tree of flavohemoglobins orthologous to *Fusarium verticillioides* genes FVEG_11186 and FVEG_13827 from fungi and oomycetes. A dataset of 570 sequences was aligned using MAFFT. *Pseudomonas aeruginosa* Q9I0H4 was used as the outgroup and the phylogeny is rooted to that sole bacterium. Maximum-likelihood trees were built using IQ-TREE (v1.6.12). ModelFinder identified the best substitution model as LG+F+R10 according to Bayesian Information Criterion (BIC). The phylogeny was run using the LG+F+R10 model with 1,000 SH-aLRT and UFBoot replicates to assess phylogenetic relationships using an alternative strategy to nonparametric bootstrap estimation of branch support. The branch labels are colored according to split support values represented as SH-aLRT support (%) / ultrafast bootstrap support (%). Clades are not collapsed and support values for relationships between samples at sub-genus level clades and at individual branches are visible in this representation. Scale bar (0.8) is at the bottom of the phylogeny. Important fungal genera are colored as follows: *Fusarium* (red), *Trichoderma* (green), *Alternaria* (blue), *Colletotrichum* (purple), *Penicillium* (orange), and *Aspergillus* (pink); other fungal genera are colored black. Tree visualization was done using FigTree (v1.4.4).

Supplementary Figure S2.4. OrthoFinder-based resolved gene tree of orthogroup (OG) OG0003335. *Fusarium verticillioides* FHB3 (FVEG_14660; EWG36354.1) is highlighted in red. Scale bar is 0.06. No support values were calculated. The tree is rooted to *F. zealandicum* NRRL 22465 FZEAL_3761 (KAF4980142.1). Tree visualization was done using FigTree (v1.4.4).

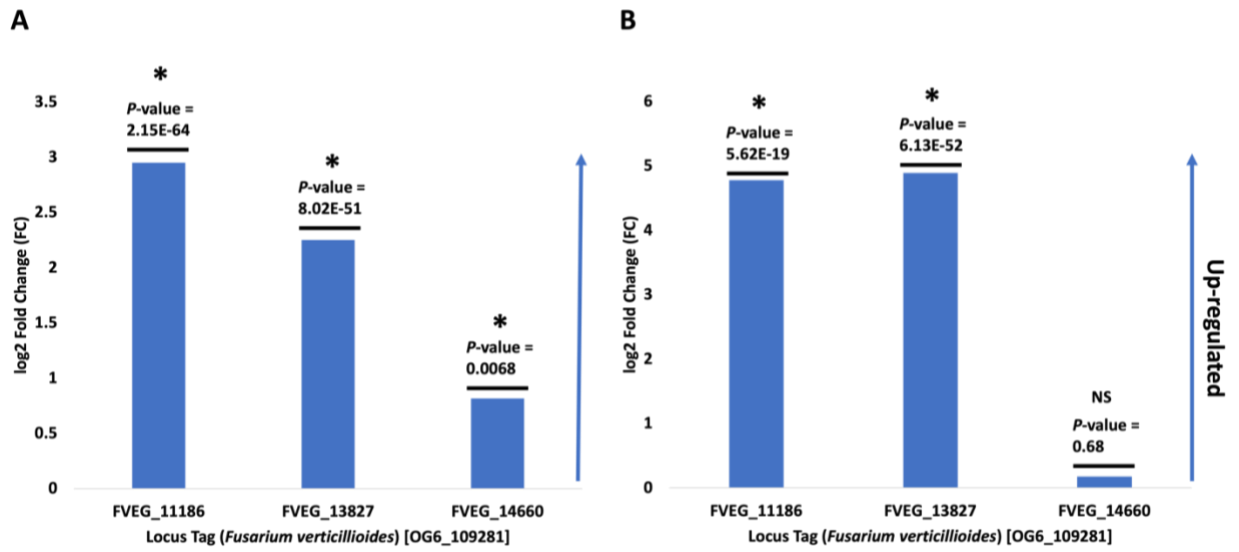

Supplementary Figure S2.5. Expression levels of all the wild type *Fusarium verticillioide* flavoHB genes within the OrthoMCL orthogroup OG6_109281 across both RNA-seq experiments. Expression levels have been transformed to log2 fold-change. Significantly up-regulated (blue) genes, as determined by *p*-value statistic, are indicated by an asterisk. (A) 0 vs. 1.5 mM DETA-NONOate; (B) Normoxia vs. Hypoxia

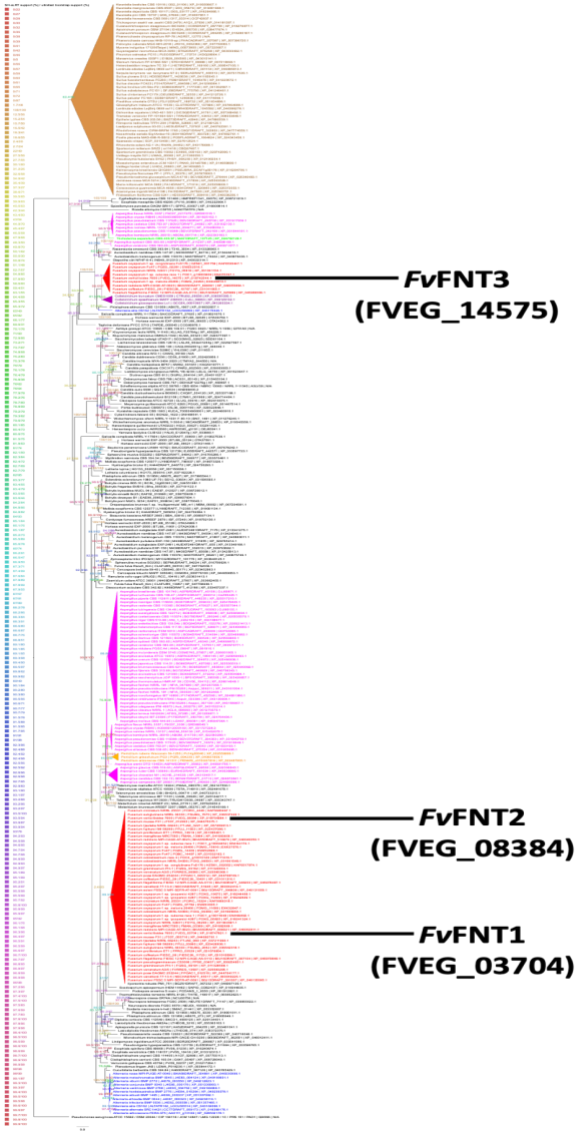

Supplementary Figure S2.6. Protein tree of formate/nitrite transporters orthologous to *Fusarium verticillioides* FVEG_03704 and FVEG_08384 from fungi and oomycetes. A dataset of 310 sequences was aligned using MAFFT. The tree is rooted to the sole bacterial protein sequence, *Pseudomonas aeruginosa* Q9I066 (outgroup). Maximum-likelihood trees were built using IQ-TREE (v1.6.12). ModelFinder identified the best substitution model as LG+R8 according to Bayesian Information Criterion (BIC). The phylogeny was run using the LG+R8 model with 1,000 SH-aLRT and UFBoot replicates to assess phylogenetic relationships using an alternative strategy to nonparametric bootstrap estimation of branch support. The branch labels are colored according to split support values represented as SH-aLRT support (%) / ultrafast bootstrap support (%). Clades are not collapsed and support values for relationships between samples at sub-genus level clades and at individual branches are visible in this representation. Scale bar (0.9) is at the bottom of the phylogeny. Important fungal genera are colored as follows: *Fusarium* (red), *Trichoderma* (green), *Alternaria* (blue), *Colletotrichum* (purple), *Penicillium* (orange), and *Aspergillus* (pink); other fungal genera are colored black. Tree visualization was done using FigTree (v1.4.4).

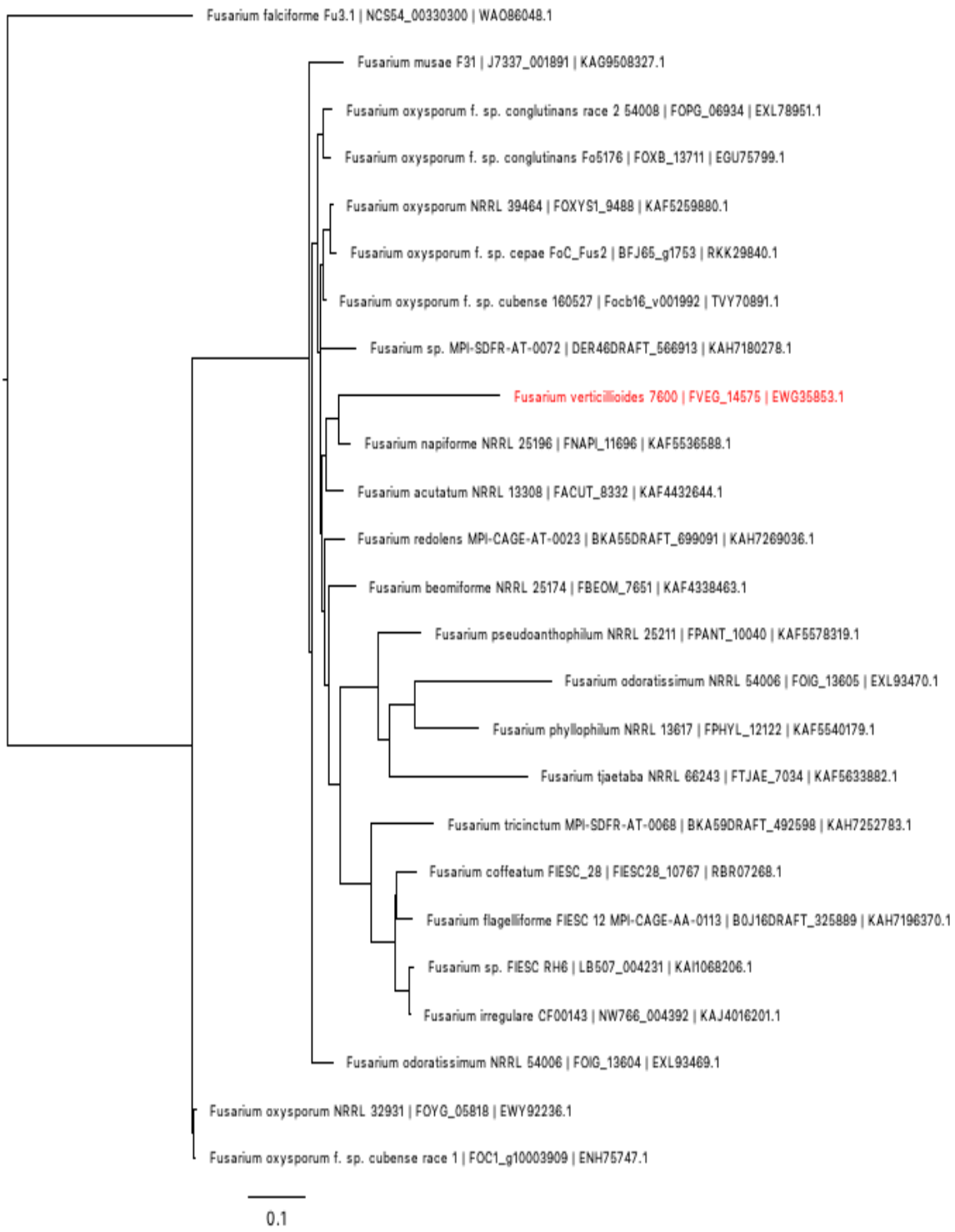

Supplementary Figure S2.7. OrthoFinder-based resolved gene tree of orthogroup (OG) OG0013118. *Fusarium verticillioides* FNT3 (FVEG_14575; EWG35853.1) is highlighted in red. Scale bar is 0.1. No support values were calculated. The tree is rooted to *F. falciforme* Fu3.1 NCS54_00330300 (WAO86048.1). Tree visualization was done using FigTree (v1.4.4).

Supplementary Figure S2.8. OrthoFinder-based resolved gene tree of orthogroup (OG) OG0000462. *Fusarium verticillioides* FNT1 and FNT2 (FVEG_03704/08384; EWG41630.1/EWG48693.1) are highlighted in red. Scale bar is 0.07. No support values were calculated. The tree is rooted to *F. zealandicum* FZEAL_9859 (KAF4971408.1). Tree visualization was done using FigTree (v1.4.4).

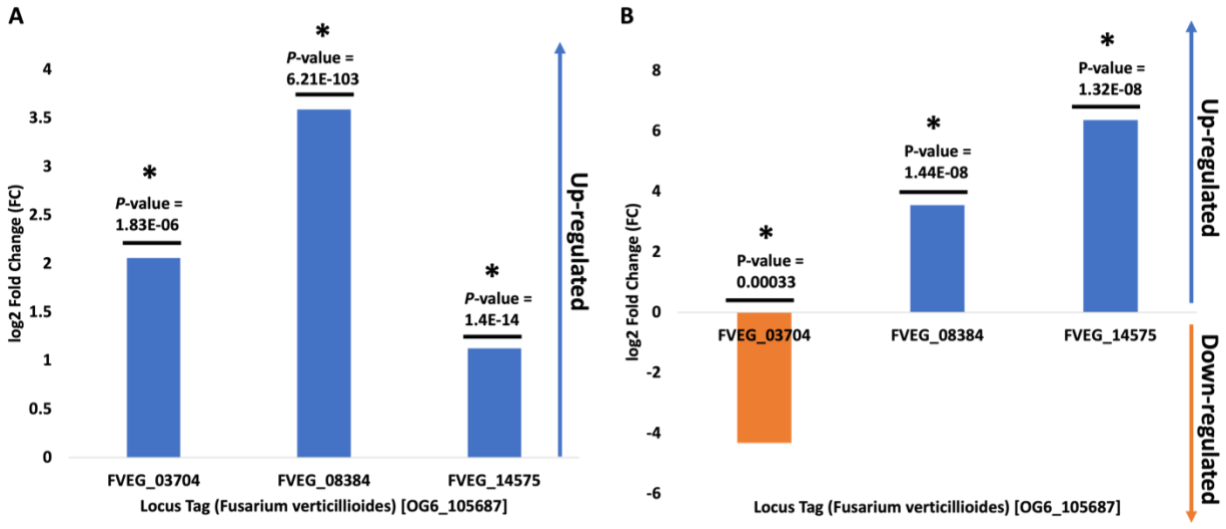

Supplementary Figure S2.9. Expression levels of all wild type *Fusarium verticillioides* FNT genes within the OrthoMCL orthogroup OG6_105687 across both RNA-seq experiments. Expression levels have been transformed to log2 fold-change. Significantly up-regulated (blue) and down-regulated (orange) genes, as determined by *p*-value statistic, are indicated by an asterisk. (A) 1.5 mM DETA-NONOate vs. 0 mM DETA-NONOate; (B) Hypoxia vs. Normoxia

CHAPTER 3

DELETION OF *FUSARIUM VERTICILLIOIDES* GENES ASSOCIATED WITH DENITRIFICATION HAS MINOR EFFECTS ON FUMONISIN PRODUCTION AND VIRULENCE IN PLANTS[2]

---

[2] Oakley BA*, Hibbs GH*, Mitchell TM, Read QD, Gold SE, and Glenn AE. To be submitted to *PhytoFrontiers*

Abstract

Denitrification is a critical microbe-mediated process in the nitrogen cycle that converts soluble nitrogen oxides such as nitrate to gaseous nitrogen oxides such as nitrous oxide. Denitrification is used by some microorganisms to survive under hypoxic or anoxic conditions. Some of these microbial denitrifiers are pathogens of humans, plants, animals, and insects. The role of denitrification in the pathogenicity of bacterial pathogens has been investigated previously, but information is lacking whether denitrification affects virulence or mycotoxin production in pathogenic fungi. *Fusarium verticillioides*, a soil-borne, plant-pathogenic, mycotoxigenic, and denitrifying fungus, is a causal agent of stalk and ear rot in maize (*Zea mays*) and contaminates ears with fumonisin mycotoxins. Here, we evaluated effects of genomic deletion of denitrification-associated genes in *F. verticillioides* on virulence and fumonisin production. Deletion of the single copy dissimilatory nitrite reductase encoding gene (*DNI1*) increased fumonisin B_1, B_2, and B_3 production compared with wild type *F. verticillioides* and other single-gene deletion mutants. Deletion of the single copy flavohemoglobin (*FHB1*) and nitric oxide reductase (*NOR1*) encoding genes marginally increased virulence as indicated by decreases in shoot height and increases in disease score. Understanding the fungal denitrification pathway and how denitrification enzymes in *F. verticillioides* may impact virulence and mycotoxin production may allow development of new methods for preventing plant infection and mycotoxin contamination by pathogenic, mycotoxigenic, denitrifying fungi.

Introduction

Agriculture's primary goal is to ensure global food security. Unfortunately, there are many issues that negatively impact our ability to produce food, such as nitrogen (N)-poor soils and disease-causing microorganisms. Growers remedy N-poor soils in agricultural systems by increasing inputs of N, an essential plant macronutrient. Anthropogenic N inputs include synthetic N fertilizers, animal wastes, increased biological N-fixation, and mineralization of organic matter and crop residues through cultivation (Mosier et al., 1998). Collectively, the industrial production of N fertilizer using the Haber-Bosch process, the fixation of N_2 by cultivated legumes, and the combustion of fuels results in more fixed N per year than all natural processes combined (210 vs. 203 Tg N $year^{-1}$, respectively) (Fowler et al., 2013). Synthetic and biological N inputs have been immensely valuable for food production and human nutrition, but human activities are disrupting the N cycle (Erisman et al., 2008; Galloway et al., 2008). The addition of N to an agricultural field is intended to maximize plant productivity, but 50% or more of the applied N is lost to the environment via abiotic and biotic processes such as leaching and denitrification, respectively (Coskun et al., 2017). These N cycle processes cause billions of dollars in losses for growers globally and cause detrimental effects to the environment and climate, including groundwater pollution, ozone degradation, and release of greenhouse gases (Vitousek et al., 1997; Smith et al., 1999).

Denitrification is a microbial process whereby plant-available N is converted to non-plant-available forms of N under hypoxic or anoxic conditions. The denitrification pathway is an alternative respiration pathway utilized by certain microbes to produce ATP via N oxides as terminal electron acceptors when oxygen (O_2) is low or absent. Canonically, denitrification is a dissimilatory pathway where nitrate (NO_3^-) is chemically reduced to dinitrogen (N_2) via

intermediates of nitrite (NO_2^-), nitric oxide (NO), and nitrous oxide (N_2O). This pathway is well-characterized in denitrifying bacteria, which use four enzymes to mediate this conversion. These enzymes are dissimilatory nitrate reductase, dissimilatory nitrite reductase, nitric oxide reductase, and nitrous oxide reductase (Zumft, 1997; Zumft and Korner, 1997). Decades ago, bacteria and archaea were thought to be the only microbial denitrifiers. Years later, fungi were found to be capable of denitrifying (Shoun and Tanimoto, 1991), but there is a key difference between prokaryotic and fungal denitrifiers in that fungi lack the nitrous oxide reductase (nosZ) that bacteria use to reduce N_2O to N_2, the inert atmospheric gas (Ye et al., 1994; Morozkina and Kurakov, 2007). This means fungi release N_2O as the final product of the fungal denitrification pathway. Without a homolog of nosZ, fungi produce N_2O in biologically relevant amounts. Indeed, fungi play the dominant role in N_2O release from agricultural soils and many other terrestrial ecosystems (Laughlin et al., 2009; Castaldi and Smith, 1998; Castellano-Hinojosa et al., 2021). N_2O is of major concern because it is a dangerous and long-lived greenhouse gas (300-fold more heat-trapping capacity than CO_2, per molecule) and, with the reduction of chlorofluorocarbons, the single most important ozone-destroying agent known (Ravishankara et al., 2009). The continuous rise in atmospheric concentrations of N_2O contributes to global warming.

Among the N_2O-emitting, denitrifying fungi are many plant pathogenic species, including several *Fusarium* species (Chapter 2). Plant pathogenic fungi likely encounter hypoxic environments (Tschiersch et al., 2012) as well as fungal- and plant-derived nitric oxide (Klessig et al., 2000; Arasimowicz-Jelonek and Floryszak-Wieczorek, 2016) during infection of their hosts, both conditions that induce the denitrification pathway in fungi (Oakley et al., in preparation). In bacteria, denitrification has been shown to be critical for pathogenicity of

opportunistic bacterial pathogens of plants and mammals (Labows et al., 1980; Baek et al., 2004; Haine et al., 2006; Fritz et al., 2002; Anjum et al., 2002; Mocca and Wang, 2012, Mocca et al., 2015; Popova et al., 2015; Truchon et al., 2022). These pathogenic bacterial denitrifiers require denitrifying respiration to survive in their hosts. Specifically, NorA and NorB, both nitric oxide reductases, and HmpX, a flavohemoglobin, cooperate to reduce NO toxicity during denitrification and plant pathogenesis in *Ralstonia solanacearum*, a bacterial wilt pathogen (Truchon et al., 2022). These NO detoxification systems are collectively essential for overcoming metabolic nitrosative stress during denitrification, for virulence and growth in the host, and for evading host defenses.

Although numerous studies have demonstrated the link between denitrification and bacterial virulence, information on the role of denitrification in fungal virulence and secondary metabolism is lacking. However, there is a link between adaptation to hypoxia and pathogenicity of fungi. Ability to adapt to hypoxia in fungi is partially regulated by the sterol regulatory element binding proteins (SREBPs) that are required for sterol homeostasis in eukaryotes (Ruan et al., 2017) and by the hypoxic induction of genes encoding oxygen-dependent enzymes involved in ergosterol biosynthesis. Loss of these genes decreases tolerance to hypoxia (Chun et al., 2007). For example, a homolog in the mammalian SREBP cholesterol biosynthesis regulatory pathway and a pathway involving a fungal-specific hybrid histidine kinase family member (Tco1) were identified in *Cryptococcus neoformans* as hypoxia regulatory pathways in fungi. *C. neoformans* mutants in either the SREBP or Tco1 pathway displayed defects in their ability to proliferate in host tissues and cause disease in infected mice (Chun et al., 2007). Vaknin et al. (2016) identified a rhomboid family protease, a novel regulator of hypoxia sensing, that is essential for hypoxic growth in *Neurospora crassa*. Deletion of the rhomboid protease

homolog *rbdA* in *Aspergillus fumigatus* resulted in an inability to grow under hypoxia, hypersensitivity to $CoCl_2$, and attenuated virulence (Vaknin et al., 2016). Since denitrification is a hypoxia-triggered pathway in fungi, we are interested in investigating how denitrification-associated enzymes affect virulence in pathogenic fungi, especially *Fusarium verticillioides*.

Fusarium is a ubiquitous and economically important fungal genus infamous for its production of mycotoxins. In some known cases *Fusarium* spp. use mycotoxins to enhance infection of their hosts (Escriva et al., 2015; Proctor et al., 2002) and cause plant diseases (Nelson et al., 1994). The mycotoxins of greatest concern produced by *Fusarium* species are fumonisins and deoxynivalenol (DON), but members of the genus also produce fusaric acid, zearalenone (ZEA), diacetoxyscirpenol (DAS), fusarins, gibberellins, moniliformin (MON), fusaproliferin, beauvericin, enniatins, nivalenol (NIV), T-2 toxin, tricarballylic acid (TCA), and naphthoquinones (Sydenham et al., 1990; Bacon et al., 1996; Jestoi, 2008; Steyn et al., 1979). Fumonisin B_1, B_2, B_3, and B_4 have been found in naturally contaminated food with B_1 being the most toxic (Soriano and Dragacci, 2004). Contamination of cereals with fumonisins has been associated with multiple human and animal diseases, such as liver cancer, keratitis, onychomycosis, esophageal cancer, equine leukoencephalomalacia (ELEM) in horses and pulmonary edema syndrome in swine (Bezuidenhout et al., 1988; Gelderblom et al., 1988; Marasas et al., 1988; Ross et al., 1990; Alangaden, 2011). Fumonisins are also a potent inducer of oxidative stress and lipid peroxidation in intestinal cells (Garbetta et al., 2015) and may increase the risk of neural tube defects (Missmer et al., 2006).

Fusarium verticillioides, a soil-borne, mycotoxigenic plant pathogen, produces fumonisins, and is a causal agent of stalk and ear rot in maize (*Zea mays*). *F. verticillioides* is a primary colonizer of maize because it can metabolize corn antimicrobials (e.g., DIMBOA,

DIBOA, MBOA, BOA) to nontoxic metabolites (Glenn et al., 2001; Yue et al., 1998). Infection pathways leading to kernel infection of maize hybrids by *F. verticillioides* include silks, stalks, seed, and roots. *F. verticillioides* infection can occur symptomatically as a pathogen (Oren et al., 2003) or asymptomatically as an endophyte (Bacon and Hinton, 1996). Symptoms of *F. verticillioides* infection on maize, include severe rotting, wilting, chlorosis, stunting, and lesion development (Blacutt et al., 2018).

Previously, genes associated with denitrification, NO detoxification, and hypoxic respiration were identified in *F. verticillioides* using RNA-seq. Some of these genes are *FvNAR1* (a dissimilatory nitrate reductase), *FvDNI1* (a dissimilatory nitrite reductase), *FvNOR1* (a cytochrome P450 nitric oxide reductase), *FvNIA1* (an assimilatory nitrate reductase), *FvNII1* (an assimilatory nitrite reductase), *FvFNT1* (a formate/nitrite transporter), and *FvFHB1* (a flavohemoglobin). We hypothesized that deletion of denitrification genes may inhibit the fungus' ability to survive under hypoxia as it is infecting the host, resulting in lower disease potential. Additionally, we hypothesized that deletion of *FvFHB1* and *FvNOR1* would decrease virulence due to the loss of nitric oxide detoxification mechanisms that cope with endogenous and exogenous NO, leading to increased NO sensitivity and lower fitness.

In this paper, we functionally characterized the role of *FvNAR1, FvDNI1, FvNOR1, FvNIA1, FvNII1, FvFNT1,* and *FvFHB1* in the pathogen's virulence on maize seedlings and fumonisin production. To reduce plant disease on maize and pre-harvest and post-harvest contamination of corn, we must expand our understanding of the *F. verticillioides*-maize pathosystem and study the potential link between fungal denitrification and pathogenesis.

Materials and Methods

Fungal and bacterial strains, culture media and growth conditions

The strains and mutants of *F. verticillioides* (*Fv*) created and used for this study are listed in Supplementary Table 1. Wild type strain FRC M-3125 (FGSC 7600) was used for genetic modification and functional characterization. For culturing, strains were grown routinely at 27° C in the dark for 3 days on either (i) potato dextrose agar (PDA; Neogen Food Safety, Lansing, MI, USA) or (ii) in potato dextrose broth (PDB; Neogen Food Safety) on a shaker incubator at 250 rpm. For the screening of transformed strains, PDA amended with 150 μg/mL hygromycin B (Invitrogen, Carlsbad, CA, USA) was used.

Construction of Δ*nor1*, Δ*fum1* and Δ*zbd1* deletion mutants and Δ*zbd1*::*ZBD1* add-back mutants was described previously (Oakley et al., submitted; Proctor et al., 1999; Gao et al., 2020). Fungal gene deletion mutants here were constructed as described in Gao et al. (2020) (Supplementary Table S3.1). To construct fungal gene deletion mutants, *Escherichia coli* (One Shot® MAX Efficiency® DH5α^{TM}-T1R, Invitrogen, Carlsbad, CA, USA) was used as the recipient of OSCAR deletion constructs and was grown in/on low-Na (0.5 g/L) Luria–Bertani (LB) medium amended with 100 μg/mL spectinomycin (Thermo Fisher Scientific, Waltham, MA, USA) at 37° C overnight. The fungal transformation was mediated by OSCAR deletion plasmid containing-*Agrobacterium tumefaciens* AGL-1 strains cultured on low-Na LB medium amended with 100 μg/mL spectinomycin at 27° C for 24-48 hours (Paz et al., 2011; Gold et al., 2017).

Construction of gene deletion mutants and complemented strains

Plasmids pSG01721_OSCAR, pSG08676_OSCAR, pSG07298_OSCAR, pSG02069_OSCAR, pSG03704_OSCAR, and pSG11186_OSCAR were created as the gene

deletion constructs for FVEG_01721 (*FvNAR1*), FVEG_08676 (*FvDNI1*), FVEG_07298 (*FvNIA1*), FVEG_02069 (*FvNII1*), FVEG_03704 (*FvFNT1*), and FVEG_11186 (*FvFHB1*), respectively, using the OSCAR method (Paz et al., 2011). Supplementary Table 3.2 summarizes the primers used in this study. Two pairs of primers for *FvNAR1, FvDNI1, FvNIA1, FvNII1, FvFNT1,* and *FvFHB1* were designed to amplify about 1-1.5 kb of the respective 5' and 3' flanks of the open reading frame (ORF). The gene deletion constructs contain two flanks separated by a hygromycin resistance cassette (HRC), all between T-DNA borders. By transformation and homologous recombination with the gene deletion construct, the coding sequence of each gene was deleted in wild type *F. verticillioides* strain FRC M-3125. Hygromycin-resistant transformants were initially screened for the presence of the HRC and loss of the ORF to identify potential gene deletion mutants, which were further subjected to single-spore purification and confirmation PCR screening. The following criteria were used during PCR screening for deletion mutants: (1) presence of the HRC and loss of the gene ORF; (2) confirmation of positionally correct replacement of gene ORF with HRC at the 5' end; and (3) confirmation of positionally correct replacement of gene ORF with HRC at the 3' end.

PCR and confirmation of genetic mutants

Wild type strains and deletion mutants were all validated by PCR screening. Fungal strain DNA was extracted using the thermolysis method (Zhang et al., 2010). Fungal strains were grown on PDA at 27° C in the dark for 4 days. Once a strain formed a colony, we used a sterile toothpick to transfer mycelia from the colony into 100 μL of lysis solution. The lysis solution contains 50 mM sodium phosphate buffer (pH 7.4), 1 mM EDTA, and 5% glycerol. We incubated the mixture at 85° C in a water bath for 30 min. The crude extracts containing genomic DNA were stored at -20° C until further use. The criteria described above for deletion mutants

generated by the OSCAR method were combined to fully assess newly created deletion mutants used in the study. PCR was carried out as described above.

Seedling disease assay

Seeds of sweetcorn Silver Queen (W. Atlee Burpee & Co., Warminster, PA, USA) were surface sterilized, imbibed and heat treated, as described previously (Glenn et al., 2008). For each fungal strain, 50 seeds were placed on a 100-mm Petri dish with 10 mL of 10^4 microconidia/mL spore suspension. For the uninoculated control, 10 mL of sterile water were added to the seeds. After overnight incubation in the dark at 27° C, seeds were planted in autoclaved potting mix (Fafard 2 Mix, Agawam, MA, USA) in 10-cm azalea pots. Three pots of 10 seeds per pot were included for each treatment. Pots were placed in plastic saucers and watered from below on days 2, 4 and 6 after planting. All subsequent watering was as needed and added from below. Plants were grown for 14 days in a growth room with 16-h light at 30°C (an average of 318 μmol/m^2/s) and 8-h dark at 20°C. At experiment conclusion, above-ground plant tissues were collected by cutting the stem at the soil line. Plant height was measured for each seedling and the proportion of seed germination and seedling death was recorded. Symptoms were visually inspected and disease severity was evaluated according to the disease scoring scale developed for *F. verticillioides* infection of *Z. mays* 'Silver Queen' (Gao et al., 2018). The scale ranges from 0 to 5 with 0 being a healthy, productive plant and 5 being an extremely diseased plant. The disease score is based on measurements of both shoot height and visual assessment of chlorotic lesions and deformations.

Pathogenicity experiments were repeated three times. The data was log-transformed because it was strictly positive and right-skewed. "Genotype" (i.e., Δ*dni1*) and "Strain" (i.e., Δ*dni1*-1, Δ*dni1*-2) were treated as fixed effects. Individual pots were arranged in a completely

randomized design, so pots were nested within a combination of "Sample" and "Trial" as an additional random intercept. For shoot weight data, a general linear mixed model (GLMM) was used with the log-transformed values of weight as the response variable. Kenward-Rogers approximation was used to calculate degrees of freedom (df) for a t-distribution that estimates the limits of the 95% confidence interval and the p-values for the t-tests of the pairwise contrasts between genotypes. For disease score data, the data is an ordered categorical variable, so we used a cumulative logistic mixed model (CLMM) with a logit link function. All individuals from the control group had a disease score of "0", so they were excluded from the model because comparisons with the control group are not statistically relevant. Seedling death and seed germination data were analyzed using a binomial GLMM with a logit link function. For disease index, seedling death and seed germination data, z-tests were used instead of t-tests. Z-tests are based on the standard normal distribution, so degrees of freedom were not calculated. Sidak adjustment was used for all multi-sample comparisons.

Fumonisin bioassay

For fumonisin analysis, fungal isolates were grown on sterile rice using an assay modified from Desjardins et al. (2000). For each assay run, 10 µL of a high concentration inoculum spore suspension from frozen single-spored stock cultures (-80ºC, in 15% glycerol) was used as inoculum for 3 mL of sterile PDB in a 10-mL snap-cap tube. Culture tubes were incubated for 3 days at 27ºC with shaking at 250 rpm in the dark. To a 20 mL glass scintillation vial, 3.0 g (+/- 0.004g) of rice (Enriched long grain rice, Kroger, Cincinnati, OH, USA) and 3.0 mL of reverse osmosis water were added. Vials were topped with foam plugs, autoclaved (121ºC, 30 min), and cooled to room temperature just prior to use. In triplicate, 250 µL of high concentration inoculum spore suspension (~10^7 microconidia per mL) from incubated PDB

flasks (or sterile water control) were added to each rice vial replicate. Inoculated rice vials were incubated for 7 days at 27ºC in the dark under either ambient or hypoxic (5% O_2) conditions. The oxygen environment was modified using a hypoxic chamber and an oxygen controller (Coy Laboratory Products, Grass Lake, MI, USA). The concentration of O_2 was decreased from 21% to 5% using a gas mixture of ~400 ppm CO_2 balanced with N_2 (Airgas Specialty Gases, Durham, NC, USA).

Following the incubation period on rice, 10 mL of a 1:1 acetonitrile (HPLC grade, Fisher, Fair Lawn, N.J., USA):distilled water extraction solution containing 5% formic acid (~98%, Sigma-Aldrich, St. Louis, Mo., USA) were added to each vial. Samples were vigorously shaken and frozen to -20ºC for at least 10 h. Prior to LC-MS/MS analysis for fumonisins, rice cultures were broken apart using sterile inoculation loops and vials were rocked for 3 h at room temperature (The Belly Dancer®, speed 6.5, Stovall Life Science, Inc., Greensboro, NC, USA). The resulting extraction solution was centrifuge-filtered (costar® SpinX HPLC Micro Centrifuge Filter, 0.45 µm, nylon, Corning Inc., Corning, N.Y., USA), diluted (100 to 10,000 fold), and analyzed via LC-MS/MS (Thermo LTQ XL). All analyses were performed in positive ion mode, and the instrument was tuned using FB_1 (PROMEC, Tygerberg, South Africa). An Imtakt Cadenza CW-C18 column (150 x 2 mm, 3 µm; Kyoto, Japan), maintained at 30ºC, was used for separations. Solvent A was distilled water with 3% acetonitrile plus 0.1% formic acid, and solvent B was acetonitrile with 3% distilled water plus 0.1% formic acid. The solvent program began at 30:70 A:B, and increased linearly to 100% B over nine min, held at 100% B for two min, and then returned to starting conditions. Samples were run along with a blank control and standard solutions of fumonisins B1, B2, and B3 (0.001 µg/g, 0.01 µg/g, and 0.1 µg/g) in 30:70 acetonitrile:distilled water plus 0.1% formic acid (PROMEC, Tygerberg, South Africa). Analytes

were identified by retention time and fragmentation pattern, as compared with standards. Levels of fumonisins were quantified by external calibration of peak areas (the MS/MS total ion current) with standards, and a new calibration curve (limit of quantitation (LOQ) = 0.045 ppb; limit of detection (LOD) = 0.013 ppb) was run with each sample set. Fumonisin amounts were reported as µg toxin per g of dried rice.

Bioassay data was fit to a GLMM with a hurdle gamma response distribution with a log link function due to the skewed distribution and the high number of 0 values in the dataset. This type of model allows us to explicitly model the probability of getting a concentration of 0, which, in this case, means that the concentration is below the LOD for the instrument. This model was fit using Bayesian methods, so the estimated means and contrasts are given as medians of the posterior predictive distribution with quantile credible intervals to show uncertainty around the means. Models were fit for each of the three fumonisin compounds (FB_1, FB_2, FB_3). As before, genotype and strain (nested within genotype) were the fixed effects, as well as oxygen level (binary) and its interactions with genotype and strain. Random intercepts were fit to each trial date. The hurdle (zero) component had the same fixed and random effects as the response. Normal(0,1) priors were assigned for fixed effect coefficients on the response, Normal(0,2) priors were assigned for fixed effect coefficients on the hurdle, and Gamma(0.1,0.1) priors were assigned to the shape parameter of the gamma distribution. Convergence of the three models was assessed using the R-hat statistic ($\hat{R} \leq 1.01$ for all parameters) (Vehtari et al., 2021) and posterior predictive check plots were plotted to assess how well the models retro-predict data. Pairwise contrasts between the posterior distributions of the means were calculated as well, back-transformed to the ratio scale using the inverse of the log link function. All posterior means were estimated averaged across oxygen levels and subsequently estimated separately for atmospheric

and hypoxic oxygen conditions. Additionally, the pairwise ratio of fumonisin production between atmospheric and hypoxic oxygen conditions was calculated for each genotype. The atmospheric:hypoxic production ratio was also calculated averaged across all genotypes excluding the uninoculated control and Δ*fum1* deletion mutants, which had zero or near-zero fumonisin production in all samples.

All statistical analysis was done using R v4.3.1 (R Core Team 2023) and Stan v2.33.1 (Stan Development Team 2023), including the R packages brms v2.20.5 (Bürkner 2018), cmdstanr v0.6.1 (Gabry & Češnovar 2023), tidybayes v3.0.4 (Kay 2022), emmeans v1.8.8 (Lenth 2023), lme4 v1.1-34 (Bates et al. 2015), and ordinal v2022.11-16 (Christensen 2022).

Results

Single-gene deletion of denitrification-associated genes have minor effects on stunting and virulence

To assess the role of denitrification-associated genes in fungal virulence, *NAR1* (Δ*nar1*), *DNI1* (Δ*dni1*), *NOR1* (Δ*nor1*), *NIA1* (Δ*nia1*), *NII1* (Δ*nii1*), *FNT1* (Δ*fnt1*), and *FHB1* (Δ*fhb1*) gene deletion mutants were generated (Supplementary Table S3.1) and shoot height, disease score, seedling death and seed germination rate of inoculated maize seeds were quantified. Deletion of *FvFHB1* and *FvNOR1* reduced shoot height of maize seedlings relative to other mutants and wild type *F. verticillioides*, but the effect was minimal (Figure 3.1). As expected, the highest shoot height recorded was for uninoculated maize seedlings with an estimated mean of 33.1 (24.7, 44.3) centimeters (cm). Of the deletion mutants listed above, Δ*nor1* (11.5 cm; 8.6, 15.4) and Δ*fhb1* (10.0 cm; 7.5, 13.4) exhibited increased inhibition of maize seedling growth. Δ*dni1* (16.3 cm; 12.2, 21.8), Δ*nia1* (16.3 cm; 12.1, 21.8), and Δ*nii1* (13.5 cm; 10.1, 18.1)

mutants were less inhibitory to shoot growth than wild type (13.0 cm; 9.7, 17.4), but differences were not statistically significant.

Disease scores, which are based on measurements of both shoot height and visual assessment of chlorotic lesions and deformations, are not reported for uninoculated seeds because it was 0 for all technical and biological replicates across all three trials. The highest disease scores were reported in Δ*fhb1* (3.7; 3.1, 4.2), Δ*nor1* (3.1; 2.6, 3.7), and Δ*nar1* (3.2; 2.6, 3.7) mutants (Figure 3.2). However, the estimated mean of the disease score for these mutants was only slightly higher than the disease score for wild type *F. verticillioides* (3.1; 2.5, 3.7). In contrast, disease scores were lowered in Δ*nia1* (2.4; 1.9, 3.0), Δ*dni1* (2.4; 1.8, 3.0), Δ*nii1* (3.0; 2.5, 3.6), and Δ*fnt1* (3.0; 2.4, 3.6) mutants compared with wild type. We also studied the loss-of-function effect of denitrification genes on seedling death and seed germination. No significant differences were observed for seedling death (data not shown), but there were significant differences between mutants in seed germination (Figure 3.3). Uninoculated seedlings had the highest estimated mean of seed germination probability (0.909; 0.819, 0.956) whereas Δ*fnt1* (0.663; 0.532, 0.774), Δ*fhb1* (0.687; 0.556, 0.794), and Δ*nor1* (0.716; 0.586, 0.818) mutants had the lowest germination proportions. For comparison, wild type *F. verticillioides* had a seed germination proportion of 0.738 (0.612, 0.834). These results indicate that denitrification genes may affect virulence in a minor way, but there are not statistically or biologically significant differences.

FvDNI1 deletion mutants show statistically significant increased production of FB_1, FB_2, and FB_3 under normoxic and hypoxic conditions

FvDNI1 deletion mutants showed significantly increased production of all fumonisin analogs (FB_1, FB_2, FB_3) regardless of whether Δ*dni1* mutants were grown under atmospheric or

hypoxic conditions (Figures 3.4-3.6). Production of fumonisins by *F. verticillioides* is a key virulence factor (Beccaccioli et al., 2021) on specific maize genotypes including cv. 'Silver Queen'. Of the deletion mutants tested, Δ*dni1* mutants were notable in terms of their overall fumonisin production capabilities [25.7 (18.9, 35.2) μg FB_1/g rice; 13.5 (9.3, 19.8) μg FB_2/g rice; 6.0 (4.1, 8.8) μg FB_3/g rice]. This level of fumonisin production is higher than what we quantified for wild type *F. verticillioides* [8.1 (6.0, 11.0) μg FB_1/g rice; 2.2 (1.5, 3.2) μg FB_2/g rice; 3.0 (2.1, 4.3 μg FB_3/g rice)]. However, the production of fumonisins in *FvDNI1* mutants pales in comparison to the *FvZBD1* mutants, which are extreme producers of fumonisins [67.7 (49.4, 92.6) μg FB_1/g rice; 18.7 (12.8, 27.3) μg FB_2/g rice; 21.9 (15.0, 31.7) μg FB_3/g rice] (Gao et al., 2020). The lowest amount of fumonisin production was reported for uninoculated rice [0.5 (0.04, 6.4) μg FB_1/g rice; 0.2 (0.008, 1.8) μg FB_2/g rice; 0.14 (0.008, 1.9) μg FB_3/g rice] and *FvFUM1* deletion mutants [0.31 (0.006, 9.8) μg FB_1/g rice); 0.08 (0.002, 2.9) μg FB_2/g rice); 0.08 (0.002, 2.5) μg FB_3/g rice] (Proctor et al., 1999). The amount of FB_1, FB_2, and FB_3 produced by mutants and wild type *F. verticillioides* differed under atmospheric and hypoxic growth conditions. In individual fungal strains, FB_1, FB_2, FB_3 production was higher when fungi were grown in 21% oxygen (O_2) compared with a low-O_2 environment. The only exception is Δ*dni1* mutants which produced more FB_3 under hypoxia than normoxia. This suggests that deletion of *FvDNI1* and hypoxia may force *F. verticillioides* to increase the ratio of FB_3 production relative to FB_1 and FB_2 production.

To further investigate this phenomenon, FB_1, FB_2, and FB_3 production levels were separately averaged across all samples, except for uninoculated rice and Δ*fum1* deletion mutants (Figure 3.7). FB_1, FB_2, and FB_3 production is higher under atmospheric conditions compared to hypoxic conditions. However, FB_3 production is higher than FB_2 production under hypoxia.

Additionally, there is a significant reduction in FB_1 production under hypoxia, whereas FB_3 production was not significantly affected by the decrease in O_2 concentration.

Discussion

In this study, the single-gene deletions of denitrification-associated genes were shown to have negligible effects on virulence as measured by shoot height, disease score, and seed germination, but significant effects on fumonisin production. We also demonstrate a significant decrease in FB_1 and FB_2 production, but not FB_3 production, as *F. verticillioides* transitions from normoxia to hypoxia. This study does not support our hypothesis that deletion of denitrification-associated genes would reduce virulence of *F. verticillioides*. The largest effect on virulence was observed in Δ*nor1* and Δ*fhb1* mutants; NOR1 and FHB1 both function to detoxify NO into N_2O and NO_3^-, respectively. The breakdown of NO to NO_3^- via flavohemoglobins may act as a system to fuel denitrification during infection when N sources in the plant are low or not easily accessible by the fungus. It is suspected that the loss of NO detoxification mechanisms blocks reduction of NO into non-toxic compounds and increases NO sensitivity in the fungus and increased efflux of NO into the plant host. Observationally, maize seedlings infected with Δ*fhb1* mutants had more necrotic lesions than maize seedlings infected with other single gene deletion mutants or wild type *F. verticillioides*, but this was not reflected in the experimental results. Phenotypic effects on virulence may have been lower than expected due to functional redundancy of denitrification enzymes. Enzymes such as *Fv*NAR1 and *FvNIA1* are functionally similar and can reduce NO_3^- to NO_2^-. Additionally, there are three homologs of flavohemoglobins (*FHB1*, *FHB2*, and *FHB3*) and formate/nitrite transporters (*FNT1*, *FNT2*, *FNT3*). These functional redundancies may mask phenotypes, so construction of double and triple gene

deletion mutants may be necessary to observe larger effects and more conclusively link fungal denitrification to virulence.

Despite inconclusive findings on the association between fungal denitrification and virulence, there was an unexpected and significant increase in fumonisin production of Δ*dni1* mutants. Δ*dni1* mutants had higher production of all three fumonisin analogs compared with other fungal strains; the only exception being Δ*zbd1* mutants. *ZBD1* (FVEG_00314) is a genetic repressor of fumonisin biosynthesis. Deletion of *ZBD1* derepresses fumonisin biosynthesis and transforms the fungus to be extremely virulent and a fumonisin super-producer (Gao et al., 2020). None of the mutants nor wild type *F. verticillioides* produced less fumonisin than *FUM1* mutants. *FUM1* is a polyketide synthase (PKS) essential for fumonisin biosynthesis (Desjardins et al., 2002; Brown et al., 2007; Sun et al., 2019). A possible explanation for increased fumonisin production in Δ*dni1* mutants is that NO_2^- cannot be reduced to NO via the N dissimilation pathway, so NO_2^- accumulates in the cytosol. This pool of NO_2^- may be partially re-routed to the N assimilation pathway where it is reduced to ammonium (NH_4^+) and incorporated into amino acids such as alanine. *FUM8,* another gene essential for fumonisin biosynthesis (Sun et al. 2018), encodes a fumarase that converts fumaric acid to L-malic acid and combines a polyketide with alanine to form a 22-carbon compound that is a precursor to fumonisin analogs. Future research will be needed to determine if deletion of *FvDNI1* leads to an increase in alanine and a parallel increase in fumonisin production. However, whatever the mechanism may be, it is not greatly impacted by O_2 concentration since production of fumonisin analogs increased regardless of the O_2 environment.

Another novel result from the fumonisin bioassay was that oxygen level is a determining factor in differential production of fumonisin analogs. The exact mechanism by which hypoxia

increases the ratio of FB_3 relative to FB_1 and FB_2 is unknown, but we hypothesize that *FUM3* may be suppressed at low-oxygen levels. The B series fumonisins differ in the number and location of hydroxyl groups attached to the carbon backbone. Fum3 is a 2-ketoglutarate-dependent dioxygenase required for C-5 hydroxylation of FB_3 into FB_1 (Ding et al., 2004). These results suggest that hypoxia may affect expression of *FUM3* and the ability of the enzyme to hydroxylate FB_3 into FB_1.

The results of this study call for additional experimentation to identify the mechanisms by which loss of *FvDNI1* increases production of FB_1, FB_2, and FB_3 no matter the oxygenation conditions and how hypoxia regulates hydroxylation of fumonisin analogs. It is critical to understand how denitrification influences *F. verticillioides* infection of the maize plant and production of mycotoxins. This work implicates denitrification-associated genes as having a role, albeit a minor one, in virulence and fumonisin production and compels us to conduct further research into fungal denitrification in mycotoxigenic, plant pathogenic fungi.

Literature Cited

Alangaden, G. J. 2011. Noscomial fungal infections: Epidemiology, infection control, and prevention. Infect. Dis. Clin. North Am. 25:201-225.

Anjum, M. F., Stevanin, T. M., Read, R. C., and Moir, J. W. B. 2002. Nitric oxide metabolism in *Neisseria meningitidis.* J. Bacteriol. 184:2987-2993.

Arasimowicz-Jelonek, M. and Floryszak-Wieczorek, J. 2016. Nitric oxide in the offensive strategy of fungal and oomycete plant pathogens. Front. Plant Sci. 7:252.

Bacon, C. W. and Hinton, D. M. 1996. Symptomless endophytic colonization of maize by *Fusarium moniliforme*. Canad. J. Bot. 74:1195-1202.

Bacon, C. W., Porter, J. K., Norred, W. P., and Leslie, J. F. 1996. Production of fusaric acid by *Fusarium* species. Appl. Environ. Microbiol. 62:4039-4043.

Baek, S.-H., Rajashekara, G., Splitter, G. A., and Shapleigh, J. P. 2004. Denitrification genes regulate *Brucella* virulence in mice. J. Bacteriol. 186:6025-6031.

Bates, D., Maechler, M., Bolker, B., and Walker, S. 2015. Fitting linear mixed-effects models using lme4. J. Stat. Softw. 67:1-48.

Beccaccioli, M., Salustri, M., Scala, V., Ludovici, M., Cacciotti, A., D'Angeli, S., Brown, D. W., and Reverberi, M. 2021. The effect of *Fusarium verticillioides* fumonisins on fatty acids, sphingolipids, and oxylipins in maize germlings. Int. J. Mol. Sci. 22:2435.

Bezuidenhout, S. C., Gelderblom, W. C. A., Gorst-Allman, C. P., Horak, R. M., Marasas, W. F. O., Spiteller, G., and Vieggaar, R. 1988. Structure elucidation of the fumonisins, mycotoxins from *Fusarium moniliforme.* J. Chem. Soc., Chem. Commun. 743-745.

Blacutt, A. A., Gold, S. E., Voss, K. A., Gao, M., and Glenn, A. E. 2018. *Fusarium verticillioides*: Advancements in understanding the toxicity, virulence, and niche adaptations of a model mycotoxigenic pathogen of maize. Phytopathology. 108:312-326.

Brown, D. W., Butchko, R. A. E., Busman, M., and Proctor, R. H. 2007. The *Fusarium verticillioides* FUM gene cluster encodes a $Zn(II)_2Cys_6$ protein that affects *FUM* gene expression and fumonisin production. Eukaryot. Cell. 6:1210-1218.

Bürkner, P.-C. 2018. Advanced Bayesian multilevel modeling with the R package brms. R J. 10:395-411.

Castaldi, S. and Smith, K. A. 1998. Effect of cycloheximide on N_2O and NO_3^- production in a forest and an agricultural soil. Biol. Fertil. Soils. 27:27-34.

Castellano-Hinojosa, A., Le Cocq, K., Charteris, A. F., Abadie, M., Chadwick, D. R., Clark, I. M., González-López, J., Bedmar, E. J., and Cardenas, L. M. 2021. Relative contributions of bacteria and fungi to nitrous oxide emissions following nitrate application in soils representing different land uses. Int. Biodeterior. Biodegradation. 159:105199.

Christensen, R. H. B. 2022. Ordinal - Regression Models for Ordinal Data. R package version 2022.11-16. https://CRAN.R-project.org/package=ordinal.

Chun, C. D., Liu, O. W., & Madhani, H. D. 2007. A link between virulence and homeostatic responses to hypoxia during infection by the human fungal pathogen *Cryptococcus neoformans*. PLoS Pathog. 3:225-238.

Coskun, D., Britto, D. T., Shi, W., and Kronzucker, H. J. 2017. How plant root exudates shape the nitrogen cycle. Trends Plant Sci. 22:661-673.

Desjardins, A. E., Manandhar, H. K., Plattner, R. D., Manandhar, G. G., Poling, S. M., and Maragos, C. M. 2000. *Fusarium* species from Nepalese rice and production of

mycotoxins and gibberellic acid by selected species. Appl. Environ. Microbiol. 66:1020-1025.

Desjardins, A. E., Munkvold, G. P., Plattner, R. D., and Proctor, R. H. 2002. *FUM1* – A gene required for fumonisin biosynthesis but not for maize ear rot and ear infection by *Gibberella moniliformis* in field tests. Mol. Plant. Microbe Interact. 15:1157-1164.

Desjardins, A. E., Plattner, R. D., and Proctor, R. H. 1996. Linkage among genes responsible for fumonisin biosynthesis in *Gibberella fujikuroi* mating population A. Appl. Environ. Microbiol. 62:2571–2576.

Ding, Y., Bojja, R. S., and Du, L. 2004. Fum3p, a 2-ketoglutarate-dependent dioxygenase required for C-5 hydroxylation of fumonisins in *Fusarium verticillioides.* Appl. Environ. Microbiol. 70:1931-1934.

Erisman, J. W., Sutton, M. A., Galloway, J., Klimont, Z., and Winiwarter, W. 2008. How a century of ammonia synthesis changed the world. Nat. Geosci. 1:636-639.

Galloway, J. N., Townsend, A. R., Erisman, J. W., Bekunda, M., Cai, Z., Freney, J. R., Martinelli, L. A., Seitzinger, S. P., and Sutton, M. A. 2008. Transformation of the nitrogen cycle: Recent trends, questions, and potential solutions. Science. 320:889-892.

Escriva, L., Font, G., and Manyes, L. 2015. *In vivo* toxicity studies of fusarium mycotoxins in the last decade: A review. Food Chem. Toxicol. 78:185-206.

Fowler, D., Coyle, M., Skiba, U., Sutton, M. A., Cape, J. N., Reis, S., Sheppard, L. J., Jenkins, A., Grizzetti, B., Galloway, J. N., Vitousek, P., Leach, A., Bouwman, A. F., Butterbach-Bahl, K., Dentener, F., Stevenson, D., Amann, M., and Voss, M. 2013. The global nitrogen cycle in the twenty-first century. Phil. Trans. Royal Soc. B. 368:20130164.

Fritz, C., Maass, S., Kreft, A., and Bange, F.-C. 2002. Dependence of *Mycobacterium bovis* BCG on anaerobic nitrate reductase for persistence is tissue-specific. Infect. Immun. 70:286-291.

Gabry, J. and Češnovar, R. 2023. cmdstanr: R Interface to 'CmdStan'. https://mc-stan.org/cmdstanr, https://discourse.mc-stan.org

Gao, M., Glenn, A. E., Gu, X., Mitchell, T. R., Satterlee, T., Duke, M. V., Scheffler, B. E., and Gold, S. E. 2020. Pyrrocidine, a molecular off switch for fumonisin biosynthesis. PLoS Pathog. 16:e1008595.

Gao, S., Gold, S. E., and Glenn, A. E. 2018. Characterization of two catalase-peroxidase-encoding genes in *Fusarium verticillioides* reveals differential responses to *in vitro* versus *in planta* oxidative challenges. Mol. Plant Pathol. 19:1127-1139.

Garbetta, A., Debellis, L., De Girolamo, A., Schena, R., Visconti, A., and Minervini, F. 2015. Dose-dependent lipid peroxidation induction on *ex vivo* intestine tracts exposed to chime samples from fumonisins contaminated corn samples. Toxicol. In Vitro. 29:1140-1145.

Gelderblom, W. C. A., Jaskiewicz, K., Marasas, W. F. O., Thiel, P. G., Horak, R. M., Vleggaar, R., and Kriek, N. P. J. 1988. Fumonisins – Novel mycotoxins with cancer-promoting activity produced by *Fusarium verticillioides*. Appl. Environ. Microbiol. 54:1806-1811.

Glenn, A. E., Hinton, D. M., Yates, I. E., and Bacon, C. W. 2001. Detoxification of corn antimicrobial compounds as the basis for isolating *Fusarium verticillioides* and some other *Fusarium* species from corn. Appl. Environ. Microbiol. 67:2973-2981.

Glenn, A. E., Zitomer, N. C., Zimeri, A. M., Williams, L. D., Riley, R. T., and Proctor, R. H. 2008. Transformation-mediated complementation of a FUM gene cluster deletion in

Fusarium verticillioides restores both fumonisin production and pathogenicity on maize seedlings. Mol. Plant Microbe Interact. 21:87-97.

Gold, S. E., Paz, Z., García-Pedrajas, M. D., and Glenn, A. E. 2017. Rapid deletion production in fungi via *Agrobacterium* mediated transformation of OSCAR deletion constructs. J. Vis. Exp. 124:e55239.

Haine, V., Dozot, M., Dornand, J., Letesson, J.-J., and De Bolle, X. 2006. NnrA is required for full virulence and regulates several *Brucella melitensis* denitrification genes. J. Bacteriol. 188:1615-1619.

Jestoi, M. 2008. Emerging *Fusarium*-mycotoxins fusaproliferin, beauvericin, enniatins, and moniliformin – A review. Crit. Rev. Food Sci. Nutr. 48:21-49.

Kay, M. 2022. tidybayes: Tidy Data and Geoms for Bayesian Models. R package version 3.0.4. http://mjskay.github.io/tidybayes/.

Kim, H. and Woloshuk, C. P. 2008. Role of *AREA*, a regulator of nitrogen metabolism, during colonization of maize kernels and fumonisin biosynthesis in *Fusarium verticillioides.* Fungal Genet. Biol. 45:947-953.

Klessig, D. F., Durner, J., Noad, R., Navarre, D. A., Wendehenne, D., Kumar, D., Zhou, J. M., Shah, J., Zhang, S., Kachroo, P., Trifa, Y., Pontier, D., Lam, E., and Silva, H. 2000. Nitric oxide and salicylic acid signaling in plant defense. Proc. Natl. Acad. Sci. U.S.A. 97:8849-8855.

Labows, J. N., McGinley, K. J., Webster, G. F., and Leyden, J. J. 1980. Headspace analysis of volatile metabolites of *Pseudomonas aeruginosa* and related species by gas chromatography-mass spectrometry. J. Clin. Microbiol. 12:521-526.

Laughlin, R. J., Rütting, T., Müller, C., Watson, C. J., and Stevens, R. J. 2009. Effect of acetate on soil respiration, N_2O emissions and gross N transformations related to fungi and bacteria in a grassland soil. Appl. Soil Ecol. 42:25-30.

Lenth, R.V. 2023. emmeans: Estimated Marginal Means, aka Least-squares Means. R package version 1.8.8. https://CRAN.R-project.org/package=emmeans.

Marasas, W. F. O., Kellerman, T. S., Gelderblom, W. C. A., Coetzer, J. A. W., Thiel, P. G., and van der Lugt, J. J. 1988. Leukoencephalomalacia in a horse induced by fumonisin B_1 isolated from *Fusarium moniliforme*. Onderstepoort J. Vet. Res. 55:197-203.

Missmer, S. A., Suarez, L., Felkner, M., Wang, E., Merrill, A. H., Rothman, K. J., and Hendricks, K. A. 2006. Exposure to fumonisins and the occurrence of neural tube birth defects along the Texas-Mexico border. Environ. Health Perspect. 114:237-241.

Mocca, B., Yin, D., Gao, Y., and Wang, W. 2015. *Moraxella catarrhalis*-produced nitric oxide has dual roles in pathogenicity and clearance of infection in bacterial-host cell co-cultures. Nitric Oxide, 51:52-62.

Mocca, B. and Wang, W. 2012. Bacterium-generated nitric oxide hijacks host tumor necrosis factor alpha signaling and modulates the host cell cycle *in vitro*. J. Bacteriol. 194:4059-4068.

Morozkina, E. V. and Kurakov, A. V. 2007. Dissimilatory nitrate reduction in fungi under conditions of hypoxia and anoxia: A review. Appl. Biochem. Microbiol. 43: 544-549.

Mosier, A., Kroeze, C., Nevison, C., Oenema, O., Seitzinger, S., and van Cleemput, O. 1998. Closing the global N_2O budget: nitrous oxide emissions through the agricultural nitrogen cycle. Nutr. Cycl. Agroecosystems. 52:225-248.

Nelson, P. E., Dignani, M. C., and Anaissie, E. J. 1994. Taxonomy, biology, and clinical aspects of *Fusarium* species. Clin. Microbiol. Rev. 4:479-504.

Oakley, B. A., Mitchell, T. R., Read, Q. D., Hibbs, G. T., Baldwin, T. T., Gold, S. E., and Glenn, A. E. 2023. Identification of a key enzyme target for reducing agricultural emissions of nitrous oxide. Sci. Adv. Submitted.

Oren, L., Ezrati, S., Cohen, D., and Sharon, A. 2003. Early events in the *Fusarium verticillioides*-maize interaction characterized by using a green fluorescent protein-expressing transgenic isolate. Appl. Environ. Microbiol. 69:1695-1701.

Paz, Z., García-Pedrajas, M. D., Andrews, D. L., Klosterman, S. J., Baeza-Montanez, L., and Gold, S. E. 2011. One Step Construction of *Agrobacterium*-Recombination-ready-plasmids (OSCAR), an efficient and robust tool for ATMT based gene deletion construction in fungi. Fungal Genet. Biol., 48:677-684.

Popova, T. G., Teunis, A., Vaseghi, H., Zhou, W., Espina, V., Liotta, L. A., and Popov, S. G. (2015). Nitric oxide as a regulator of *B. anthracis* pathogenicity. Front. Microbiol. 6:1-14.

Proctor, R. H., Desjardins, A. E., McCormick, S. P., Plattner, R. D., Alexander, N. J., and Brown, D. W. 2002. Genetic analysis of the role of trichothecene and fumonisin mycotoxins in the virulence of *Fusarium*. Eur. J. Plant Pathol. 108:691-698.

Proctor, R. H., Desjardins, A. E., Plattner, R. D., and Hohn, T. M. 1999. A polyketide synthase gene required for biosynthesis of fumonisin mycotoxins in *Gibberella fujikuroi* mating population A. Fungal Genet. Biol. 27:100-112.

R Core Team. 2023. R: A language and environment for statistical computing. R Foundation for Statistical Computing, Vienna, Austria. https://www.R-project.org/.

Ravishankara, A. R., Daniel, J. S., and Portmann, R. W. 2009. Nitrous oxide (N_2O): The dominant ozone-depleting substance emitted in the 21st century. Science. 326:123-125.

Ross, P. F., Nelson, P. E., Richard, J. L., Osweiler, G. D., Rice, L. G., Plattner, R. D., and Wilson, T. M. 1990. Production of fumonisins by *Fusarium moniliforme* and *Fusarium proliferatum* isolates associated with equine leukoencephalomalacia and a pulmonary edema syndrome in swine. Appl. Environ. Microbiol. 56:3225-3226.

Ruan, R., Chung, K.-R., and Li, H. 2017. Functional characterization of the Dsc E3 ligase complex in the citrus postharvest pathogen *Penicillium digitatum*. Microbiol. Res. 205:99-106.

Shim, W-B. and Woloshuk, C. P. 1999. Nitrogen repression of fumonisin B1 biosynthesis in *Gibberella fujikuroi*. FEMS Microbiol. Lett. 177:109-116.

Shoun, H. and Tanimoto, T. 1991. Denitrification by the fungus *Fusarium oxysporum* and involvement of cytochrome P-450 in the respiratiory nitrite reduction. J. Biol. Chem. 266:11078-11082.

Smith, V. H., Tilman, G. D., and Nekola, J. C. 1999. Eutrophication: impacts of excess nutrient inputs on freshwater, marine, and terrestrial ecosystems. Environ. Pollut. 100:179-196.

Soriano, J. M. and Dragacci, S. 2004. Occurrence of fumonisins in foods. Food Res. Int. 37:985-1000.

Stan Development Team. 2023. Stan Modeling Language Users Guide and Reference Manual, 2.33. https://mc-stan.org.

Steyn, P. S., Wessels, P. L., and Marasas, W. F. O. 1979. Pigments from *Fusarium moniliforme* Sheldon – Structue and ^{13}C nuclear magnetic resonance assignments of an azaanthraquinone and three naphthoquinones. Tetrahedron. 35:1551-1555.

Sydenham, E. W., Thiel, P. G., Marasas, W. F. O., Shephard, G. S., Van Schalkwyk, D. J., and Koch, K. R. 1990. Natural occurrence of some *Fusarium* mycotoxins in corn from low and high esophageal cancer prevalence areas of the Transkei, Southern Africa. J. Agric. Food Chem. 36:1900-1903.

Sun, L., Chen, X., Gao, J., Zhao, Y., Liu, L., Hou, Y., Wang, L. and Huang, S. 2019. Effects of disruption of five *FUM* genes on fumonisin biosynthesis and pathogenicity in *Fusarium proliferatum*. Toxins. 11:327.

Truchon, A. N., Hendrich, C. G., Bigott, A. F., Dalsing, B. L., and Allen, C. 2022. NorA, HmpX, and NorB cooperate to reduce NO toxicity during denitrification and plant pathogenesis in *Ralstonia* solanacearum. Microbiol. Spectr. 10:2.

Tschiersch, H., Liebsch, G., Borisjuk, L., Stangelmayer, A., and Rolletschek, H. 2012. An imaging method for oxygen distribution, respiration and photosynthesis at a microscopic level of resolution. New Phytol. 196:926-936.

Vaknin, Y., Hillmann, F., Iannitti, R., Baruch, N. B., Sandovsky-Losica, H., Shadkchan, Y., Romani, L., Brakhage, A., Kniemeyer, O., and Osherov, N. 2016. Identification and characterization of a novel *Aspergillus fumigatus* rhomboid family putative protease, RbdA, involved in hypoxia sensing and virulence. Infect. Immun. 84:1866-1878.

Vehtari, A., Gelman, A., Simpson, D., Carpenter, B., and Bürkner, P.-C. 2021. Rank-normalization, folding and localization: An improved ˆR for assessing convergence of MCMC (with discussion). Bayesian Anal. 16:667-718.

Vitousek, P. M., Aber, J. D., Howarth, R. W., Likens, G. E., Matson, P. A., Schindler, D. W., Schlesinger, W. H., and Tilman, D. G. 1997. Human alteration of the global nitrogen cycle: Sources and consequences. Ecol. Appl. 7:737-750.

Ye, R. W., Averill, B. A., and Tiedje, J. M. 1994. Denitrification: Production and consumption of nitric oxide. Appl. Environ. Microbiol. 60:1053-1058.

Yue, Q., Bacon, C. W., and Richardson, M. D. 1998. Biotransformation of 2-benzoxazolinone and 6-methoxy-benzoxazolinone by *Fusarium moniliforme*. Phytochemistry. 48:451-454.

Zhang, Y. J., Zhang, S., Liu, X. Z., Wen, H. A., and Wang, M. 2010. A simple method of genomic DNA extraction suitable for analysis of bulk fungal strains. Lett. Appl. Microbiol. 51:114-118.

Zumft, W. G. 1997. Cell biology and molecular basis of denitrification. Microbiol. Mol. Biol. Rev. 61:533-616.

Zumft, W. G. and Körner, H. 1997. Enzyme diversity and mosaic gene organization in denitrification. Antonie Van Leeuwenhoek. 71:43-58.

Figures

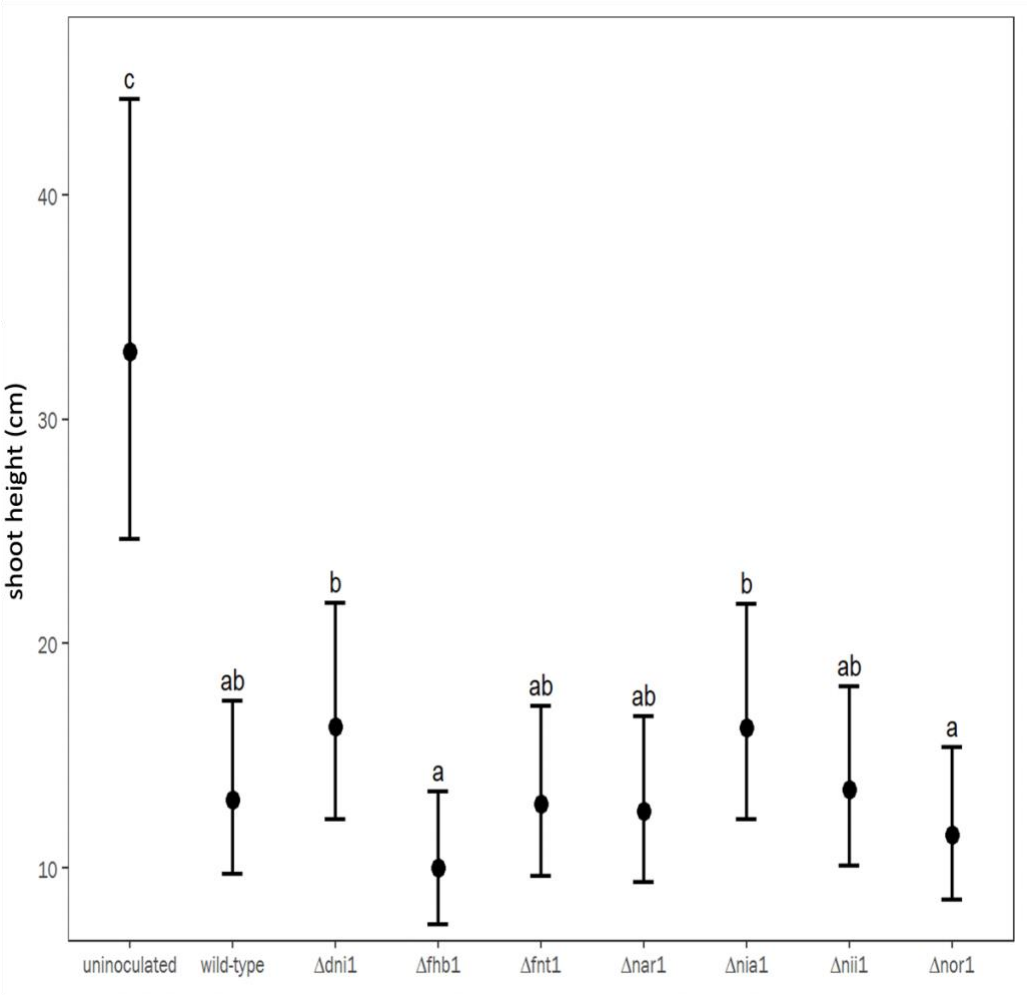

Figure 3.1. Effect of gene deletions on virulence of *Fusarium verticillioides* using shoot height as the parameter. The vertical axis represents shoot height, which was measured in cm and the horizontal axis represents the tested genotypes, including the mutant strains and wild type *F. verticillioides*. Group means that do not share a letter are significantly different based on a Šidák adjustment and error bars represent adjusted 95% confidence intervals around the modeled means.

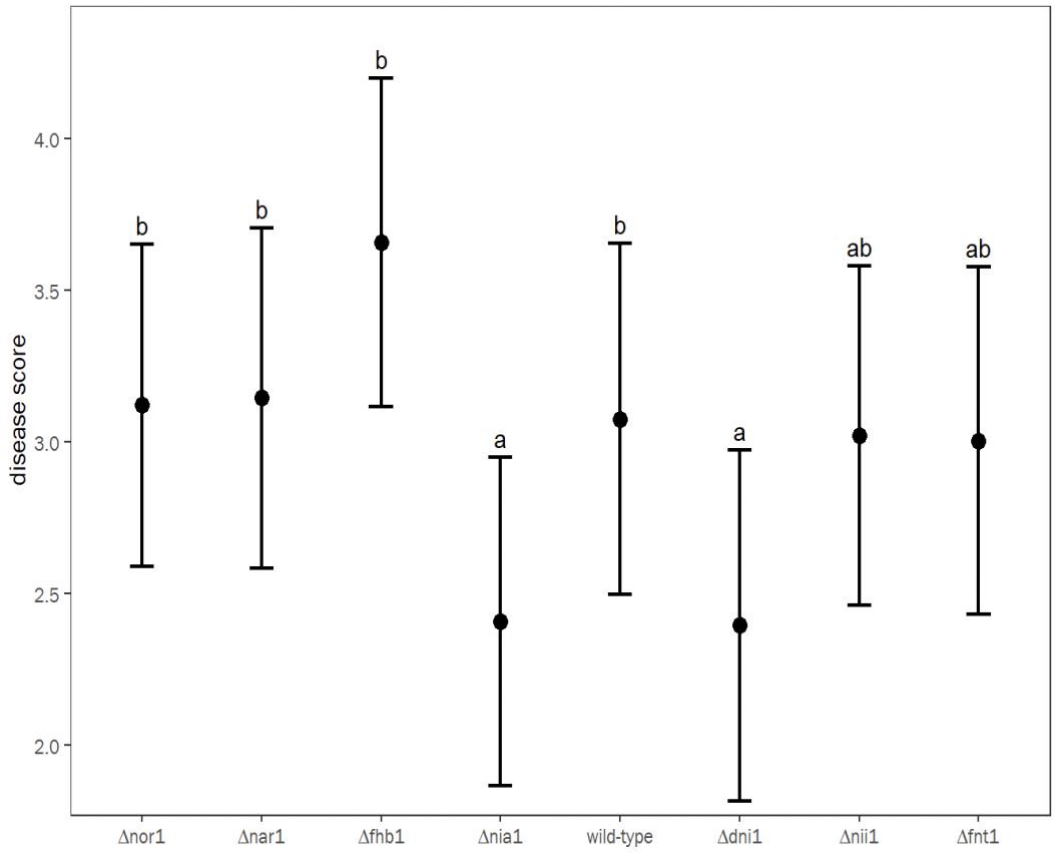

Figure 3.2. Effect of gene deletions on virulence of *F. verticillioides* as measured by disease score. Disease score was measured using the 0-5 disease score scale from Gao et al., 2018. The vertical axis is the disease score (0-5) and the horizontal axis represents the tested genotypes, including the mutant strains and wild type *F. verticillioides*. Group means that do not share a letter are significantly different based on a Šidák adjustment and error bars represent adjusted 95% confidence intervals around the modeled means.

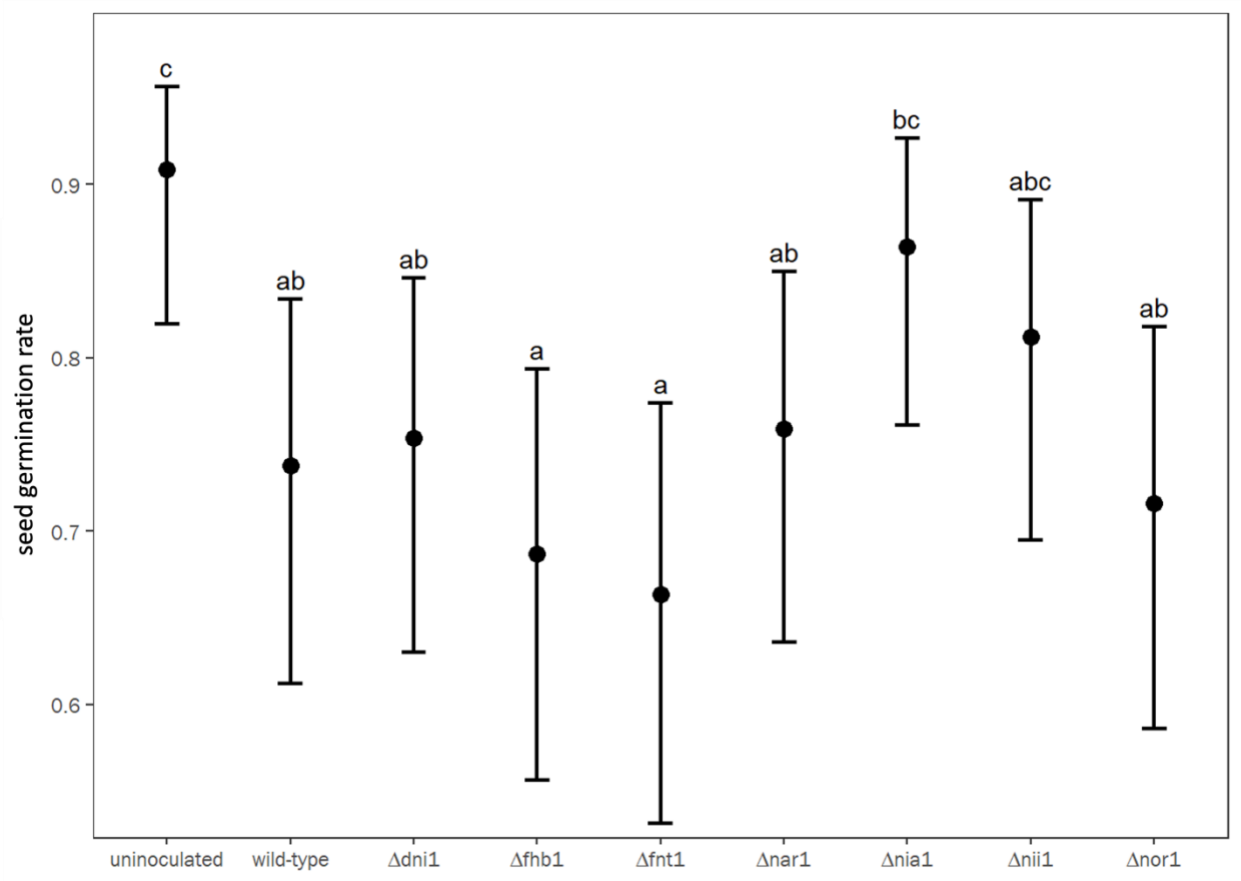

Figure 3.3. Effect of gene deletions on virulence of *Fusarium verticillioides* as measured by seed germination rates. Seedling germination was determined by the number of seeds that germinated and grew relative to seedlings that died before epicotyl emergence. The vertical axis is the seed germination probability (0.0-1.0) and the horizontal axis represents the tested genotypes, including the mutant strains, wild type *F. verticillioides*, and uninoculated seedlings. Group means that do not share a letter are significantly different based on a Šidák adjustment and error bars represent adjusted 95% confidence intervals around the modeled means.

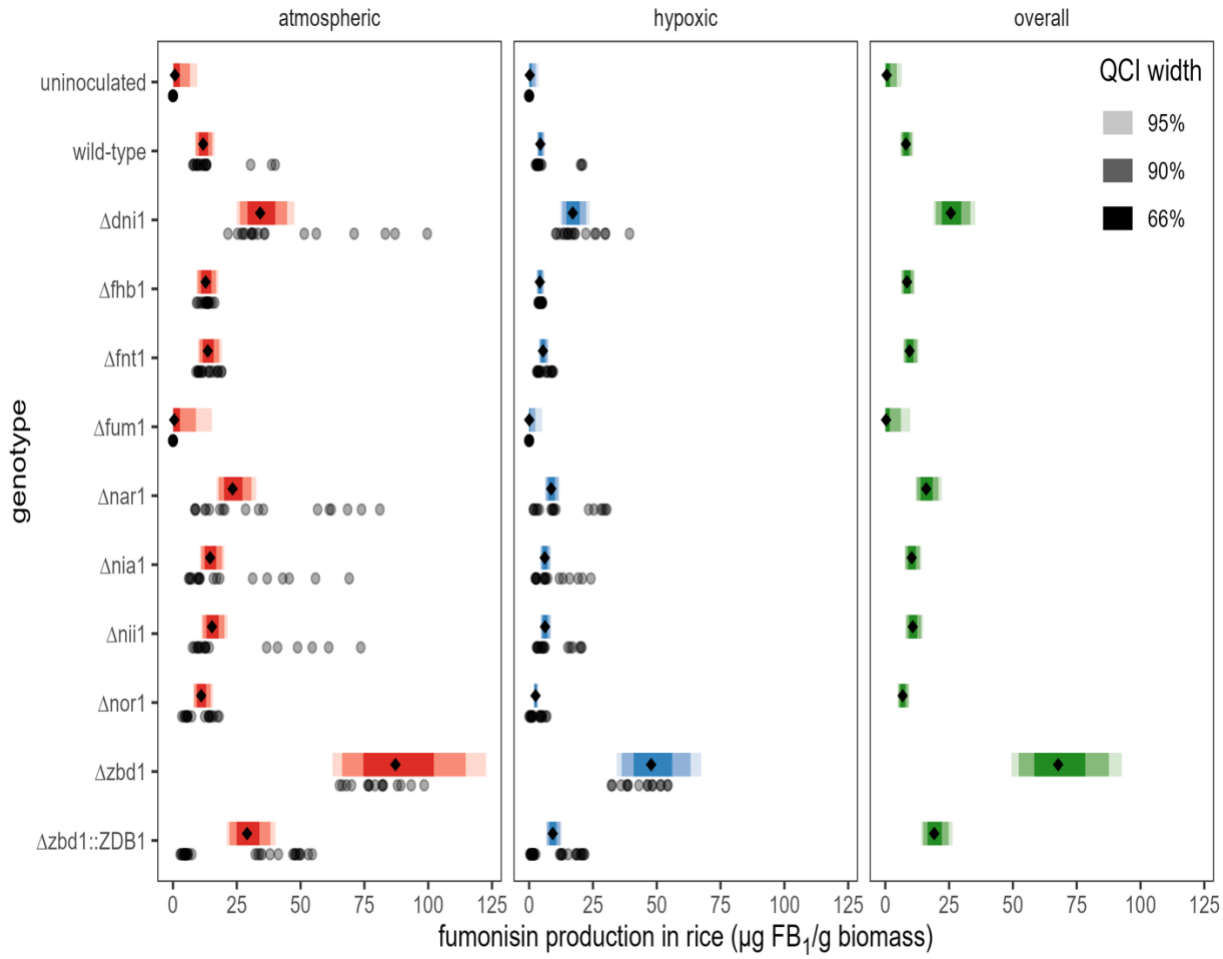

Figure 3.4. Average FB_1 production of various mutant strains of *Fusarium verticillioides* in response to normoxia or hypoxia. A genotype-level comparison of the estimated mean of FB_1 production in rice between strains grown under atmospheric and hypoxic conditions. Overall FB_1 production represents the average across both oxygen levels. The light gray dots are the raw data. The diamond-shaped point is the median of the posterior predictive distribution. The shaded blue regions show the uncertainty around the means with 66%, 90%, and 95% quantile credible intervals in progressively lighter colors. FB_1 production measured as μg FB_1/g rice biomass.

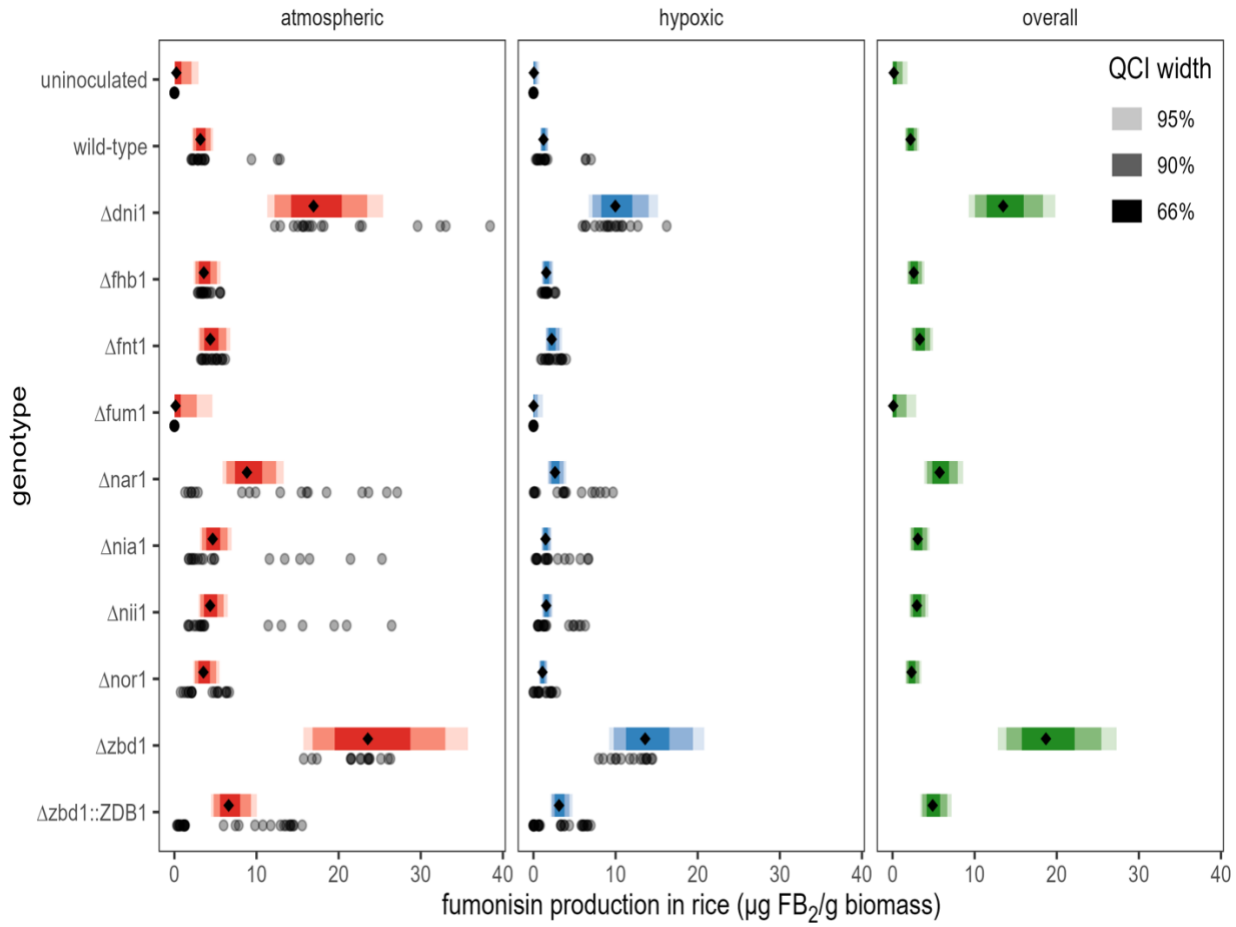

Figure 3.5. Average FB_2 production of various mutant strains of *Fusarium verticillioides* in response to normoxia or hypoxia. A genotype-level comparison of the estimated mean of FB_2 production in rice between strains grown under atmospheric and hypoxic conditions. Overall FB_2 production represents the average across both oxygen levels. The light gray dots are the raw data. The diamond-shaped point is the median of the posterior predictive distribution. The shaded blue regions show the uncertainty around the means with 66%, 90%, and 95% quantile credible intervals in progressively lighter colors. FB_2 production measured as μg FB_2/g rice biomass.

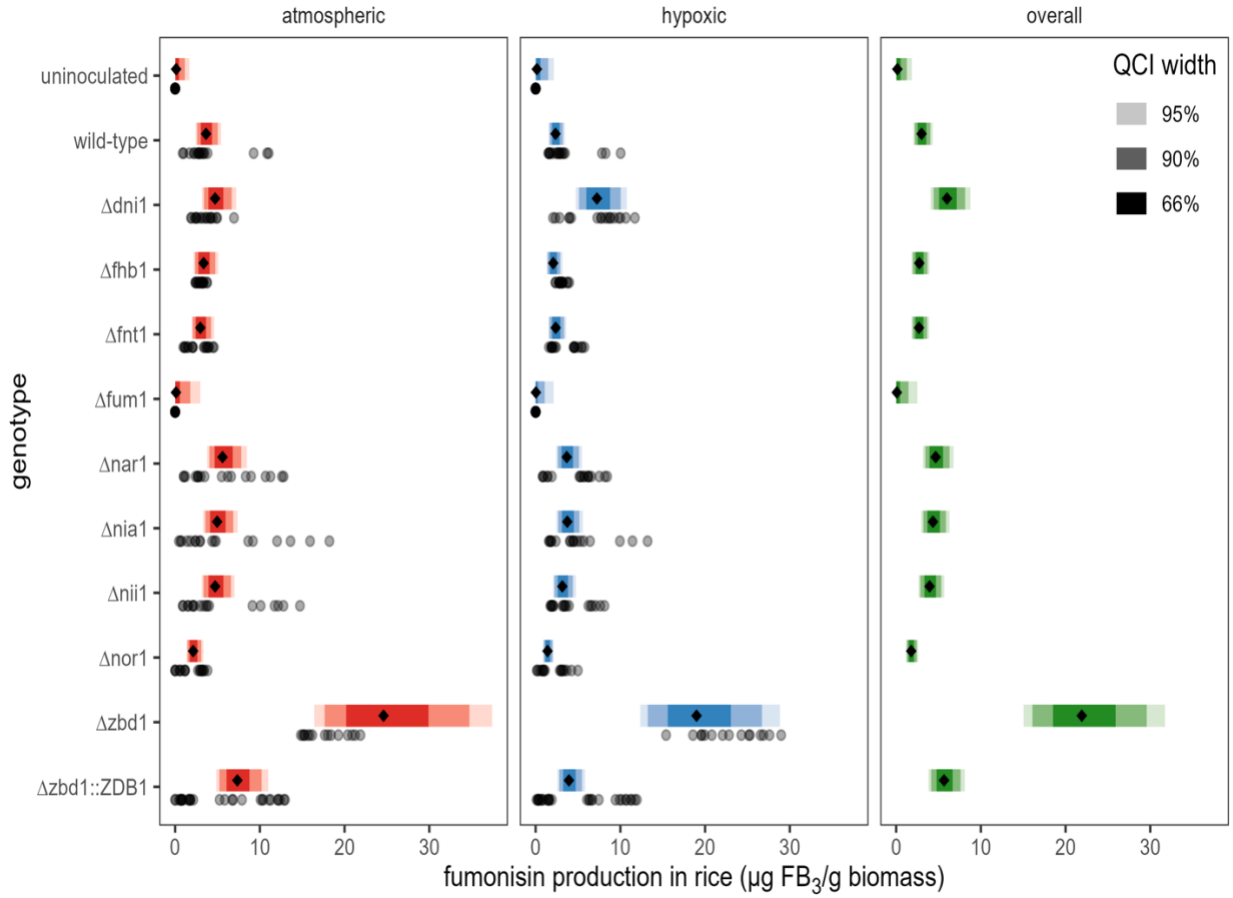

Figure 3.6. Average FB_3 production of various mutant strains of *Fusarium verticillioides* in response to normoxia or hypoxia. A genotype-level comparison of the estimated mean of FB_3 production in rice between strains grown under atmospheric and hypoxic conditions. Overall FB_3 production represents the average across both oxygen levels. The light gray dots are the raw data. The diamond-shaped point is the median of the posterior predictive distribution. The shaded blue regions show the uncertainty around the means with 66%, 90%, and 95% quantile credible intervals in progressively lighter colors. FB_3 production measured as μg FB_3/g rice biomass.

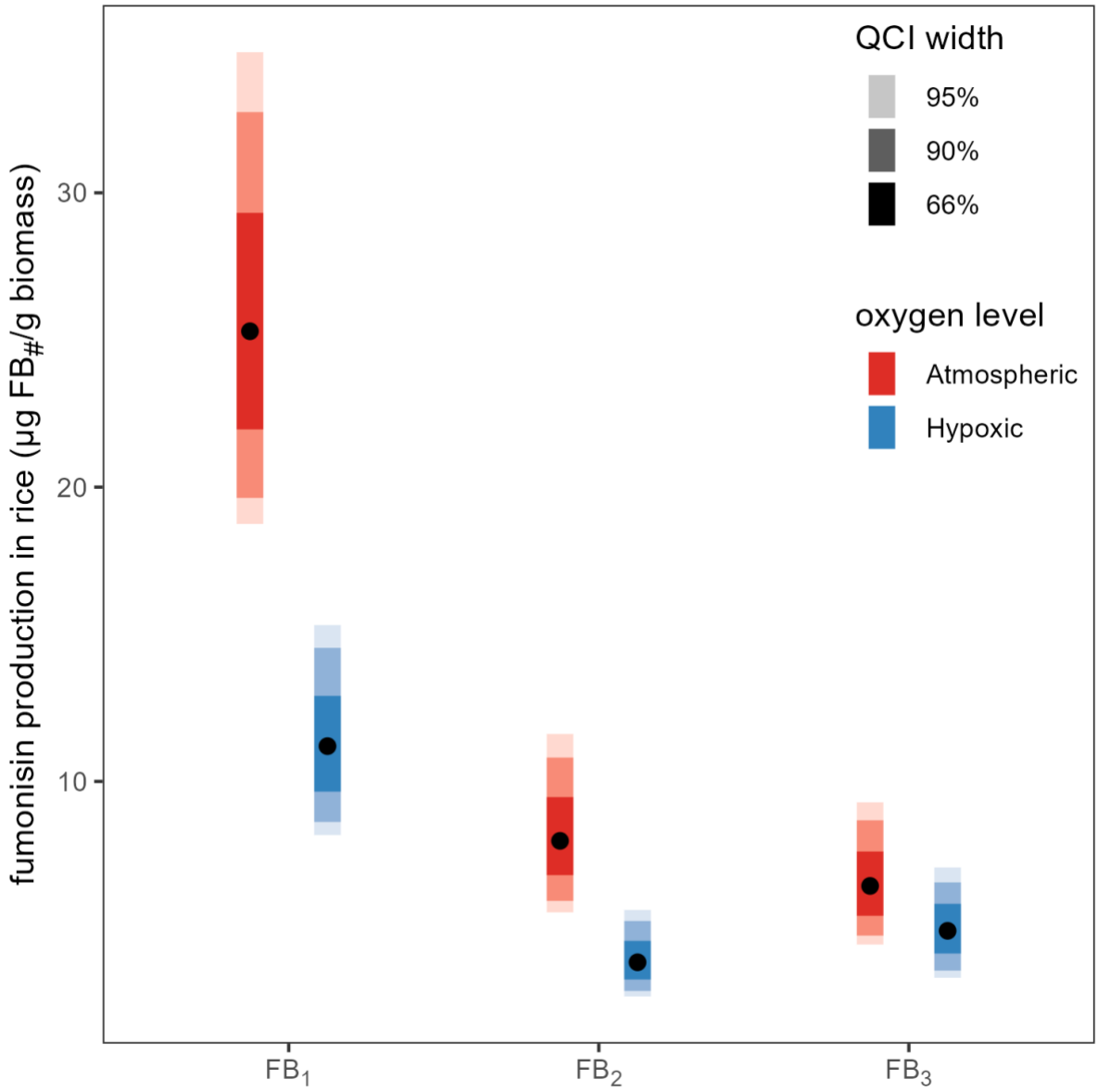

Figure 3.7. Average FB_1, FB_2, and FB_3 production across strains in response to normoxia or hypoxia. Modeled estimates of fumonisin production in rice across mutant strains grown under atmospheric or hypoxic conditions. The black dots are the point estimate (median of the posterior distribution). The shaded regions show the uncertainty with 66%, 90%, and 95% quantile credible intervals in progressively lighter colors; red and blue correspond to atmospheric and hypoxic conditions, respectively.

Supplemental Tables

Supplementary Table S3.1. *Fusarium* strains used in this study.

Strain	Genotype/Mating Type	Description
FRC M-3125[a]	Wild type *Fv/MAT1-1*	Strain used for genetic transformation and functional characterization
Δ*FvNOR1*-1	Δ*nor1/MAT1-1*	FVEG_10773 deletion mutant in FRC M-3125
Δ*FvNOR1*-2	Δ*nor1/MAT1-1*	FVEG_10773 deletion mutant in FRC M-3125
Δ*FvNAR1*-1	Δ*nar1/MAT1-1*	FVEG_01721 deletion mutant in FRC M-3125
Δ*FvNAR1*-2	Δ*nar1/MAT1-1*	FVEG_01721 deletion mutant in FRC M-3125
Δ*FvDNI1*-1	Δ*dni1/MAT1-1*	FVEG_08676 deletion mutant in FRC M-3125
Δ*FvDNI1*-2	Δ*dni1/MAT1-1*	FVEG_08676 deletion mutant in FRC M-3125
Δ*FvNIA1*-1	Δ*nia1/MAT1-1*	FVEG_07298 deletion mutant in FRC M-3125
Δ*FvNIA1*-2	Δ*nia1/MAT1-1*	FVEG_07298 deletion mutant in FRC M-3125
Δ*FvNII1*-1	Δ*nii1/MAT1-1*	FVEG_02069 deletion mutant in FRC M-3125
Δ*FvNII1*-2	Δ*nii1/MAT1-1*	FVEG_02069 deletion mutant in FRC M-3125
Δ*FvFNT1*-1	Δ*fnt1/MAT1-1*	FVEG_03704 deletion mutant in FRC M-3125
Δ*FvFNT1*-2	Δ*fnt1/MAT1-1*	FVEG_03704 deletion mutant in FRC M-3125
Δ*FvFHB1*-1	Δ*fhb1/MAT1-1*	FVEG_11186 deletion mutant in FRC M-3125
Δ*FvFHB1*-2	Δ*fhb1/MAT1-1*	FVEG_11186 deletion mutant in FRC M-3125
Δ*FvFUM1*-1[b]	Δ*fum1/MAT1-1*	FVEG_00316 deletion mutant in FRC M-3125
Δ*FvFUM1*-2[b]	Δf*um1/MAT1-1*	FVEG_00316 deletion mutant in FRC M-3125
Δ*FvZBD1*-1[c]	Δ*zbd1/MAT1-1*	FVEG_00314 deletion mutant in FRC M-3125
Δ*FvZBD1*-2[c]	Δ*zbd1/MAT1-1*	FVEG_00314 deletion mutant in FRC M-3125

Δ*FvZBD1*-1::C1[c]	Δ*zbd1*::*ZBD1*/*MAT1-1*	Δ*FvZBD1*-1 deletion mutant complemented with FVEG_00314
Δ*FvZBD1*-2::C2[c]	Δ*zbd1*::*ZBD1*/*MAT1-1*	Δ*FvZBD1*-2 deletion mutant complemented with FVEG_00314

[a] FRC, Fusarium Research Center, Pennsylvania State University; [b] NRRL, ARS Culture Collection, Mycotoxin Prevention and Applied Microbiology Research Unit, National Center for Agricultural Utilization Research, Peoria, IL; [c] RRC, Russell Research Center, Toxicology and Mycotoxin Research Unit, U.S. National Poultry Research Center, Athens, GA

Supplementary Table S3.2. Primers used in this study.

Index	Primer Name	Primer Sequence (5' → 3')	Description
P1/1	FVEG_01721 O1[a]	GGGGACAGCTTTCTTGTACAAAGTGGAA'GGGAGCCTTGGTACAATATC	Amplification of 5' flank of *FvNAR1*
P1/2	FVEG_01721 O2[a]	GGGGACTGCTTTTTTGTACAAACTTGT'GGCTCGTGTCCTATCAAATC	
P1/3	FVEG_01721 O3[a]	GGGGACAACTTTGTATAGAAAAGTTGTT'GAGAGATAGACCCGGAAAGA	Amplification of 3' flank of *FvNAR1*
P1/4	FVEG_01721 O4[a]	GGGGACAACTTTGTATAATAAAGTTGT'CAATTCCGTGAGGCGTATTA	
P1/5	FVEG_01721_ORF_F_v1	TCCTGTAGAAGGAACACATTAC	Confirmation of presence/absence of the *FvNAR1* ORF in OSCAR transformants
P1/6	FVEG_01721_ORF_R_v1	CTCTTCTGGGAATGAAACAAAG	
P1/7	FVEG_01721_5'_Out F	TTCAAGCCGCGATATCTCTCGAGAG	Confirmation of the integrity of outer sequences flanking the 5' flank of *Fv*NAR1
P1/8	FVEG_01721_3'_Out R	CGCAGCATGCATGATTCCAAATCTC	Confirmation of the integrity of outer sequences flanking the 3' flank of *Fv*NAR1
P1/9	FVEG_08676 O1[a]	GGGGACAGCTTTCTTGTACAAAGTGGAA'GCATCCCTGCTCAGAATTATATC	Amplification of 5' flank of *FvDNI1*
P1/10	FVEG_08676 O2[a]	GGGGACTGCTTTTTTGTACAAACTTGT'GTCGATCTTTATACTGCGACTAC	
P1/11	FVEG_08676 O3[a]	GGGGACAACTTTGTATAGAAAAGTTGTT'CAATGACTTCGGAGGTTTAAGAG	Amplification of 3' flank of *FvDNI1*
P1/12	FVEG_08676 O4[a]	GGGGACAACTTTGTATAATAAAGTTGT'TATAGGCATCTTGAGGAAGGTC	

P1/13	FVEG_08676_ORF_F_v1	TATACGTCAGGACAAGGAGAATA	Confirmation of presence/absence of the *FvDNI1* ORF in OSCAR transformants
P1/14	FVEG_08676_ORF_R_v1	CTTGGATAGTTGTGGTCAGTAAA	
P1/15	FVEG_08676_5'_Out F	TATACGTCAGGACAAGGAGAATA	Confirmation of the integrity of outer sequences flanking the 5' flank of *Fv*DNI1
P1/16	FVEG_08676_3'_Out R	CTTGGATAGTTGTGGTCAGTAAA	Confirmation of the integrity of outer sequences flanking the 3' flank of *Fv*DNI1
P1/17	FVEG_07298 O1[a]	GGGGACAGCTTTCTTGTACAAAGTGGAA'GCTGTAGATAAGGCAACAGAG	Amplification of 5' flank of *FvNIA1*
P1/18	FVEG_07298 O2[a]	GGGGACTGCTTTTTTGTACAAACTTGT'GTCTAAGAGGCAGCAGAAAG	
P1/19	FVEG_07298 O3[a]	GGGGACAACTTTGTATAGAAAAGTTGTT'CAGCTCTACGAGATCAGAGT	Amplification of 3' flank of *FvNIA1*
P1/20	FVEG_07298 O4[a]	GGGGACAACTTTGTATAATAAAGTTGT'CTATGCCCGACAATCATACC	
P1/21	FVEG_07298_ORF_F_v1	AGTTATAAGGTGCGAGGTTATG	Confirmation of presence/absence of the *FvNIA1* ORF in OSCAR transformants
P1/22	FVEG_07298_ORF_R_v1	CATCGGAGTATGGTGTGTATG	
P1/23	FVEG_07298_5'_Out F	AAGCAGATATGATCTCGGAAAG	Confirmation of the integrity of outer sequences flanking the 5' flank of *Fv*NIA1
P1/24	FVEG_07298_3'_Out R	TCCCAGTTCCAAACACATATAG	Confirmation of the integrity of outer sequences flanking the 3' flank of *Fv*NIA1
P1/25	FVEG_02069 O1[a]	GGGGACAGCTTTCTTGTACAAAGTGGAA'CTTAGAAGAACTTGACGCCTAAC	Amplification of 5' flank of *FvNII1*
P1/26	FVEG_02069 O2[a]	GGGGACTGCTTTTTTGTACAAACTTGT'AGTATACTTGGGAGAGAAACCC	
P1/27	FVEG_02069 O3[a]	GGGGACAACTTTGTATAGAAAAGTTGTT'T	Amplification of 3' flank of *FvNII1*

		GGGTCATTATGAGTTATGCTATG	
P1/28	FVEG_02069 O4[a]	GGGGACAACTTTGTATAATAAAGTTGT'TATCTAGCTCCTTCCTCAAGAC	
P1/29	FVEG_02069_ORF_F_v1	CGACCGATATCTCATGTTCTAC	Confirmation of presence/absence of the *FvNII1* ORF in OSCAR transformants
P1/30	FVEG_02069_ORF_R_v1	TATGGCTTCTTTCCTCTCAATC	
P1/31	FVEG_02069_5'_Out F	GGAGTCCATATTCGGTTCATATTGG	Confirmation of the integrity of outer sequences flanking the 5' flank of *Fv*NII1
P1/32	FVEG_02069_3'_Out R	ACTGCGTCTATATTCTTGGCGAAAC	Confirmation of the integrity of outer sequences flanking the 3' flank of *Fv*NII1
P1/33	FVEG_03704 O1[a]	GGGGACAGCTTTCTTGTACAAAGTGGAA'GAACGGAGCTGATTATGATAGG	Amplification of 5' flank of *FvFNT1*
P1/34	FVEG_03704 O2[a]	GGGGACTGCTTTTTTGTACAAACTTGT'CAATAGAGATATTCACACTCACCA	
P1/35	FVEG_03704 O3[a]	GGGGACAACTTTGTATAGAAAAGTTGTT'CAGGACTGTACAAGATGAGATAAA	Amplification of 3' flank of *FvFNT1*
P1/36	FVEG_03704 O4[a]	GGGGACAACTTTGTATAATAAAGTTGT'TCCAACTAGATTCGCTTCAATAC	
P1/37	FVEG_03704_ORF_F_v1	TAAGGTGTTGTTGTCTGGTATC	Confirmation of presence/absence of the *FvFNT1* ORF in OSCAR transformants
P1/38	FVEG_03704_ORF_R_v1	TATTTCCAAAGAGAGCTGGAAT	
P1/39	FVEG_03704_5'_Out F	CCACCACGTTTGGCTTAGGCATTTA	Confirmation of the integrity of outer sequences flanking the 5' flank of *Fv*FNT1
P1/40	FVEG_03704_3'_Out R	CCTCAGCAGATGATCGAATGGATGG	Confirmation of the integrity of outer sequences flanking the 3' flank of *Fv*FNT1
P1/41	FVEG_11186 O1[a]	GGGGACAGCTTTCTTGTACAAAGTGGAA'TGCTTCAAAACCCTTTCG	Amplification of 5' flank of *FvFHB1*

P1/42	FVEG_11186 O2[a]	GGGGACTGCTTTTTT GTACAAACTTGT' GGTGATGGGAATAA C	
P1/43	FVEG_11186 O3[a]	GGGGACAACTTTGTA TAGAAAAGTTGTT' GTGCATATAGCCGTC TTCTTAT	Amplification of 3' flank of *FvFHB1*
P1/44	FVEG_11186 O4[a]	GGGGACAACTTTGTA TAATAAAGTTGT' GAAAGGGCTGCAGG TATATAAT	
P1/45	FVEG_11186_ORF_F_v1	CAAGCACGTTTCTCT CTTCATC	Confirmation of presence/absence of the *FvFHB1* ORF in OSCAR transformants
P1/46	FVEG_11186_ORF_R_v1	GTGATATTCTCGTGC TTCTTAGC	
P1/47	FVEG_11186_5'_Out F	GATTTGTGCGAACTA GCATCTG	Confirmation of the integrity of outer sequences flanking the 5' flank of *Fv*FHB1
P1/48	FVEG_11186_3'_Out R	GGGAACTCGGAGTG AGATAAAT	Confirmation of the integrity of outer sequences flanking the 3' flank of *Fv*FHB1
P1/49	Hyg_F_Out	AGAGCTTGGTTGACG GCAATTTCG	Confirmation of the integrity of outer sequences flanking the 3' flank target gene
P1/50	Hyg_R_Out	GCCGATGCAAAGTGC CGATAAACA	Confirmation of the integrity of outer sequences flanking the 5' flank target gene
P1/51	HygMarker_F_v1	TGTTTATCGGCACTT TGCATCGGC	Confirmation of HRC[b] ORF during OSCAR transformation and PCR screening
P1/52	HygMarker_R_v1	AGCTGCATCATCGAA ATTGCCGTC	

[a] The ' symbol denotes the junction between 5' attB recombination site sequences for OSCAR constructs that are added extensions to the gene primers; [b] HRC, hygromycin resistance cassette

CHAPTER 4

IDENTIFICATION OF A KEY ENZYME TARGET FOR REDUCING AGRICULTURAL EMISSIONS OF NITROUS OXIDE[3]

---

[3] Oakley BA, Mitchell TM, Read QD, Hibbs GH, Baldwin TT, Gold SE, and Glenn AE. Identification of a key enzyme target for reducing agricultural emissions of nitrous oxide. Submitted to *Science Advances*, September 21, 2023.

Abstract

Nitrous oxide (N_2O) derived from fungal denitrification of synthetic nitrogen fertilizer is a major contributor to Earth's greenhouse effect. Here, a key conserved fungal denitrification enzyme for targeted inhibition of N_2O emissions was identified. Deletion of the single copy nitric oxide reductase encoding gene (*NOR1*) in the model soil-borne denitrifying maize pathogen, *Fusarium verticillioides,* eliminated N_2O emissions. Phylogenetic analysis revealed that fungal *NOR1*-like genes, with rare exceptions, are highly conserved and confined to the phylum Ascomycota suggesting potential wide efficacy of an effective inhibitor. Successful inhibition of fungal p450nor will reduce N_2O emissions and the loss of N fertilizer. Reductions in nitrogen fertilizer loss and N_2O emissions would lessen the impact of N_2O and other greenhouse gases on climate change.

Introduction

Intensive agricultural practices are necessary to produce sufficient food to feed the global population and to maintain agricultural productivity, but they generate greenhouse gas (GHG) emissions that impact the climate system. Agriculture is estimated to be responsible for 15% of total global anthropogenic emissions and ~25% of the continuing rise of GHGs (*1*). Of 2022 U.S. GHG emissions, the agricultural sector represented 11%, a 6% increase since 1990 (*2*). The three most important GHGs in order of warming impact are carbon dioxide (CO_2, 79%), methane (CH_4, 11%), and nitrous oxide (N_2O, 7%) (*2*). N_2O is particularly problematic because it has an extremely high heat-capture capacity (about 300 times the warming potential of CO_2), an atmospheric half-life 10-fold that of methane (116±9 years), and it further threatens the environment by driving stratospheric ozone depletion (*2-5*). Global N_2O emissions equal approximately 17.7 Tg N yr^{-1}, 6.7 Tg N yr^{-1} (~38%) of which is from anthropic sources (*3*). Of the estimated 6.7 Tg of human activity produced N_2O, 2.8 Tg (~42%) is derived from agricultural soils (*6*). N_2O emissions often accompany intensive fertilizer usage with agricultural soil management, including fertilizer, livestock manure, and nitrogen-fixing crops, being the largest source of N_2O emissions (74%) in the U.S. (*7*). Due to greater human reliance on N fertilizers, the atmospheric N_2O concentration has increased by 20% from 270 parts per billion by volume (ppbv) in 1750 to 322 ppbv in 2022 and continues to increase by 0.3% annually (*8, 9*). Additionally, since global efforts have reduced the presence of ozone-depleting bromine- and chlorine-based halocarbons, N_2O, unregulated by the Montreal Protocol, is now the single-most important ozone-depleting gas (*10*).

Efficient nitrogen use is challenging

Nitrogen (N) is frequently the most limiting nutrient for crop production despite the atmosphere containing 78% N_2. The Haber-Bosch process-based industrial production of synthetic N fertilizer has led to humans doubling the input of available N to the Earth's land surface (*8, 11*), and the production process itself consumes 1-2% of the world's energy, with a commensurate CO_2 footprint (*12*). During the Green Revolution (late 1940s-late 1980s) synthetic fertilizers became integral to high yields. N fertilizer usage more than quintupled between 1950 and 2019 to produce more food on less land. It is estimated that synthetic N fertilizers have supported 42% of global births over the past century (*13*). However, the efficient use of N in agricultural systems is challenging. On a global scale only about 50% of applied N fertilizer is used by crop plants, while the remainder pollutes water and the atmosphere (*14*). One of the major processes restraining nitrogen use efficiency in plants is microbial denitrification.

Microbial denitrification

Denitrification is the process of chemically reducing the N oxyanions – nitrate (NO_3^-) and nitrite (NO_2^-) – to gaseous N oxides, principally N_2O, which serves as a final alternative acceptor for electron transport phosphorylation in lieu of di-oxygen. Activation of the denitrification pathway is primarily a response to low oxygen availability (*15*). Denitrification occurs in water and on land, and the ecological role of denitrifiers from diverse natural and managed ecosystems has been previously reviewed (*16, 17*). Both prokaryotes, including bacteria and archaea, and eukaryotes, including fungi, diatoms, and foraminifers, are capable of denitrification (*18-19*), but only bacteria, archaea, and fungi are relevant for agricultural soil denitrification. Fungi, however, play the dominant role in N_2O release from agricultural soils and many other terrestrial ecosystems (*20-27*). The canonical denitrification pathways are catalyzed

by four and three enzymes in prokaryotes and fungi, respectively. Complete fungal denitrifiers possess the core three enzymes: dissimilatory nitrate reductase (dNAR), dissimilatory nitrite reductase (dNIR), and nitric oxide reductase (NOR; p450nor) (*28, 29*). Prokaryotes engage a final nitrous oxide reductase (NOS) to reduce N_2O to N_2 (Figure 1).

Bacterial vs. fungal NOR

Despite functional similarities, bacterial and fungal NORp are structurally and biochemically distinct. Fungal p450nor is an unconventional NOR among cytochrome P450s; it is a soluble, single-subunit CYP55A oxidoreductase (E.C. 1.7.1.14; 1.14.14.1) from the cytochrome P450 superfamily that is NO-reducing and lacks the N-terminal membrane anchor that is present in other eukaryotic cytochrome P450 monooxygenase enzymes (*30*). Bacterial NORp belongs to a family of evolutionarily distinct cytochrome oxidases (E.C. 1.7.2.5) (*31*). Fungal p450nor is unique in that it takes electrons directly from NAD(P)H and/or NADH (depending on CYP55A subclass) without intervention of redox proteins (*31, 32*). In denitrifying and non-denitrifying microbes, NORp detoxifies NO in response to nitrosative stress (*33*). In fungi and bacteria, flavohemoglobins (flavoHBs) commonly co-occur with p450nor (*34*). These flavoHBs are nitric oxide dioxygenases that convert NO to NO_3^- or N_2O under oxic or anoxic conditions, respectively (*35*), but are responsible for minor N_2O production compared with p450nor.

Fungal denitrification inhibitors

Target identification and methods to inhibit denitrification and its resultant N_2O emissions are a critical environmental need. Because bacterial and fungal NORs are evolutionarily and structurally distinct, it is unlikely that efficacious cross-kingdom denitrification inhibitors can be easily designed. Studies in numerous terrestrial and particularly

agricultural systems indicate that fungi are the primary microbial N_2O producers (*36-38*). Because of this, it is thought that fungal-specific denitrification inhibitors will yield significant reduction of N_2O emissions. Matsuoka et al. (*39*) have demonstrated proof-of-concept for development of fungal denitrification inhibitors targeting dNIR activity *in vitro* and *in vivo*. However, we demonstrate here that p450nor offers a novel and preferred target for suppression of fungal denitrification-associated N_2O emissions. There are limited tools to reduce N loss and N_2O emissions and there are currently no commercially available denitrification inhibitors (*40*). To effectively address climate change, new ways to limit the inefficient use of N fertilizers and rising N_2O emissions must be developed; targeting fungal p450nor offers one such solution.

***Fusarium verticillioides,* a model system for fungal denitrification**

As a denitrification test model, *Fusarium verticillioides* (*Fv*), a soil-borne denitrifying fungal phytopathogen, the causal agent of corn (*Zea mays*) stalk and ear rots, and a producer of fumonisin mycotoxins was employed (*41*). *Fusarium* is a prominent genus of soil-borne plant pathogens and soil denitrifiers. As opposed to some *Fusarium* species with multiple paralogs (e.g., *F. oxysporum* f. sp. *vasinfectum*), the *Fv* genome has a single copy of each of the three canonical denitrification genes, simplifying mutant analysis. The deletion of the single *NOR1* gene (FVEG_10773) was hypothesized to eliminate N_2O production in *F. verticillioides*.

In this report, the *FvNOR1* gene was functionally characterized and its requirement for denitrification associated N_2O emissions was conclusively demonstrated. Through comparative genomics, high structural conservation of p450nor in the phylum Ascomycota, the key group of soil N_2O emitters, was also demonstrated. Therefore, p450nor is proposed as a likely fruitful target for broad spectrum inhibitor development to reduce agricultural soil N_2O emissions.

Results and Discussion

NOR1 is essential for N_2O production

To assess its role in N_2O production, *NOR1* gene deletion mutants (Δ*nor1*) and gene add-back transformants (Δ*nor1*::*NOR1*) (Supplementary Table S4.1) were generated and N_2O emissions (Figure 4.2; Supplementary Figure S4.1B) and impacts on growth (Supplementary Figures S4.1A, S4.2-4.8) were quantified. The *NOR1* vs. Δ*nor1* genotypes did not greatly differ in growth rates. *Fv* strains with the functional *NOR1* genotype, including wild type *Fv* and two Δ*nor1*::*NOR1* add-back strains each derived from independent deletion mutants, produce 68.1 to 104.5 times more N_2O per unit fungal biomass than did Δ*nor1* strains.

To further validate N_2O production phenotypes, segregating sexual cross progeny were generated between wild type and either *i*. a Δ*nor1* deletion mutant, or *ii*. a Δ*nor1*::*NOR1* complemented mutant add-back transformant. Haploid independently assorting progeny were produced for *NOR1* (*NOR1* or Δ*nor1*) and mating type (*MAT1-1* or *MAT1-2*) genotypes (Supplementary Table S4.1). The *NOR1* genotype was 100% correlated (n = 10) with N_2O emissions. Each *NOR1* strain produced an average of more than 19.85 ppm N_2O/mg of fungal biomass, while Δ*nor1* strains (n = 6) generated a mean of less than 0.38 ppm N_2O/mg of fungal biomass (Figure 4.2; Supplementary Figure S4.9), a reduction of at least 50-fold.

N_2O production and denitrification potential in plant pathogenic *Fusarium* species

Available genomic data indicate that, in contrast to *Fv*, many *Fusarium* species possessing a p450nor ortholog lack the complete denitrification pathway. To explore this phenomenon more closely, N_2O production capabilities in three *NOR1*-possessing economically impactful phytopathogenic *Fusarium* species, namely *Fv*, *F. graminearum* (*Fg*; 1 NOR1p ortholog), and *F. oxysporum f. sp. vasinfectum* (*Fov*; 3 NOR1p orthologs) (Supplementary Table

S4.1) were assessed. *Fv* and *Fov* are known denitrifiers, but no reports on *Fg*'s ability to denitrify or produce N_2O were found. N_2O production by *Fv, Fg,* and *Fov* was 26.26, 0.08, and 39.30 ppm/mg, respectively (Supplementary Figure S4.10). As a *NOR*-possessing fungus, the low N_2O production by *Fg* was initially perplexing. Genome analysis revealed that *Fg* lacks a dNIRp ortholog; this prevents reduction of NO_2^- to NO and without a sufficient pool of NO, *Fg* NOR1p apparently cannot convert NO to N_2O in high amounts like *Fv* and *Fov* do. This implies that the singular function of *Fg* NOR1p is NO detoxification, whereas *Fv* NOR1p has dual function in energy production through denitrification and NO detoxification.

Denitrification ability is tied to the functionality of dNIR and NOR

Substantial N_2O production is tied to the functionality of only dNIR and NOR as very minor differences in N_2O production were observed between Δ*nar1* (i.e., dNAR; FVEG_01721) mutants and wild type *Fv* in preliminary studies (data not shown). Hence, the minimal denitrification pathway in fungi comprises just the two-step reduction of NO_2^- to NO to N_2O mediated by dNIR and NOR, respectively. To compare potential inhibitor target efficacy of dNIRp to NORp for inhibition of N_2O emissions, Δ*dni1* (i.e., dNIR; FVEG_08676) mutants were evaluated for their ability to produce N_2O relative to Δ*nor1* mutants and wild type *Fv*. N_2O production in Δ*dni1* and Δ*nor1* mutants is 90% and 99% lower than the wild type, respectively (data not shown). This suggests that NORp is the key enzyme involved in N_2O production and, together with its structural conservation described below, it is an ideal inhibitor target.

NOR is specific to the fungal phylum Ascomycota

Phylogenetic analysis (Figure 4.3; Supplementary Figures S4.11-S4.13) bolsters the finding that there are p450nor-possessing fungi that are not fully functional denitrifiers (i.e., they do not have a copy of dNIR and/or dNAR). This is supported by an analysis of 167 p450nor-

containing genomes in which p450nor was twice as abundant when compared with dNAR and dNIR across all genomes (*34*). This means that there are twice as many fungal genomes that contain only NOR versus genomes that contain NOR and dNAR and/or dNIR. This strengthens the argument that there is a disconnect between p450nor presence and denitrification potential as observed in *Fg*. The fungal p450nor tree revealed that *Fv* NOR1p-like proteins are widely conserved among economically important fungal genera within the phylum Ascomycota (Figure 4.3). The Hypocreales, including *Fusarium* and *Trichoderma*, is the most well-represented order in the phylogeny and is recurringly identified in surveys of soil denitrifiers (*42, 43*).

The conservation of cytochrome p450nor orthologs with high sequence similarity to *Fv* NOR1p is restricted to the Ascomycota. The only exceptions are two Basidiomycota yeasts, *Cutaneotrichosporon cutaneum* (*Cc*), which has been previously characterized as an N_2O producer (*44*), and *Trichosporon asahii* var. *asahii* (*Taa*). Genomic data indicates that neither *Cc* nor *Taa* have a dNIRp ortholog and, thus, neither fungus can denitrify. The ubiquity of p450nor in the Ascomycota does not apply to other fungal phyla or eukaryotic kingdoms. *Fv* NOR1p-like protein top BLAST hits in non-Ascomycota fungal phyla are quite dissimilar and reciprocal BLASTs of these top hits to the *Fv* genome identify genes other than p450nor as their closest match, indicating that they are not functional p450nors.

NOR1 is a valuable broad-spectrum target for reduction of agricultural N_2O emissions

Plants, microalga, and other eukaryotes produce N_2O via flavodiiron proteins, flavoHBs, and p450nor, but they are not denitrifiers (*45*, *46*); thus, they play an insignificant role in agricultural N_2O emissions relative to fungi. Because of its key role in N_2O release and denitrification, and high structural conservation, p450nor is a distinctly favorable target for reduction of N_2O emissions from soil-borne denitrifying fungi. Unlike dNIR, NORp has a highly

conserved cytochrome P450 motif. The only residues that are variable within the 10 amino acid motif are those at positions 3, 5, and 9. The cysteine at position 8 is 100% conserved across all NORp sequences because it acts as the fifth ligand for the heme iron important for reduction of NO to N_2O (Figure 4.4). This sequence conservation increases NOR1p's value as a broad-spectrum denitrification inhibitor target compared with dNIR. Off-target effects impacting non-NOR cytochrome P450 (CYP) monooxygenases need to be considered in inhibitor design.

As a consequence of soil processes and environmental conditions, 50% of applied N fertilizer is lost (*47*). It is anticipated that a p450nor-targeted inhibitor could reduce fungal-derived soil N_2O emissions significantly (*48-50*). In addition to reducing N_2O emissions, an effective inhibitor is expected to reduce N fertilizer loss in agricultural soils and save growers valuable resources and money. A reduction in N fertilizer need would save U.S. farmers tens of millions of dollars annually.

NOR1 is a highly conserved enzyme that is key for N_2O production

The work presented here conclusively shows that (1) *Fv* NOR1p is the key enzyme needed to produce biologically relevant amounts of N_2O in *Fv*, (2) *Fv* NOR1p represents a highly conserved p450nor protein in Ascomycota fungi, and (3) dNIR and p450nor are vital to fungal denitrification. This newfound knowledge about *Fv* NOR1p, its function, and conservation can be used to inform practical design strategies that reduce N_2O emissions in agriculture. Both dNIR and p450nor are essential to fungal denitrification and denitrification inhibitors targeting both of these enzymes could provide a powerful broad-spectrum tool in our fight against climate change. Addition of effective denitrification inhibitor(s) to fertilizer is expected to reduce N_2O release and make fertilizer application more efficient and environmentally benign.

Literature Cited

1. G. S. Malhi, M. Kaur, P. Kaushik, *Sustainability* **13**, 1318 (2021).

2. United States Environmental Protection Agency (EPA), "Overview of Greenhouse Gases" (EPA, 2022); https://www.epa.gov/ghgemissions/overview-greenhouse-gases

3. D. Signor, C. E. P. Cerri, *Pesq. Agropec. Trop*. **43**, 322-338 (2013).

4. Intergovernmental Panel on Climate Change, *Climate Change 2007: Synthesis Report. Contribution of Working Groups I, II and III to the Fourth Assessment Report of the Intergovernmental Panel on Climate Change*, Core Writing Team, R.K. Pachauri, and A. Reisinger, Eds. (IPCC, Geneva, Switzerland, 2007).

5.. H. Tian et al., *Nature.* 586, 248-256 (2020).

6. Denman et al., Couplings Between Changes in the Climate System and Biogeochemistry. In: *Climate Change 2007: The Physical Science Basis. Contribution of Working Group I to the Fourth Assessment Report of the Intergovernmental Panel on Climate Change*, S. Solomon, D. Qin, M. Manning, Z. Chen, M. Marquis, K. B. Averyt, M. Tignor, and H. L. Miller, Eds. (IPCC, Cambridge, UK and New York, NY, USA, 2007).

7. United States Environmental Protection Agency (EPA), "Sources of Greenhouse Gas Emissions" (EPA, 2022); https://www.epa.gov/ghgemissions/sources-greenhouse-gas-emissions

8. J. N. Galloway et al., *Science* **320**, 889-892 (2008).

9. D. E. Canfield, A. N. Glazer, P. G. Falkowski, *Science* **330**, 192-196 (2010).

10. A. R. Ravishankara, J. S. Daniel, R. W. Portmann, *Science* **326**, 123-125 (2009).

11. P. M. Vitousek et al., *Science* **7**, 737-750 (1997).

12. J. W. Erisman et al., Nitrogen: too much of a vital resource. In: *Science Brief*, N. Oerlemans, H. Strand, Eds. (WWF Netherlands, Zeist, The Netherlands, 2015).

13. J. W. Erisman, M. A. Sutton, J. Galloway, Z. Klimont, W. Winiwarter, Nat. Geosci. **1**, 636-639 (2008).

14. P. Govindasamy et al., *Front. Plant Sci.* **14**, 1-19 (2023).

15. W. G. Zumft, Microbiol. *Mol. Biol. Rev.* **61**, 533-616 (1997).

16. J. M. Tiedje, Chapter 14: Denitrifiers. In: *Methods of Soil Analysis, Part 2. Microbiological and Biochemical Properties* (Soil Science Society of America, Madison, WI, USA, 1994).

17. S. Pajares, B. J. M. Bohannan, *Front. Microbiol.* **7**, 1045 (2016).

18. M. Hayatsu, K. Tago, M. Saito, *Soil Sci. Plant Nutr.* **54**, 33-45 (2008).

19. A. Kamp, S. Høgslund, N. Risgaard-Petersen, P. Stief, *Front. Microbiol.* **6**, 1492 (2015).

20. S. D. Wankel et al., *Nat. Commun.* **8,** 15595 (2017).

21. C. L. Crenshaw, C. Lauber, R. L. Sinsabaugh, L. K. Stavely, *Biogeochemistry* **87**, 17-27 (2008).

22. Y. Yanai et al., *Soil Sci. Plant Nutr.* **53**, 806-811 (2007).

23. R. J. Laughlin, R. J. Stevens, *Soil Sci. Soc. Am. J.* **66**, 1540-1548 (2002).

24. R. J. Laughlin, T. Rütting, C. Müller, C. J. Watson, R. J. Stevens, *Appl. Soil Ecol.* **42**, 25-30 (2009).

25. A. Castellano-Hinojosa et al., *Int. Biodeterior. Biodegrad.* **159**, 105199 (2021).

26. S. Ma, J. Shan, X. Yan, *Appl. Soil Ecol.* **116,** 23-29 (2017).

27. S. Castaldi, K. A. Smith, *Biol. Fertil. Soils* **27**, 27-34 (1998).

28. R. W. Ye, B. A. Averill, J. M. Tiedje, *Appl. Environ. Microbiol.* **60**, 1053-1058 (1994).

29. E. V. Morozkina, A. V. Kurakov, *Appl. Biochem. Microbiol.* **43**, 544-549 (2007).

30. L. Zhang, T. Kudo, N. Takaya, H. Shoun, *Int. Congr. Ser.* **1233**, 197-202 (2002).

31. J. Hendriks et al., *Biochim. Biophys. Acta* **1459**, 266-273 (2000).

32. H. Shoun, S. Fushinobu, L. Jiang, S-W. Kim, T. Wakagi, *Phil. Trans. R. Soc. B* **367**, 1186-1194 (2012).

33. M. Arasimowicz-Jelonek, J. Floryszak-Wieczorek, *Mol. Plant Pathol.* **15**, 406-416 (2014).

34. S. A. Higgins, C. W. Schadt, P. B. Matheny, F. E. Löffler, *Genome Biol. Evol.* **10**, 2474-2489 (2018).

35. R. K. Poole, M. N. Hughes, *Mol. Microbiol.* **36**, 775-783 (2000).

36. Z. Xun, W. Yang, J. Liu, B. Ren, L. Bai, *Authorea* 1-19 (2020).

37. H. Chen, N. V. Mothapo, W. Shi, *Soil Biol. Biochem.* **84**, 116-126 (2015).

38. P. J. Kearns, A. N. Bulseco-McKim, H. Hoyt, J. H. Angell, J. L. Bowen, *Microbiol. Ecol.* **77**, 358-369 (2019).

39. M. Matsuoka et al., *J. Chem. Inf. Model.* **57**, 203-213 (2017).

40. G. L. Velthof, R. P. J. J. Rietra, Nitrous oxide emission from agricultural soils. In: *Wageningen Environmental Research Report 2921* (Wageningen Environmental Research, Wageningen, The Netherlands, 2018).

41. A. A. Blacutt, S. E. Gold, K. A. Voss, M. Gao, A. E. Glenn, *Phytopathology* **108**, 312-326 (2018).

42. N. Mothapo et al., *Soil Biol. Biochem.* **83**, 160-175 (2015).

43. K. Maeda et al., *Sci. Rep.* **5**, 9697 (2015).

44. S. Tsuruta et al., *FEMS Microbiol. Lett.* **168,** 105-110 (1998).

45. M. Plouviez, A. Shilton, M. A. Packer, B. Guieysse, *J. Appl. Phycol.* **31**, 1-8 (2019).

46. A. Timilsina et al., *Front. Plant Sci.* **11**, 1177 (2020).

47. B. Hirel, T. Tétu, P. J. Lea, F. Dubois, *Sustainability* **3**, 1452-1485 (2011).

48. D. Rex et al., *Nutr. Cycl. Agroecosyst.* **110**, 135-149 (2018).

49. M. Jiang, L. Zhang, M. Liu, H. Qiu, S. Zhou, *Soil Ecol. Lett.* **4**, 155-163 (2022).

50. L. Zhong et al., *Front. Microbiol.* **13**, 844663 (2022).

51. J. F. Leslie, B.A. Summerell, The *Fusarium* Laboratory Manual. *Blackwell Publishing*, 10-11 (2006).

52. A. E. Glenn, *Mycol. Res.* **110,** 211-219 (2006).

53. C. J. R. Klittich, J. F. Leslie, *Genetics* **118**, 417-423 (1988).

54. M. Gao et al., *PLoS Pathog*. **16**, 7 (2020).

55. Z. Paz et al., *Fungal Genet. Biol.* **48**, 677-684 (2011).

56. S. E. Gold, Z. Paz, M. D. García-Pedrajas, A. E. Glenn, *J Vis. Exp.* **124**, e55239 (2017).

57. A. E. Glenn, C. W. Bacon, *J. Appl. Microbiol.* **107**, 657-671 (2009).

58. S. Gao, S. E. Gold, A. E. Glenn, *Mol. Plant Pathol.* **19**, 1127-1139 (2018).

59. Y. J. Zhang, S. Zhang, X. Z. Liu, H. A. Wen, M. Wang, *Lett. Appl. Microbiol.* **51**, 114-118 (2010).

60. J. Bergsten, *Cladistics* **21**, 163-193 (2005).

61. K. Katoh, K. Misawa, K-i. Kuma, T. Miyata, Nucleic Acids Res. **30**, 3059-3066 (2002).

62. K. Katoh, D. M. Standley, *Mol. Biol. Evol.* **30**, 772-780 (2013).

63. M. N. Price, P. S. Dehal, A. P. Arkin, *Mol. Biol. Evol.* **26**, 1641-1650 (2009).

64. M. N. Price, P. S. Dehal, A. P. Arkin, PLoS ONE **5**, e9490 (2010).

65. L-T. Nguyen, H. A. Schmidt, A. von Haeseler, B. Q. Minh, *Mol. Biol. Evol.* **32**, 268-274 (2015).

66. S. Kalyaanamoorthy, B. Q. Minh, T. K. F. Wong, A. von Haeseler, L. S. Jermiin, *Nat. Methods* **14**, 587-589 (2017).

67. C. Kosiol, N. Goldman, *Mol. Biol. Evol.* **22**, 193-199 (2005).

68. D. T. Jones, W. R. Taylor, J. M. Thornton, *Comput Appl. Biosci.* **8**, 275-282 (1992).

69. Z. Yang, *Genetics* **139**, 993-1005 (1995).

70. J. Soubrier et al., *Mol. Biol. Evol.* **29**, 3345-3358 (2012).

71. Z. Yang, *J. Mol. Evol.* **39**, 306-314 (1994).

72. D. T. Hoang, O. Chernomor, A. von Haeseler, B. Q. Minh, L. S. Vinh, *Mol. Biol. Evol.* **35**, 518-522 (2018).

73. S. Guindon et al., *Syst. Biol.* **59**, 307-321 (2010).

74. B. Q. Minh, M. A. T. Nguyen, A. von Haeseler, *Mol. Biol. Evol.* **30**, 1188-1195 (2013).

75. J. Felsenstein, *Evolution* **39**, 783-791 (1985).

76. N. P. Brown, C. Leroy, C. Sander, *Bioinformatics* **14**, 380-381 (1998).

77. F. Madeira et al., Nucleic Acids Res. **50**, W276-W279 (2022).

78. A. C. E. Darling, B. Mau, F. R. Blattner, N. T. Perna, *Genome Res.* **14**, 1394-1403 (2004).

79. A. E. Darling, B. Mau, N. T. Perna, *PLoS ONE* **5**, e11147 (2010).

80. P. Rice, I. Longden, A. Bleasby, *Trends Genet*. **16**, 276-277 (2000).

81. G. E. Crooks, G. Hon, J-M. Chandonia, S. E. Brenner, *Genome Res.* **14**, 1188-1190 (2004).

82. T. D. Schneider, R. M. Stephens, *Nucleic Acids Res.* **18**, 6097-6100 (1990).

83. N. V. Mothapo, H. Chen, M. A. Cubeta, W. Shi, *Soil Biol. Biochem.* **66**, 94-101 (2013).

84. O. Van Cleemput, A. H. Samater, *Fertil. Res.* **45**, 81-89 (1996).

85. P. T. Mørkved, P. Dörsch, L. R. Bakken, *Soil Biol. Biochem.* **39**, 2048-2057 (2007).

86. R. B. Lavrent'ev, S. A. Zaitsev, I. I. Sudnitsyn, A. V. Kurakov, *Mosc. Univ. Soil Sci. Bull.* **63**, 178-183 (2008).

87. S. E. Gold, D. W. Brown, B. D. Nadon, F. N. Williams, V. T. Vo, C. E. Miller, submitted.

88. Z. Šidák, *J. Am. Stat. Assoc.* **62,** 626-633 (1967).

89. R Core Team (2021). R: A language and environment for statistical computing. R Foundation for Statistical Computing, Vienna, Austria. https://www.R-project.org/.

Stan Development Team. 2019. Stan Modeling Language Users Guide and Reference Manual, 2.28. https://mc-stan.org.

90. D. Bates, M. Mächler, B. M. Bolker, S. C. Walker, *J. Stat. Softw.*, **67**, 1 (2015).

91. A. Kuznetsova, P. B. Brockhoff, R. H. B. Christensen, J Stat. Softw. **82**, 13 (2017).

92. Lenth RV (2022). emmeans: Estimated Marginal Means, aka Least-Squares Means. R package version 1.7.3. https://CRAN.R-project.org/package=emmeans.

93. T. Hothorn, F. Bretz, P. Westfall, Biom J. **50**, 346-363 (2008).

94. Gabry J, Cesnovar R (2021). cmdstanr: R Interface to 'CmdStan'. https://mc-stan.org/cmdstanr, https://discourse.mc-stan.org.

95. P-C. Bürkner, R J., **10**, 395-411 (2018).

96. Kay M (2022). tidybayes: Tidy Data and Geoms for Bayesian Models. doi: 10.5281/zenodo.1308151, R package version 3.0.2. http://mjskay.github.io/tidybayes/.

Figures

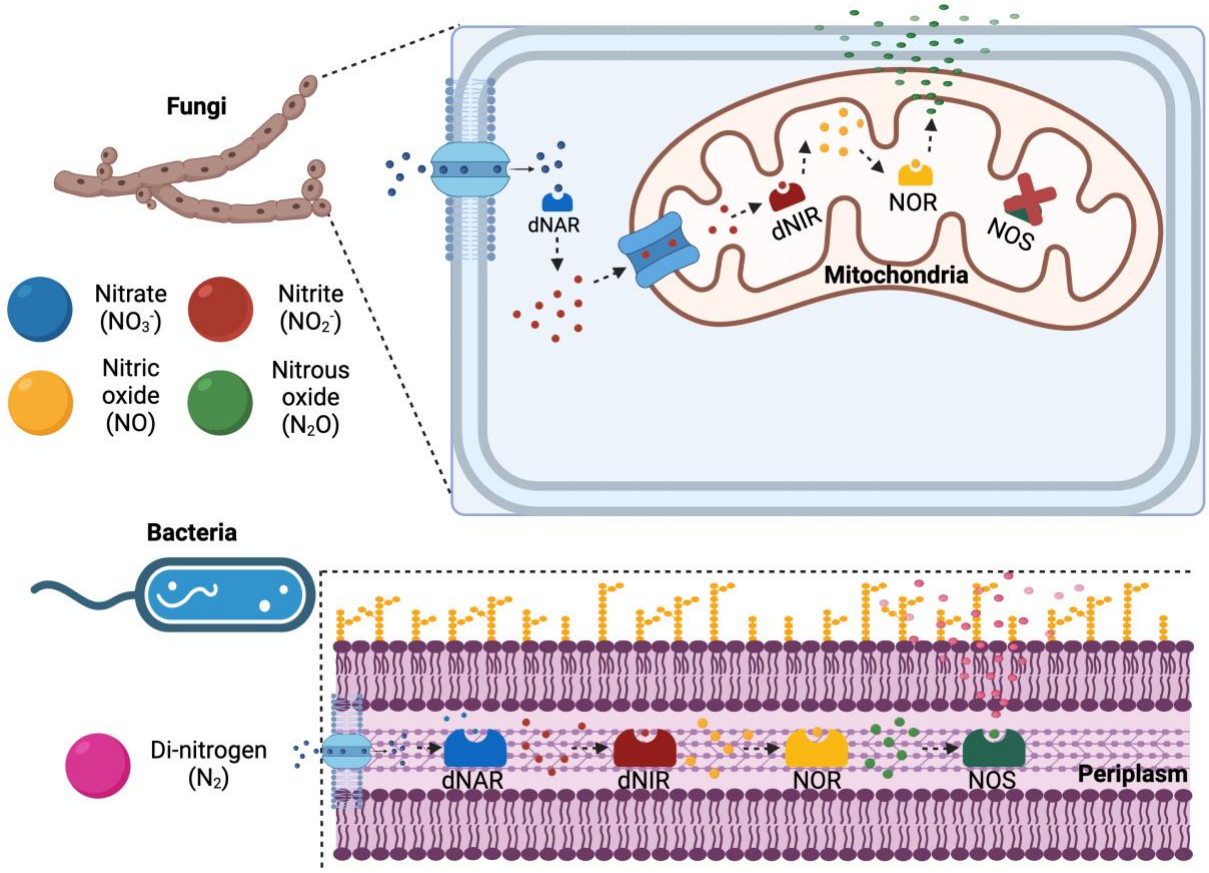

Figure 4.1. Comparison between the major players of the denitrification pathway in fungi vs. bacteria. Fungi lack the NOS enzyme and thus produce N_2O as the final product instead of di-nitrogen (N_2) as in bacteria. Localization of reductases is kingdom- and species-specific. Fungal denitrification enzymes can be found in the mitochondrion or the cytosol and are soluble. Bacterial denitrification enzymes are found in the periplasm and sometimes in the cytoplasm. dNAR = dissimilatory nitrate reductase; dNIR = dissimilatory nitrite reductase; NOR = nitric oxide reductase; NOS = nitrous oxide reductase. Created with BioRender.com.

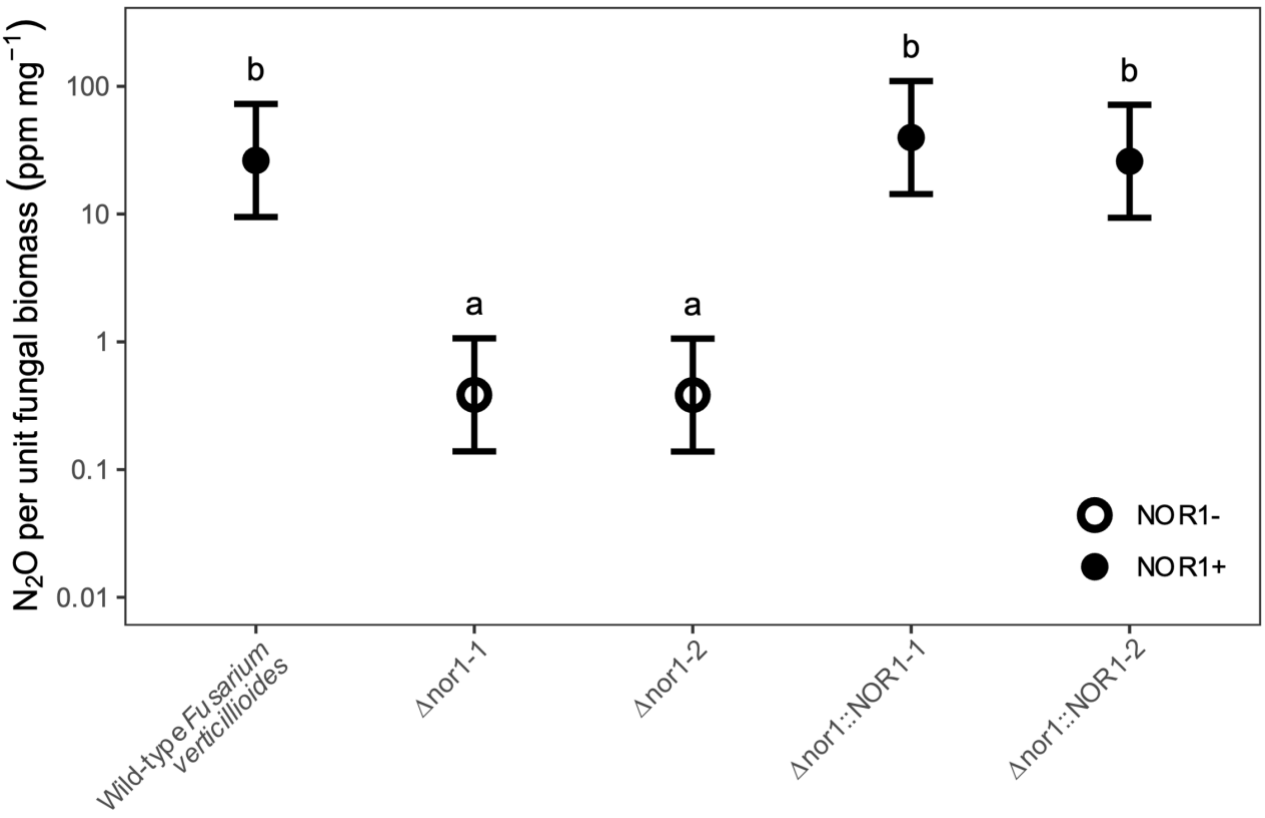

Figure 4.2. Role of p450nor in N_2O production. Analysis of *NOR1* in *Fusarium verticillioides* across wild type, deletion mutants (Δ*nor1*-1 and Δ*nor1*-2) and add-back (Δ*nor1*-1::NOR1 and Δ*nor1*-2::NOR1) genotypes. Open circles indicate a *F. verticillioides* strain with *NOR1* absent from its genome; closed black circles indicate strains having *NOR1* present in its genome. The vertical axis is transformed to a log-scale for easier visualization. Group means that do not share a letter are significantly different based on a Šidák adjustment and error bars represent adjusted 95% confidence intervals.

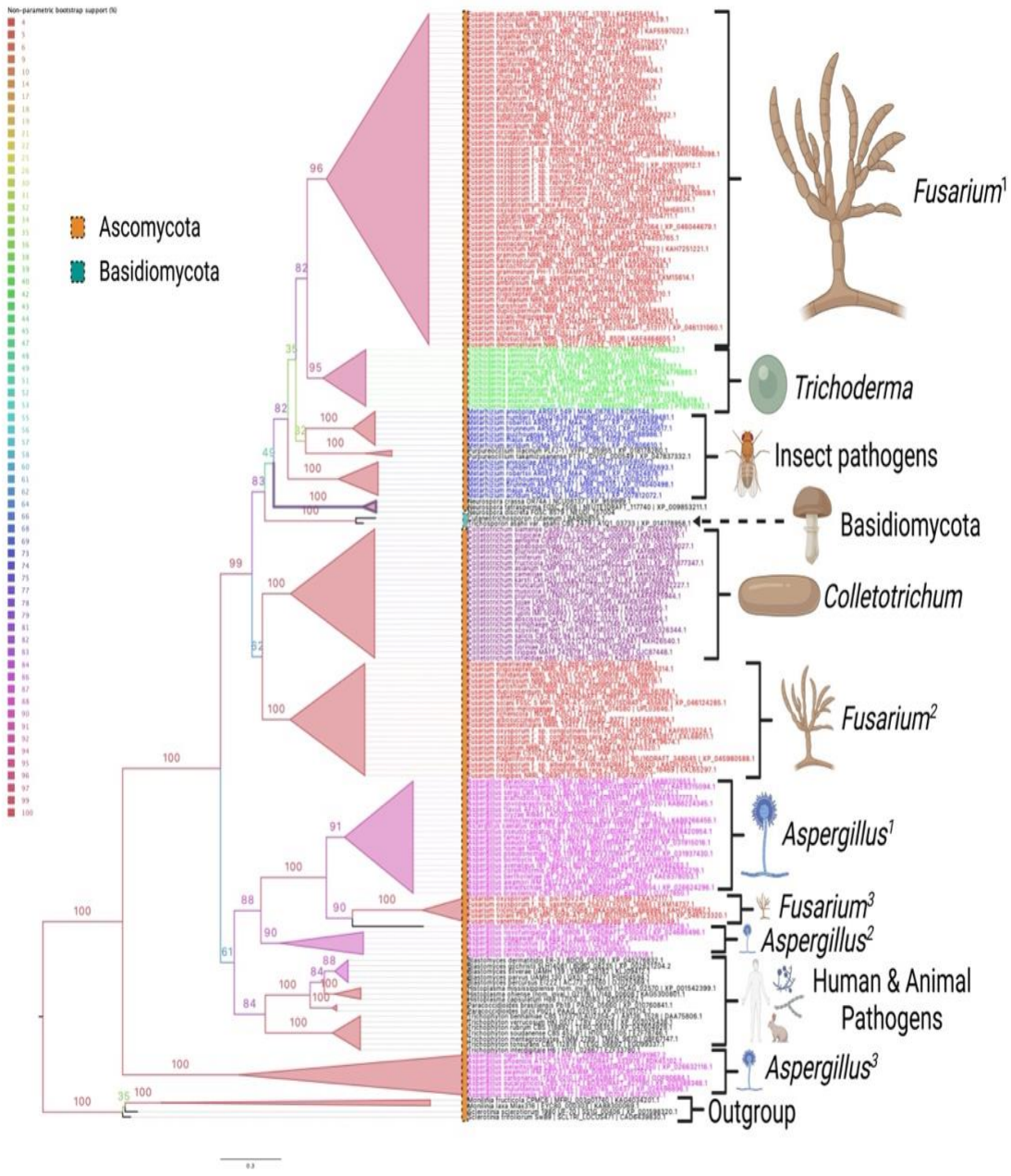

Figure 4.3. Protein tree of nitric oxide reductase (NOR; CYP55A subfamily) in fungi. A dataset of 198 sequences was aligned using MAFFT. The protein tree is rooted to the most basal sister clade (i.e., outgroup) which was determined in preliminary analyses using FastTree. Maximum-likelihood trees were built using IQ-TREE (v1.6.12). ModelFinder identified the best substitution model as JTTDCMut+R5 according to Bayesian Information Criterion (BIC). The phylogeny was assessed with 100 bootstrap replicates using nonparametric bootstrap estimation. The tree branches and branch labels are colored according to the nonparametric bootstrap support (%). Scale bar (0.3) is at the bottom of the tree. Tree visualization was done using FigTree (v1.4.4). The numerical superscripts for *Fusarium* and *Aspergillus* enumerate the three different clades of each genus. Created with BioRender.com.

Figure 4.4. Sequence logo of the cytochrome P450 motif. 159 of the 198 protein sequences from the fungal phylogeny of nitric oxide reductase were characterized by a canonical 10 amino acid cytochrome P450 motif with a highly conserved cysteine that is important for reduction of NO to N_2O. Motifs were extracted from each protein sequence and sequences were aligned using MAFFT. This logo consists of stacks of letters and there is one stack for each position in the amino acid sequence. The overall height of each stack indicates the sequence conservation at that position. The height of symbols within the stack reflect the relative frequency of the amino acid at that position. This sequence logo was created with WebLogo 2.8.2.

Supplemental Materials and Methods

Fungal and bacterial strains, culture media, and growth conditions

The strains of *Fusarium verticillioides* created and used for this study are listed in Supplementary Table 1. The sequenced wild type strain FRC M-3125 (also known as FGSC 7600) was used for genetic modification and functional characterization. For culturing, strains were grown routinely at 27° C in the dark for 3 days on either (i) potato dextrose agar (PDA; Neogen Food Safety, Lansing, MI, USA) or (ii) in potato dextrose broth (PDB; Neogen Food Safety) on a shaker incubator at 250 rpm. For fungal growth bioassay, strains were grown in a semi-synthetic minimal medium (MM) based on Czapek-Dox medium (*51*) with supplements. For N_2O detection/quantification experiments, strains were grown in PDB, double-distilled water, and MM without and with supplements. This modified basal medium (per liter) contains: 1.0 g KH_2PO_4, 0.50 g $MgSO_4 \bullet 7H_2O$, 0.50 g KCl, 30.0 g Sucrose, and 200 μL of Trace Element Solution (TES). The TES (per 100 mL) contains: 5.0 g citric acid, 5.0 g $ZnSO_4 \bullet 6H_2O$, 1.0 g $Fe(NH_4)_2(SO_4)_2 \bullet 6H_2O$, 0.25 g $CuSO_4 \bullet 5H_2O$, 0.05 g $MnSO_4$, 0.05 g H_3BO_3, 0.05 g $Na_2MoO_4 \bullet 2H_2O$. MM was supplemented with 1.28 g $NaNO_3$ (15 mM) or 1.04 g $NaNO_2$ (15 mM) and with or without 0.15 g L-Lysine (1 mM) (Merck/MilliporeSigma, Burlington, MA, USA). For selection of transformed strains, PDA amended with 150 μg/mL hygromycin B (Invitrogen, Carlsbad, CA, USA) and/or 300 μg/mL geneticin (Thermo Fisher Scientific, Waltham, MA, USA) was used. Water agar (3%) plates were used for single spore isolation of conidia and ascospores (*52*). Sexual crosses were performed on carrot agar (*53*) at 27° C with 16 h light/8 h dark grow light cycles.

Fungal gene deletion mutants were constructed as described in Gao et al. (*54*). To construct fungal gene deletion mutants, *Escherichia coli* (One Shot® MAX Efficiency®

DH5α^{TM}-T1R, Invitrogen) was used as the recipient of OSCAR deletion constructs and was grown in/on low-Na (0.5 g/L) Luria–Bertani (LB) medium amended with 100 μg/mL spectinomycin (Thermo Fisher Scientific) at 37° C overnight. The fungal transformation was mediated by OSCAR deletion plasmid containing-*Agrobacterium tumefaciens* AGL-1 strains cultured on low-Na LB medium amended with 100 μg/mL spectinomycin at 27° C for 24-48 hours (*55, 56*).

Construction of gene deletion mutants and complemented strains

Plasmid pSG10773_OSCAR was created as the gene deletion construct for FVEG_10773 (*FvNOR1*) using the OSCAR method (*55*). pSG10773_OSCAR was verified by sequencing (Eurofins Genomics LLC, Louisville, KY, USA). Supplementary Table 2 lists the primers used in this study. Two pairs of primers for *FvNOR1* were designed to amplify approximately 1 kb each of the 5' (primers P1/1 and P1/2) and 3' (primers P1/3 and P1/4) flanks of the open reading frame (ORF). The OSCAR gene deletion construct contains two flanks separated by a hygromycin resistance cassette (HRC), all between the T-DNA borders. By *Agrobacterium tumefaciens* mediated transformation (ATMT) and homologous recombination with the gene deletion construct, the gene coding sequence of FVEG_10773 was deleted from the wild type genome of strain FRC M-3125. Hygromycin-resistant transformants were initially screened for the presence of the HRC (primers P1/11 and P1/12) and loss of the ORF (primers P1/5 and P1/6) to identify potential gene deletion mutants, which were further subjected to single spore purification and confirmation PCR screening. The following criteria were used during PCR screening for deletion mutants: (1) presence of the HRC (primers P1/11 and P1/12); (2) loss of the FVEG_10773 ORF (primers P1/5 and P1/6); (3) confirmation of positionally correct replacement of *FvNOR1* ORF with HRC at the 5' end (primers P1/7 and P1/10); and (4)

confirmation of positionally correct replacement of *FvNOR1* ORF with HRC at the 3' end (primers P1/9 and P1/8).

Complemented strains were constructed via protoplast-mediated co-transformation. The wild type amplicon of *FvNOR1* (total length, 3,601 bp) was generated with primers P1/23 and P1/24 to include the ORF (1,650 bp) and the sequences both upstream (containing 1,487 bp 5' of the predicted start codon) and downstream (containing 464 bp 3' of the stop codon). The reaction was prepared with TaKaRa high fidelity LA Taq polymerase (TaKaRa Bio, Kyoto, Japan) following the manufacturer's protocol. The amplicons were purified (QIAquick PCR purification kit, Qiagen, Inc., Valencia, CA, USA) and combined with undigested pGEN-NotI (1 μg) for PEG- mediated co-transformation of protoplasts (*57*) generated from the Δ*nor1* deletion strains. Transformants were selected on both geneticin (300 μg/mL) and hygromycin (150 μg/mL) and screened by ORF primer pairs P1/5 + P1/6 to confirm ectopic complementation fragment integration of *FvNOR1*. PCR reactions were carried out with Q5® High-Fidelity 2X Master Mix (New England Biolabs, Ipswich, MA, USA) following the manufacturer's protocol. PCR conditions were as follows: T_m was calculated using the Tm Calculator (v1.13.1; New England Biolabs); primer concentration in the mixture was 500 nM; extension time was estimated as 1 min/1,000 bp of expected amplicon size; 30 reaction cycles. The length of amplified products was determined on a 0.8% agarose gel. Gel staining was performed using Biotium Gel Red Agarose (Biotium, Fremont, CA, USA). The gel was visualized using an Invitrogen iBright 1500 (Invitrogen). Ectopic insertion of the complementing fragment was confirmed by retention of the HRC in all complemented strains. Complemented transformants were confirmed by PCR for the reintroduction of the target gene (primers P1/5 and P1/6 for *FvNOR1*), the geneticin resistance cassette (primers P1/13 and P1/14), and the mating type gene (primers P1/15 and P1/16 for

MAT1-1 and primers P1/17 and P1/18 for *MAT1-2*). Strains that were complemented (with *FvNOR1*) were obtained.

Sexual crosses were done to generate mutants that comprise a collection of $NOR1^+$ and $NOR1^-$ progeny of both MAT1-1 and MAT1-2 mating types (*53, 58*). The two parents were a (1) MAT1-2 near-isogenic line of wild type *F. verticillioides* FRC M-3125 and (2) a MAT1-1 Δ*FvNOR1* mutant or Δ::*FvNOR1* complemented add-back. The female strain (MAT1-2; *F. verticillioides* NIL) was grown on carrot agar at 27° C for 5-7 days in the dark. 1-2 mL of 3-day-old PDB culture of the male strain (MAT1-1; *F. verticillioides* FRC M-3125) was spread gently and evenly over the female growth. The fertilized plates were incubated at 27° C with 16 h light and 8 h dark cycles. After 2-3 weeks, the cirrhi were visible at the tip of the perithecia and were transferred with an inoculation needle into 0.7 mL of sterile water to disperse the ascospores. Alternatively, forcibly discharged ascospores were collected from the lids of the Petri dishes in 0.7 mL of sterile water. Fifty micro-liter aliquots of the ascospore suspension were plated onto 3% water agar for single spore isolation of F_1 progeny. Crosses were done in triplicate. Progeny (Δ*FvNOR1*xNIL and Δ::*FvNOR1*xNIL) were used in subsequent experimentation.

PCR confirmation of genetic mutants and sexual progeny

Wild type strains, deletion and add-back mutants, and sexual cross progeny were all validated by PCR screening. Fungal strain DNA was extracted using the thermolysis method (*59*). Fungal strains were grown on PDA at 27° C in the dark for 4 days. Once a strain formed a colony, we used a sterile toothpick to transfer mycelia from the colony into 100 μL of lysis solution. The lysis solution contains 50 mM sodium phosphate buffer (pH 7.4), 1 mM EDTA, and 5% glycerol. We incubated the mixture at 85° C in a water bath for 30 minutes. The crude extracts containing genomic DNA were stored at -20° C until further use.

The criteria described above for deletion mutants generated by the OSCAR method and add-backs generated by protoplast complementation were combined to fully assess each fungal strain used in the study: (1) presence of the HRC (primers P1/13 and P1/14); (2) loss of the FVEG_10773 ORF (primers P1/5 and P1/6); (3) confirmation of positionally correct replacement of the *FvNOR1* ORF with HRC at the 5' end (primers P1/9 and P1/12); (4) confirmation of positionally correct replacement of *FvNOR1* ORF with HRC at the 3' end (primers P1/10 and P1/11); (5) presence of the geneticin resistance marker (primers P1/17 and P1/18); and (6) mating-type gene specificity (primers P1/19 and P1/20 for *MAT1-1* and primers P1/21 and P1/22 for *MAT1-2*). PCR was carried out as described above.

Construction of the NOR1 phylogeny

The *Fv*NOR1 protein sequence was downloaded from FungiDB (Release 57; April 21, 2022) in FASTA format. The NCBI blastp (protein-protein BLAST) algorithm (BLAST+ v2.13.0) was used to identify protein sequences that are similar to *Fv*NOR1. Searches were confined to the non-redundant protein sequences (nr) database with "Uncultured/environmental sample sequences" excluded. Algorithm parameters, including general and scoring parameters and filters and masking, were all default settings. The only parameters that were adjusted were max target sequences (5,000, not 100), word size (6, not 5) and filtering of low complexity regions. The initial blastp search set included 5,000 sequences. Additional sequence data was added to the dataset in the form of the *Fv*NOR1 ortholog group (OG6_110453) from OrthoMCL DB (Release 6.11; June 23, 2022). Over 5,000 sequences were filtered and culled iteratively to exclude Bacteria and Archaea and remove duplicate sequences, redundant sequences from different strains of the same species, uninformative or exotic fungal genera, and any sequences that were abnormally short or long causing long branch attraction (*60*). Other non-fungal

eukaryotes have NOR1-like proteins. These non-fungal eukaryotes include green algae (*Raphidocelis, Chlamydomonas, Scenedesmus, Gonium, Chlorella, Volvox*) and rotifers (*Rotaria, Adineta*) and they are commonly found in aquatic habitats. Lichen fungal symbionts (*Lobaria, Hypocenomyce, Sticta*) found in terrestrial habitats across a wide range of temperatures also have NOR1 orthologs. However, none of these organisms are known as denitrifiers nor are they relevant to agricultural N_2O emissions, so they were excluded from the phylogenetic analysis. All the most closely related fungal NOR1 proteins are represented in this phylogeny because of our interest in fungal denitrification. Any fungal NOR1-like protein that is not present either belongs to a fungal genus that is unimportant in the context of fungal denitrification in agricultural settings (e.g., *Hirsutella*) or its sequence similarity is less than that of the bacterial NOR sequences.

The final dataset consisted of 198 sequences. These sequences were subjected to multiple sequence alignment (MSA) using MAFFT (v7.490; *61, 62*) in Geneious Prime® 2022.2.1 (Build 2022-07-07 13:25). FastTree (v2.1.11; *63, 64*) was used to evaluate the preliminary phylogeny. The most basal clade was identified via the FastTree maximum-likelihood (ML) tree. The protein alignment was re-used to build a ML tree using IQ-TREE (v1.6.12; *65*). ModelFinder (*66*) was used to identify the best substitution model for the dataset. “JTTDCMut+R5” was determined to be the best amino-acid exchange rate matrix according to the Bayesian Information Criterion (BIC; 60267.9648). The JTTDCMut protein model (*67*) is a revised JTT matrix (*68*) that uses the FreeRate model (*69, 70*) with 5 categories. The FreeRate model generalizes the discrete Gamma model (+G; *71*) by relaxing the assumption of Gamma-distributed rates. The FreeRate model regularly fits data better than the +G model and is recommended for large dataset analysis. For

more information regarding IQ-TREE sequence alignment, substitution model, and tree statistics, see Supplementary Table S3.

The phylogeny was reassessed using the JTTDCMut+R5 substitution model and 100 bootstrap replicates (Figure 3; Supplementary Figure S11). Additionally, the phylogeny was run using 1000 and 10000 bootstrap replicates (Supplementary Figure S12-S13) of the Ultrafast Bootstrap (UFBoot; *72*) analysis in combination with the SH-like approximate likelihood ratio test (SH-aLRT branch test; *73*). Shimodaira–Hasegawa (SH)-aLRT is a nonparametric version of aLRT based on a method similar to SH tree selection. The strength and confidence of the phylogenetic relationships were evaluated using two different support methods to reduce any inherent bias built into each method.

Recommendations to perform the SH-aLRT test (*73*) in concert with UFBoot (*72*) were followed where one can begin to rely on a clade if SH-aLRT >= 80% and UFBoot > 95%. UFBoot (*72, 74*) was used to overcome the computational costs required by the nonparametric bootstrap (*75*) and validate the tree with a larger number of replicates (e.g., 100 vs. 1000 or 10,000). UFBoot is much faster than the standard process and produces relatively unbiased branch support values (a clade is likely true if support is > 95%). This has a different meaning than normal bootstrap support though (a clade is likely true if support is >80%). Unfortunately, this means it is inappropriate to compare bootstrap (BS) support (%) to UFBoot %. There is a risk with UFBoot that branch supports may be overestimated due to severe model violations; however, no severe model violations could be identified in the dataset, so the nearest neighbor interchange (NNI) search option was not used. The resulting phylogenies were visualized in FigTree (v1.4.4) and edited in Microsoft PowerPoint (v 16.59). Convincingly, there were no

differences in topology or clade relationships between the resulting phylogenies using nonparametric bootstrap support estimation or SH-aLRT and UFBoot.

Synteny analysis

*Fv*Nor1 (XP_018758113) was used as a reference sequence and was aligned to the orthologous NOR1 sequences in *Trichosporon asahii* var. *asahii* (*Taa*; XP_018758113) and *Cutaneotrichosporon cutaneum* (*Cc*; BAB60855) using MAFFT as described before. MSA was visualized using MView (v1.63; *76, 77*) with default settings for input and output parameters. The location of NOR1 and its orthologs in each respective species' genome was determined and the corresponding contigs/scaffolds with annotations (.gbff) encompassing those genomic locations were downloaded from NCBI and imported into Geneious Prime® 2022.2.1 (Build 2022-07-07 13:25). The three genomic sequences were aligned using Mauve (*77*) and the progressiveMauve algorithm (*79*). Seed weight and minimum LCB score were automatically calculated and locally collinear blocks were computed for the full alignment. Synteny was analyzed using the Mauve genome alignment viewer. Synteny analysis was performed to assess the retention of gene order surrounding *Nor1* for potential evidence of horizontal gene transfer (HGT) to *Cc/Taa*.

Motif analysis

Motif analysis was performed on all 198 fungal species in the NOR1 phylogeny (Figure 3; Supplementary Figures S11-S13) by aligning the sequences with MAFFT (v7.490) and using the EMBOSS (v.6.5.7) tool 'fuzzpro' in Geneious Prime® 2022.2.1 (Build 2022-07-07 13:25; *80*). Motif predictions were completed by screening protein sequences against the PROSITE motif that is characteristic of canonical cytochrome P450s: [FW][SGNH]x[GD]{F}[RKHPT]{P}C[LIVMFAP][GAD]. The maximum number of

mismatches was designated as 0. The consensus sequence for all 198 fungal species was "FGFGDHRCIA". The P450 motif was extracted from only 159 out of 198 fungal species (80.30%). This means that 39 fungal *Fv*NOR1-like sequences do not possess this exact motif. Using a sub-sample of the original dataset, all 159 fungal sequences that did contain the P450 motif were re-aligned using MAFFT (v7.490) and the MSA was submitted to WebLogo (2.8.2.) (*81*) to create a sequence logo of the cytochrome P450 motif (*82*; Figure 4).

Fungal growth bioassay

Spore concentrations were calculated using a Luna Cell Counter (Logos Biosystems, Aligned Genetics, Inc., Anyang, Gyeonggi, Republic of Korea) with its protocol preset to "Fusarium conidia". Growth curve analysis was performed with wild type *Fv*, wild type *Fv* near-isogenic line (NIL), two confirmed independent deletion mutants and their complemented strains, and four sexual cross progeny that satisfy a variety of mating types and $NOR1^{+/-}$ genotypes. This was done in a Bioscreen C automated system (Growth Curves USA, Piscataway, NJ, USA). Fungal strains were inoculated in MM amended with either $NaNO_3$ or $NaNO_2$ (15 mM) and L-Lysine (1 mM) (4.0×10^3 microconidia per 200 μL MM per well) using 100-well Bioscreen honeycomb microtiter plates (Growth Curves Ab Ltd., Helsinki, Finland) and grown under either normoxia (21% O_2) or hypoxia (5% O_2). The oxygen environment was manipulated using a hypoxic chamber and an oxygen controller (Coy Laboratory Products, Grass Lake, MI, USA). The concentration of O_2 was decreased from 21% to 5% using a gas mixture of ~400 ppm CO_2 balanced with N_2 (Airgas Specialty Gases, Durham, NC, USA). As noted in Gao et al. (*54*), *F. verticillioides* grows as a nearly pure culture of conidia under these conditions and the optical density (OD) readings are similar to those of yeast cultures. Ten replicates were prepared for each fungal strain. The microtiter plates were incubated for 148 hours at 28° C with intermittent

shaking at a slow speed with low amplitude, and OD_{600} measurements were recorded every hour. The brown (OD_{600}) filter was determined to be the best for monitoring *F. verticillioides* growth. For the presentation of the growth curves, all 1-h incremental time points were plotted starting at 3 h post initiation. The experiment was conducted three times for each combination of conditions (media:oxygen environment).

For statistical analysis, data without removing any outliers across triplicate experiments for each condition combination were used. All raw data was plotted with all replicates within each run and summary statistics were calculated to visualize differences between strains and treatments. Logistic or sigmoid growth curves were fit to the data; parameters were estimated using Bayesian methods. The basic functional form of the curve is as follows where *L* is the carrying capacity or maximum "plateau" value of the curve, *k* is the growth rate or slope of the curve, and t_{mid} is the time in hours required to reach 50% of the maximum value:

$$y(t) = \frac{L}{1 + e^{-k(t - t_{mid})}}$$

The parameter *L* is allowed to vary by strain, treatment, and experimental run, using a combination of fixed and random effects. The models include fixed effects for the 12 strains (12 levels), oxygen level (two levels, hypoxic and normoxic), and presence/absence of nitrite (two levels, MM + 1 mM L-Lysine and MM + 15 mM $NaNO_2$ + 1 mM L-Lysine) and all two-way and three-way interactions between them. Each run was assigned its own random intercept for the *L* parameter, with two plates per experimental run. The *k* and t_{mid} parameters only have random intercepts for each run and no fixed effects. The three nonlinear parameters, *L, k,* and t_{mid}, were all exponentiated to constrain them to be positive values. Uninformative prior

distributions (normal distributions with mean = 0 and SD = 1 for the logarithm of *L* intercept and all its fixed effects; normal distributions with mean = -2 and SD = 2 for the logarithm of *k* intercept; normal distributions with mean = 4 and SD = 2 for the logarithm of t_{mid} intercept) were set on all the parameters to keep the sampling algorithm within a reasonable range and ensure convergence. Standard deviation parameters of the random effects and the overall model residuals were all given exponential priors with $\lambda = 1$. The Hamiltonian Monte Carlo algorithm was used to sample from the joint posterior distribution of the model parameters. There were four Markov chains that were run for 2000 iterations of warm-up that were discarded and 1000 iterations to sample from the posterior distribution. All Markov chains were initialized with all parameter values at 0 to achieve convergence. Models were run on the USDA-ARS SCINet High-Performance Computer Systems.

Before model results were examined, diagnostics were viewed to ensure the model converged and fit the data sufficiently (maximum R-hat < 1.05). A posterior predictive check plot was examined to ensure the model fit the data adequately well. Estimated marginal means of the carrying capacity parameters were calculated for each sample from the posterior distribution for each strain averaged across all treatments, for each oxygen × medium treatment combination averaged across strains, and for each combination of strain × oxygen × medium. Contrasts between strains were estimated by taking the ratio of the back-transformed estimated marginal mean of carrying capacity at each sample from the posterior distribution. Contrasts were taken between each pair of strains averaged across treatment combinations, as well as within each treatment combination (Supplementary Figures S2-S8).

N_2O detection/quantification assay

The methods employed here are modified from Mothapo et al. (*83*). Spore concentrations were calculated as described above. For each culture being assayed, micro-conidial concentrations were adjusted to 4.0 x 10^4/mL (1.0 x 10^6/25 mL). Two replicates per fungus:medium combination were aseptically inoculated into a 50 mL Erlenmeyer flask containing 25 mL liquid MM supplemented with $NaNO_2$ (15 mM) and L-Lysine (1 mM). The flask was closed with jumbo cotton balls (Wal-Mart Stores, Inc., Bentonville, AR, USA) and incubated at 27° C for 3 days. During this time, Whatman® Filter Paper No. 4 (15.0 cm; Filter Speed:Retention = Fast:Qualitative) was dried at 72° C for 48 h and blank weight was measured. After 3 days, the cotton ball was removed and each flask was sealed with a rubber septum sleeve stopper (Thomas Scientific, Swedesboro, NJ, USA) to prevent air exchange and induce hypoxia. After 24 h incubation, 3 mL headspace gas was sampled from the flask using a 22-gauge hypodermic needle (Air-Tite, Virginia Beach, VA, USA) attached to a 5 mL syringe (Becton, Dickinson, and Company, Franklin Lakes, NJ, USA) with a one-way stopcock (Cole-Parmer/Antylia Scientific, Vernon Hills, IL, USA). The sample was then injected through the septum of a 10-mL amber vial with a crimped cap (LEAP PAL Parts and Consumables, Raleigh, NC, USA). Nitrous oxide concentration in each gas sample was analyzed using a Shimadzu GC-2010 gas chromatograph equipped with electron capture detector (ECD) (Shimadzu Scientific Instruments, Inc., Durham, NC, USA) and an AOC-6000 autosampler (PAL System, Distribution by Archer Science, Lake Elmo, MN, USA). The carrier gas was a P-5 mixture (Gasco, Oldsmar, FL, USA) of 5% methane (CH_4) and 95% argon (Ar). The column responsible for the separation process was a non-polar PorapakQ column (Agilent Technologies, Inc., Santa Clara, CA, USA) of 2.0 mm internal diameter (2.74 m long). GCMS Real Time Analysis program (Shimadzu

Scientific Instruments) was used to setup instrumentation and operation conditions for experimentation. The operation conditions included: a primary pressure of 500-900 kPa, an oven temperature of 60° C, an injection temperature of 125° C with a direct injection mode, an ECD temperature of 250° C with a current of 1.30 nA. For the program, the GC-ECD was held at 60° C for 5 min for the first sample and between samples. After autosampler injection, the rate of temperature change was 20° C/min with a final temperature of 125° C and a hold time of 1.5 min. A 10-min running time was used for each gas sample; chromatographic peaks for carbon dioxide (CO_2) and N_2O were at 0.8 min and 2.4 min, respectively. CO_2 values were recorded (data not shown) to confirm that CO_2 did not vary greatly from sample to sample. The total flow was 20 mL/min and the purge flow was 1.0 mL/min.

N_2O was detected by the GC-ECD and visualized as a peak on a chromatogram that could be viewed and evaluated using the GCMS Postrun Analysis program. N_2O was quantified ppm by running a set of five analytical standards of 1, 10, 100, 1,000, and 10,000 ppm of N_2O (Gasco, Oldsmar, FL, USA) to generate a calibration curve. The calibration curve was used to convert raw N_2O to N_2O ppm by fitting the data to a logarithmic regression model. Across all runs and trials, R^2 values between 0.970 and 0.998 for observed versus expected values of the five N_2O analytical standards suggest that the relationship between them is roughly linear; this can be visualized in the log-log plot of the calibration curve (Supplementary Figure S4.14; Supplementary Table S4.4).

It is worth mentioning that the analytical standards only spanned 1 to 10,000 ppm. Thus, N_2O amounts below 1 ppm or above 10,000 ppm were not able to be quantified accurately. We are aware that ambient levels of N_2O are at approximately ~320 ppb according to the U.S. Environmental Protection Agency (*2*). Ambient air samples were used as a control to compare

against. A majority of the reported raw N_2O values fell within this range (1-10,000 ppm); the values that did not fit within this range were extrapolated. This particular set of standards was used because there are very few commercial options for N_2O standards that captured the range of N_2O produced by our fungi. Headspace gas samples were also taken after 48 h incubation to ensure that the N_2O measurement was authentic (*83*). In all cases, N_2O measurements at 48 h were numerically similar to measurements made at 24 h. Because of this consistency, these samples were only taken during preliminary studies and those values are not reported. The liquid media was filtered through Whatman® Filter Paper No. 4 to obtain a filtrate that was meant to be microbe-free. Due to the method of collection, sterile filtration was not possible. Acetonitrile (CH_3CN) was added to the filtrate before post-assay pH assessment at a final concentration of >10% to eliminate all microbial activity. A measurement of fungal growth (biomass; dry weight) was collected for each isolate after drying each sample for 48 h at 70° C (*83*). Fungal biomass was calculated by subtracting the weight of the fungus and the filter paper from the blank filter paper. The pH of liquid MM was measured before inoculation and at the end of the sampling period to check the possibility of chemodenitrification (i.e., chemical N_2O production in the presence of Fe(II)). Whether N_2O production from the culture medium was due to a chemical or fungal pathway was evaluated using proper controls because chemical reactions can contribute to N_2O production under acidic pH conditions (*84-86*). Uninoculated liquid media served as a control for possible chemodenitrification. The N_2O-producing activity of *F. graminearum* and *F. oxysporum* f. sp. *vasinfectum* were also measured following the protocol described above. To gauge substrate-specific effects on N_2O production, rich and minimal media with assorted N amendments were compared in wild type *F. verticillioides* and a near-isogenic line of wild type *F. verticillioides* (*87*; Supplementary Figures S4.15-S4.17).

General linear mixed models were fit to the fungal biomass dataset and the logarithmic transformation of the N_2O flux. Homogeneity of variance and normality of residuals were diagnostically checked to confirm that there were no severe deviations from the assumption of normally distributed residuals with constant variance. In each model, fungal sample was included as a fixed effect, and a random intercept was fit to each trial. Models with nested random effects were fit for experimental run within each trial, but the data did not support estimating these intercepts, resulting in singularities (not shown). Therefore, only the models that include random intercepts for each trial were presented. Strain-by-strain pairwise statistical comparisons (t-tests) were performed for each possible pair of samples with Šidák adjustment, a method to control the family-wise error rate and counteract the problem of multiple comparisons (*88*). Letters indicate statistical differences between groups ($p < 0.05$) after multiple comparisons adjustment. The Kenward-Roger method was used for degrees of freedom approximation. The estimated marginal means and their 95% confidence intervals were calculated for all 18 samples; N_2O flux means and confidence interval endpoints were back-transformed from the logarithmic scale. Analysis of variance (ANOVA) with Type III sum of squares and Kenward-Roger approximation of the denominator degrees of freedom for the F-distribution was used to examine 1) the effect of inorganic N sources, medium type (rich or minimal), and absence or presence of L-lysine on uninoculated medium (Supplementary Figure S4.18) and 2) the effect of NOR1 genotypes, MAT mating types of fungal isolates, and different *Fusarium* species on N_2O production and growth (Supplementary Figures S4.1, S4.9-S4.10, S4.15-S4.17, and S4.19-S4.20). Normalized N_2O is reported as ppm mg^{-1}. Error bars represent 95% confidence intervals around the estimated marginal means. This experiment was repeated in triplicate. Data from all three experiments was analyzed and visualized independently and together.

All statistical analyses were done using R software version 4.1.2 (*89*), including the lme4 (*90*), lmerTest (*91*), emmeans (*92*), and multcomp (*93*) packages. Bayesian models were fit using CmdStan software version 2.28.2 (Stan Development Team 2019), using the cmdstanr (*94*), brms (*95*), and tidybayes (*96*) packages to interface between CmdStan and R.

Supplementary Text

Fungal growth bioassay

FvNOR1 deletion did not dramatically affect fungal biomass measured in a comparative N_2O flux experiment, so a more in-depth analysis of fungal growth was performed using absorbance measurements with higher stringency on oxygen levels and overall growth conditions. As expected, fungal growth in all samples was higher in nitrite and L-lysine-amended MM compared with MM amended with L-lysine exclusively. Fungal growth was also higher across the sample collection in the same medium conditions in a normoxic compared with a hypoxic environment. There was substantial statistical evidence for growth differences among wild type *F. verticillioides*, complemented, and Δ*nor1* deletion mutant strains under the same experimental conditions. Averaging across media and oxygen conditions, the largest relative differences were between wild-type *F. verticilloides* and Δ*nor1*-1 (carrying capacity ratio 1.193; 95% credible interval [1.190, 1.196]) and between wild-type and Δ*nor1*::*NOR1*-1 (carrying capacity ratio 1.142; 95% credible interval [1.140, 1.145]). All other carrying capacity ratios between pairs of strains were between 0.9 and 1.1, where 1 indicates no difference (Supplemental Figure S4.7). These differences are statistically robust but biological significance is nominal.

N_2O detection/quantification assay

Across all experiments, N_2O is produced in minor quantities in $NOR1^-$ strains relative to $NOR1^+$ strains. The amount of N_2O produced is slightly higher than ambient levels of N_2O or N_2O levels derived from chemodenitrification in uninoculated conditions (i.e., non-biological reduction of NO_2^- to NO). Roughly equivalent amounts of N_2O are produced by the wild type fungus if grown in a medium with nitrate and L-lysine or nitrite/nitrate exclusively. If no

inorganic N source is added to the medium, there is no detectable N_2O production. The highest levels of N_2O production were detected in nitrite-amended MM with addition of L-lysine (Supplementary Figures S4.15-S4.17). Nitrite without other inorganic or organic N sources is inhibitory to conidial germination and results in reduced overall growth (data not shown); the addition of L-lysine allows the fungus to germinate and metabolize nitrite. Nitrate is a less toxic, inorganic N substrate but also a poor inducer of N_2O production; thus, nitrate was not used as the standardized inorganic N source in the comparative N_2O flux or substrate studies. In our substrate studies, nitrite was shown to be an overall better inducer of N_2O production than nitrate, so nitrite was used as the only inorganic N source in subsequent studies.

Synteny analysis

Based on the Mauve alignment, there is seemingly no synteny between *Fv* and the two basidiomycetes in the region surrounding *FvNOR1* because contiguous genes upstream and downstream of *FvNOR1* are absent in *Cc* and *Taa* (data not shown).

Supplementary Tables

Supplementary Table S4.1. *Fusarium* strains used in this study.

NOR1 (+/-)	Strain	Genotype/Mating Type	Description
+ (1)	FRC M-3125[b]	Wild type *Fv*/*MAT1-1*	Strain used for genetic transformation and functional characterization
+ (1)	FRC M-3125 NIL	Wild type *Fv/MAT1-2*	Back cross 6 progeny of FRC-M3125 crossed with JFL A00999
- (0)	Δ*FvNOR1*-1	Δ*nor1/MAT1-1*	FVEG_10773 deletion mutant in FRC M-3125
- (0)	Δ*FvNOR1*-2	Δ*nor1/MAT1-1*	FVEG_10773 deletion mutant in FRC M-3125
+ (1)	Δ*FvNOR1*-1::C1	Δ*nor1*::*NOR1*/*MAT1-1*	Δ*FvNOR1*-1 deletion mutant complemented with FVEG_10773
+ (1)	Δ*FvNOR1*-2::C2	Δ*nor1*::*NOR1*/*MAT1-1*	Δ*FvNOR1*-2 deletion mutant complemented with FVEG_10773
- (0)	Δ*FvNOR1*xNIL-1	Δ*nor1/MAT1-1*	F_1 progeny of FRC-M3125 NIL crossed with Δ*FvNOR1*-1 (#1)
- (0)	Δ*FvNOR1*xNIL-2	Δ*nor1/MAT1-1*	F_1 progeny of FRC-M3125 NIL crossed with Δ*FvNOR1*-1 (#2)
- (0)	Δ*FvNOR1*xNIL-3	Δ*nor1/MAT1-2*	F_1 progeny of FRC-M3125 NIL crossed with Δ*FvNOR1*-1 (#3)
- (0)	Δ*FvNOR1*xNIL-4	Δ*nor1/MAT1-2*	F_1 progeny of FRC-M3125 NIL crossed with Δ*FvNOR1*-1 (#4)
+ (1)	Δ*FvNOR1*xNIL-5	Δ*nor1*::*NOR1/MAT1-1*	F_1 progeny of FRC-M3125 NIL crossed with Δ*FvNOR1*-1 (#5)
+ (1)	Δ*FvNOR1*xNIL-6	Δ*nor1*::*NOR1/MAT1-2*	F_1 progeny of FRC-M3125 NIL crossed with Δ*FvNOR1*-1 (#6)
+ (1)	Δ::*FvNOR1*xNIL-1	Δ*nor1*::*NOR1*/*MAT1-1*	F_1 progeny of FRC-M3125 NIL crossed with Δ*FvNOR1*-1::C1 (#1)
+ (1)	Δ::*FvNOR1*xNIL-2	Δ*nor1*::*NOR1*/*MAT1-1*	F_1 progeny of FRC-M3125 NIL crossed with Δ*FvNOR1*-1::C1 (#2)
+ (1)	Δ::*FvNOR1*xNIL-3	Δ*nor1*::*NOR1*/*MAT1-2*	F_1 progeny of FRC-M3125 NIL crossed with Δ*FvNOR1*-1::C1 (#3)
+ (1)	Δ::*FvNOR1*xNIL-4	Δ*nor1*::*NOR1*/*MAT1-2*	F_1 progeny of FRC-M3125 NIL crossed with Δ*FvNOR1*-1::C1 (#4)
+ (3)[a]	F17-5AS1	Wild type *F. oxysporum* f. sp. *vasinfectum*	Strain used for N_2O comparative analysis
+ (1)[a]	NRRL 31084[c]	Wild type *F. graminearum*	Strain used for N_2O comparative analysis

[a] The number of NOR1 homologs in wild type *Fusarium oxysporum* f. sp. *vasinfectum* and *Fusarium graminearum* based on predictive bioinformatics and phylogenetic analysis; [b] FRC, Fusarium Research Center, Pennsylvania State University; [c]NRRL, ARS Culture Collection, Mycotoxin Prevention and Applied Microbiology Research Unit, National Center for Agricultural Utilization Research, Peoria, IL

Supplementary Table S4.2. Primers used in this study.

Index	Primer Name	Primer Sequence (5' → 3')	Description
P1/1	FVEG_10773 O1[c]	GGGGACAGCTTTCTTGTACAAAGTGGAA' TGCTTCAAAACCCTTTCG	Amplification of 5' flank of *FvNOR1*
P1/2	FVEG_10773 O2[c]	GGGGACTGCTTTTTTGTACAAACTTGT' GGTGATGGGAATAAC	
P1/3	FVEG_10773 O3[c]	GGGGACAACTTTGTATAGAAAAGTTGTT' GTGCATATAGCCGTCTTCTTAT	Amplification of 3' flank of *FvNOR1*
P1/4	FVEG_10773 O4[c]	GGGGACAACTTTGTATAATAAAGTTGT' GAAAGGGCTGCAGGTATATAAT	
P1/5	FVEG_10773_ORF_F_v1	ATTGATAGGGAACTCCTTGATTAC	Confirmation of presence/absence of the *FvNOR1* ORF in OSCAR transformants and for screening of complements and sexual cross progeny
P1/6	FVEG_10773_ORF_R_v1	CTTGAGATCTGGAAACTTCTGATA	
P1/7	FVEG_10773_5'_Out F	GAATGCTTCTTGACCTTCATTT	Confirmation of the integrity of outer sequences flanking the 5' flank of *Fv*NOR1
P1/8	FVEG_10773_3'_Out R	GAATTAGTACAGCAACTGGAAAG	Confirmation of the integrity of outer sequences flanking the 3' flank of *Fv*NOR1
P1/9	Hyg_F_Out	AGAGCTTGGTTGACGGCAATTTCG	Confirmation of the integrity of outer sequences flanking the 3' flank target gene
P1/10	Hyg_R_Out	GCCGATGCAAAGTGCCGATAAACA	Confirmation of the integrity of outer sequences flanking the 5' flank target gene
P1/11	HygMarker_F_v1	TGTTTATCGGCACTTTGCATCGGC	Confirmation of HRC[a] ORF during OSCAR transformation and PCR screening
P1/12	HygMarker_R_v1	AGCTGCATCATCGAAATTGCCGTC	
P1/13	GenMarker_F	GAGAGGCTATTCGGCTATGACTG	Confirmation of GRC[b] ORF
P1/14	GenMarker_R	GAACTCGTCAAGAAGGCGATAGA	
P1/15	MAT1-1_F	GTTCATCAAAGGGCAAGCG	Confirmation of mating type *MAT1-1*

P1/16	MAT1-1_R	TAAGCGCCCTCTTAACGCCTTC	
P1/17	MAT1-2_F	AGCGTCACCATTCGATCAAG	Confirmation of mating type *MAT1-2*
P1/18	MAT1-2_R	CTACGTTGAGAGCTGTACAG	
P1/19	NOR1_Proto_F	GTATATCCGATACAACCTCAACAAC	Amplification of the wild type *FvNOR1* ORF and the surrounding genomic region
P1/20	NOR1_Proto_R	GAGTAGAATGGGTAAAGATGGTAAAG	

[a] HRC, hygromycin resistance cassette; [b] GRC, geneticin resistance cassette; [c] the ’ symbol denotes the junction between 5’ attB recombination site sequences for OSCAR constructs that are added extensions to the gene primers.

Supplementary Table S4.3. IQ-TREE sequence alignment, substitution model, and tree statistics.

Sequence Alignment			
Input Data	# of Invariant Sites	# of Parsimony Informative Sites	# of Distinct Site Patterns
198 sequences with 784 amino acid sites	247 (= 31.5% of all sites)	414	711

Substitution Process		
Model of Substitution	Model of Rate Heterogeneity	Site Proportion and Rates
JTTDCMut+R5	FreeRate with 5 categories	1) (0.2208, 0.1013) 2) (0.1819, 0.3258) 3) (0.2360, 0.7541) 4) (0.2279, 1.5639) 5) (0.1333, 2.8795)

Maximum Likelihood Tree							
Log-Likelihood of the Tree	Unconstrained Log-Likelihood (without tree)	# of Free Parameters [a]	AIC[b]	AICc[c]	BIC[d]	Total Tree Length (Sum of Branch Lengths)	Sum of Internal Branch Lengths
-28797.8 (s.e. 1178.7)	-5108.7	401	58397.5	59241.5	60268.0	19.9	11.4 (57.3% of tree length)

[a] Number of branches + number of model parameters
[b] Akaike Information Criterion score
[c] Corrected Akaike Information Criterion score
[d] Bayesian Information Criterion score

Supplementary Table S4.4. Coefficients of determination and parameters of the calibration curve for N_2O analytical standards.

Trial	Run	Intercept (*b*)	Slope (*a*)	R^2
1	1	-7.807	0.970	0.970
1	2	-9.740	1.102	0.989
2	1	-10.685	1.134	0.995
2	2	-10.662	1.136	0.996
3	1	-11.624	1.194	0.998
3	2	-11.369	1.180	0.998

This table contains the intercept, slope, and R-squared value for three trials, and two independent runs within each trial, for five analytical standards of N_2O (1, 10, 100, 1,000, and 10,000 ppm). All equations are of the formula $\log N_{true} = a \log N_{measured} + b$, where *a* is the slope and *b* is the intercept.

Supplementary Figures

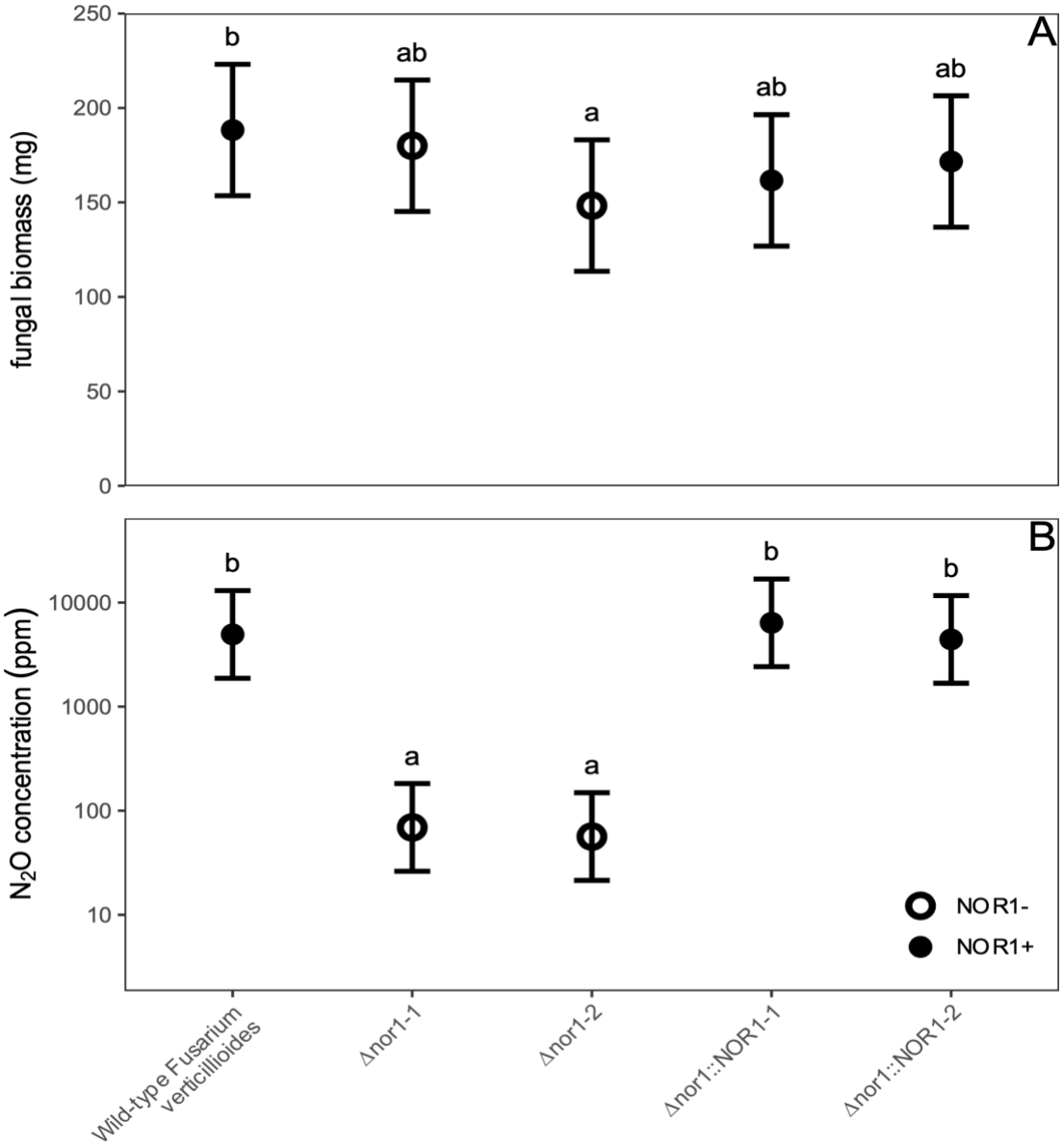

Supplementary Figure S4.1. Evaluation of fungal biomass and N_2O production from wild-type *Fusarium verticillioides*, deletion mutants and complemented gene add-back mutants. **(A)** Fungal biomass (dry weight); **(B)** Nitrous oxide concentration reported in parts per million (ppm). Complementation analysis of *NOR1* in *F. verticillioides* across wild type, deletion mutant (Δ*nor1*-1 and Δ*nor1*-2) and add-back mutant (Δ*nor1*-1::NOR1 and Δ*nor1*-2::NOR1) genotypes. Open circles mean *NOR1* is absent; closed black circles indicate *NOR1* is present in genome. The vertical axis of S4.1A has an arithmetic scale; the vertical axis of S4.1B has a logarithmic scale. Group means that do not share a letter are significantly different based on a Šidák adjustment and error bars represent adjusted 95% confidence intervals around the modeled means.

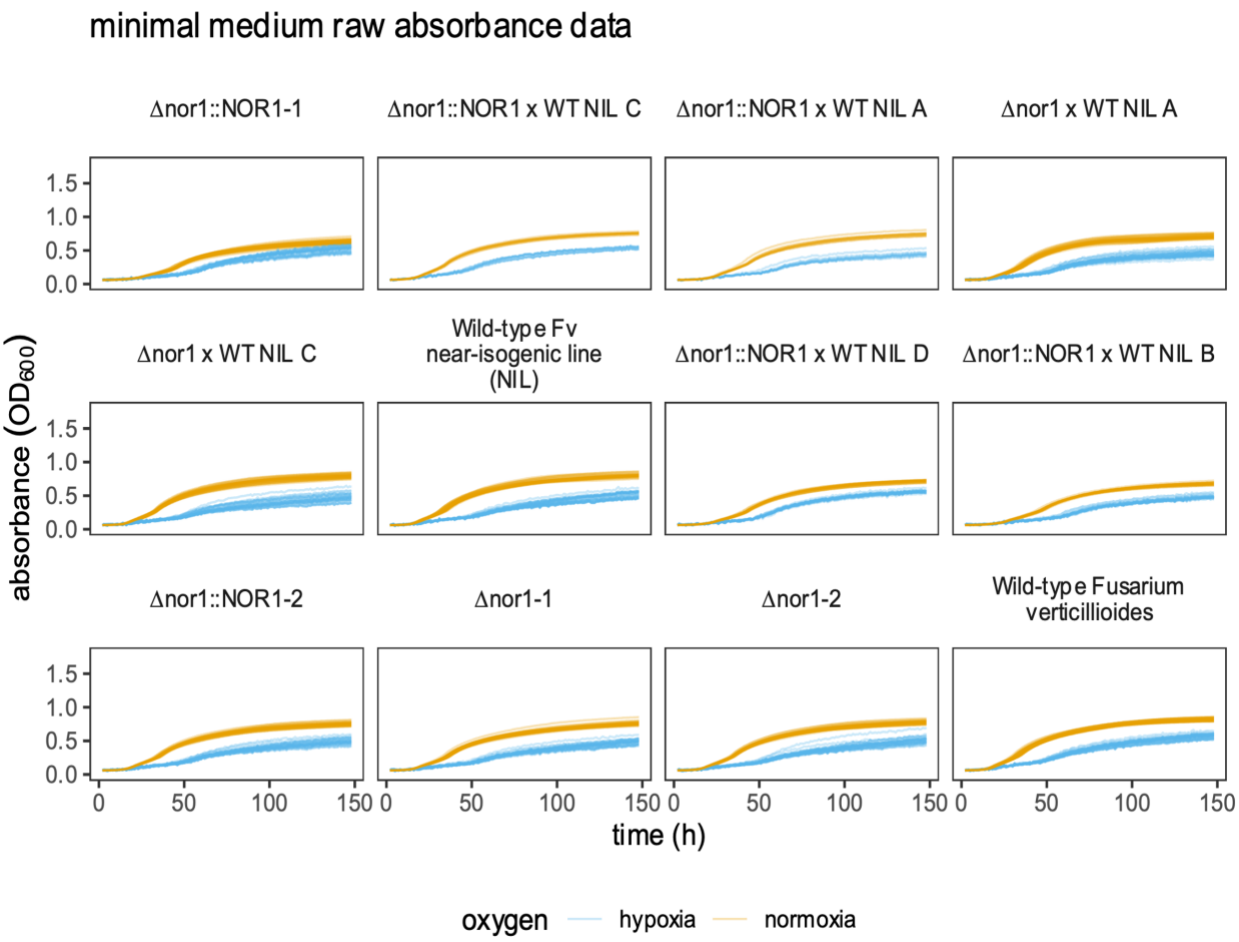

Supplementary Figure S4.2. Evaluation of fungal growth in minimal medium (MM) + L-lysine under normoxia or hypoxia. Time series of fungal growth in MM + L-lysine for all strains with all replicates within each run. All individual replicates' time series are plotted as semitransparent lines.

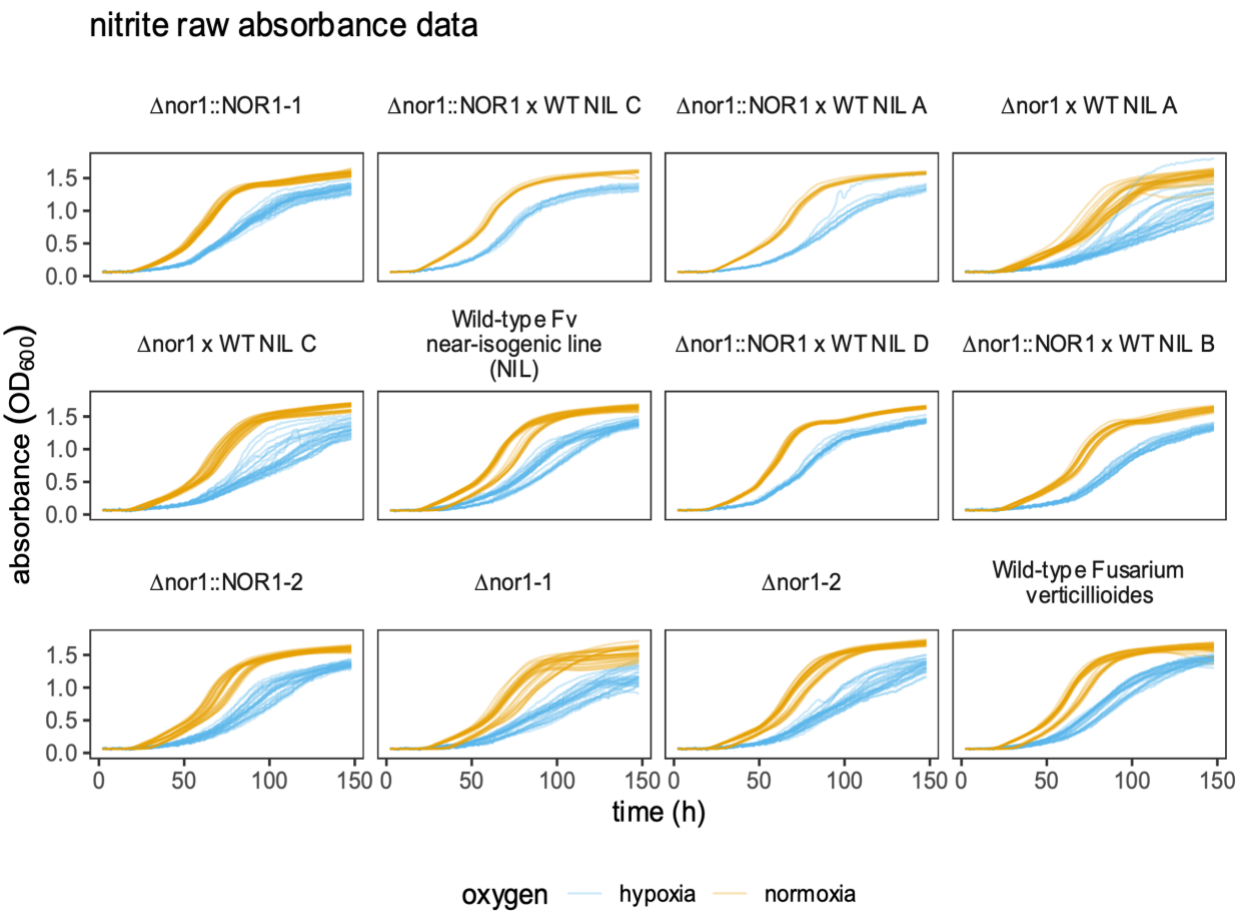

Supplementary Figure S4.3. Evaluation of fungal growth in minimal medium (MM) + $NaNO_2$ + L-lysine under normoxia or hypoxia. Time series of fungal growth in MM + $NaNO_2$ + L-lysine for all strains with all replicates within each run. All individual replicates' time series are plotted as semitransparent lines.

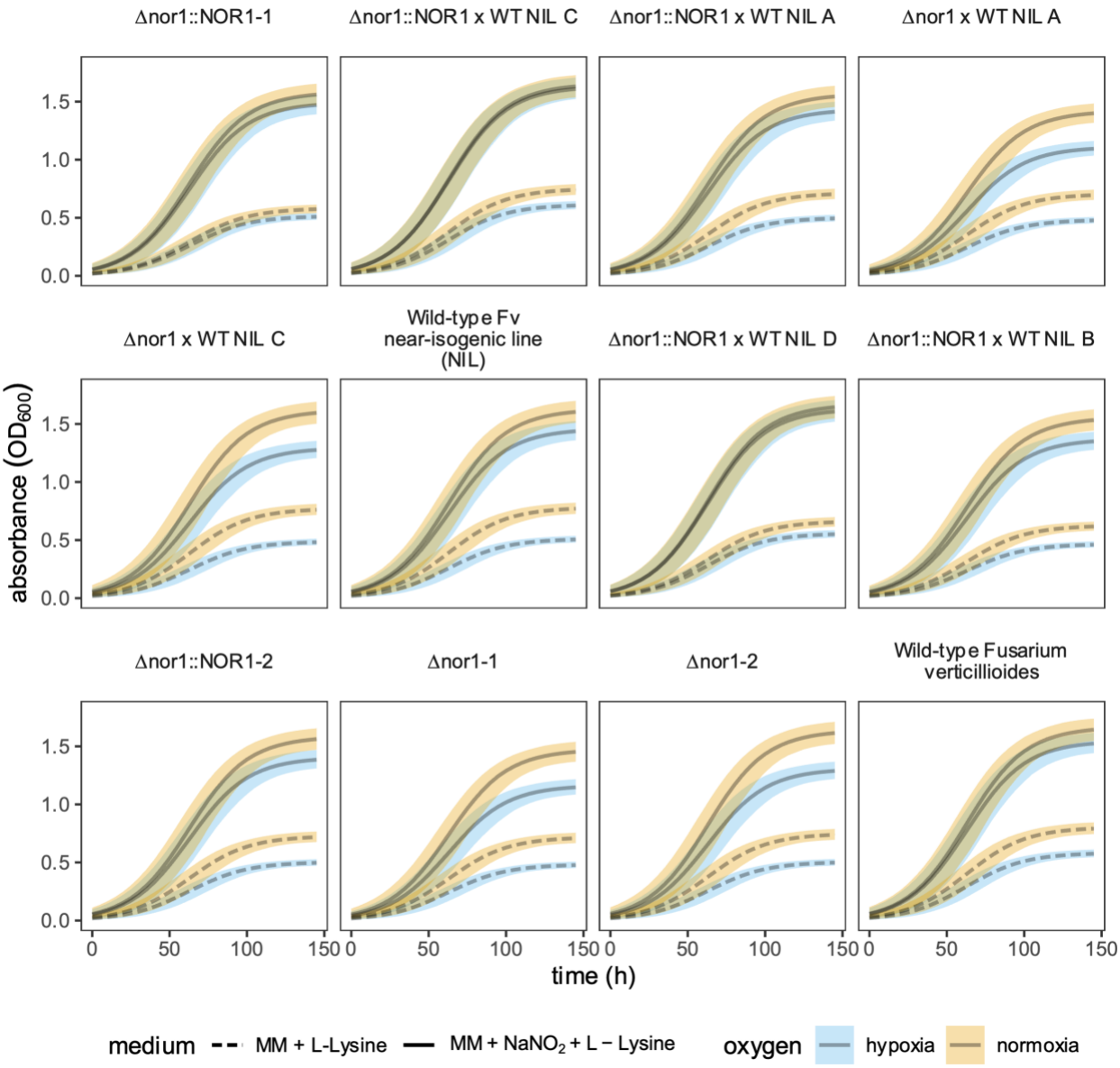

Supplementary Figure S4.4. Fitted fungal growth curves from model prediction. Plots of fitted curves of fungal growth data predicted from the model. Minimal medium + L-lysine and minimal medium + $NaNO_2$ + L-lysine are displayed with dashed and solid lines, respectively (median of posterior predictive distribution). The shaded credible intervals are colored by blue (hypoxia) or orange (normoxia). The 95% quantile credible interval of the posterior estimate of the prediction is shown as shading around the growth curve. The 66% and 90% quantile credible intervals of the posterior estimate of the prediction are not shown.

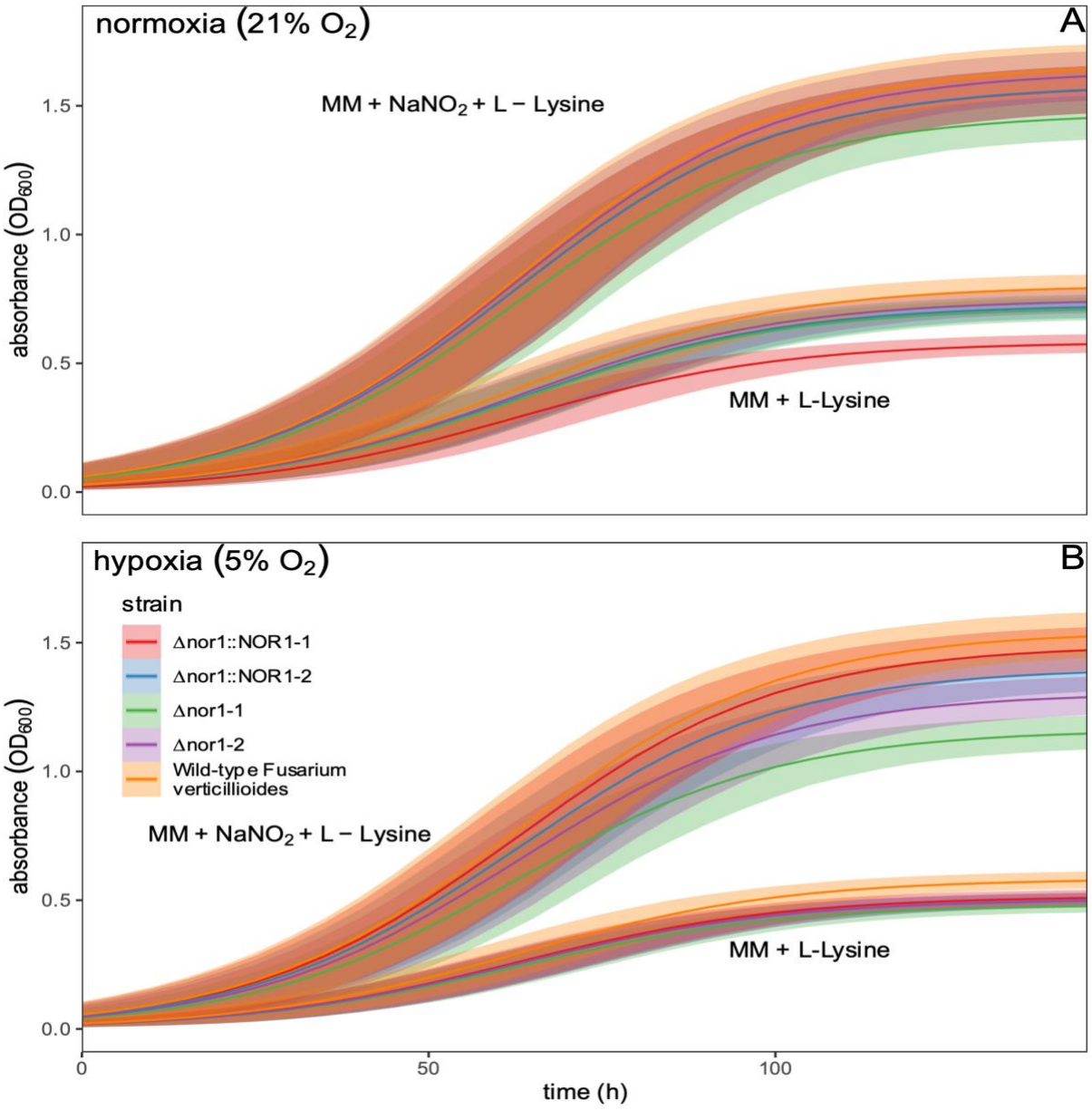

Supplementary Figure S4.5. Assessment of fungal growth over time in wild-type *Fusarium verticillioides* and mutants in different media and oxygenation conditions. Time plot of fungal growth using Bioscreen C instrumentation. Each growth experiment ran for 148 hours at 27º C in minimal medium + NaNO2 + L-lysine. Medium choice was informed by the N substrate study (Supplementary Figures S4.15-S4.17). Growth across different oxygen environments was compared among wild type *F. verticillioides*, Δ*nor1* deletion mutants, and Δ*nor1::NOR1* add-back mutants. Data plotted are the fitted expected (mean) values with credible intervals; only the 95% credible intervals are plotted as shaded regions around the line representing the median expected value from the posterior predictive distribution. A. Normoxia (21% O_2); B. Hypoxia (5% O_2; 95% N_2; 400 ppm CO_2).

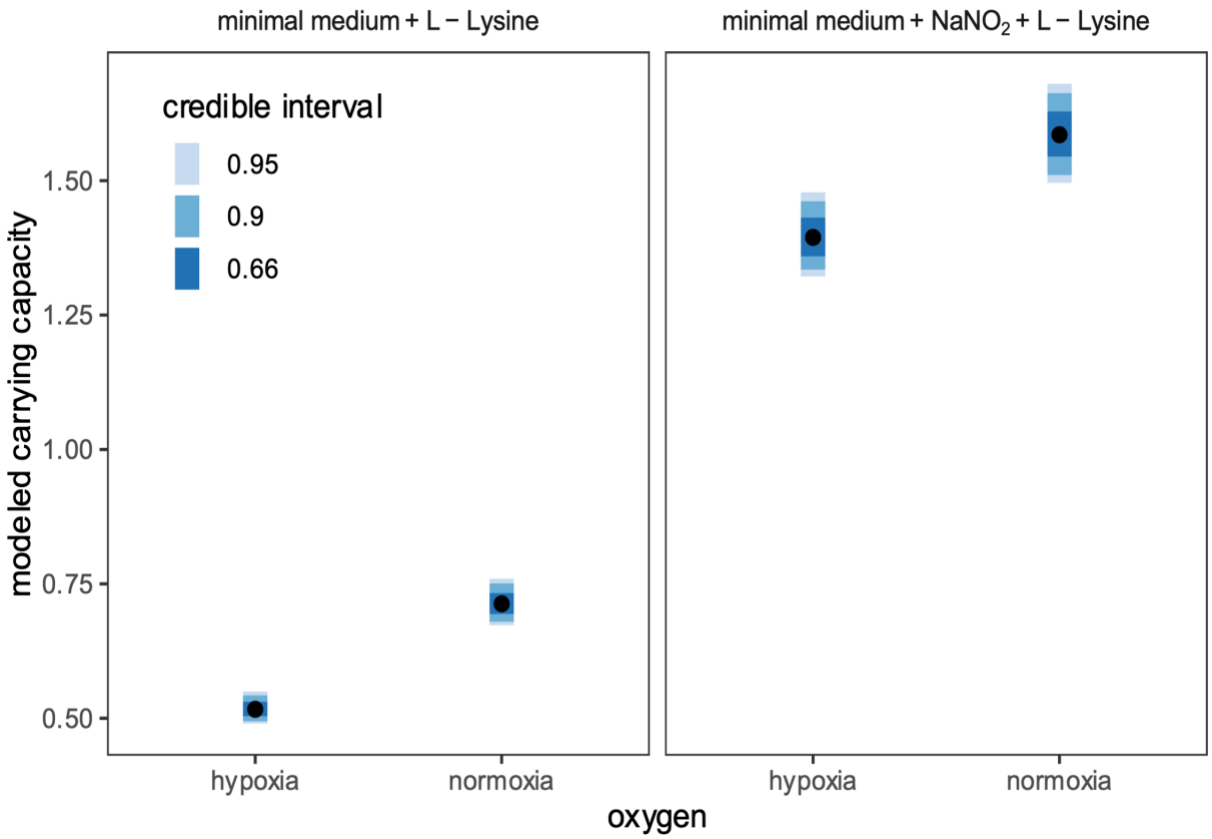

Supplementary Figure S4.6. **Average fungal growth across all strains in two different media under normoxia or hypoxia.** Comparison of carrying capacity parameters between oxygen treatments, averaged across strains in two different media (minimal medium without and with nitrite). The posterior estimates of the back-transformed carrying capacity parameter *L* are shown in the plot. The black dots are the point estimate (median of the posterior distribution). The shaded blue regions show the uncertainty with 66%, 90%, and 95% quantile credible intervals in progressively lighter colors.

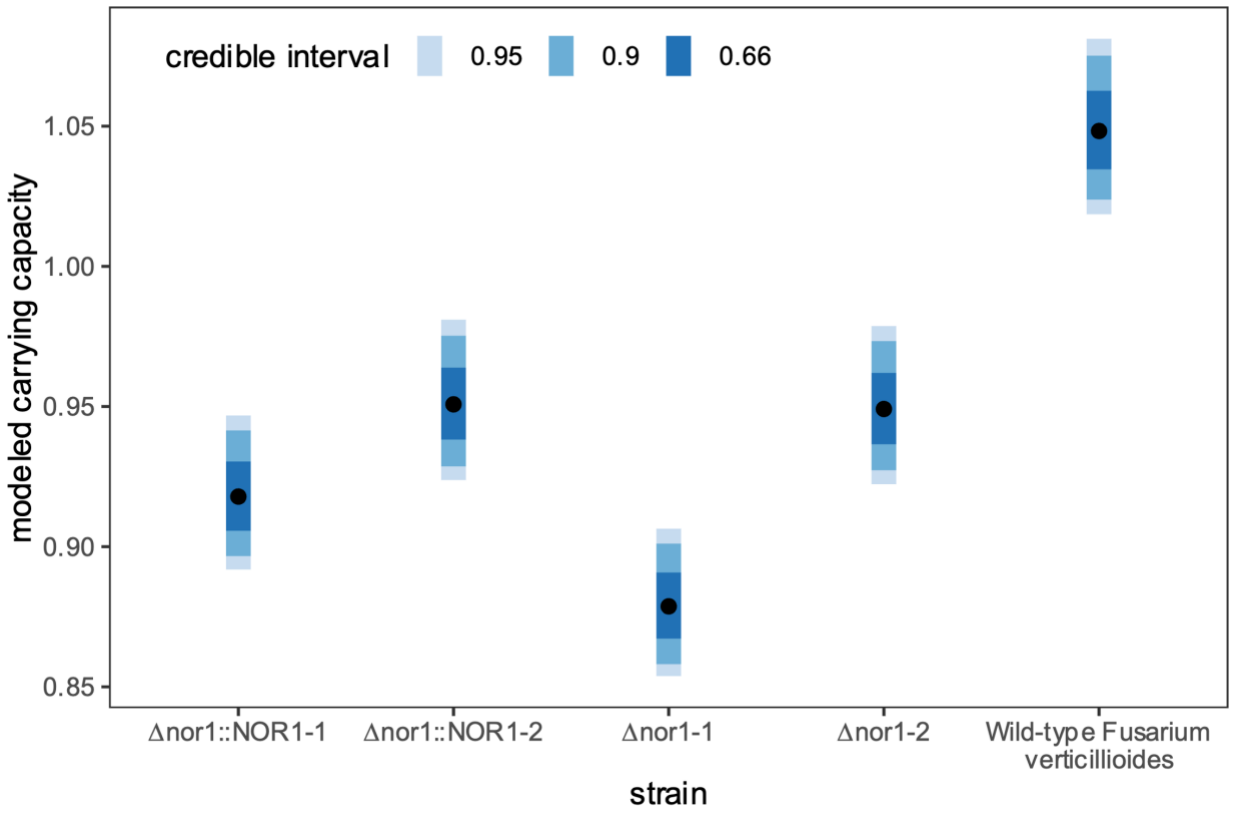

Supplementary Figure S4.7. Average fungal growth across all strains, media, and oxygen levels. The posterior estimates of the back-transformed carrying capacity parameter *L* for each of the mutant strains, averaged across the effects of medium and oxygen environment, are shown in the plot. The black dots are the point estimate (median of the posterior distribution). The shaded blue regions show the uncertainty with 66%, 90%, and 95% quantile credible intervals in progressively lighter colors.

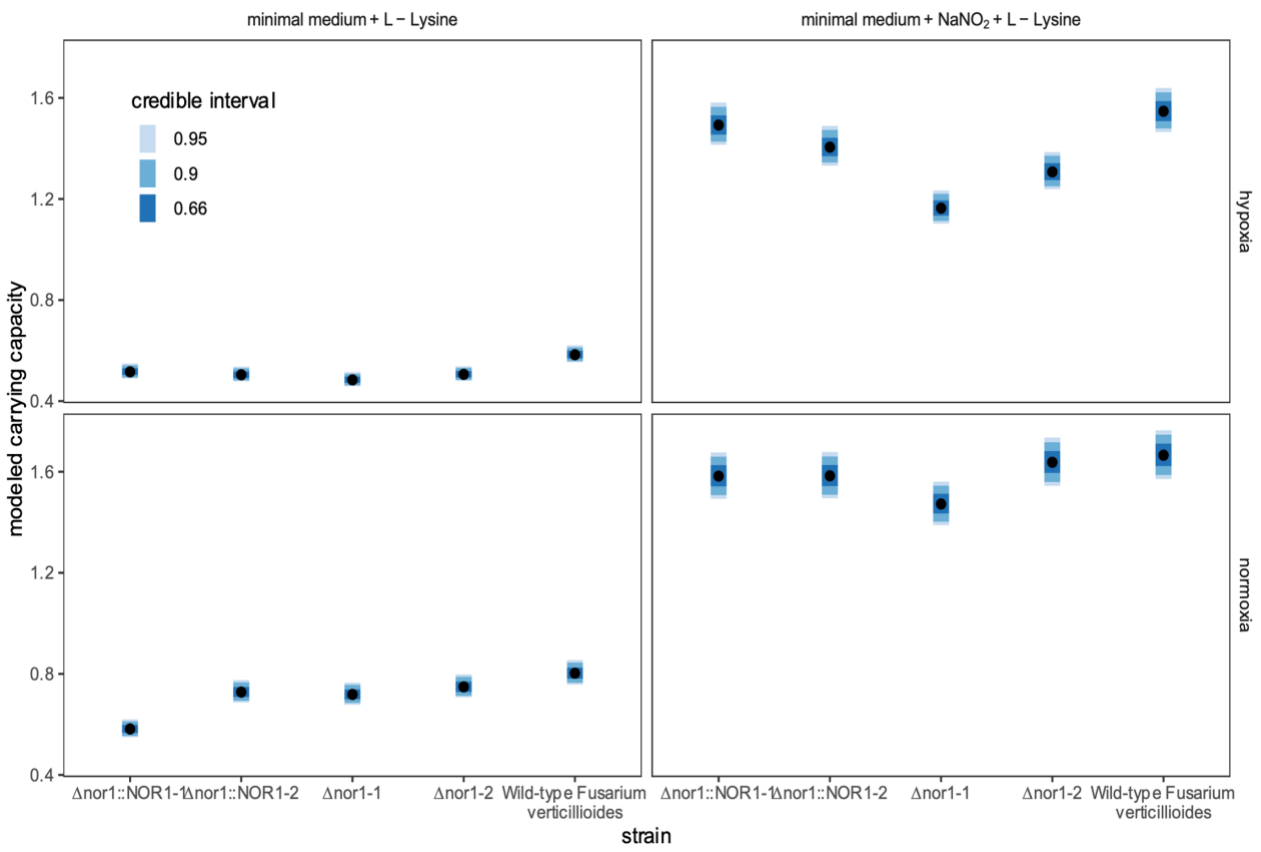

Supplementary Figure S4.8. Average fungal growth of various mutant strains in response to N amendments and oxygenation levels. A comparison of carrying capacity parameters between strains within each combination of medium and oxygen environment. The posterior estimates of the back-transformed carrying capacity parameter *L* are shown in the plot. The black dots are the point estimate (median of the posterior distribution). The shaded blue regions show the uncertainty with 66%, 90%, and 95% quantile credible intervals in progressively lighter colors. The modeled carrying capacities are shown separately for each of the medium:oxygen environment combinations: minimal medium (MM) + L-lysine:Hypoxia (top left), MM + L-lysine:Normoxia (bottom left), MM + $NaNO_2$ + L-lysine:Hypoxia (top right), and MM + NaNO2 + L-lysine:Normoxia (bottom right).

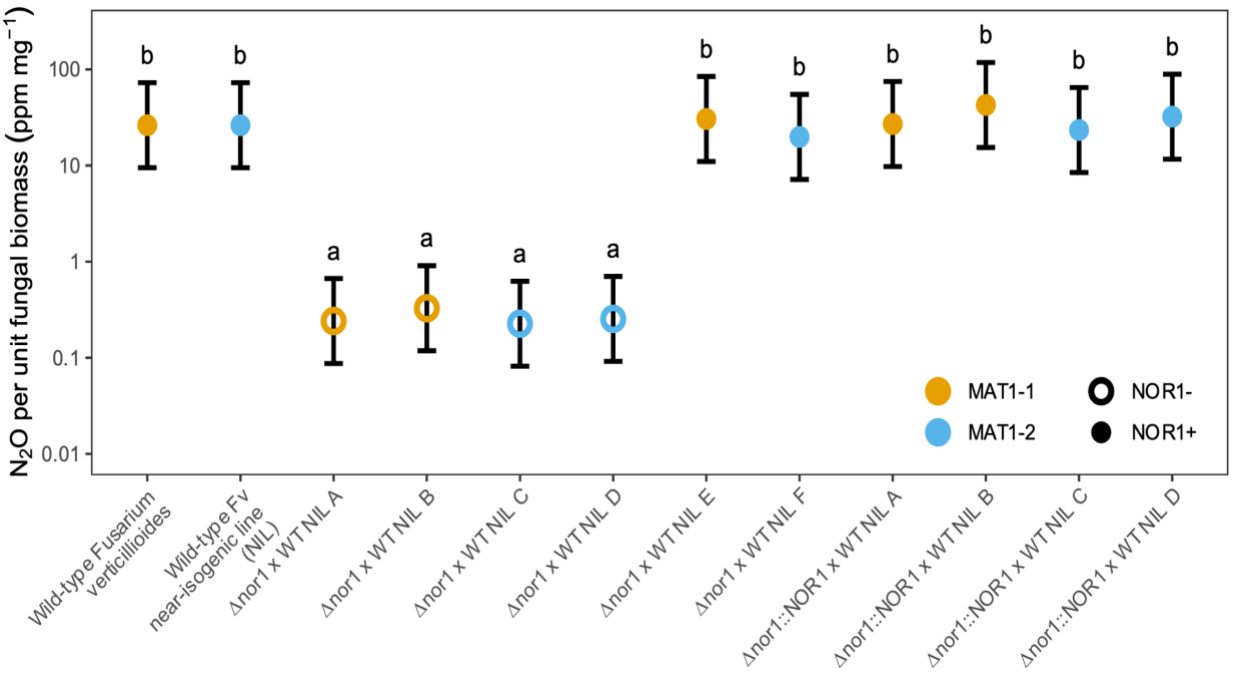

Supplementary Figure S4.9. Genetic analysis of the role of NOR1 in N_2O production per unit of fungal biomass in sexual cross progeny. The role of NOR1 in N_2O production per unit of fungal biomass was determined in wild type *Fusarium verticillioides*, a near-isogenic line (NIL) of wild type *Fv*, and a collection of sexual cross progeny that are the product of the wild type *Fv* NIL crossed with a single Δ*nor1*-1 deletion mutant (A-F) or a single Δ*nor1*-1::NOR1 add-back mutant (A-D). Orange circles represent MAT1-1 mating type; blue circles represent MAT1-2 mating type. Open circles represent the $NOR1^-$ genotype; closed circles represent the $NOR1^+$ genotype. The vertical axis is on a logarithmic scale. Group means that do not share a letter are significantly different based on a Šidák adjustment and error bars represent adjusted 95% confidence intervals around the modeled means.

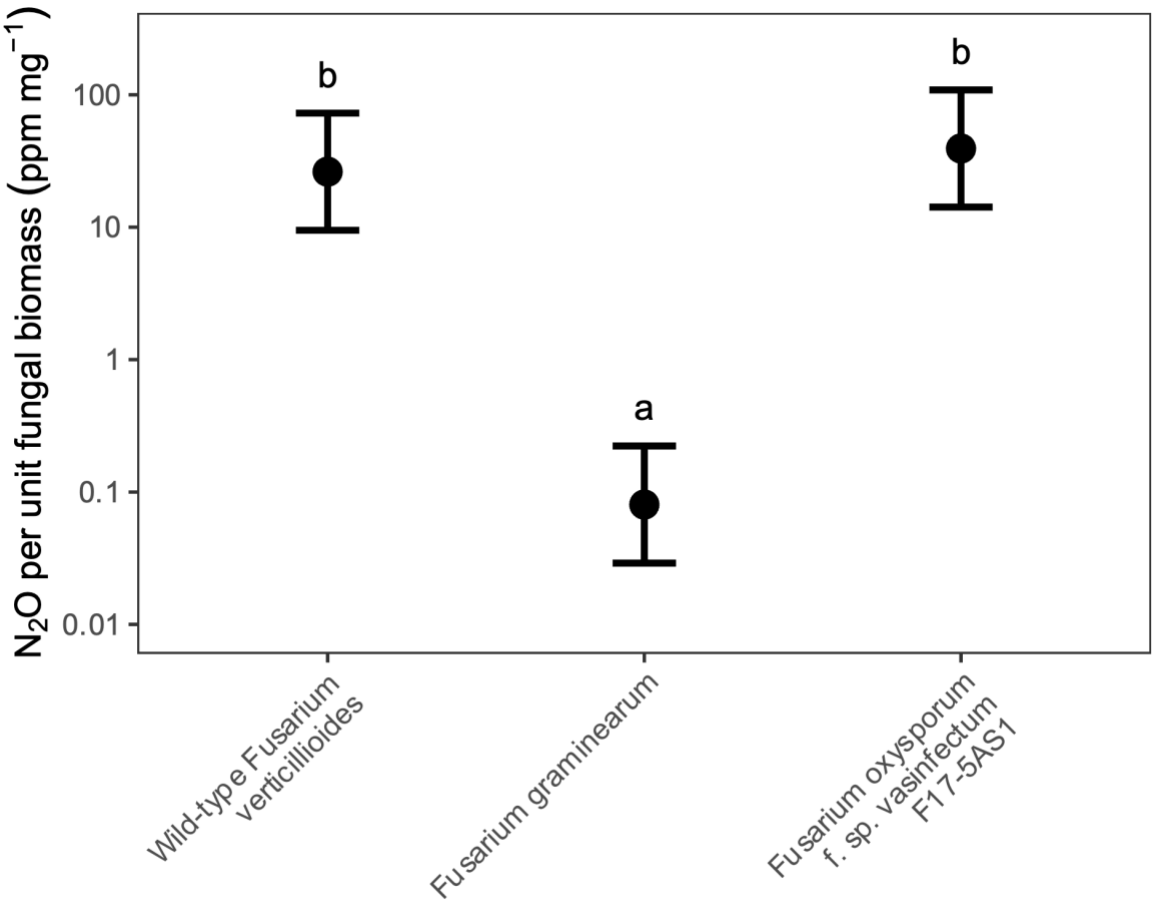

Supplementary Figure S4.10. Comparative assessment of N_2O production per unit of fungal biomass in three important plant pathogenic *Fusarium* species. Normalized nitrous oxide concentration were compared among *Fusarium verticillioides* FRC M-3125, *Fusarium graminearum,* and *Fusarium oxysporum* f. sp. *vasinfectum* F17-5AS1. The vertical axis is on a logarithmic scale. Group means that do not share a letter are significantly different based on a Šidák adjustment and error bars represent adjusted 95% confidence intervals around the modeled means.

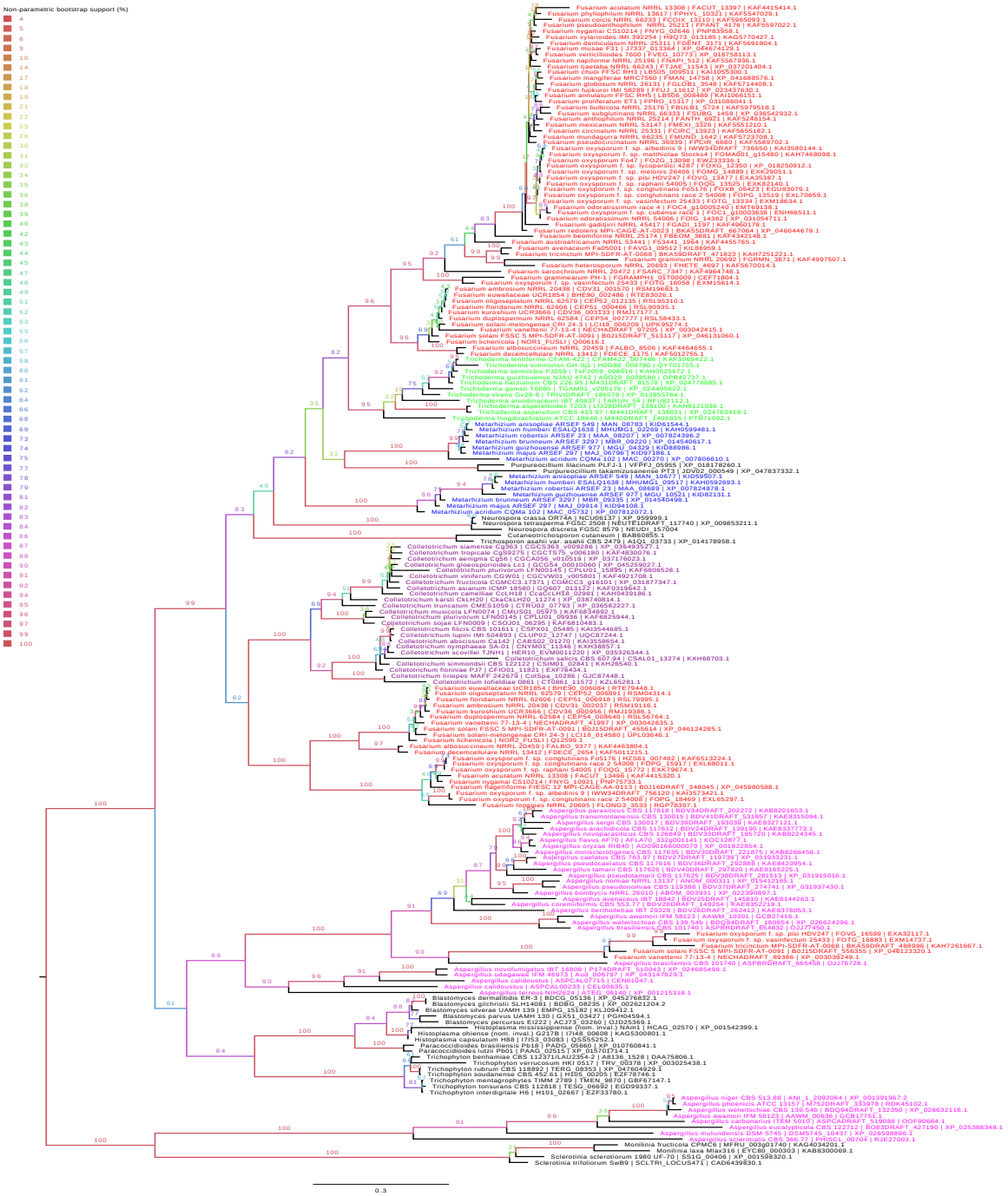

Supplementary Figure S4.11. p450nor protein tree built using non-parametric bootstrap estimation of 100 replicates. This is the same NOR protein tree depicted in Figure 4.3. Clades are not collapsed and support values for relationships between samples at sub-genus level clades and at individual branches are shown in this representation. Important fungal genera are colored as follows: *Fusarium* (red), *Trichoderma* (green), *Metarhizium* (blue), *Colletotrichum* (purple), and *Aspergillus* (pink); other fungal genera are colored black.

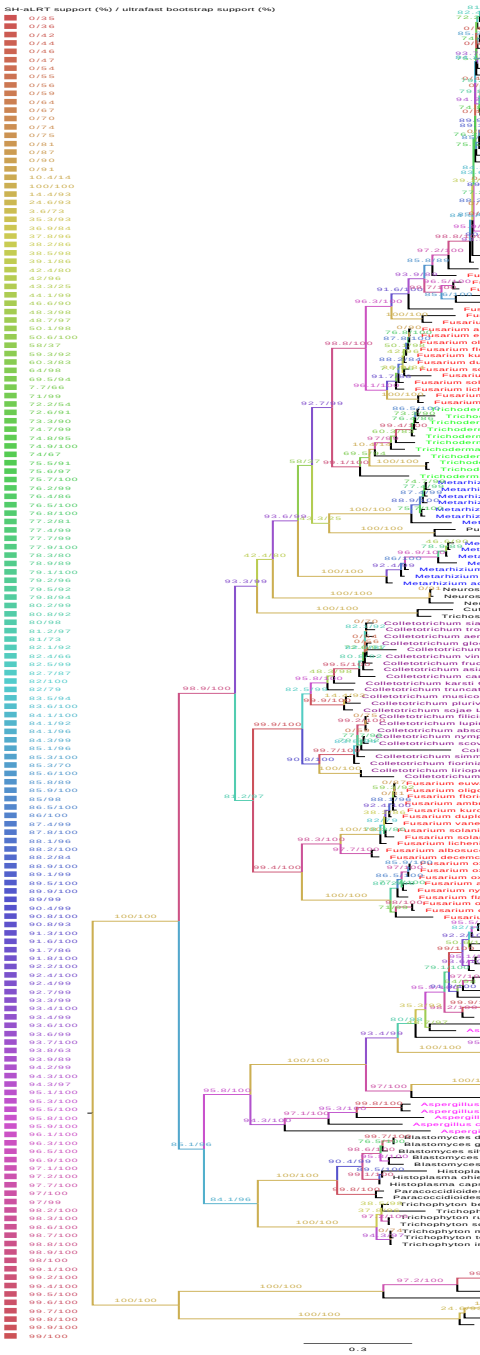

Supplementary Figure S4.12. p450nor protein tree built using SH-aLRT and UFBoot with 1,000 SH-aLRT and UFBoot replicates. The protein tree from Figure 4.3 and Fig. S4.11 was re-run using the JTTDCMut+R5 model with 1,000 SH-aLRT and UFBoot replicates to assess phylogenetic relationships using an alternative strategy to non-parametric bootstrap estimation of branch support. Clades are not collapsed and support values for relationships between samples at sub-genus level clades and at individual branches are shown in this representation. The legend is colored according to split support values represented as SH-aLRT support (%) / ultrafast bootstrap support (%). Important fungal genera are colored as in Fig. S4.11.

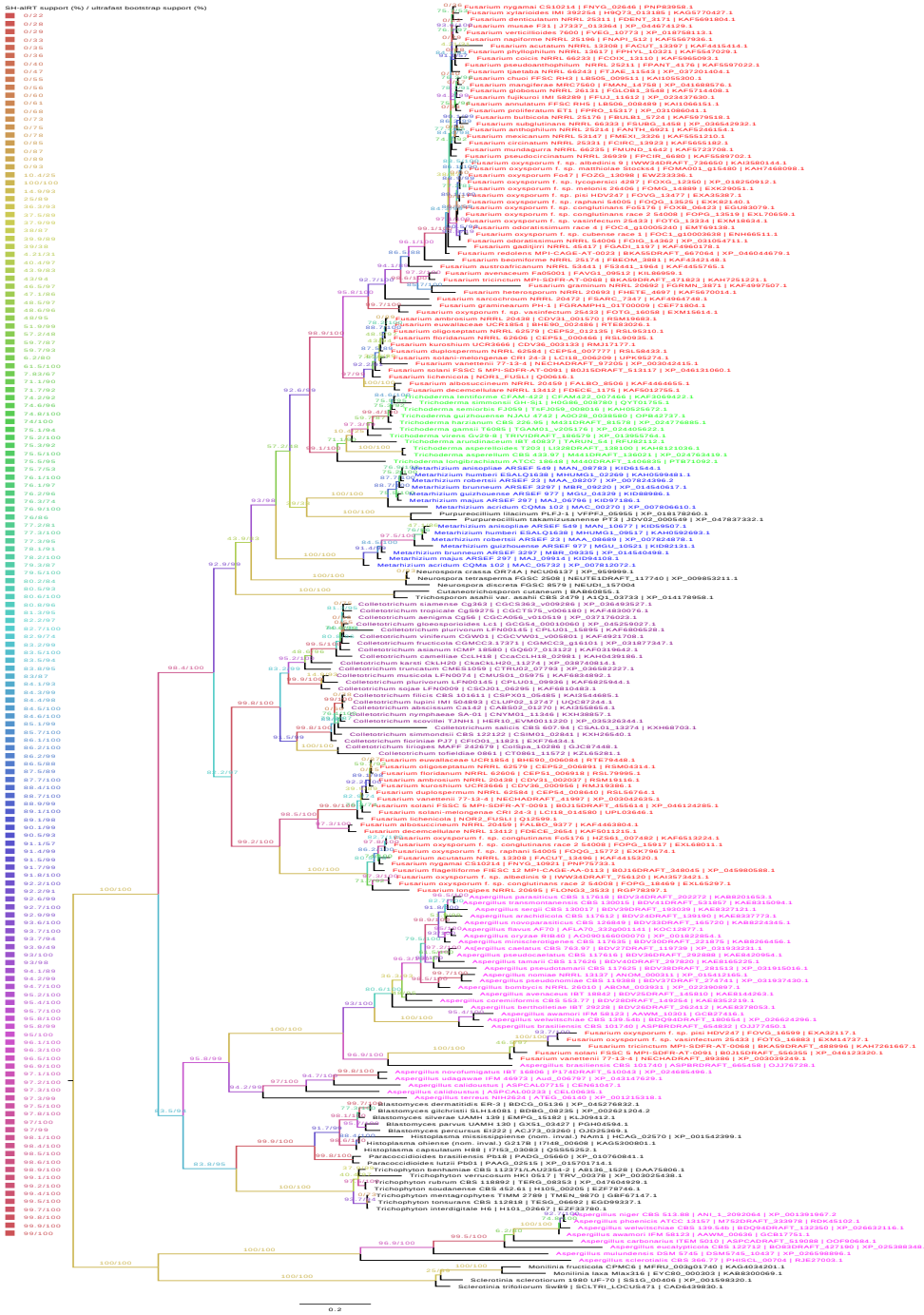

Supplementary Figure S4.13. p450nor protein tree built using SH-aLRT and UFBoot with 10,000 SH-aLRT and UFBoot replicates. The protein tree from Figure 4.3 and Fig. S4.11 was re-run using the JTTDCMut+R5 model with 10,000 SH-aLRT and UFBoot replicates. Clades are not collapsed and support values for relationships between samples at sub-genus level clades and at individual branches are shown in this representation. The legend is colored according to split support values represented as SH-aLRT support (%) / ultrafast bootstrap support (%). Important fungal genera are colored as in Fig. S4.11.

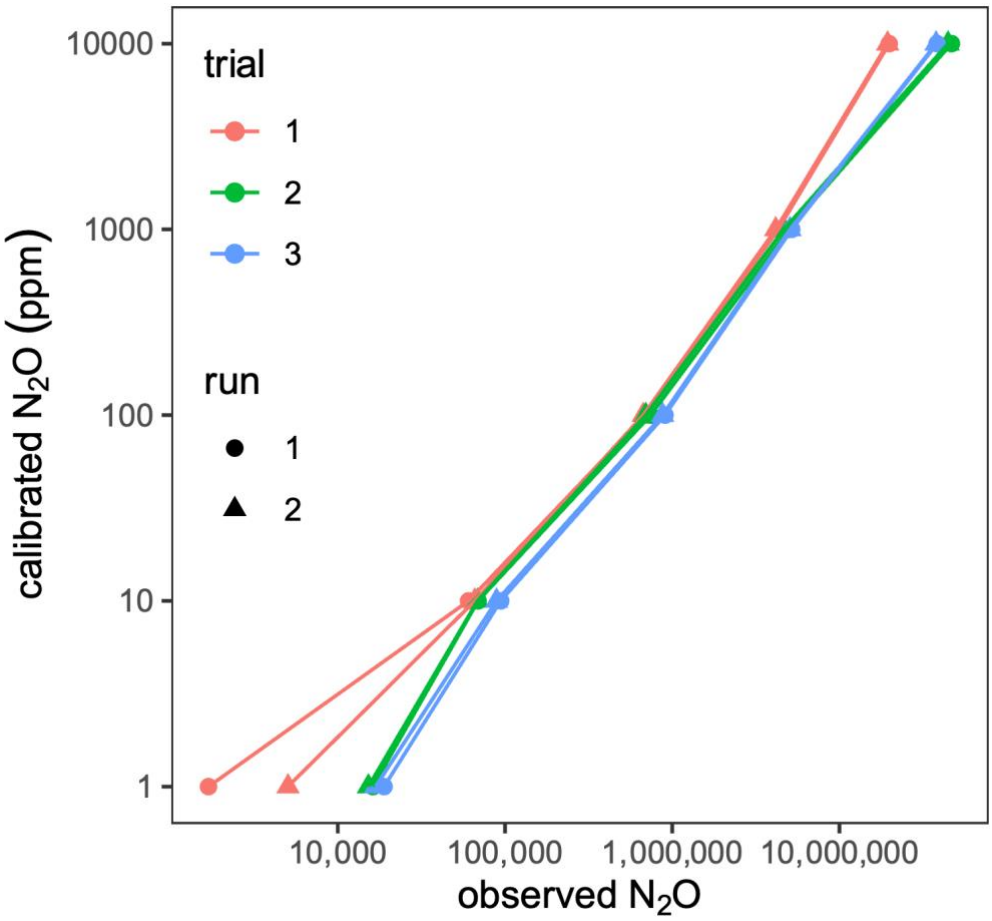

Supplementary Figure S4.14. Estimation of observed amounts of N_2O based on known amounts of N_2O. A calibration graph generated using five analytical standards of N_2O in amounts of 1, 10, 100, 1,000, and 10,000 ppm. All markers indicate the reported unknown values of N_2O that are calculated by manual integration of the chromatographic peaks using GCMS Real-Time Analysis. Both axes are on logarithmic scales.

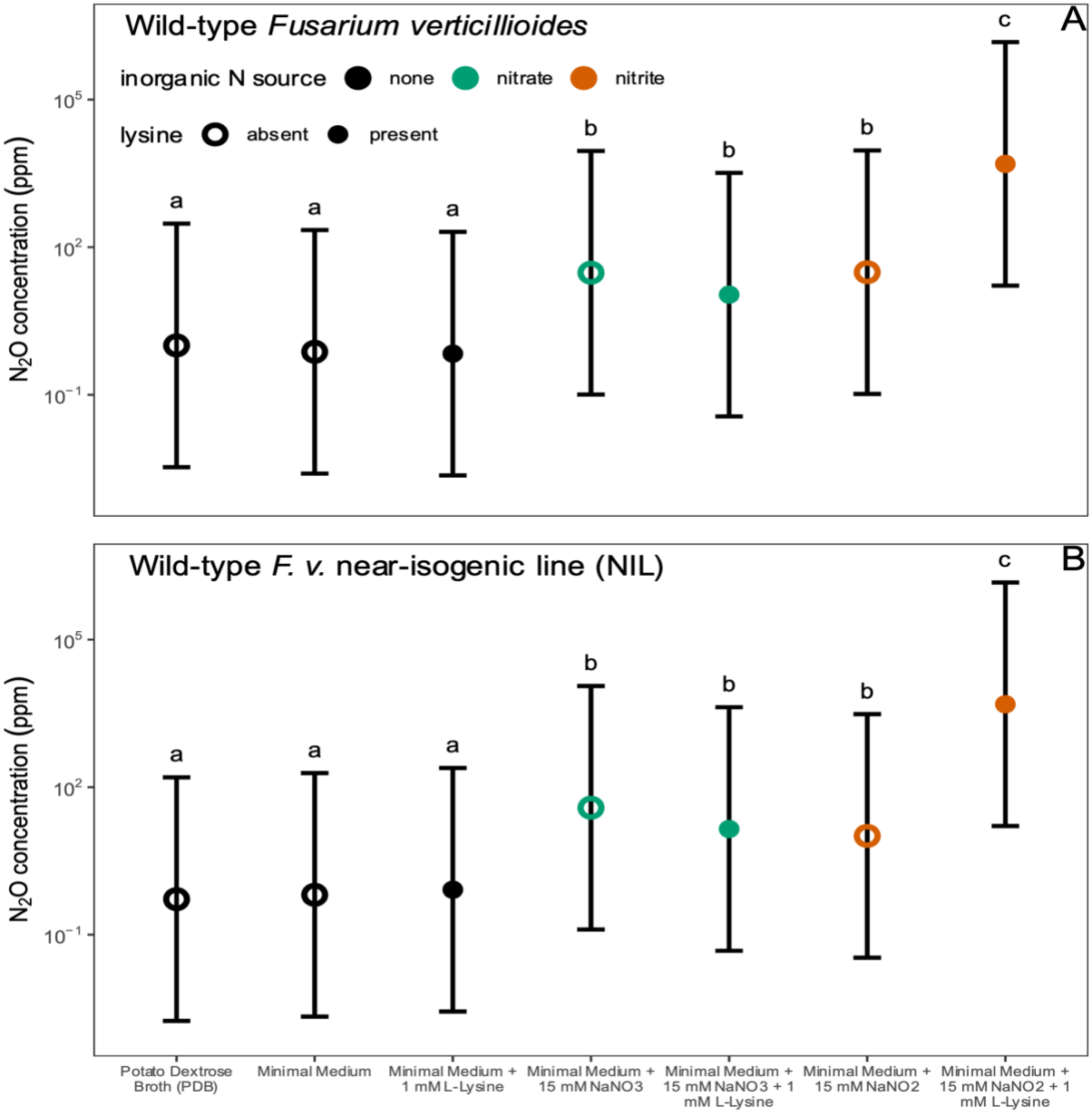

Supplementary Figure S4.15. Evaluation of N_2O production across rich and minimal medium and various nitrogen substrate amendments. Wild type *F. verticillioides* (*Fv*) (MAT1-1) and the wild type *Fv* NIL (MAT1-2) were used to confirm NOR1 N_2O production phenotypes in both mating types. Empty circles indicate L-lysine is absent from the medium; filled circles mean L-lysine (1 mM) is present; black circles mean no inorganic N source; green circles indicate the presence of nitrate (NO_3^-; 15 mM) in the medium; and orange circles indicate the presence of nitrite (NO_2^-; 15 mM) in the medium. Group means that do not share a letter are significantly different based on a Šidák adjustment and error bars represent adjusted 95% confidence intervals around the modeled means. Both vertical axes are on a logarithmic scale.

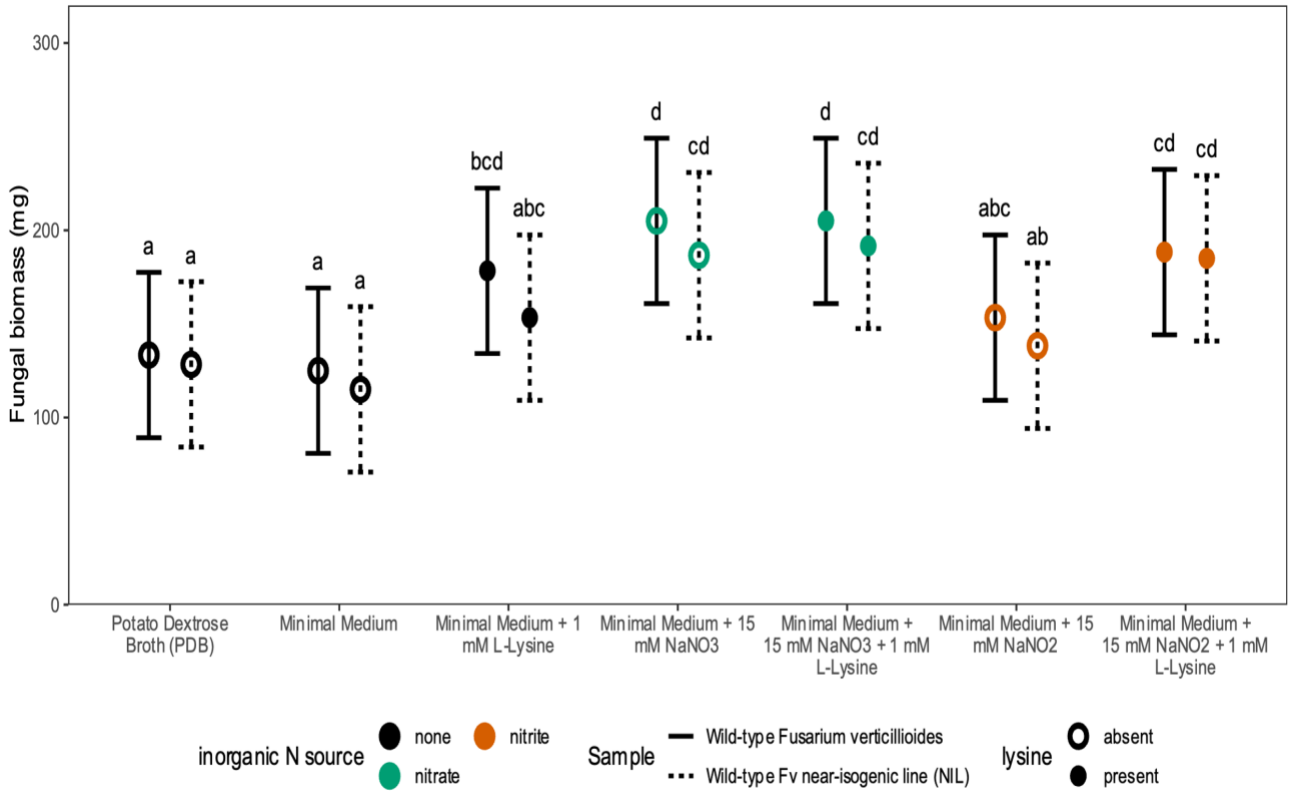

Supplementary Figure 4.16. Evaluation of fungal biomass across rich and minimal media with various nitrogen substrate amendments. Wild type *Fusarium verticillioides* (*Fv*) (MAT1-1) and the wild type *Fv* near-isogenic line (MAT1-2) were used to confirm NOR1 N_2O production phenotypes in both mating types. Solid lines represent wild type *Fv*; dashed lines represent wild type *Fv* NIL; empty circles indicate L-lysine is absent from the medium; filled circles mean L-lysine (1 mM) is present; black circles mean there is no inorganic N source; green circles represent the presence of nitrate (NO_3^-; 15 mM) in the medium; and orange circles represent the presence of nitrite (NO_2^-; 15 mM) in the medium. Group means that do not share a letter are significantly different based on a Šidák adjustment and error bars represent adjusted 95% confidence intervals around the modeled means.

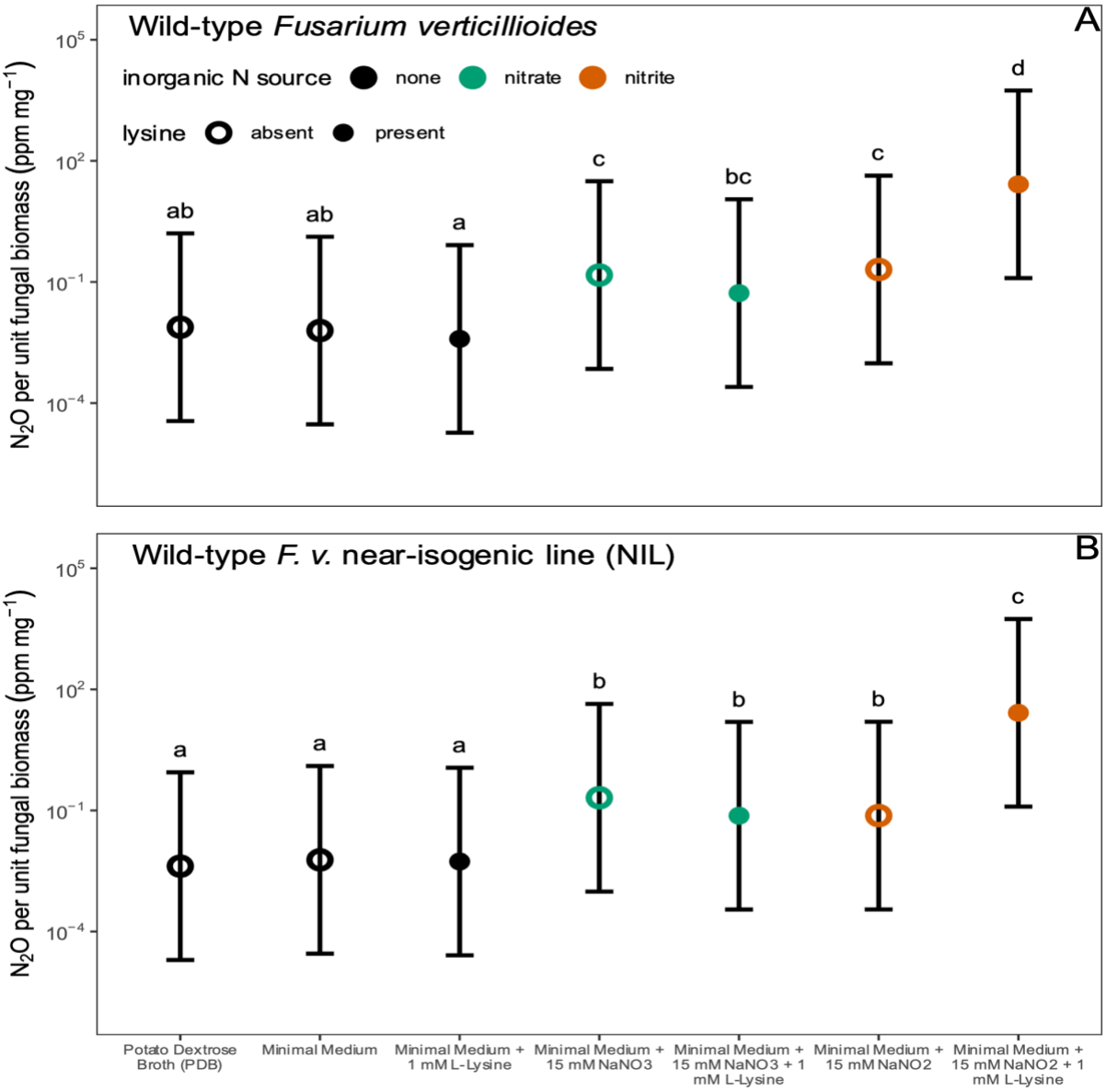

Supplementary Figure S4.17. Evaluation of N_2O production normalized to fungal biomass across rich and minimal medium with various nitrogen substrate amendments. Wild type *F. verticillioides* (*Fv*) (MAT1-1) and the wild type *Fv* NIL (MAT1-2) were used to confirm NOR1 N_2O production phenotypes in both mating types. Empty circles indicate L-lysine is absent from the medium; filled circles mean L-lysine (1 mM) is present; black circles mean there is no inorganic N source; green circles represent the presence of nitrate (NO_3^-; 15 mM) in the medium; and orange circles represent the presence of nitrite (NO_2^-; 15 mM) in the medium. Group means that do not share a letter are significantly different based on a Šidák adjustment and error bars represent adjusted 95% confidence intervals around the modeled means. Both vertical axes are on a logarithmic scale.

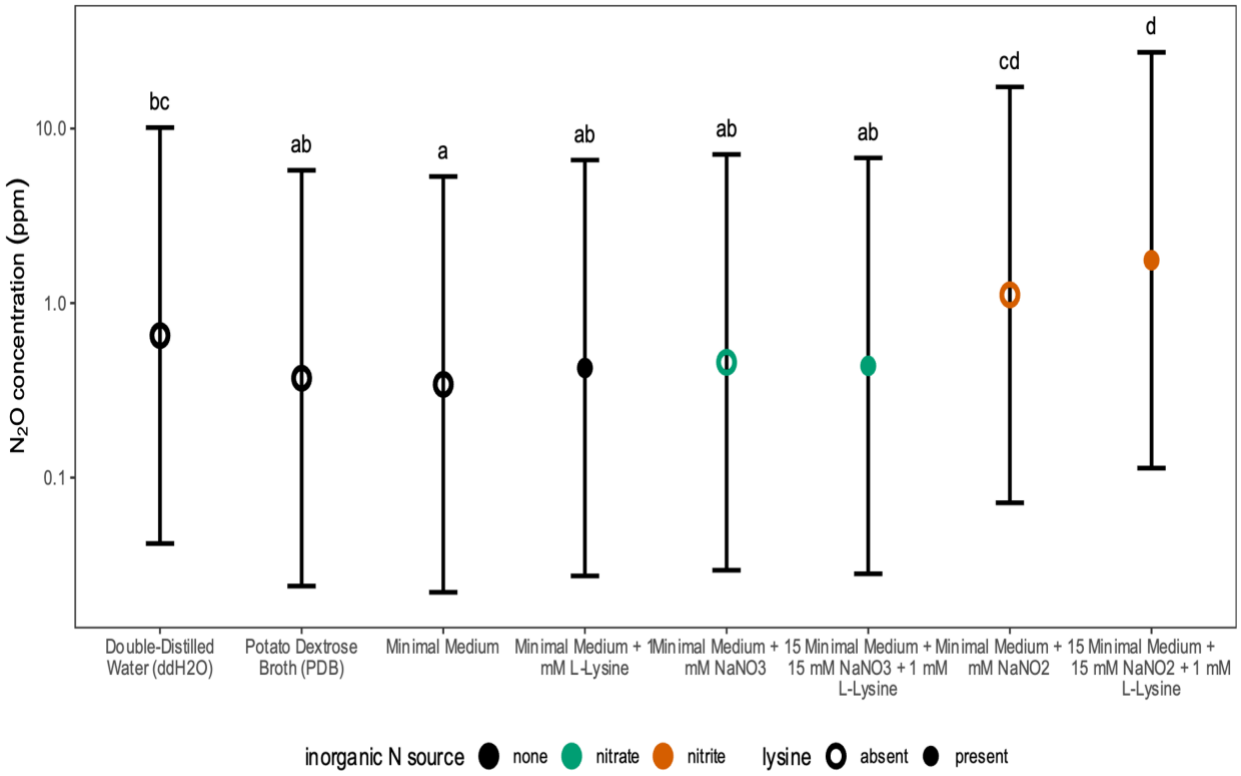

Supplementary Figure S4.18. **Evaluation of N_2O production from uninoculated media.** Empty circles mean L-lysine is absent from the medium; filled circles mean L-lysine (1 mM) is present in the medium; black circles mean there is no inorganic N source; green circles represent the presence of nitrate (NO_3^-; 15 mM) in the medium; and orange circles represent the presence of nitrite (NO_2^-; 15 mM) in the medium. Group means that do not share a letter are significantly different based on a Šidák adjustment and error bars represent adjusted 95% confidence intervals around the modeled means. The vertical axis is on a logarithmic scale.

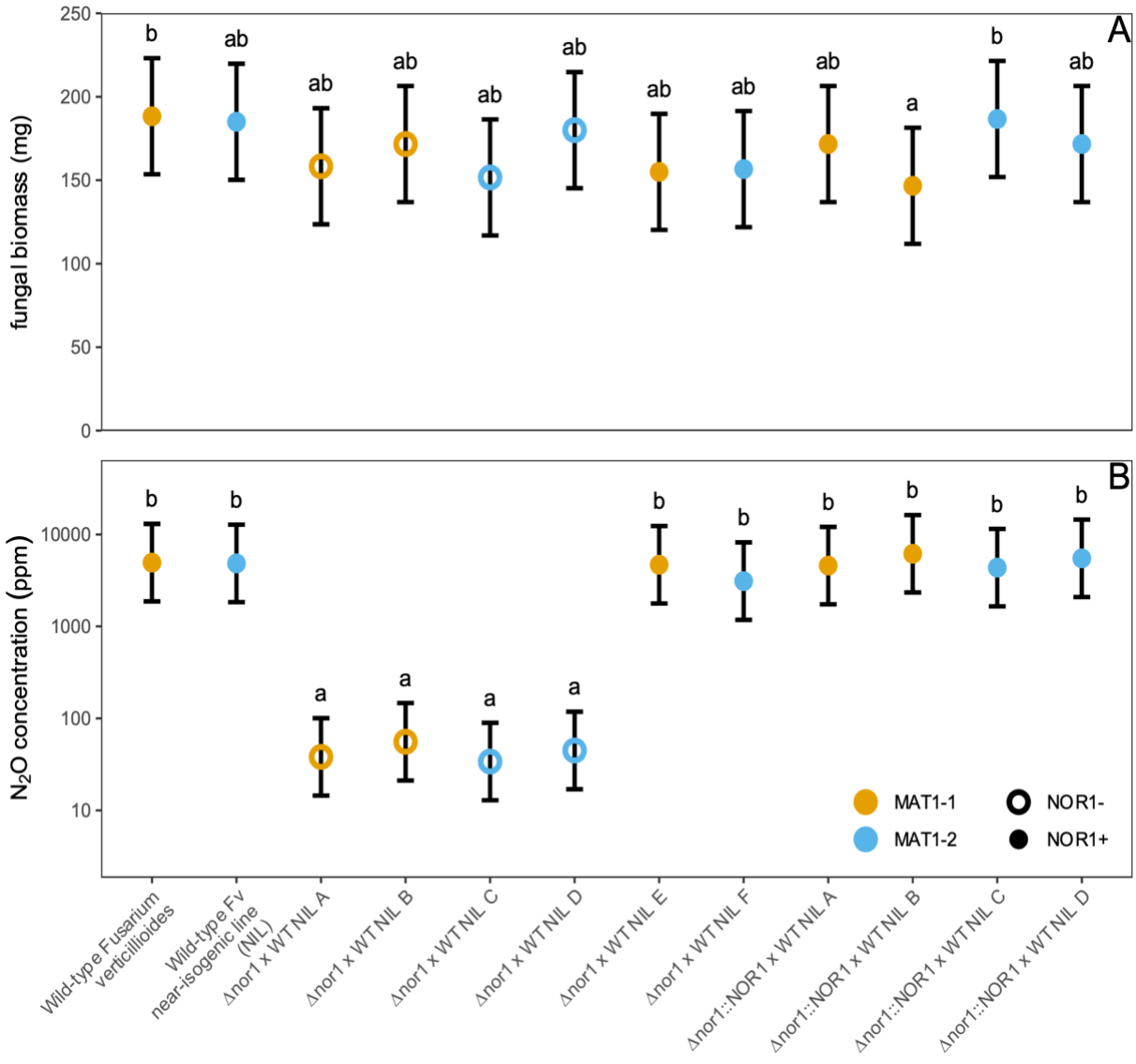

Supplementary Figure S4.19. Genetic analysis of the role of NOR1 in fungal biomass and N_2O production in sexual cross progeny. (A) Fungal biomass (dry weight) was measured in milligrams (mg); **(B)** Nitrous oxide concentration was reported in parts per million (ppm). The role of NOR1 in fungal biomass and N_2O production was determined in wild type *Fv*, a near-isogenic line (NIL) of wild type *Fv*, and a collection of sexual cross progeny that are the product of the wild type *Fv* NIL crossed with a single Δ*nor1*-1 deletion mutant (A-F) or a single Δ*nor1*-1::NOR1 add-back complemented mutant strain (A-D). Orange circles represent MAT1-1 mating type; blue circles represent MAT1-2 mating type. Open circles represent the $NOR1^-$ genotype; closed circles represent the $NOR1^+$ genotype. The y-axis is on a logarithmic scale. Group means that do not share a letter are significantly different based on a Šidák adjustment and error bars represent adjusted 95% confidence intervals around the modeled means.

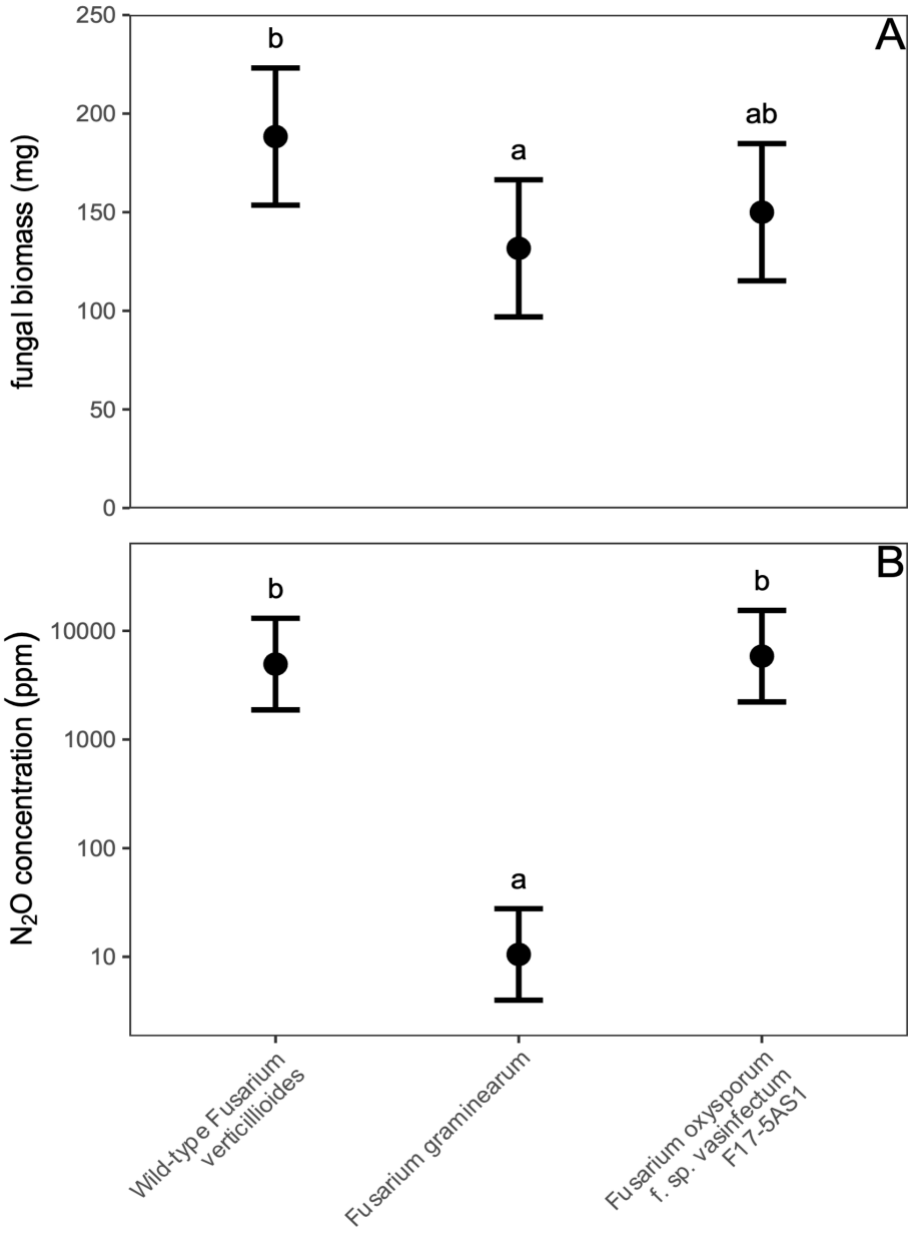

Supplementary Figure S4.20. **Comparative assessment of fungal biomass and N_2O production in three important plant pathogenic *Fusarium* species. (A)** Fungal biomass measured mg; **(B)** Nitrous oxide concentration reported in ppm. Biomass and raw nitrous oxide concentration were compared among *Fusarium verticillioides* FRC M-3125, *Fusarium graminearum*, and *Fusarium oxysporum* f. sp. *vasinfectum* F17-5AS1. The vertical axis is on a logarithmic scale. Group means that do not share a letter are significantly different based on a Šidák adjustment and error bars represent adjusted 95% confidence intervals around the modeled means.

CHAPTER 5

CONCLUSIONS

Fungal denitrification was studied in fungi as an avenue for better understanding the underlying mechanisms of nitrogen dissimilation in fungal-derived nitrous oxide (N_2O) emissions, lifestyles of pathogenic fungi, and mechanisms of virulence and fumonisin production. In Chapter 2, a prior transcriptome study of the soil-borne, mycotoxigenic plant pathogen, *Fusarium verticillioides* provided a list of genes of interest. These were differentially expressed genes responding to either diethylenetriamine (DETA) NONOate, which is a nitric oxide (NO) donor, or hypoxic conditions. From this RNA-seq study, 16 genes presumed to be associated with denitrification, survival under hypoxia, and/or nitrogen metabolism were identified. I geared the rest of my research towards a subset of these 16 genes. Using phylogenetics, phylogenomics, and our own independent RNA-seq dataset and publicly available transcriptomic data, I found the following:

1. Denitrification genes (*dNAR*, *dNIR*, and *p450nor*) are highly up-regulated *in planta* during maize (*Zea mays*) root infection by *F. verticillioides* and *in vitro* under specific culture conditions.
2. Fungal orthologs of dNAR, dissimilatory nitrate reductase, are uncommon, but their assimilatory counterpart is found in almost all filamentous fungi.

3. Fungal orthologs of dNIR (dissimilatory nitrite reductase) and p450nor (a unique fungal cytochrome P450 nitric oxide reductase) are mostly limited to the phylum Ascomycota and a few orders.
4. Lifestyle features in *Fusarium* spp. may be partially influenced by the ability, or inability, to denitrify.

Based on the findings from Chapter 2, I hypothesized that denitrifying plant pathogenic fungi utilize the N dissimilation pathway to survive under fluctuating oxygen conditions, to infect plant hosts, overcome plant defense responses, and cause disease. In Chapter 3, this hypothesis was tested using single-gene deletion mutants for *NAR1* (dNAR), *DNI1* (dNIR), *NOR1* (p450nor), *NIA1* (aNAR), *NII1* (aNIR), *FHB1* (flavoHB), and *FNT1*. Mutants were assessed for virulence in maize seedlings and fumonisin production. From this study, I determined the following:

1. Maize seedlings inoculated with Δ*fhb1* or Δ*nor1* deletion mutants exhibit severe stunting.
2. Deletion of *FHB1* has the largest effect on virulence *in planta* and increases necrotic lesion formation.
3. Deletion of *DNI1* significantly increased fumonisin ($FB_{1,2,3}$) production under normoxia and hypoxia relative to wild type *F. verticillioides*.
4. Hypoxia induces a phenotypic switch where FB_3 production exceeds FB_1 and FB_2 production.

It is unclear how much of a role denitrification plays in the virulence of plant pathogenic fungi, but deletion of some denitrification-associated genes in *F. verticillioides* have a measurable impact on virulence and fumonisin production. Additionally, the function of some

denitrification-associated proteins has yet to be determined because we were unable to do isolated studies for all 16 genes identified by RNA-seq in Chapter 2.

I also focused my attention on identifying a denitrification enzyme that could be targeted for inhibition of fungal denitrification and, thus, reduction of nitrogen loss and N_2O emissions from agricultural fields. In Chapter 4, I assessed fungal growth and N_2O production in the Δ*nor1* deletion mutants. After observing a striking decrease in N_2O emissions of Δ*nor1* deletion mutants, I used protoplast complementation to add the wild type *FvNOR1* gene back into the Δ*nor1* genome to see if we could restore the wild type phenotype for N_2O production. I also validated my results using progeny from a sexual cross between *MAT1-1* Δ*nor1* or Δ*nor1*::*NOR1* mutants and a *MAT1-2* near-isogenic line of wild type *F. verticillioides*. Using these various fungal strains of $NOR1^+$ or $NOR1^-$ genotypes, I determined the following:

1. Nitrite (NO_2^-) is the best inorganic nitrogen source for induction of N_2O production.
2. NOR1 is the key enzyme involved in N_2O production in *F. verticillioides* and its deletion reduces N_2O by up to 99%.
3. dNIR and p450nor are vital to produce biologically relevant amounts of N_2O.
4. NOR1 orthologs are conserved in a variety of plant, insect, and animal fungal pathogens.

My long-term goal is to develop fungal denitrification inhibitors that effectively target key denitrification enzymes like dNIR and p450nor. Pennerman et al. (in preparation) used molecular docking and pharmacological modeling approaches to screen a chemical database for compounds that may bind to the active site of orthologs of dNIR and p450nor in fungi. All candidate compounds were subjected to a Griess assay to assess conversion of NO_3^- to NO (i.e., N loss). Two candidates have been identified that reduce N loss by 7-10%. In the future, I aim to

evaluate the effect of these candidate inhibitors on N_2O production, the soil microbiome, and plant health.

Understanding the nature of denitrification enzymes in fungi is central to developing denitrification mitigation and inhibition strategies. Advanced mitigation/inhibition strategies and knowledge regarding N cycle global processes will assist in alteration of agricultural practices to increase N use efficiency, increase plant growth and productivity, reduce N fertilizer loss due to denitrification, limit N_2O emissions, reduce economic loss and environmental pollution, reduce adverse effects to local and global ecosystems, and decrease anthropogenic forcing of the climate system. In conclusion, my project used a multi-disciplinary approach to increase understanding of the fungal denitrification pathway, phylogenetic rarity of denitrification genes, mechanisms for production of N_2O in denitrifying fungi, and the interconnection between denitrification and pathogenesis. The combination of my results across all studies was translated into an updated hypothetical model of the denitrification pathway in *F. verticillioides* (Figure 5.1). Overall, this research will contribute towards a synthesis of relationships across a range of microbial and plant systems that will drive research focusing on the atmosphere-plant-microbe-soil continuum.

Figures

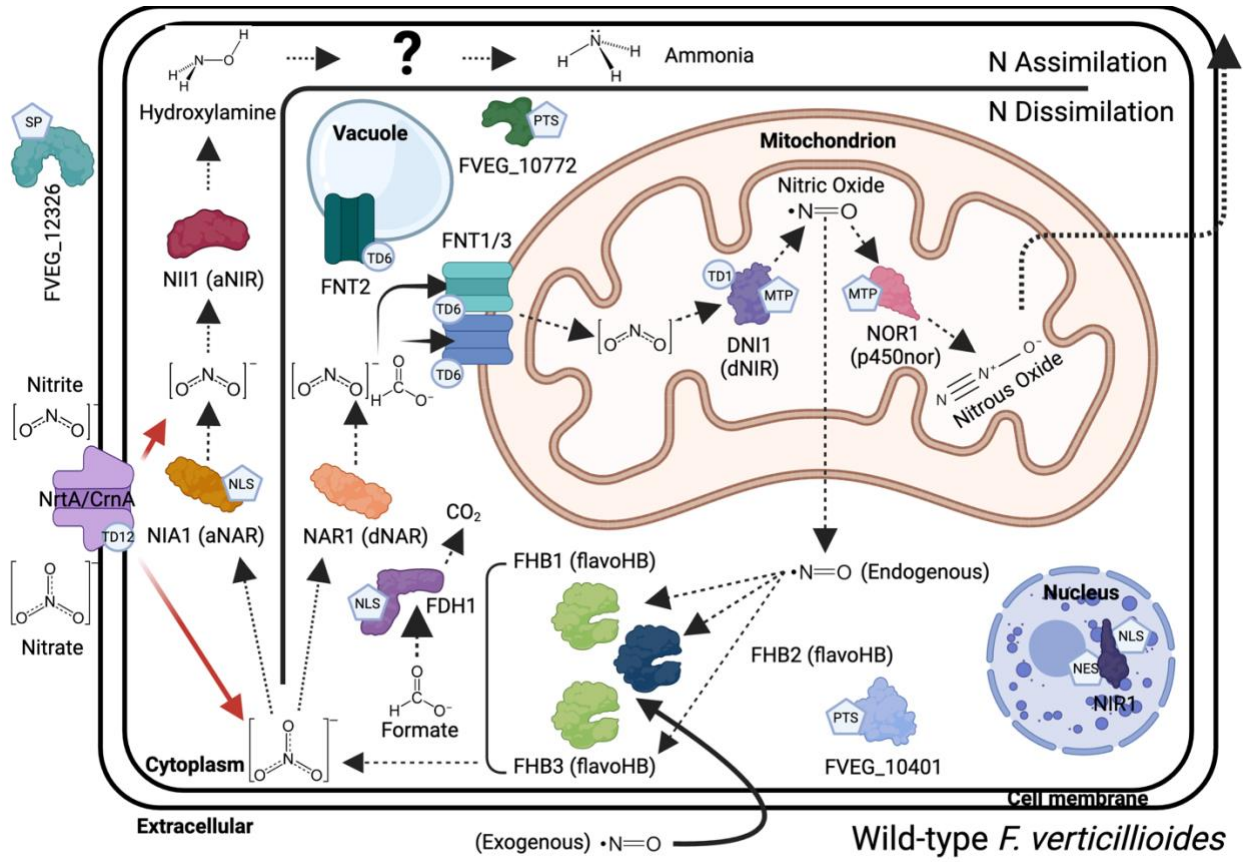

Figure 5.1. Hypothetical model of the nitrogen dissimilation and assimilation pathways with accessory proteins in *Fusarium verticillioides.* This hypothetical model is based on a combination of RNA-seq analysis results and bioinformatic prediction of signal peptide presence, transmembrane helices, and subcellular localization. The model includes proteins outside of the three enzymes commonly associated with fungal denitrification (dNAR, dNIR, NOR). Localization signals and the number of transmembrane domains is pictured for each protein for which it is relevant. Subcellular components are labeled. PTS = peroxisomal targeting signal; MTP = mitochondrial transit peptide; NLS = nuclear localization signal; NES = nuclear export signal; SP = signal peptide; TD = transmembrane domain. Created with BioRender.com.